Tachyon Condensation in String Field Theory

by

Nicolas Moeller

Submitted to the Department of Physics
in partial fulfillment of the requirements for the degree of

Doctor of Philosophy in Physics

at the

MASSACHUSETTS INSTITUTE OF TECHNOLOGY

June 2003

Author .....
Department of Physics
May 2, 2003

Certified by .....
Barton Zwiebach
Professor of Physics
Thesis Supervisor

Accepted by .....
Thomas J. Greytak
Professor of Physics; Associate Department Head for Education

Tachyon Condensation in String Field Theory

by

Nicolas Moeller

Submitted to the Department of Physics
on May 2, 2003, in partial fulfillment of the
requirements for the degree of
Doctor of Philosophy in Physics

Abstract

In this thesis, we present some results that strongly support Sen's conjectures on tachyon condensation on a bosonic D-brane. Our main tool of analysis is level truncated open bosonic string field theory

We use level truncation to check that the energy difference between the local maximum and the local minimum of the open bosonic tachyon effective potential is equal to the tension of a space-filling D-brane (Sen's first conjecture). Our results prove this equality within a precision of about 0.1%.

We then construct lump solutions of open bosonic string field theory, which are conjectured by Sen (third conjecture) to be D-branes of lower dimensions. We check that indeed the tensions of lumps of codimension one and two, coincide with the tensions of the respective D-branes within a precision of a few percent.

We also give evidence for Sen's second conjecture; that in the nonperturbative tachyon vacuum all open string degrees of freedom must disappear. We show that this is guaranteed if we can write the identity string field $\mathcal{I}$ in the form $\mathcal{I} = QA$, where A is some string field and Q is the BRST operator in the true vacuum. We show evidence that the identity can indeed be written in this form.

We also analyze the dynamics of tachyon condensation by studying time-dependent solutions of p-adic string theory and level truncated string field theory. Although our rolling solutions conserve energy, their pressure oscillates with diverging amplitudes. These results therefore don't support Sen's proposal of a pressureless tachyon matter.

Thesis Supervisor: Barton Zwiebach
Title: Professor of Physics

Acknowledgments

I am indebted to my advisor Barton Zwiebach for introducing me to the subject of string field theory and for advising me, during all the course of my research at MIT, through many enlightening collaborations and discussions. I thank Ian Ellwood, Bo Feng, Yang-Hui He, Martin Schnabl, Ashoke Sen and Washington Taylor for collaborations and discussions, Hiroyuki Hata for correspondence, and Joe Minahan and Leonardo Rastelli for discussions. I also thank the members of my thesis committee, Roman Jackiw, Washington Taylor and Barton Zwiebach, for proofreading my thesis. Finally, I am grateful to my family, and in particular to my wife Marina, for their constant support and encouragements.

Contents

Chapter 1

Introduction

The main protagonist of this thesis is the tachyon, a particle of negative mass-squared, that is well known for signaling us that we are expanding the theory around the wrong vacuum. String theory was barely born, and still known as dual resonance model, when a tachyon was found in its spectrum. We will thus start this chapter with a short (and necessarily incomplete) history of the role of tachyons in string theory that will start from the time of the dual models.

Dual models were originally invented as a theory of the strong interaction, as physicists were trying to understand the multitude of new hadrons found in collision experiments. These theories, shown to be realized as theories of a relativistic string, possess an infinite tower of resonances of arbitrarily high masses and spins; a situation qualitatively similar to the experimental data. But it was clear that string theory in its bosonic form is not devoid of problems. Requiring it to be free of ghosts indicated that it favors a 26-dimensional spacetime, a disturbing fact for a theory of hadrons (we now know that it has to be 26, or 10 for superstring theories, in order to cancel conformal anomalies). More seriously, it has a tachyon in its spectrum, whose presence means, at least, that the theory is formulated around an unstable vacuum. For the theory to make any serious sense, it should be reformulated around a stable vacuum. While this situation is under control when we know the tachyon potential, like for example for the Higgs field in the standard model, the situation in string theory is more difficult since we do not know a priori the string theory tachyon potential, that

must be evaluated from the off-shell dynamics of the theory. Some early attempts to find a stable vacuum of the dual models were made in [1, 2],

It was soon discovered, however, that the correct theory of hadrons is QCD, a nonabelian gauge theory with an $SU(3)$ color gauge group. But that didn't make string theory obsolete; instead, it changed its aims, as it was soon proposed that string theory's ability to describe particles of high spin could be useful in the quest of a quantum theory of gravity. While this was becoming more and more concrete, string theorists were relegating bosonic string theory to an inconsistent model, while focusing on the supersymmetric string theories (superstring theories). These were in fact more likely to provide us with a unified theory of gravity and matter, one obvious reason being that superstring theories contain fermions, while the bosonic string only describes bosons. Another very attractive feature is that these theories can be made tachyon-free. Indeed, it is possible to consistently truncate the superstring spectrum by imposing so-called GSO projections, which in some cases project out the tachyon. In total there are five consistent superstring vacua without tachyons, those are type I, type IIA, IIB, $E_8 \times E_8$ heterotic and $SO(32)$ heterotic. We know today that these five theories are all particular limits of one underlying theory named M-theory.

But the vacuum of a theory is not quite the end of the story. And in fact, when nonperturbative objects (D-branes) that can break supersymmetry, were being discovered and understood, it was found that tachyons often live on their worldvolume.

D-branes were first defined as hyperplanes on which open strings can end. It was subsequently discovered that they have their own dynamics; they have a tension and are thus sources for closed strings (which carry gravity); also superstring D-branes can be sources of Ramond-Ramond fields. For example, type IIA or IIB superstring theories possess BPS Dp-branes[1] for, respectively, any even or odd $p < 10$. BPS D-branes are stable since they conserve some supersymmetries and can carry conserved R-R charges. But the type II theories also admit non BPS D-branes (when p has the wrong parity) that break all supersymmetries, and are unstable. Indeed these don't carry R-R charge, and moreover supersymmetry is not here to protect their mass.

[1] A Dp-brane is extended in p spatial dimensions and one time dimension.

This instability is actually signaled by the presence of a tachyon in the spectrum of the non BPS D-branes. Also one can construct configurations of coincident D-branes and anti-D-branes. These too break all supersymmetries, and are unstable as is suggested by the fact that a D-brane and an anti D-brane can annihilate. Moreover, the spectrum of open strings that have one end attached to a D-brane and the other end attached to a coincident anti-D-brane, contains a tachyon.

We have just seen that the superstring tachyons are related to D-brane instabilities. Can we say the same about the tachyons of bosonic string theory? In bosonic string theory, there are D-branes of any dimension, that are all unstable. Let us consider a Dp-brane sitting in a closed string theory background. In this configuration, we can have two kinds of strings:

- Closed strings that are free to propagate in the whole spacetime.
- Open strings, whose endpoints must be attached to the D-brane.

So it looks like we have an open string theory living on the D-brane, although we were considering a closed string theory background. What happens now if we consider $p = 25$? Our D-brane fills all of spacetime, and the open string endpoints are unconstrained. And therefore open bosonic string theory can be seen as closed bosonic string theory with a space-filling D-brane. And in analogy with the previous superstring examples, the instability of the D25-brane is related to the open[2] bosonic string theory tachyon.

We will actually make this claim much more precise. In fact, the process of tachyon condensation (by which we mean the tachyon building a nonzero vacuum expectation value (vev) so as to minimize its effective potential) corresponds to the decay of the unstable system of D-brane on which the tachyon was living. This was formulated in a precise way by Sen [3, 4, 5, 6, 7, 8, 9] in a set of three conjectures, which we describe here for the case of the open bosonic string theory. It should be understood however that these conjectures generalize to any unstable system of D-branes in string theory.

[2]Bosonic string theory also has a closed string tachyon which is still, at this time, very poorly understood. This tachyonic instability is not related to any D-brane instability.

First conjecture. The tachyon effective potential has a local minimum, and the difference in energy between the local maximum and the local minimum of the potential, must exactly cancel the tension T_{25} of the space-filling D25-brane.

This situation is shown in Figure 1-1. The perturbative vacuum at $\phi = 0$ is on

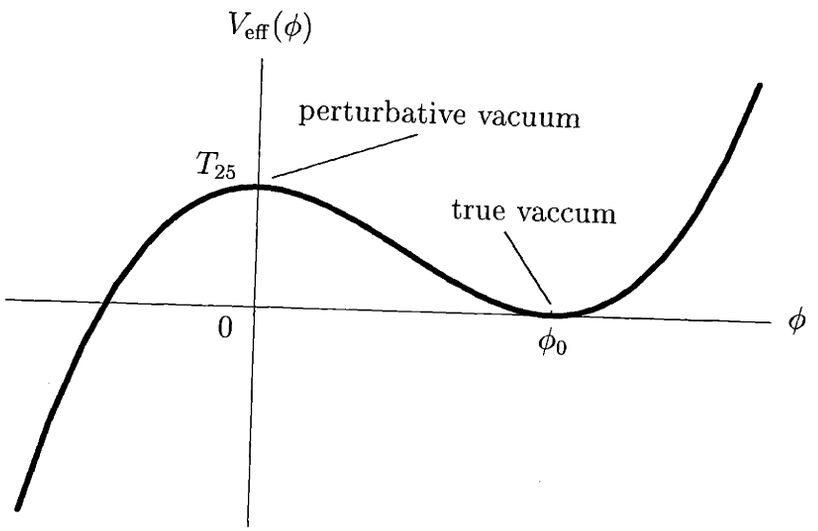

Figure 1-1: The effective potential of the open bosonic string tachyon. The perturbative vacuum is at $\phi = 0$, on the local maximum of the potential. The local minimum at $\phi = \phi_0$ is the true vacuum of open bosonic string theory. The potential is unbounded on the left. Sen's conjectures assert that the height of the potential at $\phi = 0$ is equal to the tension T_{25} of a space-filling D25-brane, and that the physics around $\phi = \phi_0$ doesn't contain open strings.

the local maximum of the effective tachyon potential. There is a local minimum at $\phi = \phi_0$. Note that the left part of the effective potential is poorly understood. It might actually be unbounded; it has been suggested that tachyon condensation on the left is related to closed string tachyon condensation.

Second conjecture. Once the tachyon has condensed to its local minimum, all open string degrees of freedom must disappear.

Indeed, a D-brane is a hyperplane on which the open strings can end. Once it has decayed, there is no place left for the endpoints of the open strings. Only the closed strings survive.

In the particular case of open bosonic string theory, one can formulate a slightly

stronger version of the second conjecture, namely that the stable vacuum of open bosonic string theory should be precisely the perturbative vacuum of closed bosonic string theory.

Third conjecture. Solitonic configurations of the tachyon condensate are D-branes of lower dimensions.

For example, we see from the effective potential (Figure 1-1) that one can have lump configurations, for which the tachyon tends to ϕ_0 far away from the lump. Since around $\phi = \phi_0$ there can be no open strings, these must be localized on the core of the lump, precisely what we expect from a D-brane. The lumps are unstable, in accordance with the fact that all bosonic D-branes are unstable. Let us mention that the tachyon effective potential on a non-BPS D-brane of type IIA or IIB, is even and has two global minima. There, we can therefore have kink solutions that are stable, this is consistent with the fact that a D-brane of one less dimension is BPS.

The first and third conjectures have been proved in the context of Boundary String Field Theory (BSFT) [10, 11, 12]. Unfortunately, this theory only describes the tachyon field without giving any explicit information on the fields of higher mass. But Sen claimed that these conjectures could be verified in the context of open String Field Theory (SFT), a theory of open strings (describing all its degrees of freedom) that is able to describe nonperturbative dynamics, and which we now introduce.

First, let us say that the usual perturbative formulation of string theory is a *first-quantized* theory whose degrees of freedom are fields living on the two-dimensional worldsheet (that we parameterize with (σ, τ)). The worldsheet Polyakov action provides us with the means to calculate any amplitude of *on-shell* external strings. This restriction to on-shell states is due to the fact that only these states are conformally invariant; and conformal invariance is central in perturbative string theory, in that it allows us to map any string diagram with n external legs to a Riemann surface with n punctures. For example, an open string tree diagram can be mapped to a disk, whose boundary is punctured n times; and a closed string tree diagram is mapped to

a punctured sphere. Loop diagrams are mapped to Riemann surfaces of higher genus.

The tachyon condensate, that we will study in much details, involves nonzero vev of not only the tachyon, but also of scalar fields of arbitrarily high masses. The condensate must be Poincaré invariant and thus it must have zero momentum, but since the masses of the condensate's fields are not zero, it cannot be on-shell. And the techniques mentioned above cannot be applied to compute interactions of the condensate, that we need in order to calculate the tachyon effective potential.

To calculate off-shell amplitudes in the first-quantized theory, we would need to keep track of the complete histories of the interactions, and integrate over all of them; a seemingly formidable task. But there is no such problem in usual particle field theory that is done in the *second quantization*, where the degrees of freedom are fields in spacetime. There we can use Feynman rules and propagators to calculate any off-shell diagram. And indeed, it is a second-quantized version of string theory, namely string field theory, that we have to use to calculate off-shell amplitudes. String field theory's fundamental degree of freedom is the string field Φ, a functional of string embeddings $\{X^\mu(\sigma), b(\sigma), c(\sigma)\}$, where b and c are the reparameterization ghosts. For concreteness, we can expand the string field in terms of first-quantized modes; for every vertex operator that appears in the first quantized theory, there corresponds an element in the string field. For example, considering only the tachyon and massless states, the string field of open bosonic string theory starts with

$$|\Phi\rangle = \int d^{26}p \left(\phi(p) + A_\mu(p)\, \alpha_{-1}^\mu + B(p)\, b_{-1}c_0 + \ldots\right) |p\rangle\,,$$

where $|p\rangle$ is the perturbative ground state (the tachyon) with momentum p. The "..." denote the infinitely many fields of arbitrarily high masses that we haven't written here. The formulation of string field theory that we will use in this thesis is Witten's cubic string field theory [13]. It has a Chern-Simons action

$$S = \frac{1}{2}\int \Phi \star Q\Phi + \frac{g}{3}\int \Phi \star \Phi \star \Phi\,,$$

where Q is the BRST operator and g is the open string coupling constant. The symbol

"$\star$" stands for the star-algebra product, defined by the interaction of strings joining by their midpoint. In short, if the right-half of the first string coincides with the left-half of the second, then the $\star$-product of the first and the second string is the string whose left-half is the left-half of the first string, and whose right-half is the right-half of the second string. The $\star$-algebra is not commutative but it is associative. Its explicit expression in terms of the infinitely many first quantized fields is actually very intricate since it mixes fields of all different masses. Indeed, although the equations of motion

$$Q\Phi + g\Phi \star \Phi = 0$$

look very simple in this closed form, we presently don't know any exact nontrivial classical solution.

An approximation technique to solve this equations was proposed in [14]. It is called *level truncation*, and consists of keeping only a finite number of fields in the action, those fields whose mass is lower than a fixed level. The authors of [14] found that physical quantities calculated in the level truncation, converge as the level is increased. They used this method to find a stable vacuum for the open bosonic string; but at that time, D-branes were not yet known, and it was unclear how to interpret the energy of this new vacuum, and what kind of physics to expect around it. Shortly after Sen made its conjectures, Sen and Zwiebach [15] used the same method of level truncation to check the first conjecture. They found that, indeed, the energy gap between the two extrema of the potential, converges to the tension of the D25-brane when the level is increased.

In the next four chapters of this thesis, we use level-truncated cubic open bosonic string field theory to test further Sen's three conjectures for the case of open bosonic string theory. Of course, the bosonic string isn't as interesting as the superstring if one wants to make phenomenological predictions. But it is nevertheless worth studying it for two reasons. First, string field theory calculations are in general much easier in bosonic string theory than is superstring theory; and it is thus a good idea to do research in bosonic string theory, which results we can then try to generalize

to the case of the superstring. The other reason is more speculative; one can imagine that bosonic string theory is linked to the web of M-theory, and that maybe closed tachyon condensation makes it flow to some point in the moduli space of M-theory. The study of this question would probably make use of closed string field theory, and is beyond the scope of this thesis.

The solutions needed to verify Sen's conjectures are all static solutions (either homogeneous or solitonic). But it would be very interesting if we were able to find time dependent solutions describing tachyon condensation. That would help us understand, for example, by which mechanism the open string degrees of freedom freeze when we reach the stable vacuum, or how the rest energy of the D-brane gets dissipated into closed strings. The natural picture that we would expect is that the tachyon rolls to the minimum of its effective potential, and then oscillates around it as it dissipates its energy into radiation of closed strings. Sen has addressed this problem in the context of boundary conformal field theory, and he found that, surprisingly, even if one switches off the coupling to closed strings, the tachyon rolls asymptotically towards the true vacuum without oscillating, and tends to a state of positive energy density and zero pressure, called *tachyon matter* [16, 17, 18]. It would be very interesting to verify this picture in the full string field theory. There, however, the time dependence comes with infinitely many time derivatives, making the problem technically difficult and fundamentally different from an initial value problem. The same kind of time dependence is found in p-adic string theory, a much simpler theory of the open bosonic tachyon. We present, in the last chapter, rolling tachyon solutions of p-adic string theory as well as in Wick-rotated SFT. Our results don't give any evidence for a pressureless tachyon matter.

Outline

In Chapter 2, we calculate the cubic action of open bosonic string field theory describing zero-momentum interactions of up to level 20 between scalars of level 10 or less. These results are used to study the tachyon effective potential and Sen's first conjecture. We show that, when including fields up to level 10, 99.91% of the energy

from the bosonic D-brane tension is canceled in the nonperturbative stable vacuum. We show that the perturbative expansion of the effective tachyon potential has a small but finite radius of convergence, and we find evidence for a critical point in the tachyon effective potential at a small negative value of the tachyon field corresponding to the radius of convergence. Also, we study the branch structure in the effective potential in the vicinity of this point and speculate that the tachyon effective potential could be globally nonnegative. We end this chapter by a summary of recent works, from different authors, that give some nice improvements to some questions studied in this chapter.

In Chapter 3, we address the question of verifying that the tachyonic lump solution of the open bosonic string field theory describing a D-brane represents a D-brane of one lower dimension. For this, we place the lump on a circle of finite radius and develop a variant of the level expansion scheme that allows systematic account of all higher derivative terms in the string field theory action, and gives a calculational scheme that can be carried to arbitrary accuracy. Using this approach, we find lump masses that agree with expected D-brane masses to an accuracy of about 1%. We find convincing evidence that in string field theory the lump representing a D-brane is an extended object with a definite profile.

In Chapter 4, we extend the work of Chapter 3 to lumps of codimension two and we verify that their mass is close to the expected mass of a D-brane of two lower dimensions. We also compare these solutions with codimension two lumps from a pure ϕ^3 theory and from pure tachyonic string field theory (string field theory where we keep only the tachyon and all its derivatives).

In Chapter 5, we show that the absence of any open string state in the true vacuum is guaranteed if the identity $\mathcal{I}$ of the string field theory star-algebra can be written as $\mathcal{I} = QA$, where A is a string field and Q is the BRST charge at the stable vacuum. We use level truncation to find such a string field A, and we find that, to truncation level nine, the Q-exactness of the identity is realized with an accuracy of about 3%. This is in support of Sen's second conjecture. As a by-product, a new and simple expression for the identity string field in terms of Virasoro operators is established.

Finally, in Chapter 6, we address the problem of time dependent solutions of string field theory. We find such solutions in the simpler model of p-adic string theory. This is a nice toy model since both in string field theory and in p-adic string theory the equations of motion involve infinite number of time derivatives. We argue that the initial value problem is qualitatively different from that obtained in the limit of many time derivatives in that the space of initial conditions becomes strongly constrained. We calculate the energy-momentum tensor and study in detail time dependent solutions representing tachyons rolling on the p-adic string theory potentials. For even potentials we find surprising small oscillations at the tachyon vacuum. These are not conventional physical states but rather anharmonic oscillations with a nontrivial frequency–amplitude relation. When the potentials are not even, small oscillatory solutions around the bottom must grow in amplitude without a bound. Open string field theory resembles this latter case, the tachyon rolls to the bottom and ever growing oscillations ensue. We discuss the significance of these results for the issues of emerging closed strings and tachyon matter.

The results described in this thesis have also appeared in several publications during the last three years [19, 20, 21, 22, 23, 24].

Chapter 2

Level truncation and the tachyon in open bosonic string field theory

The appearance of a tachyon in the spectrum of both open and closed bosonic strings has appeared to be a fundamental obstacle to a physical interpretation of these theories since the early days of the dual resonance model. Early work on the subject indicated the possible existence of a more stable nonperturbative vacuum which can be reached by a condensation of the tachyon and other string fields in the open bosonic string theory [1, 14]. At that time, however, the connection between open strings and Dirichlet branes [25] had not yet been realized, so that the significance of the nonperturbative stable vacuum was not widely appreciated.

It was recently pointed out by Sen [9] that the condensation of the tachyon in open bosonic string theory should correspond to the process of annihilation of an unstable D25-brane. The nonperturbative stable vacuum of the open string should simply be the vacuum corresponding to empty space, and the energy difference between the stable and unstable vacua should therefore be given by the mass of the D25-brane. Sen suggested that it should be possible to precisely calculate this energy gap using open string field theory. In fact, it was found over a decade ago by Kostelecky and Samuel that truncating open bosonic string field theory at low mass levels gives a systematic approximation scheme which seems to converge to a finite value for the energy difference between the unstable and stable vacua [14, 26]. Sen and Zwiebach

have carried out a calculation of this type and have shown that including fields up to mass level 4 and interactions up to mass level 8 gives a mass gap of 98.6% of the D25-brane energy. Similar calculations of tachyon condensation have recently been performed in open superstring field theory [27, 28]. The level-truncation approach to string field theory has also been used to study lower-dimensional Dp-branes as solitonic lumps [29, 28]. In all these calculations, truncation of string field theory to the first few levels seems to give a sequence of successively better approximations to nonperturbative physical quantities.

In this chapter we extend the level truncation approach to open bosonic string field theory to include scalar fields of mass levels > 4, following earlier work in [30]. We use the level-truncated theory as a tool for exploring various features of the tachyon and its condensation into a stable vacuum. We compute all terms in the string field theory action involving fields of level less than or equal to 10 and interactions of up to mass level 20. We perform a nonperturbative calculation of the energy gap between the stable and unstable vacua and find that 99.91% of the D25-brane tension is produced in the level (10, 20) truncated theory.

We study the structure of the tachyon effective potential in some detail using the various level-truncated theories. We compute the first 60 coefficients c_n of ϕ^n in the effective tachyon potential in several successive level truncations up to level (10, 20). We find that the effective tachyon potential has a radius of convergence which decreases to an apparently finite asymptotic value as the level number increases. This radius of convergence is substantially smaller than the tachyon value corresponding to the stable vacuum, although the associated singularity is at a negative value of ϕ while the stable vacuum arises at $\phi > 0$. We investigate the branch structure of the tachyon effective potential near the singular point, and use our numerical results to speculate about the behavior of the effective potential beyond this point.

In Section 2.1 we review the level truncation approach to string field theory and outline our calculation of the action up to level (10, 20). In Section 2.2 we use our results to analyze the perturbative expansion of the tachyon effective potential, and in Section 2.3 we discuss the nonperturbative stable vacuum and the branch structure

of the effective tachyon potential.

2.1 Level truncation of string field theory

In this section we briefly review the level truncation approach to string field theory and describe our calculation of interactions between scalar string fields of level ≤ 10. Throughout this chapter we follow the conventions and notation of [14, 30] except for the state associated with the tachyon field that we denote here by $|\Omega\rangle$. This state is given by $|\Omega\rangle = c_1 |0\rangle$, where $|0\rangle$ is the SL(2,$\mathbb{R}$) invariant vacuum.[1] For more detailed reviews of open string field theory see [63, 31].

2.1.1 The scalar potential in open bosonic string field theory

String field theory is described in terms of a string field Φ which contains a component field for every state in the first-quantized string Fock space. For the open bosonic string, a particularly simple string field theory was suggested by Witten [13] in which the action takes the cubic form

$$S = \frac{1}{2\alpha'} \int \Phi \star Q\Phi + \frac{g}{3!} \int \Phi \star \Phi \star \Phi, \tag{2.1}$$

where Q is the BRST operator and $\star$ is the string field theory star product.

In Feynman-Siegel gauge, the string field can be expanded in the form

$$\Phi = \left(\phi + A_\mu \alpha^\mu_{-1} + \frac{1}{\sqrt{2}} B_{\mu\nu} \alpha^\mu_{-1} \alpha^\nu_{-1} + \beta b_{-1} c_{-1} + \cdots \right) |\Omega\rangle \tag{2.2}$$

The expansion (2.2) contains an infinite series of fields. The level of each field in the expansion is defined to be the sum of the level numbers of the creation operators which act on $|\Omega\rangle$ to produce the associated state. Thus, the tachyon is the unique field of level 0, the gauge field A_μ is the unique field of level 1, etc. The states associated

[1] This notation for the tachyon field is different from the notation used in [19], where the content of this chapter was originally published. It has been changed here so that it is consistent throughout all of this thesis. This is the only notation that has been changed from the published versions of the work presented in this thesis.

with these fields are all in the subspace $\mathcal{H}$ of the full string Hilbert space containing states of ghost number 1.

In this chapter we are interested in the behavior of the tachyon field ϕ. In particular, we wish to study questions related to the appearance of a Lorentz-invariant stable vacuum in the theory when the tachyon and other scalar fields acquire nonzero condensates. Because all the questions we will address here involve Lorentz-invariant phenomena, we can restrict attention to scalar fields in the string field expansion. We write the string field expansion in terms of scalar fields as

$$\Phi = \sum_{i=1}^{\infty} \psi^i |s_i\rangle \tag{2.3}$$

where $|s_i\rangle$ are all the scalar states in $\mathcal{H}$. The scalar states at levels 0 and 2 are

$$\begin{aligned} |s_1\rangle &= |\Omega\rangle \\ |s_2\rangle &= \alpha_{-1} \cdot \alpha_{-1} |\Omega\rangle \\ |s_3\rangle &= b_{-1} c_{-1} |\Omega\rangle \end{aligned}$$

The associated scalar fields can be related to the fields in the expansion (2.2) through

$$\begin{aligned} \phi &= \psi^1 \\ B_{\mu\nu} &= \sqrt{2} \eta_{\mu\nu} \psi^2 \\ \beta &= \psi^3 \end{aligned}$$

We will often refer to the tachyon field ψ^1 simply as ϕ. (Note that a superscript on ψ will always indicate a field index while a superscript on ϕ indicates an exponent.) For the calculations of interest here, contributions from scalar fields of odd level cancel due to a twist symmetry [14, 15]. Thus, we need only consider scalar fields of even level number. All scalar states at levels 0, 2, 4 and 6 are listed in Appendix A.1.

An explicit algorithm for computing the terms in the string field theory action (2.1) using the oscillator modes of the matter fields and ghost fields of the bosonic conformal

field theory was given in [32, 33, 34]. The aspects of this formalism needed for the computations in this chapter are reviewed in [30]. The quadratic term evaluated on a state $|s\rangle$ is simply

$$\int |s\rangle \star Q|s\rangle = \langle s|c_0 \left(\alpha' p^2 + \frac{1}{2}M^2\right)|s\rangle \tag{2.4}$$

where $\frac{1}{2}M^2$ is the level of s minus 1, p is the momentum of the state s, $\langle s|$ is the BPZ dual state to $|s\rangle$ produced by acting with the conformal transformation $z \to -1/z$, and the dual vacuum satisfies $\langle\Omega|c_0|\Omega\rangle = 1$. The cubic interaction terms in the string field action can be described in terms of Witten's vertex operator V through

$$\int \Phi \star \Phi \star \Phi = \langle V|(\Phi \otimes \Phi \otimes \Phi) \tag{2.5}$$

where V is a state in the tensor product space $\mathcal{H}^* \otimes \mathcal{H}^* \otimes \mathcal{H}^*$, given in terms of oscillator modes by

$$\begin{aligned}\langle V| = \delta(p_{(1)} + p_{(2)} + p_{(3)}) \left(\langle\Omega|c_0^{(1)} \otimes \langle\Omega|c_0^{(2)} \otimes \langle\Omega|c_0^{(3)}\right) \times \\ \times \exp\left(\frac{1}{2}\alpha_n^{(r)\mu} N_{nm}^{rs} \eta_{\mu\nu} \alpha_m^{(s)\nu} + c_n^{(r)} X_{nm}^{rs} b_m^{(s)}\right).\end{aligned} \tag{2.6}$$

The coefficients N_{nm}^{rs}, X_{nm}^{rs} can be calculated from formulae in [32, 33, 34]; explicit tables of these coefficients for $n, m \leq 8$ are given in [30].

Using the equations (2.4, 2.5) for the quadratic and cubic terms in the string field theory action, the potential for the zero momentum scalar fields in $\mathcal{H}$ can be written as

$$V = \sum_{i,j} d_{ij}\psi^i\psi^j + g\kappa \sum_{i,j,k} t_{ijk}\psi^i\psi^j\psi^k \tag{2.7}$$

where g is the string coupling constant and

$$\kappa = \frac{3^{7/2}}{2^7}.$$

has been chosen so that $t_{111} = 1$. Throughout the chapter we set $\alpha' = 1$. The

coefficients d_{ij}, t_{ijk} can be explicitly computed for any given values of the indices. The action can be truncated by only including fields up to a fixed level L and interactions including terms whose total level does not exceed another fixed value I. In [14], the complete action with $(L, I) = (2, 6)$ was calculated and shown to be

$$\begin{aligned} V &= -\frac{1}{2}\phi^2 + 26(\psi_2)^2 - \frac{1}{2}(\psi_3)^2 \\ &\quad +\kappa g\left[\phi^3 + \phi^2\left(-\frac{5\cdot 26}{9}\psi_2 - \frac{11}{9}\psi_3\right)\right. \\ &\qquad +\phi\left(\frac{4\cdot 7\cdot 13\cdot 83}{3^5}(\psi_2)^2 + \frac{4\cdot 5\cdot 11\cdot 13}{3^5}\psi_2\psi_3 + \frac{19}{3^4}(\psi_3)^2\right) \\ &\qquad -\frac{2^3\cdot 3\cdot 7\cdot 13\cdot 41\cdot 73}{3^9}(\psi_2)^3 - \frac{2^2\cdot 7\cdot 13\cdot 11\cdot 83}{3^8}(\psi_2)^2\psi_3 \\ &\qquad \left.-\frac{2\cdot 5\cdot 13\cdot 19}{3^7}\psi_2(\psi_3)^2 - \frac{1}{3^4}(\psi_3)^3\right] \end{aligned}$$

(Note that we have lowered indices on the fields ψ^2, ψ^3 for clarity.) Results using the complete action with $(L, I) = (4, 12)$ were described in [26]. In [15] calculations were performed at level $(L, I) = (4, 8)$.

With the help of the symbolic manipulation program *Mathematica*, we have calculated all terms in the action up to levels $(L, I) = (10, 20)$. There are 252 fields at levels ≤ 10 and 138,202 distinct cubic interaction terms between fields whose total level is ≤ 20, so it is clearly impractical to reproduce the full action here. It is worth mentioning, however, some points which help to simplify the calculation.

One significant simplification arises from the fact that the matter and ghost fields almost completely decouple in the action. In fact, it is clear from (2.6) that this decoupling is complete in the cubic terms, and from (2.4) that the only coupling in the quadratic terms arises from the appearance of the total level of the scalar field in question, including the levels of both the matter and ghost oscillators needed to produce the state. Because of this decoupling, we find that it is convenient to decompose the Hilbert space into the matter and ghost Hilbert spaces

$$\mathcal{H} = \mathcal{H}_{\text{mat}} \otimes \mathcal{H}_{\text{gh}} \tag{2.8}$$

and to separately enumerate the scalar fields in the matter and ghost sectors $|\eta_m\rangle \in \mathcal{H}_m, |\chi_g\rangle \in \mathcal{H}_g$. The first few states in each of these component Hilbert spaces are

$$\begin{aligned} |\eta_1\rangle = |\chi_1\rangle &= |\Omega\rangle \\ |\eta_2\rangle &= \alpha_{-1} \cdot \alpha_{-1} |\Omega\rangle \\ |\chi_2\rangle &= b_{-1} c_{-1} |\Omega\rangle \end{aligned}$$

Given the decomposition (2.8) of the Hilbert space we can write each of the scalar fields $|s_i\rangle$ in $\mathcal{H}$ as a tensor product

$$|s_i\rangle = |\eta_{m(i)}\rangle \otimes |\chi_{g(i)}\rangle \tag{2.9}$$

Thus, for example, $m(1) = 1$ and $g(1) = 1$. A list of matter and ghost scalars up to level 6 is given in Appendix A.2, and the decomposition of the scalars in $\mathcal{H}$ into matter and ghost factors is given in Appendix A.1 for the scalars of level ≤ 6.

From the decomposition into matter and ghost components, we can now write the quadratic and cubic coefficients (2.4,2.5) as

$$\begin{aligned} d_{ij} &= \frac{2(\text{level}(i) - 1)}{(\text{level}(m(i)) - 1) \cdot (\text{level}(g(i)) - 1)} d^{\text{mat}}_{m(i)m(j)} d^{\text{gh}}_{g(i)g(j)} \\ t_{ijk} &= t^{\text{mat}}_{m(i)m(j)m(k)} t^{\text{gh}}_{g(i)g(j)g(k)} \end{aligned} \tag{2.10}$$

where $d^{\text{mat}}_{mn}, d^{\text{gh}}_{gh}, t^{\text{mat}}_{mnp}$ and t^{gh}_{ghj} are the quadratic and cubic coefficients in the matter and ghost sectors, and where $\text{level}(i) = \text{level}(g(i)) + \text{level}(m(i))$ indicates the level of the state $|s_i\rangle$. Quadratic and cubic coefficients of the matter and ghost scalars appearing in scalar fields up to level 6 are tabulated in Appendix A.3. From these coefficients and (2.10) one can reproduce the entire string field theory action for zero momentum scalars up to level 6 fields and level 16 interactions. We have carried out the calculation of all matter and ghost interactions up to fields of level 10 and interactions of level 20. While we do not reproduce here the complete results of this calculation, we will use these results to study questions of physical interest in the

remainder of the chapter.

We end this section with a brief discussion of the approach used in [15], in which a reduced Hilbert space of background-independent fields was used. It was pointed out in [9] that it is possible to truncate the Hilbert space $\mathcal{H}$ in a consistent fashion by considering the subspace $\mathcal{H}_1$ obtained by considering only those states produced by acting with the ghost fields b, c and the Virasoro generators $L_{-n}, n \geq 2$ associated with the stress tensor of the matter fields. In the stable vacuum of the theory, only scalar fields in $\mathcal{H}_1$ acquire nonzero expectation values. At level 4 and above, the number of scalars in $\mathcal{H}_1$ is less than the number of scalars in $\mathcal{H}$, so that particularly when the level number becomes very large the effective action for the level-truncated theory is significantly simplified by restricting attention to the truncated Hilbert space. To compare the number of scalars in $\mathcal{H}$ at a fixed level n, which we denote h_n, with the number of scalars in $\mathcal{H}_1$, which we denote h_n^1, we can write generating functions

$$f(x,y) = \prod_{p=2}^{\infty} \frac{1}{(1-x^p)^{\lfloor \frac{p}{2} \rfloor}} \prod_{q=1}^{\infty} (1+x^q y)(1+\frac{x^q}{y}) = \sum_{n,m} h_{n,m} x^n y^m \qquad (2.11)$$

$$f_1(x,y) = \prod_{p=2}^{\infty} \frac{1}{(1-x^p)} \prod_{q=1}^{\infty} (1+x^q y)(1+\frac{x^q}{y}) = \sum_{n,m} h^1_{n,m} x^n y^m \qquad (2.12)$$

in terms of which

$$h_n = h_{n,0}$$
$$h_n^1 = h_{n,0}^1$$

The number of scalars in $\mathcal{H}$ and $\mathcal{H}_1$ at each even level up to $n = 20$ is tabulated in Table 2.1. Up to the level 10 fields we consider in this chapter, the difference between

n	0	2	4	6	8	10	12	14	16	18	20
h_n	1	2	7	21	60	161	415	1021	2432	5620	12639
h_n^1	1	2	6	17	43	102	231	496	1027	2060	4010

Table 2.1: The number of scalars h_n and h_n^1 in $\mathcal{H}$ and $\mathcal{H}_1$ at level n

$\mathcal{H}$ and $\mathcal{H}_1$ is less than a factor of 2, so that there is no extraordinary advantage to be gained by using the smaller Hilbert space. Clearly, however, as the level becomes much larger than 10, the reduced size of the truncated Hilbert space would make explicit calculations much easier, assuming that calculations in $\mathcal{H}_1$ could be done just as efficiently as corresponding calculations in $\mathcal{H}$.

In our calculations we have worked with the complete oscillator Hilbert space $\mathcal{H}$ and not with $\mathcal{H}_1$. The main reason for this is that at this point no method has been developed for computing cubic interactions between fields in $\mathcal{H}_1$ which is as systematic and efficient as the oscillator method described above for computing cubic interactions between fields in $\mathcal{H}$. It is possible to calculate cubic interactions in $\mathcal{H}_1$ by computing the relevant correlation functions in the open bosonic string theory [63], but this method is somewhat more complicated than the straightforward oscillator approach. Of course, the interactions in $\mathcal{H}_1$ can always be computed by rewriting each state in terms of the oscillator basis and then using (2.6), but this requires just as much work as the computation directly in the oscillator basis. In any case, the results in Appendix A.3 for fields up to level 6 are given in the oscillator basis of $\mathcal{H}$; these interactions can easily be translated into an action for fields in $\mathcal{H}_1$ by explicitly writing the Virasoro generators L_{-n} in terms of the oscillator basis.

2.2 Tachyon effective potential: perturbation expansion

Given the (rational) coefficients in the scalar potential (2.7) truncated at level (L, I), we can perform a number of interesting calculations. In particular, we can study the effective potential of the tachyon field and identify the stable vacuum or vacua of the theory.

An effective potential for the tachyon field ϕ can be determined by starting with the complete set of terms in the cubic potential (2.7) truncated at level (L, I), fixing a value of $\phi = \psi^1$, solving for all fields $\psi^i, i > 1$, and plugging back into the potential

to rewrite it as a function of ϕ. If there are N scalar fields involved, this means that we need to solve a system of $N-1$ simultaneous quadratic equations. In principle there are many solutions of this system of equations, but if we are interested in the branch of the solution on which all fields vanish when $\phi = 0$, it is easy to determine which branch to choose for each of the quadratic equations (an explicit example of this choice is described below). Clearly when N becomes large it is impractical to find an exact analytic form for the effective tachyon potential. Various numerical methods can be used to approximate the effective potential arising from integrating out a large number of fields; for example, a numerical analysis of the effective potential was performed in [14] using the level 2 action with the two fields ψ^2, ψ^3 integrated out. In Section 2.3.2 we extend these results by analyzing the structure of the effective potential at levels 4 and 6 using numerical methods.

Another approach to studying the effective potential, which we consider in this section, is to determine the terms in a power series expansion of the potential around the unstable vacuum $\phi = 0$. In Section 2.2.1 we describe an algebraic method for efficiently summing all diagrams contributing to the ϕ^n term in the effective potential. In Section 2.2.2 we summarize the results of our calculation of these coefficients up to $n = 60$ at level $L \leq 10$, and discuss the implications of these results. In particular, we find that the power series expansion of the tachyon effective potential seems to have a radius of convergence which approaches a finite but nonzero value as the level number is increased. As we will discuss in the next section, the stable vacuum of the theory lies outside the radius of convergence of this power series.

2.2.1 Summing planar diagrams

In the vicinity of the unstable vacuum $\psi^i = 0$ we can perform a power series expansion of the effective tachyon potential

$$V(\phi) = \sum_{n=2}^{\infty} c_n (g\kappa)^{n-2} \phi^n = -\frac{1}{2}\phi^2 + g\kappa\phi^3 + \cdots \tag{2.13}$$

There are a number of ways in which we might try to calculate the coefficients c_n in this expansion. Given a cubic potential (2.7) for N fields, one approach to determining the coefficients c_n would be to write the quadratic equations of motion for each of the $N-1$ fields which we wish to integrate out, expand each field $\psi^i, i > 1$ as a formal power series in ϕ, and solve a linear system of equations at each order in ϕ, plugging the final results back into the cubic potential. We will not directly use this method, although it is technically equivalent to the graphical approach we will use.

An alternative approach to calculating the coefficients in the effective tachyon potential is to treat (2.7) as the action for a 0-dimensional field theory and to use Feynman diagrams to sum all terms contributing to a given coefficient c_n. This method was used by Kostelecky and Samuel in [14] to calculate the level 2 and level 4 approximations to the quartic coefficient c_4, which they had calculated exactly in [35]. They found that at level 2, 72% of the exact coefficient is generated, and at level 4 this increases to 84%. This calculation was extended in [30], where contributions from all fields up to level 20 were included, generating 96-97% of the exact term c_4.

We can use the exact cubic terms we have found up to level (10, 20) as cubic interaction vertices in Feynman diagrams which we can then sum to find the contributions to each of the coefficients c_n. Because the combinatorics of the Feynman diagrams grows exponentially, we will find it useful to use an algebraic simplification to expedite the summation over graphs. The essence of the simplification we will use is that because we are summing over planar tree graphs, we can write a recursion relation relating the set of graphs G_k with k external ϕ edges and single external ψ^i edge to the sets of graphs $G_{k'}$ with $k' < k$. This relationship is indicated schematically by

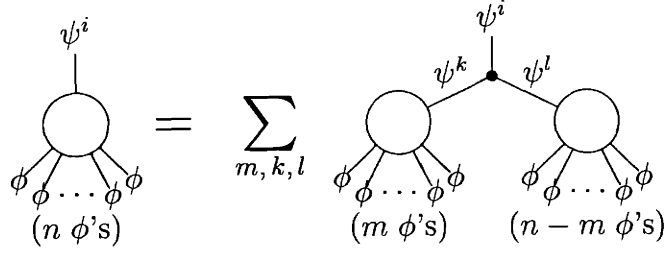

Algebraically, we can define an N-dimensional vector v_n^i for each n, representing the summation over all graphs with n external ϕ edges and a single external ψ^i (including the propagator for ψ). We then have

$$\begin{aligned} v_1^i &= \delta_1^i \\ v_n^i &= \frac{3}{2}\sum_{m=1}^{n-1} d^{ij}\, t_{jkl}\, \hat{v}_m^k \hat{v}_{n-m}^l \end{aligned} \tag{2.14}$$

where d^{ij} is the inverse matrix to d_{ij} and

$$\hat{v}_n^i = \begin{cases} 0, & i = 1 \text{ and } n > 1 \\ v_n^i, & \text{otherwise} \end{cases} \tag{2.15}$$

has been defined to project out internal ϕ edges. In terms of the vectors v_n^i, the coefficients c_n are given by

$$c_n = \frac{1}{n} v_{n-1}^1 \tag{2.16}$$

In fact, the recursion relations (2.14) precisely encode the relations we would find between the coefficients of the fields ψ^i expanded in powers of ϕ if we used the power series approach to solving the $N-1$ quadratic equations term by term in ϕ as described in the first paragraph of this subsection. The terms v_n^i are precisely the coefficients of ϕ^n in the expansion of the field ψ^i.

In any case, using this recursive formalism, the computation of c_n becomes a polynomial-time algorithm taking time of order $\mathcal{O}(N^3 n^2)$, instead of an exponentially hard algorithm such as we would encounter if we tried to directly sum over all Feynman diagrams. It may be helpful to illustrate this approach with a simple example. Consider a single massive field ψ which couples to ϕ only through a term of the form $\phi^2\psi$ in the potential

$$V = -\frac{1}{2}\phi^2 + g\kappa\phi^3 + \frac{1}{2}\psi^2 + g\kappa\left(\frac{\gamma}{6}\psi^3 + \beta\phi^2\psi\right). \tag{2.17}$$

In this case we can explicitly solve for ψ

$$\psi = \frac{1}{g\kappa\gamma}\left(-1 + \sqrt{1 - 2g^2\kappa^2\beta\gamma\phi^2}\right) \tag{2.18}$$

As mentioned above, we have chosen the branch of the square root which gives $\psi = 0$ when $\phi = 0$. Substituting (2.18) into (2.17) gives us the effective potential for ϕ on the branch containing the unstable vacuum

$$V = -\frac{1}{2}\phi^2 + g\kappa\phi^3 + \frac{1}{3g^2\kappa^2\gamma^2}\left(1 - 3g^2\kappa^2\beta\gamma\phi^2 - (1 - 2g^2\kappa^2\beta\gamma\phi^2)^{3/2}\right) \tag{2.19}$$

The coefficients in a power series expansion of this potential are

$$c_{2n} = -\frac{(2n-5)!!}{n!}\beta^n\gamma^{n-2} \tag{2.20}$$

for $2n \geq 4$.

To derive these coefficients using the recursive formalism (2.14) we need the coefficients

$$\begin{aligned} d_{11} &= -\frac{1}{2} & t_{112} &= \frac{\beta}{3} \\ d_{22} &= \frac{1}{2} & t_{222} &= \frac{\gamma}{6} \end{aligned}$$

which give the recursion relations

$$\begin{aligned} v_1^1 &= 1 \\ v_n^1 &= -2\beta\sum_{m=1}^{n-1}\hat{v}_m^1\hat{v}_{n-m}^2 = -2\beta v_{n-1}^2, \qquad n > 1 \\ v_1^2 &= 0 \\ v_2^2 &= \beta\hat{v}_1^1\hat{v}_1^1 = \beta \\ v_n^2 &= \frac{\gamma}{2}\sum_{m=1}^{n-1}v_m^2 v_{n-m}^2, \qquad n > 2. \end{aligned}$$

We begin by solving for v_n^2. These terms clearly vanish unless n is even. Defining

$$w_m = v_{2m}^2 \tag{2.21}$$

we have

$$\begin{aligned} w_1 &= \beta \\ w_m &= \frac{\gamma}{2}\sum_{k=1}^{m-1} w_k w_{m-k}. \end{aligned} \tag{2.22}$$

Defining a generating function

$$f(x) = \sum_{m=1}^{\infty} w_m x^{2m} \tag{2.23}$$

The equations (2.22) are equivalent to the quadratic equation

$$f = \frac{\gamma}{2} f^2 + \beta x^2 \tag{2.24}$$

with solution

$$f = \frac{1}{\gamma}(1 - \sqrt{1 - 2\beta\gamma x^2}) = \sum_{m=1}^{\infty} \frac{(2m-3)!!}{m!}\beta^m \gamma^{m-1} x^{2m} \tag{2.25}$$

So

$$c_{2n} = \frac{1}{2n}(-2\beta)w_{n-1} = -\frac{(2n-5)!!}{n!}\beta^n \gamma^{n-2} \tag{2.26}$$

in agreement with (2.20).

2.2.2 Coefficients of the effective tachyon potential

We have used the method described in the previous subsection to calculate the coefficients c_n in the perturbative expansion of the effective tachyon potential around the unstable vacuum for $n \leq 60$ in each of the level-truncated theories up to (10, 20). In Table 2.2 we have tabulated the successive approximations to c_n for a representative

set of values of n at various levels. There are several observations we can make based

n	(2, 6)	(4, 12)	(6, 18)	(8, 20)	(10, 20)
3	1	1	1	1	1
4	-1.2592	-1.4724	-1.5562	-1.6004	-1.6276
5	5.9478	7.8370	8.6398	9.0756	9.3479
6	-27.909	-43.529	-50.768	-54.816	-57.353
7	143.67	269.25	333.83	371.36	395.12
8	-786.81	-1777.5	-2346.7	-2691.9	-2913.4
9	4513.9	12323.	17345.	20529.	22606.
10	$-26845.$	$-88690.$	$-133179.$	$-162693.$	$-182299.$
20	$-4.0710 \cdot 10^{12}$	$-9.2769 \cdot 10^{13}$	$-2.6957 \cdot 10^{14}$	$-4.5477 \cdot 10^{14}$	$-6.0780 \cdot 10^{14}$
30	$-1.3415 \cdot 10^{21}$	$-2.1308 \cdot 10^{23}$	$-1.2050 \cdot 10^{24}$	$-2.8154 \cdot 10^{24}$	$-4.4920 \cdot 10^{24}$
40	-6.017310^{29}	$-6.6758 \cdot 10^{32}$	$-7.3563 \cdot 10^{33}$	$-2.3817 \cdot 10^{34}$	$-4.5372 \cdot 10^{34}$
50	$-3.1889 \cdot 10^{38}$	$-2.4732 \cdot 10^{42}$	$-5.3126 \cdot 10^{43}$	$-2.3840 \cdot 10^{44}$	$-5.4231 \cdot 10^{44}$

Table 2.2: Level truncation approximations to coefficients c_n in effective tachyon potential

on these results. In [30] successive approximations to the coefficient c_4 were computed using fields at up to level 20. It was found that while the level truncation method gives a monotonic sequence of approximations which seem to converge to the known exact value for this coefficient $c_4 \approx -1.75$, the convergence to the asymptotic value is fairly slow. For c_4, the contribution from the set of graphs including at least one field of level k but no fields of level $k+1$ decreases as k increases. The same is true for successive approximations to c_n for small n, but as n increases we find that at $n = 8$, the contribution from graphs with some fields of level 4 exceeds that of graphs with only fields of level 2. At $n = 15$, the contribution from graphs with some fields of level 6 exceeds that of graphs with fields of level at most 4. The corresponding thresholds where fields of levels 8 and 10 dominate the contributions from lower levels are $n = 26$ and $n = 43$ respectively. The fact that higher level fields become more relevant for higher order terms in the effective potential is a natural consequence of the trade-off between the exponential growth in the number of diagrams contributing to c_n and the suppression of higher order diagrams by $(g\kappa)^{n-2}$. From this behavior, however, we see that for large n it will be necessary to include fields of increasingly

high level in order to have a good approximation to the coefficients c_n.

One interesting question which we can explore using our results for the coefficients c_n is the radius of convergence of the power series expansion of the effective potential after truncating at a fixed level. Because of the square root branch cuts which arise from the quadratic equations of motion for the fields, at some finite value of ϕ the effective potential becomes singular for any given level truncation. For example, the effective potential arising from (2.17) has a radius of convergence $r_c = 1/(g\kappa\sqrt{2\beta\gamma})$, which is manifest in (2.19) and which can be seen from the asymptotic form of the coefficients $c_{2n} \sim \alpha n^{\eta}(\sqrt{2\beta\gamma})^{2n}$ where α, η are numerical constants. It was found in [14] that after truncation at level 2, there is a singularity at $-\phi = r_c \approx 0.35/g$. This radius of convergence can be seen from the coefficients of the effective potential in the level 2 truncated theory, which for large n go as

$$|c_n| \sim \alpha n^{\eta} \frac{1}{(g\kappa r_c)^n} \tag{2.27}$$

A graph of $(\ln|c_n|)/n$ as a function of n is shown for each level truncation in Figure 2-1. The asymptotic value of $(\ln|c_n|)/n$ gives the (logarithm of the inverse of the)

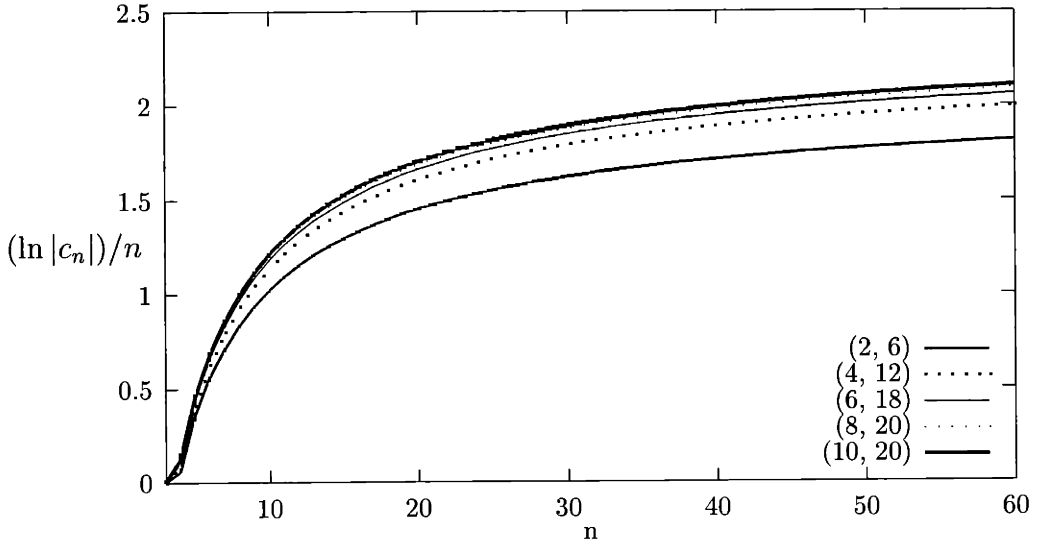

Figure 2-1: $(\ln|c_n|)/n$ for coefficients c_n in effective tachyon potential in different level truncations

radius of convergence of the effective potential at each level. It is clear from the graph that this radius of convergence is decreasing and seems to be approaching a nonzero limiting value. By matching the c_n trajectories to a 3-parameter family of functions of n of the form (2.27) we can find a close approximation to the radius of convergence at each of the levels we have computed. Table 2.3 shows the approximate radius of convergence at each level; we see that in the limiting theory the radius of convergence approaches something like

$$r_c \approx 0.25/g\,. \tag{2.28}$$

Because the signs of the coefficients c_n are alternating, this corresponds to a singularity in the effective potential at $g\phi \sim -0.25$. We study the behavior of the effective potential in the vicinity of this singularity in more detail in Section 2.3.2.

level	(2, 6)	(4, 12)	(6, 18)	(8, 20)	(10, 20)
gr_c	≈ 0.345	≈ 0.283	≈ 0.265	≈ 0.256	≈ 0.252

Table 2.3: Approximate radius of convergence of effective potential in different level truncations

From this analysis of the perturbative effective potential using string field theory we have found several things. First, we find that we can in principle determine any coefficient in the perturbative expansion of the effective tachyon potential to an arbitrary degree of accuracy with a finite calculation in string field theory, but that the size of the calculation needed to determine the coefficients c_n increases significantly as n increases. Second, we have found that the resulting effective potential has a radius of convergence on the order of (2.28). As we will discuss in the next section, the stable vacuum of the theory lies well outside this radius, near $\phi \approx 1.1/g$. It is tempting to conclude from this that, even in principle, the existence and structure of the stable vacuum of the theory are fundamentally nonperturbative phenomena.

2.3 The true vacuum and other nonperturbative features

The appearance of a stable vacuum in the open bosonic string field theory was first shown by Kostelecky and Samuel in [14]. They found the vacuum in the $(2, 6)$ level-truncated theory. In later work, Kostelecky and Potting extended this analysis to the $(4, 12)$ level-truncated theory and reported that the energy density and the values of the scalar fields in the new vacuum both seemed to be rapidly converging as the level number was increased. In [9], Sen argued that the energy difference between the false and true vacua should precisely correspond to the tension of the bosonic D25-brane. Strong evidence for this conclusion was given by Sen and Zwiebach in [15], where they showed that at level $(4, 8)$ the energy gap between the stable and unstable vacua was 98.64% of the D-brane energy.

In this section we use our results for the level-truncated string field action to compute some nonperturbative features of the open bosonic string. In Section 2.3.1 we determine the values of the scalar fields and the total energy of the system in the stable vacuum including fields of up to level 10. At level (10, 20) we find that the energy gap between the stable and unstable vacua corresponds to 99.91% of the D25-brane energy. In Section 2.3.2 we study the effective potential of the tachyon, focusing on the branch structure of the effective potential in the region $\phi < 0$.

2.3.1 The stable vacuum

In order to find the stable vacuum of the level-truncated string field theory action in the zero momentum sector it is necessary to solve a system of N coupled quadratic equations, where N is the number of scalar string fields involved. In general, as N becomes large it is difficult to rapidly solve such a system of equations to a high degree of precision. Because we know which branch of each quadratic equation the physical solution lies on, however, we can use an iterative approximation algorithm to rapidly converge on the true vacuum.

As discussed in Section 2.2, the branch of the solution for each of the N quadratic equations arising from the level-truncated string field theory action is determined by the condition that the stable vacuum lies on the same branch as the unstable vacuum which has all fields vanishing. Thus, the choice of branch for each field is dictated by the sign of the quadratic term in the string field action. For most fields ψ^i, therefore, the value of the field can be expressed in terms of the remaining fields $\psi^j, j \neq i$ through

$$\psi^i = \frac{-b + \text{sign}(d_{ii})\sqrt{b^2 - 4ac}}{2a} \tag{2.29}$$

where

$$\begin{aligned} a &= 3t_{iii} \\ b &= \sum_{j\neq i} 6t_{iij}\psi^j + 2d_{ii} \\ c &= \sum_{j,k\neq i} 3t_{ijk}\psi^j\psi^k + \sum_{j\neq i} 2d_{ij}\psi^j \end{aligned} \tag{2.30}$$

There are some exceptions to this general rule, however. For the tachyon $\phi = \psi$ we choose the + branch of the square root even though the kinetic term is negative. In addition, for most fields with ghost excitations the quadratic term in the action is off-diagonal. For example, the level 4 fields ψ^8, ψ^{10} are coupled through the quadratic term $d_{8\,10} = -3/2$. For fields such as this we use the equation of motion for field ψ^i to solve for the dual field $\tilde{\psi}^i$ which has ghost and antighost modes exchanged through $c_{-n} \leftrightarrow b_{-n}$.

We have used (2.29, 2.30) to solve iteratively for the stable vacuum. We begin by solving (2.29) for all fields ψ^i, using zero for all fields appearing on the RHS. We then insert the first-round solutions for the fields back on the RHS to solve again for all the ψ^i, and repeat this process many times. This algorithm is numerically very stable near the nonperturbative vacuum and converges quite rapidly to a simultaneous solution of all N equations. At level 6, for example, including all interactions up to level 18, after 30 rounds of this procedure the energy stabilizes to 10 digits, and after 50 rounds the values of all fields stabilize to 10 digits.

In the units we are using here, the tension of the bosonic D25-brane is [9]

$$T_{25} = \frac{1}{2\pi^2 g^2} \tag{2.31}$$

In Table 2.4 we have tabulated the results of our calculation of the exact vacuum in the theory truncated at various levels. The value of the tachyon is given in units of

level	$g\langle\phi\rangle$	V/T_{25}
(0, 0)	0.91236	-0.68462
(2, 4)	1.08318	-0.94855
(2, 6)	1.08841	-0.95938
(4, 8)	1.09633	-0.98640
(4, 12)	1.09680	-0.98782
(6, 12)	1.09602	-0.99514
(6, 18)	1.09586	-0.99518
(8, 16)	1.09424	-0.99777
(8, 20)	1.09412	-0.99793
(10, 20)	1.09259	-0.99912

Table 2.4: Tachyon VEV and vacuum energy in stable vacua of level-truncated theory

$1/g$ (with $\alpha' = 1$), and the vacuum energy difference from the unstable vacuum is given as a proportion of the D25-brane tension. The results at levels (2, 4) and (2, 6) agree with those of [14], and the results at level (4, 8) agree with [15].

We see from Table 2.4 that at level $(10, 20)$ the energy gap between the unstable and stable vacua is 99.91% of the D25-brane tension. This seems to affirm the prediction of Sen in [9] beyond any reasonable doubt. It is interesting to note that the error in the vacuum energy $(1 + V/T_{25})$ is multiplied by approximately $1/3 \approx \kappa$ as each new level is added. It would be nice to have a theoretical explanation for this rate of convergence.

In [14] it was found that the vacuum energy and tachyon expectation values change very little between the (2, 4) and (2, 6) level truncations. In [15] a calculation was performed at level (4, 8) giving 98.6% of the D-brane tension. The improvement on this result given by including level 10 and 12 interactions between level 4 fields is fairly small. We have found that this pattern persists at higher level. The results at

level (6, 18) are not very different from those found at level (6, 12), and the results at level (8, 20) are very close to those at level (8, 16). If, however, we drop cubic interactions at the same level as the quadratic interactions at that level, for example by truncating all cubic interactions to level (6, 6), the energy of the stable vacuum varies much more wildly and can even decrease below $-T_{25}$. For this reason, we do not think that it would be useful to consider including higher level fields unless the level of cubic interactions calculated could be increased to at least twice the level number. Using our rather inefficient program it would take a significant amount of computer time to go to level (12, 24) on a standard desktop machine. We discuss in the last section the prospects for continuing these numerical studies to higher levels of truncation of the full theory.

As we can see from Table 2.4, the expectation value of the tachyon in the stable vacuum converges fairly quickly as the level number is increased. The same is true of all the scalar fields; in Appendix A.1 the values of the scalar fields at levels ≤ 6 are given for the level $(4, 12)$, $(6, 18)$ and $(10, 20)$ truncations. The tachyon field itself converges to a value near

$$g\langle\phi\rangle \approx 1.09 \tag{2.32}$$

In [15] Sen and Zwiebach observed that the level 2 fields with canonical normalization

$$\begin{aligned} u &= -\psi^3 \\ v &= \frac{1}{2\sqrt{13}}\psi^2 \end{aligned}$$

take almost identical expectation values in the level $(4, 8)$ truncation. This led these authors to conjecture that in the exact theory these fields would take identical expectation values, possibly due to some hidden symmetry in the theory. Checking this relationship in the vacua of the higher level truncations, we find that this conjecture is not supported. While at level $(4, 8)$ these fields differ by about 0.1%, at level $(10, 20)$ the difference has grown to over 5%. The values of these fields in the different level-truncated vacua are graphed in Figure 2-2, using the value $g = 2$ to conform with

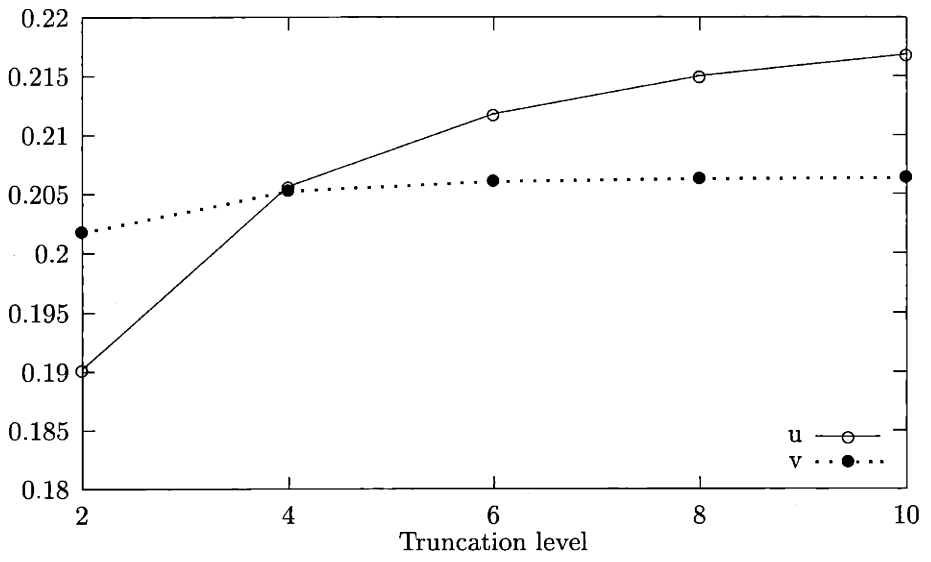

Figure 2-2: Expectation values of fields $u = -\psi^3$ and $v = \psi^2/\sqrt{52}$ for $g = 2$ in different level truncations

the conventions of [15]. The failure of this equality to hold in the asymptotic theory indicates that it may be more difficult than previously thought to implement the suggestion made in [15] of finding an exact solution for the nonperturbative vacuum in the full theory using a hidden symmetry relating fields of this type.

As a check on our results, we can verify that the vacuum expectation values of the fields ψ^i are such that the nonperturbative vacuum lies in the truncated Hilbert space H_1 described in [9]. For example, the level 4 fields should obey the linear relation

$$\langle\psi^4\rangle - 2\langle\psi^5\rangle - 4\langle\psi^6\rangle = 0 \tag{2.33}$$

in the vacuum. We have checked this relation and other analogous relations for higher level fields and find that they are satisfied up to the level of accuracy (10 significant digits) to which we have calculated the vacuum expectation values.

Now that we have identified the stable vacuum of the theory after truncating at levels up to (10, 20), a natural next step is to investigate the structure of the theory around this stable vacuum. The stable vacuum should correspond to the empty vacuum of the closed bosonic string theory, with modes corresponding to the open

string fields on the D25-brane decoupling from the theory. Of particular interest in this regard is the fate of the U(1) vector field A^μ on the brane [36, 37, 38]. Some progress in understanding the structure of the theory around the stable vacuum was made in [14]. It would be interesting to study this question further and to investigate the spectrum of modes around the stable vacuum using the more detailed picture we have given of the expectation values of the scalar string fields in this vacuum. We leave these questions to further work.

2.3.2 Effective tachyon potential

In Section 2.2.2 we studied the effective potential of the tachyon through its power series expansion around the unstable vacuum $\psi^i = 0$. We found that the perturbation series had a finite radius of convergence in each of the level-truncated theories, indicating a possible singularity near $\phi \approx -0.25/g$. In this section we study the non-perturbative effective potential, and investigate the branch structure of the potential near the singularity.

For a fixed value of the tachyon field, there are in general many solutions of the equations for the remaining fields $\psi^i, i > 1$ which correspond to different branches of the effective potential. The perturbative expansion describes only one branch of the effective potential, the one which is connected to the unstable vacuum. We will refer to this as branch 1. For levels higher than (2,4), we cannot exactly integrate out all the non-tachyonic fields, so we are forced to use numerical methods to study the effective potential outside its radius of convergence or on other branches. We have used Newton's method to find the zeros of the partial derivatives of the potential. The choice of initial values for the fields determines on which branch the algorithm will converge. At mass level 2, we can find all the solutions, and thus determine all the branches. We can then use the field values from these branches as initial values for the algorithm at higher levels in order to stay on the same branch.

In Figure 2-3, we have plotted branch 1 of the effective potential at levels (2,6), (4,12) and (6,18). At level (4,12), our algorithm stops converging after $g\phi \approx 1.8$. At level (6,18), the algorithm becomes unstable after $g\phi \approx 1.6$. This may indicate either

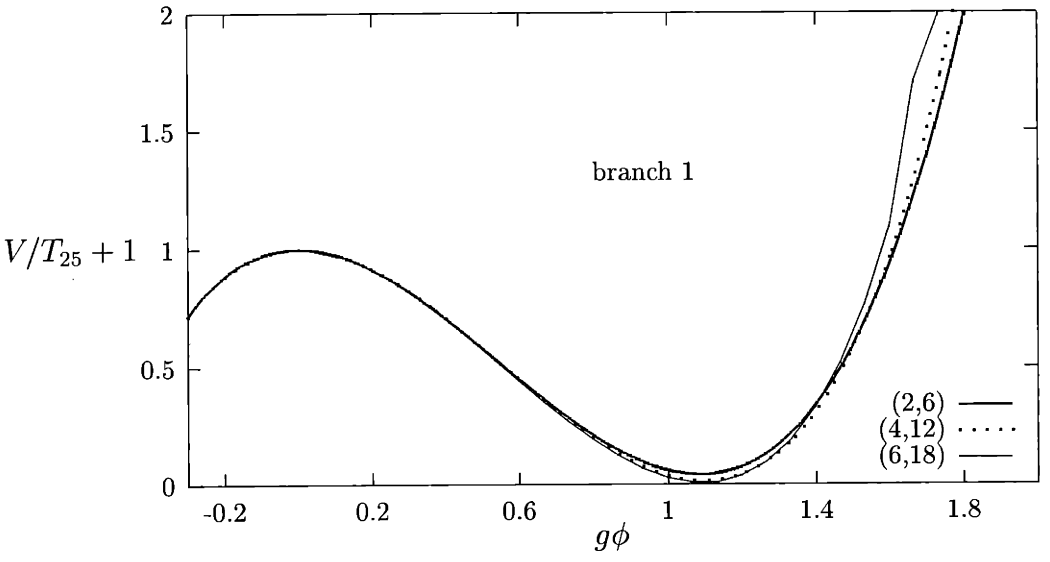

Figure 2-3: Branch 1 of the effective tachyon potential at different truncation levels

that the branch ends at that point or that it meets one or more other branches which play the role of attractors, making it difficult to converge to the chosen branch. A similar breakdown of convergence also happens at level (2, 6) around $g\phi \approx 6$, where a new pair of branches appear [14].

A particularly interesting physical question is to determine the structure of the tachyon effective potential for negative values of ϕ. In the level 0 truncated theory, this potential decreases to $-\infty$ as $\phi \to -\infty$. If this behavior is not modified by higher level corrections, it poses the natural question of why the D25-brane would choose to condense to the stable vacuum rather than the runaway solution at negative ϕ.

When we attempt to continue branch 1 of the effective potential to include arbitrary negative values of the tachyon field, we find that at each level our algorithm stops converging very near the radius of convergence given in Table 2.3, which we calculated using the perturbative expansion coefficients of the effective potential. In [14], Kostelecky and Samuel studied the effective potential at mass level 2 near this point. They found that the branch connected to the unstable and stable vacua (branch 1) ends at a singularity at $g\phi \approx -0.35$ and, at that point, meets another branch (branch 2) which continues upward for increasing values of ϕ. This branch then meets a third

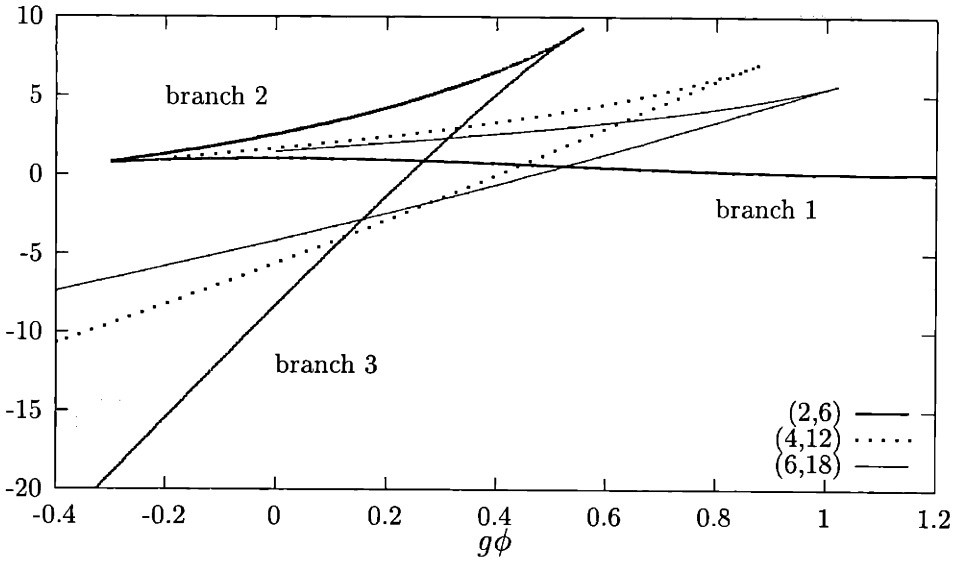

Figure 2-4: Structure of branches 1, 2, and 3 at different levels

branch (branch 3) which continues downward for decreasing values of ϕ. We have studied the branch structure of the effective potential in level truncations (4, 12) and (6, 18) and we find precisely the same branch structure, although the shape of the branches changes noticeably at each level. In Figure 2-4, a graph is given of the branch structure of the effective potential at each of these levels. We observe that branch 3 becomes less steep as we go at higher levels, and that it begins to approach the singular point where branch 1 meets branch 2. While branch 3 does not seem to approach the singular point of branch 1 exponentially quickly, its rate of approach seems compatible with the rate of convergence of the coefficients in the perturbative expansion of the tachyon effective potential. Although we only have limited evidence for this suggestion at this time, we conjecture that in the limit of the full string field theory, branch 3 precisely intersects the singular point connecting branches 1 and 2. The physical effect of this would be to create a critical point near $g\phi \approx -0.25$ at which there would be a higher-order phase transition in the tachyon effective potential. Unlike the effective potential on branch 1, the structure of the effective potential on branch 3 changes dramatically with each additional level of string fields which are included. Thus, we cannot trust our low-level truncation of the theory to accurately

describe the effective potential beyond the critical point. It is natural to speculate that the effective potential becomes nonnegative (relative to the energy of the stable vacuum) for all values of ϕ in the full string field theory.

It would be very nice to have some better understanding of the physics of open bosonic string theory beyond the critical point; there must also be a natural physical explanation for the existence of the critical point, which might be understood from the point of view of bosonic D-branes. We leave these questions for further research, but we conclude this section by pointing out one possible amusing scenario: it is quite possible that the numerical difficulties we have encountered in extending branch 1 of the effective potential near $g\phi \approx 1.6$ indicate a second critical point at approximately the same energy as that we have found at $g\phi \approx -0.25$. If this is indeed the case, it may be that these two critical points should be physically identified in the full theory, so that the tachyon effective potential will essentially become (in some coordinates) periodic, and perhaps even smooth. This would provide a satisfying resolution to the question of what happens when the tachyon rolls in the negative direction: it would simply bring the system to the same stable vacuum as if it rolled in the positive direction. More evidence is needed before this possibility can be taken seriously, but it would provide a nice scenario in which the effective potential for the tachyon has a unique global minimum corresponding to the stable vacuum, just as occurs for the superstring [28]. One potentially serious drawback to this scenario, however, is that it seems to predict the existence of a stable 24-brane kink for whose existence there is no evidence in the bosonic string theory.

2.4 Conclusions

In this chapter we have used the level-truncation approach to string field theory to perform a detailed study of the tachyonic instability of the open bosonic string. We have calculated the cubic string field theory potential up to terms of mass level 20, including fields up to level 10. We have used these results to analyze the effective tachyon potential and the nonperturbative stable vacuum of the system. Our results

for the perturbative form of the effective potential indicate that the radius of convergence of this potential decreases to an apparently finite value as higher level fields are included, indicating a critical point in the effective potential near $\phi \approx -0.25/g$. The stable vacuum lies well outside this radius of convergence, although the critical point and the stable vacuum lie on opposite sides of the unstable vacuum so there is no phase transition between the two vacua. We have found that while the coefficients in the effective potential converge relatively slowly using the level truncation method, the energy of the stable vacuum solution and the values of the fields in this vacuum converge much more quickly. We found that the discrepancy between the exact D-brane tension and the vacuum energy calculated in the truncated string field theory decreases by approximately a factor of $1/3$ when string fields at each additional mass level are included, although we do not have a theoretical explanation for this rate of convergence.

It is perhaps somewhat surprising that this method converges more rapidly for the vacuum energy calculation, which is a truly nonperturbative feature of the system, than for the coefficients of the effective potential, which are in principle computable using perturbative methods. This finding seems to indicate that string field theory has the potential to be an extremely useful tool in studying detailed aspects of non-perturbative string physics. Even if it is not possible to find an exact analytic solution of string field theory describing the nonperturbative vacuum, it would be of great interest to carry out a more detailed analysis of the asymptotic properties of the level truncation approach.

The methods used in this chapter give us a fairly complete picture of the behavior of the effective tachyon potential when $-0.25 < g\phi < 1.5$. We have found that a critical point appears in the tachyon potential near $g\phi \approx -0.25$, beyond which it is difficult to precisely determine the physics. We have speculated that the effective potential stays above the stable vacuum energy for negative ϕ beyond the critical point, but we do not yet have conclusive evidence for this conclusion. It would be very nice to have a better understanding of the behavior of the theory in the regime where the tachyon is large and negative. We have outlined one possible scenario, in

which the tachyon effective potential becomes periodic and the stable vacuum appears at the unique minimum of this potential. If this scenario is realized it would provide a simple answer to the question of how the theory behaves if the tachyon chooses to roll in the negative direction. This would also provide a picture in which unstable bosonic D-branes could naturally be interpreted as sphalerons, as advocated in the supersymmetric case in [39].

There are many directions in which it would be interesting to extend the work in this chapter. One obvious question is to ask how far it is possible to extend the level truncation method in the open bosonic string field theory. For the results in this chapter where we included fields at level 10 we have computed 138,202 distinct cubic vertices. Because many of these vertices involve hundreds of possible index contraction combinations, this computation is already rather time-consuming using a higher-level symbolic manipulation program such as *Mathematica* on a desktop PC. To continue to level (12, 24), over a million vertices (1,381,097) would be needed, each involving hundreds or thousands of index contractions. With a more efficient program and a powerful computer, it might be possible to push as far as level (16, 32) or higher in the foreseeable future if there are physical questions of sufficient interest to motivate further development in this direction (at this level there are over 10^8 cubic vertices). Although the number of vertices grows as the cube of the number of fields at the level at which the theory is truncated, both the number of fields and the complexity of computing each vertex grows exponentially, so that unless a better theoretical understanding of the structure of the theory is developed it will probably never be feasible to perform calculations in this theory beyond interactions of total level 40 or so.

There are a number of other questions of significant interest which could be investigated using truncations of bosonic string field theory at levels considered in this chapter. As discussed in Section 2.3.1 it is clearly important to attain a better understanding of the structure of the theory around the nonperturbative vacuum. While some progress was made in this direction in [14], we do not yet have a very clear picture of how the open string fields such as the U(1) gauge field decouple from the

theory in the stable vacuum. Another question of interest which can be addressed in the bosonic theory is the existence of vacua which break Lorentz symmetry. Such vacua have been shown to exist and to converge up to level (6, 18) truncations of the theory [14, 26]. It would be nice to have a better theoretical understanding of the significance of these vacua.

A related question which can be addressed using open bosonic string field theory is that of describing the structure of Dp-branes with $p < 25$ as unstable configurations of open string fields. Solutions of this type have been found in conformal field theory [40, 41, 42, 43]. The possibility of realizing a bosonic D$(p-1)$-brane as a tachyonic lump on a Dp-brane was discussed in [7]. The use of the level truncation approach to string field theory in this context was suggested in [15], and was implemented by Harvey and Kraus [29], who found numerical evidence for Dp-branes with $p > 18$ as lumps on the D25-brane after including effects of some level 2 fields. It would be very interesting to extend this work to higher level truncations and to see whether the physics of all Dp-branes is indeed accurately described in level-truncated string field theory.

The open bosonic string is an interesting model in which string field theory is particularly simple. Studying this theory further may allow us to refine our understanding of certain qualitative aspects of D-brane physics and tachyonic instabilities. Nonetheless, if string theory is ever to make concrete contact with observable phenomenology it will almost certainly be in the context of a supersymmetric theory. Given that the open string field theory seems to be able to access interesting nonperturbative structure in string theory, it is clearly of substantial interest to develop an equally systematic approach to performing nonperturbative calculations using superstring field theory. While Witten's formulation of open string field theory can be extended to the supersymmetric theory [44, 45], this formalism may be problematic due to the necessity of considering higher order contact interactions [46, 47]. Several alternative formulations of open superstring field theory have been suggested [48, 49, 50]. Recently Berkovits has used his alternative formulation of the supersymmetric open string field theory [50] to carry out a first approximation of the energy

gap in a tachyonic brane system, and has found that 60% of the brane energy is reproduced even in the first truncation of the theory [27]. This formalism has been more explicitly developed and the calculation of the energy gap has been extended by Berkovits, Sen and Zwiebach [28], who showed that including the three scalar fields at the next relevant level gives 85% of the brane energy. If explicit calculations in open superstring field theory can indeed be systematically carried out in high-level truncations as we have done for the bosonic theory, this promises to provide an exciting new tool for investigating in detail nonperturbative issues in string theory such as the description of non-BPS D-branes as brane-antibrane bound states [3, 4, 51] and the associated connection between D-brane charges and K-theory [37, 52].

2.5 Present status

The content of this section is not part of the author's work, it is a summary of results that appeared in [107, 108]. These new results are directly related to the content of the present chapter; and they give such a substantial improvement in the understanding of the level-truncated effective potential, that we thought they had to be mentioned in this thesis.

Extrapolation of the coefficients in the effective potential

The first of these results was proposed by Taylor [107]. It suggests that the coefficients of the effective potential in (2.13), calculated at level L, behave approximately like a polynomial in $1/L$. For example, we can try to interpolate the values for c_4 given in Table 2.2 with the polynomial $a + b/L + c/L^2$. And we find that those five values are very well fitted with[2]

$$c_4^{[L]} \approx -1.743 + 0.598\, L^{-1} - 0.115\, L^{-2}\,. \tag{2.34}$$

[2]The numbers from Table 2.2 are not all from levels $(L, 2L)$. This is why the numbers in (2.34) are slightly different from those in [107].

If we extrapolate this approximation to $L \to \infty$, we find

$$c_4^{[\infty]} \approx -1.743$$

which is in very good agreement with the exact value $c_4 \approx -1.742 \pm 0.001$ that was calculated in [14, 35, 109]. Including more powers of $1/L$ in the fit gives even better extrapolations.

Padé approximants

We could expect that these extrapolations to the coefficients can give us an improved value for the minimum of the potential; but we saw that unfortunately the radius of convergence of the effective potential is smaller than the vev of the tachyon at the minimum. And therefore the effective potential given by a polynomial in ϕ cannot be used to find the difference of energy between the two vacua. It was however shown in [107] that one can extend the convergence of the effective potential beyond the nonperturbative vacuum if one uses a Padé approximant instead of a polynomial.

The Padé approximant $P_N^M(x)$ of a function $f(x)$ is the unique rational function whose numerator is of degree M and whose denominator is of degree N, which agrees with the series expansion of $f(x)$ up to order $M + N$. Taylor showed in [107] that the Padé approximants $P_n^{n+2}(x)$ to the polynomial effective potential, reproduce well the effective potential beyond the radius of convergence, far enough to include the local minimum. These Padé approximants can thus be used to evaluate the energy gap between the two vacua; and since they are calculated from the coefficients c_n, they can be extrapolated to higher level. The qualitative behavior of the energy gap extrapolated to level L is shown in Figure 2-5. The energy approaches -1 downward until it overshoots it, then it decreases to smaller values until it reaches a minimum $V_{\min}/T_{25}$ at a level $L_{\min}$ of approximately 28. And it finally turns back and converges monotonically to a value V_∞/T_{25} very close to -1. Extrapolating the coefficients c_n with more powers of $1/L$ leads to values of V_∞/T_{25} that are even closer to -1.

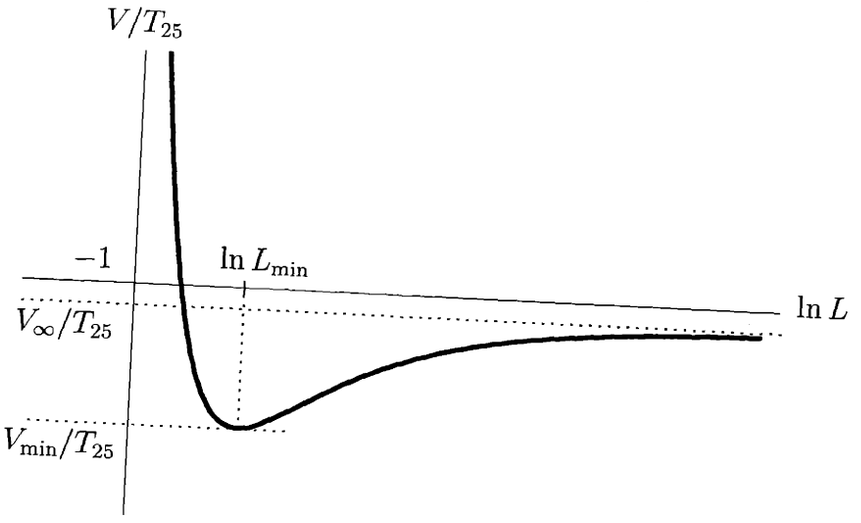

Figure 2-5: The qualitative behavior of the extrapolated energy gap as a function of the logarithm of the level.

Higher level truncation

In [108], Gaiotto and Rastelli have calculated the action to level (18, 54) using an efficient program written in C++. Their results to level 10 agree perfectly with our results; at level 12 their energy continues to approach -1; and for levels 14 and higher their energies overshoot -1, in very good agreement with Taylor's extrapolation [107].

In order to extrapolate their effective potential, they use an idea similar to Taylor's: Let us denote by $V_L(\phi)$ the effective potential obtained, at level L, by integrating out massive fields as in Section 2.3.2. They then define the extrapolation of order M by

$$V_L^{(M)}(\phi) = \sum_{n=0}^{M/2} \frac{a_n(\phi)}{(L+1)^n},$$

where the functions $a_n(\phi)$ are determined from the conditions $V_L^{(M)}(\phi) = V_L(\phi)$ for $L = 0, 2, \ldots, M$ and $\forall \phi \in I$, where I is a finite interval containing the minimum of the potential. The energy at the minimum of the potential $V_L^{(M)}(\phi)$, behaves with L like in Figure 2-5. As the order of the extrapolation M is increased, the value V_∞/T_{25} approaches -1. Indeed, their best estimate for the energy gap is for $M = 16$ where $V_\infty/T_{25} = -1.000030$, a result very close to the conjectured value.

Finally, we emphasize that one of the conclusions of [107, 108] is that extrapolation allows us, in some cases, to evaluate some nonperturbative quantities with a good precision and with a relatively short calculation.

Chapter 3

D-branes as tachyon lumps in string field theory

The 26-dimensional critical bosonic string theory admits Dirichlet p-branes (D-p-branes) for all $p \leq 26$. Each of these D-p-branes admits a tachyonic mode T of mass$^2 = -1$, in units where the tension of the fundamental string is equal to $(2\pi)^{-1}$ ($\alpha' = 1$). It has been conjectured that the potential for the tachyon field has a non-trivial translationally invariant (local) minimum at some value T_{vac} where the sum of the tachyon potential and the tension of the original brane vanishes [7]. Thus at $T = T_{vac}$ the total energy density vanishes, and hence this configuration can be identified as the vacuum of the closed string theory without any D-branes. It has also been conjectured that although this vacuum does not have any perturbative open string excitations, it contains lump-like soliton configurations which approach the vacuum $T = T_{vac}$ asymptotically far away from the core of the soliton and represent D-branes of lower dimension [40, 41, 43, 7]. Similar conjectures have also been made involving the tachyon living on the coincident D-brane anti-D-brane pair, or on a non-BPS D-brane of type IIA and IIB superstring theories [3, 4, 5, 37, 6, 52].

Various pieces of evidence for these conjectures have been found in both the first [40, 41, 43, 7, 3, 4, 5], and second (Chapter 2 and [15, 30, 19, 29, 53, 27, 28, 54, 55]) quantized string theory, and also using AdS/CFT correspondence [39, 56]. The first quantized description has been successful in verifying the conjectures relating the

tachyonic solitons to lower dimensional D-branes, but it can only supply indirect evidence for the equivalence between the (local) minimum of the tachyon potential and the vacuum without a D-brane. On the other hand, the second quantized description – open string field theory [13] – can provide direct evidence for this conjecture by explicitly computing the (negative) value of the tachyon potential at the minimum and comparing it with the tension of the original D-brane system. Although open string field theory contains infinite number of fields, and the problem of finding a translationally invariant stationary point of the potential involves solving the equations of motion of the infinite number of zero momentum modes of these fields, the calculations are made feasible by using the level expansion scheme proposed by Kostelecky and Samuel [26, 35]. The procedure is as follows. Using the correspondence between the modes of the string field and states in the conformal field theory describing the first quantized string, we define the level of a mode of the string field as the difference between the $\widehat{N}$ eigenvalue of the first quantized string state representing this mode, and the $\widehat{N}$ eigenvalue of the state representing the zero momentum tachyon, where $\widehat{N}$ is the total 'number operator' of the matter and ghost system. The level truncation scheme to order (M, N) then corresponds to an approximation in which we keep in the string field theory action all modes of level $\leq M$, and all interaction terms for which the sum of the levels of all the modes appearing in the term is $\leq N$. This gives a potential (which, for a static field configuration, is just the negative of the action up to a normalization constant) with finite number of fields and a finite number of terms. Thus we can find its extremum and calculate its value at the extremum. The larger the values of (M, N), the larger is the number of modes and the number of terms in the potential, and the better is the accuracy.

The calculation of ref. [26, 35] for the tachyon potential was revisited and extended in [15] in terms of background independent fields. It was shown there that the total negative potential energy at the stationary point cancels the energy of the D-brane represented by the string field theory to an accuracy of <1.5% at the level (4,8) approximation. This calculation was extended in Chapter 2 (ref. [19]) to level (10,20). At this level the contribution from the tachyon potential was found to cancel the

tension of the D-brane to an accuracy of about 0.1%. Similar calculations have also been performed [27, 28, 54, 55] in open superstring field theory [50, 57, 58]. At the level (2,4) approximation the tachyon potential has been shown to cancel about 90% of the tension of the original brane configuration.[1]

The success of string field theory in verifying the conjecture relating the translationally invariant stationary point of the tachyon potential and the vacuum without any D-brane encourages one to ask whether string field theory can also be used in studying the conjectured relation between the tachyonic lump solutions and lower dimensional D-branes. This study was initiated by Harvey and Kraus [29]. In this paper they started with the level (0,0) contribution to the tachyon potential in open bosonic string field theory on a D-p-brane, and identified a 'bounce solution' in this field theory as the D-$(p-1)$ brane. At this level the tension associated with this solution turns out to be about 78% of the known value of the D-$(p-1)$-brane tension. This result receives correction not only from the higher level fields, but also from the momentum dependence of the interaction terms which were neglected in the initial analysis. While there is no systematic expansion scheme for taking into account these momentum dependent corrections, a naive expansion of the interaction term in powers of momentum, keeping only the zeroth and first order terms, reduced the tension of the soliton to about 70% of the conjectured answer. On the other hand, taking into account the correction to the potential to level (2,4) increased the answer back to about 82% of the conjectured answer. A systematic method for taking into account the momentum dependent terms in the interaction was suggested in ref. [53], but this procedure did not give rise to an appreciable change in the tension of the lump. A similar analysis has also been carried out for solitons in the open superstring field theory [28, 59, 60]. Although the answer turns out to be close to the expected answer, it is likely to be an accidental result, as there is no reason to assume that the corrections due to the momentum dependent terms are small in this case.

The purpose of this chapter will be to develop a systematic approximation scheme

[1] At present there seems to be some disagreement between refs. [54] and [55] about the level (2,4) results.

for studying these solitons in string field theory and calculating their tension. We shall focus on the codimension one lump on a Dp-brane of the bosonic string theory – which is conjectured to be equivalent to a D-$(p-1)$-brane – but it will become clear that the scheme is general enough to be applicable to the study of higher codimension solitons, as well as to solitons in superstring field theory. In the case of a codimension one soliton, we are dealing with a field configuration on the Dp brane which depends on only one of the spatial coordinates (say x) on the brane, and is independent of time, as well as the other $(p-1)$ spatial coordinates. We study this problem by compactifying the coordinate x on a circle of radius R instead of letting it span the whole real line. In this case, since all field configurations must be periodic in x, we can decompose all fields into modes carrying discrete momenta along x in units of $(1/R)$, and the solitonic field configuration that we are looking for must be obtained as an appropriate superposition of these modes. We can now define the level of any such mode as the difference between the L_0 eigenvalue of the first quantized string state representing this mode, and that of the zero momentum tachyon state, where L_0 denotes the zeroth component of the Virasoro generator of the combined matter ghost system.[2] This allows us to define a level (M, N) approximation to the potential exactly as before. Working with the potential up to a given level, we can now look for x dependent solutions of the string field equations by extremizing the potential with respect to the modes appearing in the potential to this level.

This is precisely the procedure we follow in this chapter for studying the tachyonic lump solution on a D-p-brane.[3] We study this problem for various radii at various levels of approximation, and compare the tension of the lump with the tension of a D-$(p-1)$-brane. The results for the tension of the lump turn out to be remarkably close to the known tension of the D-$(p-1)$-brane. Whereas for $R = \sqrt{3}$ and $\sqrt{15/2}$ we are able to get a lump tension within 1% of the tension of the D-$(p-1)$-brane, for larger radii ($R = \sqrt{12}$ and $\sqrt{35/2}$) we get answers within 3% of the expected

[2]Since for the zero momentum states the eigenvalue of the number operator is the same as the L_0 eigenvalue of the state, the two prescriptions agree for these states.

[3]The discretization of the momentum is reminiscent of the procedure followed in ref. [53], although the precise relationship between these two approaches is not clear.

answer. We also compare the profile of the tachyon field corresponding to the lump for different values of R, – obtained by superposition of $\cos(nx/R)$ for integer n – and find remarkable agreement between the profiles for different values of R.

At this point we should note that the problem of formation of the tachyonic lump on a circle was addressed using the first quantized approach in ref. [61]. There a renormalization group analysis was used to show that the mass of the tachyonic lump on a D-p-brane is indeed equal to that of a D-$(p-1)$-brane.[4] In view of this result one might ask whether the string field theory analysis carried out in this chapter gives any new insight into this problem. To this end, we note, first of all, that the relationship between the renormalization group analysis in the first quantized approach, and the string field theory analysis based on the level truncation scheme, is as yet quite unclear, and hence it is certainly illuminating to independently verify the equivalence of the D-$(p-1)$-brane, and the tachyonic lump on the D-p-brane in string field theory. Furthermore, string field theory provides us with a definite picture of the tachyon profile as superposition of $\cos(nx/R)$ for different n with definite coefficients. In contrast the analysis based on the renormalization group flow only tells us that a perturbation by the leading relevant operator $\cos(x/R)$ takes the original D-p-brane to a D-$(p-1)$-brane, and does not tell us how the higher harmonics mix with $\cos(x/R)$ to produce the soliton. Indeed most of the higher harmonics correspond to irrelevant perturbation, and hence their coefficients vanish in the infra-red.[5] Furthermore, the rigorous results of ref.[42] have not yet been generalized to superstring theory. Thus we believe that despite the exact results based on the renormalization group analysis of the first quantized theory, the present analysis throws new light on the tachyonic soliton solutions.

The rest of the chapter is organized as follows. In Section 3.1 we outline the general procedure of level expansion scheme of the string field theory, discuss the possibility of restricting the string field to a background independent subspace for

[4]This followed earlier work of ref. [42] on the renormalization group flow of the two dimensional field theory under a perturbation corresponding to switching on a tachyon background proportional to $\cos(x/R)$.

[5]Presumably if we could determine the exact location of the infrared fixed point in the space of coupling constants, then the shape of the lump will be determined in this approach.

studying the lump solution, and give details of computation of a few terms in the potential. In Section 3.2 we give in detail the results for the potential, the lump solution and its energy for a specific radius $R = \sqrt{3}$. We also compare the profile of the lump at different levels of approximation. In Section 3.3 we give the results for several other radii, both larger ($\sqrt{15/2}$, $\sqrt{12}$ and $\sqrt{35/2}$) and smaller ($\sqrt{11/10}$) than $\sqrt{3}$, and compare the profile of the lump for each radii with the profile at $R = \sqrt{3}$. We conclude in Section 3.4 by discussing possible generalization of this analysis and some speculations.

3.1 Level expansion and the string field

In this section we will set up a variant of the level expansion method to deal with the problem of finding the profile and mass of the tachyon lump in string field theory. As reviewed at the beginning of this chapter, such method is desirable as previous computations of lump masses in string field theory have not been very accurate. After explaining this method we will discuss the background independent expansion of the string field suitable for the problem. Then we discuss two methods for estimating the lump mass. We conclude by showing a few samples of typical calculations needed to evaluate the string field action for the lump.

3.1.1 Modified level expansion

When calculating the tachyon potential in search for a spacetime independent vacuum state, all spacetime fields are set to constants, and the evaluation of the string field action does not require the inclusion of terms with spacetime derivatives. The string field is at zero momentum and is thus built by a superposition of zero momentum states times constants representing the zero momentum modes of the spacetime fields. The states are built by acting on a zero-momentum vacuum with oscillators of the relevant conformal field theory (CFT). In this case the level expansion was defined as follows [26, 35]. Let $\widehat{N}$ be the number operator, representing the contribution to L_0 from the system of matter and ghost oscillators. Let N_0 ($=-1$) denote the eigenvalue

of $\widehat{N}$ for the zero momentum tachyon: $\widehat{N}\,|T_0\rangle = N_0\,|T_0\rangle$. For a given state $|\Phi_i\rangle$, with number eigenvalue N_i ($\widehat{N}\,|\Phi_i\rangle = N_i\,|\Phi_i\rangle$) we define the level $l(\Phi_i)$ of the state $|\Phi_i\rangle$ as

$$l(\Phi_i) \equiv N_i - N_0\,. \tag{3.1}$$

As defined, level is a dimensionless number. For the case of bosonic string theory the levels are all integers while for NS superstrings they can also be half integral. We now define the level (M, N) approximation to the action as follows:

- We keep only those fields with level $\leq M$.
- We keep only those terms in the action for which the sum of the levels of all the fields in the term is $\leq N$.

In order that the quadratic term of all fields with level $\leq M$ are kept in the action, we must have $N \geq 2M$. While variants are possible, it seems most effective when calculating any physical object to use its level $(M, 2M)$ approximation, as experience shows that increasing the number of terms in the potential keeping the number of fields fixed does not improve the results very much. While there is yet no theoretical explanation for the convergence of the level expansion, the numerical evidence collected thus far is impressive.

Consider now the problem at hand. While all of our discussion applies to soliton solutions on non-BPS D-branes, and D-brane anti- D-brane pairs of superstring theory, we will consider here explicitly only the case of the unstable D-branes of bosonic string theory. Consider therefore, an unstable bosonic D-brane extending over a number of spatial dimensions. We now wish to select one of these dimensions, call it x and construct a tachyon lump such that the solution depends only on the x-coordinate. (Again our discussion applies to lumps depending on more than one coordinates, but we shall not analyze these cases here.) As the lump is not invariant under translation along x, we now need to include x-momentum modes in the string field expansion and x-derivatives, or x-momentum dependent terms in the string field action. In order to do this systematically we compactify x over a circle of radius R, namely $x \sim x + 2\pi R$.

This quantizes the x-momentum as $p_x = n/R$ for integer n. For each of the zero momentum states $|\Phi_i\rangle$ we had before, we now have discrete states of the type $|\Phi_{i,n}\rangle$ that only differ by the fact that they are built on vacua having x-momentum n/R. For such states there is a natural generalization of the level. This is the difference between the L_0 eigenvalue of the state and that of the zero momentum tachyon, where $\{L_n\}$ denote the Virasoro generators of the combined matter and ghost system. This is because (with $\alpha' = 1$) we have that $L_0 = p_x^2 + \widehat{N}$. For zero momentum this is just the previous definition. Still denoting by N_i the number eigenvalue of $|\Phi_{i,n}\rangle$ we have

$$l(\Phi_{i,n}) = L_0(\Phi_{i,n}) - L_0(T_0) = \frac{n^2}{R^2} + N_i - N_0\,. \tag{3.2}$$

The level is still a dimensionless number as R here is measured in units of $\sqrt{\alpha'}$ (which has been set to one). We can now define the level (M, N) approximation for the action exactly as before. Since the L_0 eigenvalue of a state plays a crucial role in the conformal map that inserts the state into the disk representing the interaction terms in the action, this is a natural generalization of the level truncation scheme of ref. [26, 35]. This chapter will present evidence that this modified version of the level truncation scheme also works very well.

In calculating in this setup in the level $(M, 2M)$ approximation for any given radius we will have to include states $|\Phi_i\rangle \equiv |\Phi_{i,0}\rangle$ and "harmonics" $|\Phi_{i,n}\rangle$, and clearly the condition $l(\Phi_{i,n}) \leq M$ will give an upper bound on n for each i. This also requires $l(\Phi_{i,0}) \leq M$, and thus we have a finite number of modes to be included at a given level of approximation. Each term in the action including modes whose sum of levels does not exceed $2M$ is computed exactly. It is manifest that in a cubic string field theory the level $(M, 2M)$ approximation will only require a finite number of computations[6].

3.1.2 Background independent string field

The general setup required to study a lump is similar to that developed in [9] to study the mass of the D-brane. To begin with, we assume that the background space-time

[6]This will also be the case for the NS superstring field theory discussed in ref. [27, 28, 54, 55].

is the product of a (2+1) dimensional flat space-time, labelled by a pair of space-like coordinates (x, y) and a time like coordinate x^0, and an arbitrary Euclidean manifold $\mathcal{M}$ described by a conformal field theory of central charge 23. We take the spatial direction y to be non-compact, but x to be compact with radius R. We let X, Y and X^0 denote the three scalar fields on the string world-sheet associated with the coordinates x, y and x^0.

We now consider a D-brane with the following properties. For an open string ending on the D-brane we put Neumann boundary condition on the fields X and X^0 and Dirichlet boundary condition on the field Y.[7] We leave the boundary condition on the fields associated with the coordinates on $\mathcal{M}$ arbitrary, with the only restriction that all the fields on which we put Neumann boundary condition are associated with compact coordinates. This means that all directions tangential to the D-brane are compact, and hence the D-brane has finite mass. From the point of view of the full space-time, this D-brane describes a D-p brane for some $p \geq 1$, with $(p-1)$ directions wrapped on an internal $(p-1)$ cycle of $\mathcal{M}$, and one direction wrapped on the circle of radius R labelled by x. On the other hand from the point of view of an observer who only sees the (2+1) dimensional space-time labelled by (x, y, x^0), this system corresponds to a D1-brane wrapped on a circle of radius R. From now on we shall refer to this system as the D1-brane or the D-string; with its tension defined as the total energy per unit length along x. Of course, an ordinary D-string will be a special case of this system, obtained by putting Dirichlet boundary condition on all the fields associated with the coordinates on $\mathcal{M}$.

The dynamics of an open string with ends on this D-brane is described by a boundary conformal field theory of central charge 26, which is a direct sum of the boundary conformal field theories associated with the fields X, Y, X^0 and the manifold $\mathcal{M}$. We shall denote by CFT(X), CFT(Y) and CFT(X^0) the boundary conformal field theories (each with central charge 1) associated with the fields X, Y and X^0 respectively, and by CFT($\mathcal{M}$) the boundary conformal field theory with central charge 23

[7] As in ref. [9], the extra non-compact direction y with Dirichlet boundary condition provides a direction along which the brane can move, and we can calculate the tension of the brane by studying its motion in this direction.

associated with the manifold $\mathcal{M}$. We also define

$$\text{CFT}' = \text{CFT}(Y) \oplus \text{CFT}(X^0) \oplus \text{CFT}(\mathcal{M})\,, \tag{3.3}$$

so that CFT′ has central charge 25. We denote by L_n^X and L'_n the Virasoro generators of CFT(X) and CFT′ respectively. If we denote by L_n^{ghost} the Virasoro generators of the ghost system, then the total Virasoro generators of the system will be given by $L_n = L_n^{ghost} + L_n^X + L'_n$.

The compact direction x corresponds to the direction in which we shall eventually form the lump. If we follow the normalization convention of ref.[15], then the tension $\mathcal{T}_1$ of the D-string described above is related to the coupling constant g_o of the open string field theory describing the wrapped D-string by the relation:

$$2\pi R\mathcal{T}_1 = \frac{1}{2\pi^2 g_o^2}\,. \tag{3.4}$$

In this normalization convention, a time independent string field configuration represented by a state $|\Phi\rangle = \Phi(0)|0\rangle$ in the Hilbert space of first quantized string theory, will have a potential

$$\text{Potential} = -S(\Phi) = \frac{1}{g_o^2}\mathcal{V}(\Phi) = 2\pi R\mathcal{T}_1 \cdot 2\pi^2\mathcal{V}(\Phi)\,, \tag{3.5}$$

where

$$\mathcal{V}(\Phi) = \frac{1}{2}\langle\, \Phi, Q\Phi\,\rangle + \frac{1}{3}\langle\, \Phi, \Phi * \Phi\,\rangle\,. \tag{3.6}$$

Here Q denotes the BRST charge, $\langle , \rangle$ denotes BPZ inner product between two states, and $*$ denotes the $*$-product of Witten's open bosonic string field theory [13].

A basis of states in CFT(X) is obtained by acting on $e^{inX/R}(0)|0\rangle$ with the oscillators α_{-m}^X of X. It follows by a simple counting argument that an alternate basis can be formed out of the Verma module, containing states obtained by acting on $e^{inX/R}(0)|0\rangle$ with the operators L_{-m}^X, *as long as these states are all linearly independent.* This is the case if there are no null states in the spectrum. The condition for

the appearance of a null state is given by [62],

$$\frac{n^2}{R^2} = \frac{(p-q)^2}{4} \quad \rightarrow \quad \frac{n}{R} = \frac{(p-q)}{2}, \tag{3.7}$$

where p and q are integers. Since n is an integer, we can avoid null states for $n \neq 0$ with an appropriate choice of R. Even if we work with a value of R for which there are null states, the choice of basis described above is good below the level where the first null state appears. From now on we shall restrict our analysis to situations where this choice of basis based on Verma module is good. In fact our explicit work in later sections will be based on R values that are not rational, and thus there will be no null states for $n \neq 0$.

For $n = 0$, however, there are null states and hence the basis of states obtained by applying L^X_{-m} on $|0\rangle$ is not complete. For example, $L^X_{-1}|0\rangle$ is null, and this requires us to explicitly include the primary state $\alpha^X_{-1}|0\rangle$ in the basis. There are further null states in the Verma module over $\alpha^X_{-1}|0\rangle$, and hence there are new primary states at higher level which must be explicitly included in the basis. Let us denote by $\{|\varphi^i_e\rangle = \varphi^i_e(0)|0\rangle_X\}$ and $\{|\varphi^i_o\rangle = \varphi^i_o(0)|0\rangle_X\}$ the set of zero momentum primary states which are respectively even and odd under the reflection $X \rightarrow -X$. The complete basis of zero momentum states in CFT(X) is obtained by acting on $\{|\varphi^i_e\rangle\}$ and $\{|\varphi^i_o\rangle\}$ with L^X_{-n}'s, and removing the null states.

A generic string field configuration is represented by an arbitrary state in the Hilbert space $\mathcal{H}$ of ghost number one in the combined matter, ghost conformal field theory. We now claim that in order to discuss a lump along the x coordinate, we can restrict the string field $|\Phi\rangle$ to a subspace $\widehat{\mathcal{H}}$ of $\mathcal{H}$, built by acting with the oscillators

$$\{L^X_{-1}, L^X_{-2}, \cdots; L'_{-2}, L'_{-3}, \cdots; c_1, c_{-1}, c_{-2}, \cdots; b_{-2}, b_{-3}, \cdots\} \tag{3.8}$$

on the following primary states:

- The zero momentum even primaries $\varphi^i_e(0)|0\rangle$ (and removing the null states), and,

- The Fock vacuum states of the form

$$\cos\left(\frac{n}{R}X(0)\right)|0\rangle = \frac{1}{2}\left(e^{inX(0)/R} + e^{-inX(0)/R}\right)|0\rangle = \frac{1}{2}\left(\left|\frac{n}{R}\right\rangle + \left|-\frac{n}{R}\right\rangle\right) \quad n \neq 0\,, \tag{3.9}$$

where $|0\rangle$ is the SL(2,$\mathbb{R}$) vacuum of the combined matter, ghost conformal field theory. A few points should be made. The Virasoro operator L'_{-1} is not required for it kills the above primary states (this is not the case for L^X_{-1}). b_{-1} and b_0 also annihilate the vacuum $|0\rangle$, and hence have been omitted from the list. We have not included the oscillator c_0 because we work in the Siegel gauge, where all states must be annihilated by b_0. Finally we can restrict ourselves to states of even twist [31]. This simply requires that the eigenvalue of the number operator $\widehat{N}$ must be odd (same as that for the tachyon).

In order to show that the above is a consistent truncation of the string field, one must show that there is no term in the action that couples a single state in $(\mathcal{H} - \widehat{\mathcal{H}})$ to a state in $\widehat{\mathcal{H}}$ via the quadratic term, or to a pair of states in $\widehat{\mathcal{H}}$ via the interaction term. This is readily done by listing the states in $(\mathcal{H} - \widehat{\mathcal{H}})$. We carry along all ghost oscillators and classify the states by their behavior under the matter operators. In this way we get the following disjoint sets:

- States with nonzero momentum k_0 along X^0.

- States obtained by acting with the oscillators in (3.8) on Fock vacua of the type $\sin(\frac{nX(0)}{R})\,|0\rangle$, or on a state of the form $\varphi^i_o(0)|0\rangle$.

- States obtained by acting with (3.8) on states that (i) have $k_0 = 0$, (ii) are non-trivial primaries of CFT′ (of dimension greater than zero, by unitarity), and (iii) are CFT(X) primaries.

It is manifest by momentum conservation that a state in the first set cannot couple to states in $\widehat{\mathcal{H}}$. The symmetry $X \to -X$ of CFT(X) insures that a state in the second set also cannot couple to states in $\widehat{\mathcal{H}}$. The same is true for the last set as Virasoro Ward identities can be used to show that a correlator involving two states in $\widehat{\mathcal{H}}$ and

a state in the last set is proportional to the one point function of the CFT′ primary in question. Since this primary must have dimension greater than zero, its one point function vanishes. This completes our justification for the use of $\widehat{\mathcal{H}}$.

Since the choice of basis described above requires the use of the basis $\{|\varphi_e^i\rangle\}$, it will be useful to determine at which level the first zero momentum primary (other than the vacuum state) appears. For this we can compare the full partition function of CFT(X) for states even under $X \to -X$

$$Z_{even}(q) \equiv Tr_{even}(q^{L_0^X - \frac{1}{24}}) = \frac{1}{2} q^{-\frac{1}{24}} \Big(\prod_{n=1}^{\infty} \frac{1}{1-q^n} + \prod_{n=1}^{\infty} \frac{1}{1+q^n} \Big) \tag{3.10}$$

with the Virasoro character for $(c = 1, h = 0)$ [62],

$$\chi_{c=1,h=0}(q) = q^{-\frac{1}{24}} \prod_{n \geq 2} \frac{1}{1-q^n} \,. \tag{3.11}$$

It can be easily checked that

$$Z_{even}(q) - \chi_{c=1,h=0}(q) = q^{-\frac{1}{24}} (q^4 + O(q^5)) \,. \tag{3.12}$$

Thus the first non-trivial primary $|\varphi_e^1\rangle$ even under $X \to -X$ appears at level four. Indeed, the available descendants at this level, $L_{-4}^X |0\rangle$, $L_{-2}^X L_{-2}^X |0\rangle$, do not suffice to represent the nonvanishing X-even states $\alpha_{-3}^X \alpha_{-1}^X |0\rangle$, $\alpha_{-2}^X \alpha_{-2}^X |0\rangle$, $(\alpha_{-1}^X)^4 |0\rangle$.

3.1.3 Mass of the lump

To begin with, the wrapped D-p brane, which we have been calling a D-1 brane wrapped on a circle of radius R, has mass $2\pi R \mathcal{T}_1$, where $\mathcal{T}_1$, as defined earlier, is the tension of this D1-brane. We want to compute the mass of the system in a situation where the tachyon field on this D1-brane develops a lump along a circle of radius R (this direction is represented by the world sheet field X). If we denote by $\vec{T}$ the multicomponent string field configuration on the D1 brane, restricted to $\widehat{\mathcal{H}}$, then, using eq.(3.5), the rest mass energy plus potential energy of the D1 brane stretched

on the circle can be written as

$$E(D1) = \mathcal{T}_1(2\pi R)\,(1 + 2\pi^2\mathcal{V}(\vec{T})) \tag{3.13}$$

where $\mathcal{V}$ has been defined in eq.(3.6). Before condensation, $\vec{T} = 0$ and $\mathcal{V}(\vec{T}) = 0$, and thus the energy formula correctly reproduces the mass of the D1-brane. Recall that for the nontrivial translationally invariant vacuum $\vec{T}_{vac}$, one expects $\mathcal{V}(\vec{T}_{vac}) = -1/(2\pi^2)$ and the energy formula correctly gives zero (as the D1 brane has disappeared). Using $\mathcal{V}(\vec{T}_{vac}) = -1/(2\pi^2)$ we can write the energy formula as

$$E(\mathrm{D1}) = \mathcal{T}_1\, 2\pi R \cdot 2\pi^2\,(\mathcal{V}(\vec{T}) - \mathcal{V}(\vec{T}_{vac})) \tag{3.14}$$

The mass of the tachyonic lump solution, represented by the configuration $\vec{T}_{lump}$, is obtained by replacing $\vec{T}$ by $\vec{T}_{lump}$ on the right hand sides of eqs.(3.13) or (3.14). This tachyonic lump on the D-string (wrapped D-p-brane) is conjectured to be equivalent to a D0-brane (a wrapped D-$(p-1)$-brane) of mass $\mathcal{T}_0$. With $\alpha' = 1$, the ratio of the tension of a D-p brane and a D-$(p-1)$-brane is $1/(2\pi)$; using this we get,

$$\mathcal{T}_0 = 2\pi\mathcal{T}_1\,. \tag{3.15}$$

This gives

$$r \equiv \frac{E_{lump}}{\mathcal{T}_0} = 2\pi^2 R\,(\,\mathcal{V}(\vec{T}_{lump}) - \mathcal{V}(\vec{T}_{vac}))\,. \tag{3.16}$$

The predicted answer for this ratio is 1.

This prediction can be tested for various values of R, and independently of the chosen value we must obtain unity, since the mass of a D0-brane on a circle of radius R does not depend on R. At fixed R and at any level of approximation in the level expansion it is possible to use (3.16) in two ways. We can use that $2\pi^2\mathcal{V}(\vec{T}_{vac})$ at the exact vacuum is indeed -1 and thus we check how accurately

$$r^{(1)} \equiv R\,(2\pi^2\mathcal{V}_{(M,N)}(\vec{T}_{lump}) + 1) \tag{3.17}$$

approaches unity. Here $\mathcal{V}_{(M,N)}$ is the potential calculated at the specified level of approximation. Alternatively we can use the translationally invariant vacuum that is obtained with the same level of approximation used to compute the lump.[8] This gives

$$r^{(2)} \equiv R\,(2\pi^2\mathcal{V}_{(M,N)}(\vec{T}_{lump}) - 2\pi^2\mathcal{V}_{(M,N)}(\vec{T}_{vac})) \tag{3.18}$$

We will find that $r^{(1)}$ approaches unity monotonically from above as we increase the level of approximation. On the other hand $r^{(2)}$ provides a more accurate answer.

3.1.4 Setup and sample computations

Let us now describe explicitly the string field we will be using to analyze the bosonic string lump. The zero momentum tachyon $|T_0\rangle = c_1\,|0\rangle$ now becomes the lowest in a family of states

$$|T_n\rangle = c_1 \cos\Big(\frac{n}{R}X(0)\Big)\,|0\rangle\ , \quad l(T_n) = \frac{n^2}{R^2} \tag{3.19}$$

where $l(T_n)$ denotes the level of T_n. For any given computation only a finite number of tachyon modes are required. In the zero-momentum computation the next modes that contribute are $|U_0\rangle = c_{-1}\,|0\rangle$ and $|V_0\rangle = L^{matt}_{-2}\,|0\rangle$. In view of our remarks around (3.9) these states actually give rise to three towers

$$\begin{aligned}
|U_n\rangle &= c_{-1}\ \cos\Big(\frac{n}{R}X(0)\Big)\,|0\rangle\ , \quad l(U_n) = 2 + \frac{n^2}{R^2}\,,\\
|V_n\rangle &= c_1 L^X_{-2}\cos\Big(\frac{n}{R}X(0)\Big)\,|0\rangle\ , \quad l(V_n) = 2 + \frac{n^2}{R^2}\,,\\
|W_n\rangle &= c_1 L'_{-2}\cos\Big(\frac{n}{R}X(0)\Big)\,|0\rangle\ , \quad l(W_n) = 2 + \frac{n^2}{R^2}\,.
\end{aligned} \tag{3.20}$$

In addition to these three towers there is one more, where the $n = 0$ state happens to vanish:

$$|Z_n\rangle = c_1\,L^X_{-1}L^X_{-1}\cos\Big(\frac{n}{R}X(0)\Big)\,|0\rangle\ , \quad n \geq 1, \quad l(Z_n) = 2 + \frac{n^2}{R^2}\,. \tag{3.21}$$

[8] The value of $\mathcal{V}_{(M,N)}(\vec{T}_{vac})$ can be read from Chapter 2 or refs. [15, 19].

No new fields or towers arise until level four, and for the purposes of the present chapter we shall not carry computations that far. Therefore we will use the string field

$$\begin{aligned}\left|\vec{T}\right\rangle \;=\;& t_0\left|T_0\right\rangle + t_1\left|T_1\right\rangle + t_2\left|T_2\right\rangle + \cdots \\ &+ u_0\left|U_0\right\rangle + u_1\left|U_1\right\rangle + \cdots \\ &+ v_0\left|V_0\right\rangle + v_1\left|V_1\right\rangle + \cdots \\ &+ w_0\left|W_0\right\rangle + w_1\left|W_1\right\rangle + \cdots \\ &+ z_1\left|Z_1\right\rangle + \cdots\end{aligned} \tag{3.22}$$

Which fields and which interactions must be kept for any fixed level computation depends on the chosen radius, and this will be discussed in the following sections. We conclude here with some basic comments about the evaluation of the potential (or the action) for a string field of the above type.

This is simply the evaluation of $\mathcal{V}(\vec{T})$ as given in (3.6)

$$\mathcal{V}(\vec{T}) = \frac{1}{2}\langle \vec{T}, Q\vec{T}\,\rangle + \frac{1}{3}\langle \vec{T}, \vec{T} * \vec{T}\,\rangle\,. \tag{3.23}$$

We work in units where $\alpha' = 1$. The stress tensor for the compact coordinate X is $T_X = -\frac{1}{4}\partial X\,\partial X$ with $X(z)X(w) \sim -2\ln(z-w)$, $T(z)e^{ip\cdot X(w)} \sim \frac{p^2}{(z-w)^2}e^{ip\cdot X(w)}$ and $e^{ip_1\cdot X(z)}e^{ip_2\cdot X(w)} = (z-w)^{2p_1\cdot p_2}e^{ip_1\cdot X(z)+ip_2\cdot X(w)}$, where z and w are coordinates on the real line with $z > w$. With these conventions $L_0\left|p\right\rangle = L_0 e^{ip\cdot X(0)}\left|0\right\rangle = p^2\left|p\right\rangle$. In addition, the inner product is normalized as

$$\left\langle \frac{n}{R}\right| c_{-1}c_0c_1 \left|\frac{m}{R}\right\rangle = \delta_{n,m} \tag{3.24}$$

Consider, for example contributions from the tachyon tower to the action. By momentum conservation all kinetic terms must be diagonal. Using (3.9) we see that the

contribution from t_n $(n \geq 1)$ to V is

$$\frac{1}{2}\frac{t_n}{2}\frac{t_n}{2}\Big(\Big\langle -\frac{n}{R}\Big| + \Big\langle \frac{n}{R}\Big|\Big) c_{-1}c_0 L_0 c_1 \Big(\Big|\frac{n}{R}\Big\rangle + \Big|-\frac{n}{R}\Big\rangle\Big) \tag{3.25}$$

By momentum conservation there are two cross terms that do not vanish and give identical contributions. We thus get

$$\frac{1}{4}t_n^2 \Big\langle \frac{n}{R}\Big| c_{-1}c_0\Big(-1+\frac{n^2}{R^2}\Big)c_1 \Big|\frac{n}{R}\Big\rangle = -\frac{1}{4}\Big(1-\frac{n^2}{R^2}\Big)t_n^2 \tag{3.26}$$

For t_0 the normalization factor differs by a factor of two. All this together gives us that the quadratic terms are

$$\begin{aligned}\mathcal{V}(t_0,t_1,t_2,\cdots)^{(2)} &= -\frac{1}{2}t_0^2 - \frac{1}{4}\sum_{n=1}^{\infty}\Big(1-\frac{n^2}{R^2}\Big)t_n^2 \\ &= -\frac{1}{2}t_0^2 - \frac{1}{4}\Big(1-\frac{1}{R^2}\Big)t_1^2 - \frac{1}{4}\Big(1-\frac{4}{R^2}\Big)t_2^2 + \cdots \end{aligned} \tag{3.27}$$

We will use the first tachyon harmonic t_1 to drive the unstable vacuum into the lump solution. Note that t_1 is tachyonic whenever $R > 1$. We will choose different values of $R > 1$ to examine how the lump forms. As R increases, more and more tachyon harmonics become tachyonic.

It is not difficult to compute the interactions of the various tachyon harmonics. One can use the oscillator expressions for the states and contract them against the 3-string vertex bra $\langle V_{123}|$ [32, 34, 33]. Alternatively one can use the conformal field theory definition [63]

$$\langle \vec{T}, \vec{T} * \vec{T}\rangle \equiv \langle h_1 \circ T(0) h_2 \circ T(0) h_3 \circ T(0)\rangle \ . \tag{3.28}$$

where $T(0)$ denotes the vertex operator associated to the state $\big|\vec{T}\big\rangle$. Here h_1, h_2 and h_3 are a set of familiar conformal transformations reviewed in [9]. For illustration purposes consider three tachyon harmonics t_n, t_m and t_{n+m}, with $n \neq m \neq 0$. Such

fields contribute to $\mathcal{V}$ the following interaction

$$\frac{1}{3}\cdot 6\cdot\frac{t_n}{2}\cdot\frac{t_m}{2}\cdot\frac{t_{n+m}}{2}\cdot 2\,\langle\, h_1\circ(ce^{\frac{inX}{R}})(0)\; h_2\circ(ce^{\frac{imX}{R}})(0)\; h_3\circ(ce^{\frac{-i(n+m)X}{R}})(0)\rangle \quad (3.29)$$

The factor (1/3) is in the definition of $\mathcal{V}$. The factor of 6 appears because this is the number of ways three different fields can be assigned to the three punctures in the disk. Then come the fields, and then a factor of two, as there are two momentum conserving combinations giving equal contributions. Evaluation of the above gives

$$\frac{1}{2}\,t_n\,t_m\,t_{n+m}\,K^{3-\frac{1}{R^2}(n^2+m^2+(n+m)^2)}, \quad K\equiv\frac{3\sqrt{3}}{4} \quad (3.30)$$

Slightly different combinatorics are required for terms of the form $t_0t_n^2$ and $t_n^2t_{2n}$. Combining all such terms together we obtain

$$\begin{aligned}\mathcal{V}(t_0,t_1,\cdots)^{(3)} &= \frac{1}{3}K^3t_0^3+\frac{1}{2}\sum_{n=1}^{\infty}t_0\,t_n^2\;K^{3-\frac{2n^2}{R^2}}+\frac{1}{4}\sum_{n=1}^{\infty}t_n^2\,t_{2n}\;K^{3-\frac{6n^2}{R^2}}\\ &\quad+\frac{1}{2}\sum_{n\geq 1}^{\infty}\sum_{m>n}^{\infty}t_n\,t_m\,t_{n+m}\,K^{3-\frac{2}{R^2}(n^2+m^2+nm)}\,. \quad (3.31)\end{aligned}$$

Equations (3.27) and (3.31) give the complete potential for the tachyon tower.

3.2 Calculating the action in the level expansion for $R=\sqrt{3}$

In this section we will consider different truncation levels to calculate the lump tension. For this we will write explicitly the action at different levels. Though we will work with a fixed radius $R=\sqrt{3}$, all our equations will contain R as a variable for further use. Once we know the action we can solve the equations of motion numerically for the one-lump solution by giving a nonzero initial value to t_1. At the end of the section, we will be able to study the convergence of our level truncation scheme by using both (3.17) and (3.18).

Level	Fields
0	t_0
1/3	t_1
4/3	t_2
2	$u_0,\ v_0,\ w_0$
7/3	$u_1,\ v_1,\ w_1,\ z_1$
3	t_3

Table 3.1: The list of fields appearing at various levels when $R = \sqrt{3}$.

We will do these calculations at levels $(1/3, 2/3)$, $(4/3, 8/3)$, $(2, 4)$, $(7/3, 14, 3)$ and $(3, 6)$. This will require the fields listed in Table 3.1 with their respective levels (using (3.19), (3.20) and (3.21)). In order to study the truncation method at various levels, we define $V(m, n)$ to be the part of the whole potential satisfying the three following conditions:

1. All terms in $V(m, n)$ have level n.

2. All terms in $V(m, n)$ contain only fields of level smaller than or equal to m.

3. All terms in $V(m, n)$ contain at least one field of level m.

This definition ensures that various $V(m, n)$'s are disjoint (i.e. $V(m, n)$ and $V(m', n')$ don't contain common terms for $(m, n) \neq (m', n')$). It now follows that the total potential at level (M, N) is given by

$$\mathcal{V}_{(M,N)} = \sum_{m \leq M} \sum_{n \leq N} V(m, n) \tag{3.32}$$

We shall now compute $V(m, n)$ for $m \leq 3$ and $n \leq 6$. Though here we will restrict ourselves to levels (M, N) of the form $(M, 2M)$, eq.(3.32) and the results for $V(m, n)$ given below can be used to construct the potential $\mathcal{V}_{(M,N)}$ for arbitrary level (M, N)

as long as $M \leq 3$ and $N \leq 6$. We shall first list all possible terms appearing in each $V(m,n)$ consistent with momentum conservation, separating the quadratic and cubic terms. We then use the methods described in Section 3.1 to explicitly calculate the coefficients of each possible term in the $V(m,n)$'s.

The list of interactions that must be computed is generated conveniently with the help of the following function:

$$\begin{aligned}\mathcal{Z}(x,y,s) \equiv \prod_{n=0}^{\infty}\Big\{&\Big(1-t_n x(y^n+y^{-n})s^{n^2/R^2}\Big)\Big(1-u_n x(y^n+y^{-n})s^{2+n^2/R^2}\Big)\\ &\Big(1-v_n x(y^n+y^{-n})s^{2+n^2/R^2}\Big)\Big(1-w_n x(y^n+y^{-n})s^{2+n^2/R^2}\Big)\\ &\Big(1-z_{n+1} x(y^{n+1}+y^{-n-1})s^{2+(n+1)^2/R^2}\Big)\cdots\Big\}^{-1}\end{aligned} \tag{3.33}$$

Here the formal variables x, y and s are used to count number of fields, momentum, and level, respectively. If we write

$$\mathcal{Z}(x,y,s) = \sum_{m,n} \mathcal{Z}(m,n,s)\, x^m y^n\,. \tag{3.34}$$

The momentum conserving cubic interactions appear in $\mathcal{Z}(3,0,s)$ and an expansion in s gives

$$\mathcal{Z}(3,0,s) = \sum_{l} \mathcal{Z}(l)\, s^l\,. \tag{3.35}$$

Let $\{\psi^i\}$ denote the complete set of modes $(t_n, u_n, \cdots)$. Then $\mathcal{Z}(l)$ has an expression of the form $\mathcal{Z}(l) \sim \sum a_{ijk}\psi^i\psi^j\psi^k$ where each a_{ijk} is an integer. If $a_{ijk} \neq 0$ the interaction $\psi^i\psi^j\psi^k$ must be included in the level l contribution to the potential. Thus $\mathcal{Z}(l)$ supplies the complete list of momentum conserving cubic interactions of level l. When useful, we split by hand the terms in $\mathcal{Z}(l)$ to obtain the possible terms which appear in various $V(m,l)$'s.

The list of all terms for the various $V(m,n)$'s with $n \leq 6$ (and $R = \sqrt{3}$) are given in Table 3.2.

	Quadratic terms	Cubic terms
$V(0,0)$	t_0^2	t_0^3
$V(1/3,2/3)$	t_1^2	$t_0t_1^2$
$V(4/3,2)$		$t_1^2t_2$
$V(2,2)$		$t_0^2u_0,\ t_0^2v_0,\ t_0^2w_0$
$V(4/3,8/3)$	t_2^2	$t_0t_2^2$
$V(2,8/3)$		$t_1^2u_0,\ t_1^2v_0,\ t_1^2w_0$
$V(7/3,8/3)$		$t_0t_1u_1,\ t_0t_1v_1,\ t_0t_1w_1,\ t_0t_1z_1$
$V(2,4)$	$u_0^2,\ v_0^2,\ w_0^2$	$t_0u_0^2,\ t_0v_0^2,\ t_0w_0^2,\ t_0u_0v_0,\ t_0u_0w_0,\ t_0v_0w_0$
$V(7/3,4)$		$t_1t_2u_1,\ t_1t_2v_1,\ t_1t_2w_1,\ t_1t_2z_1$
$V(2,14/3)$		$t_2^2u_0,\ t_2^2v_0,\ t_2^2w_0$
$V(7/3,14/3)$	$u_1^2,\ v_1^2,\ w_1^2,\ z_1^2,$ v_1z_1	$t_0u_1^2,\ t_0v_1^2,\ t_0w_1^2,\ t_0u_1v_1,\ t_0u_1w_1,\ t_0v_1w_1,$ $t_1u_0u_1,\ t_1u_0v_1,\ t_1u_0w_1,\ t_1v_0u_1,\ t_1v_0v_1,$ $t_1v_0w_1,\ t_1w_0u_1,\ t_1w_0v_1,\ t_1w_0w_1,$ $t_0z_1^2,\ t_0u_1z_1,\ t_0v_1z_1,\ t_0w_1z_1,$ $t_1u_0z_1,\ t_1v_0z_1,\ t_1w_0z_1$
$V(3,14/3)$		$t_1t_2t_3$
$V(2,6)$		$u_0^3,\ v_0^3,\ w_0^3,\ u_0^2v_0,\ u_0^2w_0,\ u_0v_0^2,\ u_0w_0^2,\ v_0^2w_0$ $v_0w_0^2,\ u_0v_0w_0,$
$V(7/3,6)$		$t_2u_1^2,\ t_2v_1^2,\ t_2w_1^2,\ t_2u_1v_1,\ t_2u_1w_1,\ t_2v_1w_1,$ $t_2z_1^2,\ t_2u_1z_1,\ t_2v_1z_1,\ t_2w_1z_1$
$V(3,6)$	t_3^2	$t_0t_3^2$

Table 3.2: Quadratic terms and interactions appearing at various levels when $R = \sqrt{3}$.

3.2.1 The terms in the potential

The explicit interactions corresponding to the various terms appearing in the table will be listed here. With $K = \frac{3\sqrt{3}}{4}$, as in eq.(3.30), we have at the lowest level:

$$V(0,0) = -\frac{1}{2}t_0^2 + \frac{1}{3}K^3 t_0^3 . \tag{3.36}$$

At first nontrivial level we have:

$$V(1/3,2/3) = -\frac{1}{4}\left(1-\frac{1}{R^2}\right)t_1^2 + \frac{1}{2}K^{3-2/R^2}t_0 t_1^2 . \tag{3.37}$$

At level 2 we have:

$$\begin{aligned} V(4/3,2) &= \frac{1}{4}K^{3-6/R^2}t_1^2 t_2 \\ V(2,2) &= \frac{K}{32}t_0^2\left(22\,u_0 - 5\,(v_0+25w_0)\right) . \end{aligned} \tag{3.38}$$

At level 8/3 :

$$\begin{aligned} V(4/3,8/3) &= -\frac{1}{4}\left(1-\frac{4}{R^2}\right)t_2^2 + \frac{1}{2}K^{3-8/R^2}t_0 t_2^2 \\ V(2,8/3) &= K^{1-2/R^2}t_1^2\left(\frac{11}{32}u_0 + \frac{1}{2}\left(\frac{1}{R^2}-\frac{5}{32}\right)v_0 - \frac{125}{64}w_0\right) \\ V(7/3,8/3) &= \frac{1}{32}K^{1-2/R^2}t_0 t_1\left(22u_1 - \left(5+\frac{16}{R^2}\right)v_1 - 125w_1 + \left(\frac{-44}{R^2}+\frac{32}{R^4}\right)z_1\right) . \end{aligned} \tag{3.39}$$

At level 4:

$$\begin{aligned} V(2,4) &= -\frac{1}{2}u_0^2 + \frac{1}{4}(v_0^2+25w_0^2) + K\left\{\frac{1}{576}t_0\left(76\,u_0^2+179\,v_0^2+9475\,w_0^2\right)\right. \\ &\left. +\frac{625}{864}\,t_0 v_0 w_0 - \frac{55}{432}\,t_0 u_0(v_0+25w_0)\right\} \end{aligned}$$

$$V(7/3,4) = \frac{1}{64}K^{1-6/R^2}t_1t_2\left(22u_1 - \left(5 - \frac{48}{R^2}\right)v_1 - 125w_1 + \left(-\frac{44}{R^2} + \frac{288}{R^4}\right)z_1\right). \tag{3.40}$$

At level 14/3:

$$\begin{aligned}
V(2,\frac{14}{3}) &= \frac{1}{64}K^{1-8/R^2}t_2^2\left(22u_0 - \left(5 - \frac{128}{R^2}\right)v_0 - 125w_0\right) \\
V(\frac{7}{3},\frac{14}{3}) &= \frac{1}{8}\left(1+\frac{1}{R^2}\right)\left(-2u_1^2 + \left(1+\frac{8}{R^2}\right)v_1^2 + 25w_1^2\right. \\
&\quad \left. + \left(\frac{8}{R^2} + \frac{16}{R^4}\right)z_1^2 + \frac{24}{R^2}v_1z_1\right) \\
&\quad + K^{1-2/R^2}\left\{\frac{19}{288}t_0u_1^2 + \frac{1}{3456}\left(537 + \frac{8864}{R^2} + \frac{256}{R^4}\right)t_0v_1^2 + \frac{28425}{3456}t_0w_1^2\right. \\
&\quad - \frac{11}{864}t_0u_1\left(\left(5+\frac{16}{R^2}\right)v_1 + 125w_1\right) + \frac{125}{1728}\left(5+\frac{16}{R^2}\right)t_0v_1w_1 \\
&\quad + \frac{19}{144}t_1u_0u_1 - \frac{11}{864}t_1u_0\left(\left(5+\frac{16}{R^2}\right)v_1 + 125w_1\right) \\
&\quad - \frac{11}{864}\left(5-\frac{32}{R^2}\right)t_1v_0u_1 + \frac{1}{1728}\left(537 + \frac{944}{R^2} - \frac{512}{R^4}\right)t_1v_0v_1 \\
&\quad + \frac{25}{1728}\left(25 - \frac{160}{R^2}\right)t_1v_0w_1 - \frac{1375}{864}t_1w_0u_1 + \frac{25}{1728}\left(25+\frac{80}{R^2}\right)t_1w_0v_1 \\
&\quad + \frac{28425}{1728}t_1w_0w_1 + \frac{1}{216}\frac{1}{R^2}\left(384 + \frac{1145}{R^2} + \frac{336}{R^4} + \frac{64}{R^6}\right)t_0z_1^2 \\
&\quad + \frac{11}{864}\frac{1}{R^2}\left(-44 + \frac{32}{R^2}\right)t_0u_1z_1 + \frac{1}{432}\left(\frac{2359}{R^2} + \frac{1672}{R^4} - \frac{128}{R^6}\right)t_0v_1z_1 \\
&\quad + \frac{125}{432}\frac{1}{R^2}\left(11 - \frac{8}{R^2}\right)(t_0w_1z_1 + t_1w_0z_1) \\
&\quad \left. + \frac{1}{864}\frac{1}{R^2}\left(11\left(-44+\frac{32}{R^2}\right)t_1u_0z_1 + \left(2158 - \frac{2832}{R^2} + \frac{512}{R^4}\right)t_1v_0z_1\right)\right\}
\end{aligned}$$

$$V(3,\frac{14}{3}) = \frac{1}{2}K^{3-14/R^2}t_1t_2t_3\,. \tag{3.41}$$

And at level 6:

$$
\begin{aligned}
V(2,6) \;=\; & K\left\{\frac{1}{144}u_0^3+\frac{8321}{93312}v_0^3-\frac{219775}{10368}w_0^3-\frac{95}{7776}u_0^2\left(v_0+25w_0\right)\right. \\
& \left.+\frac{1969}{15552}u_0v_0^2+\frac{104225}{15552}u_0w_0^2-\frac{22375}{31104}v_0^2w_0-\frac{47375}{31104}v_0w_0^2+\frac{6875}{23328}u_0v_0w_0\right\}
\end{aligned}
$$

$$
\begin{aligned}
V(\frac{7}{3},6) \;=\; & K^{1-6/R^2}\left\{\frac{19}{576}t_2u_1^2+\frac{1}{2304}\left(179-\frac{1696}{R^2}+\frac{768}{R^4}\right)t_2v_1^2+\frac{9475}{2304}t_2w_1^2\right. \\
& -\frac{11}{1728}\left(5-\frac{48}{R^2}\right)t_2u_1v_1-\frac{1375}{1728}t_2u_1w_1+\frac{1}{72}\left(\frac{625}{48}-\frac{125}{R^2}\right)t_2v_1w_1 \\
& +\frac{1}{144}\left(-\frac{128}{R^2}+\frac{723}{R^4}-\frac{2064}{R^6}+\frac{1728}{R^8}\right)t_2z_1^2+\frac{11}{432}\left(\frac{-11}{R^2}+\frac{72}{R^4}\right)t_2u_1z_1 \\
& \left.+\frac{1}{288}\left(-\frac{67}{R^2}-\frac{808}{R^4}+\frac{1152}{R^6}\right)t_2v_1z_1+\frac{125}{864}\left(\frac{11}{R^2}-\frac{72}{R^4}\right)t_2w_1z_1\right\}
\end{aligned}
$$

$$
V(3,6) \;=\; \frac{1}{4}\left(-1+\frac{9}{R^2}\right)t_3^2+\frac{1}{2}K^{3-18/R^2}t_0t_3^2\,. \tag{3.42}
$$

3.2.2 Potentials at various truncation levels and mass calculations

From these formulae one can construct the potentials at various truncation levels using (3.32). As we will use them, we give below the explicit sums for $\mathcal{V}_{(1/3,2/3)}$, $\mathcal{V}_{(4/3,8/3)}$, $\mathcal{V}_{(2,4)}$, $\mathcal{V}_{(7/3,14/3)}$ and $\mathcal{V}_{(3,6)}$:

$$
\begin{aligned}
\mathcal{V}_{(1/3,2/3)} &= V(0,0)+V(1/3,2/3) \\
\mathcal{V}_{(4/3,8/3)} &= \mathcal{V}_{(1/3,2/3)}+V(4/3,2)+V(4/3,8/3) \\
\mathcal{V}_{(2,4)} &= \mathcal{V}_{(4/3,8/3)}+V(2,2)+V(2,8/3)+V(2,4) \\
\mathcal{V}_{(7/3,14/3)} &= \mathcal{V}_{(2,4)}+V(7/3,8/3)+V(7/3,4)+V(2,14/3)+V(7/3,14/3) \\
\mathcal{V}_{(3,6)} &= \mathcal{V}_{(7/3,14/3)}+V(3,14/3)+V(2,6)+V(7/3,6)+V(3,6)
\end{aligned} \tag{3.43}
$$

Field	(1/3, 2/3)	(4/3, 8/3)	(2, 4)	(7/3, 14/3)	(3, 6)
t_0	0.181034	0.214757	0.25703	0.265131	0.269224
t_1	-0.344389	-0.343566	-0.384575	-0.394396	-0.394969
t_2	...	-0.0955972	-0.107424	-0.12046	-0.125011
u_0	...	...	0.0888087	0.0900609	0.0969175
v_0	...	...	-0.00675676	-0.0175367	-0.0172906
w_0	...	...	0.0317837	0.0299617	0.0320394
u_1	...	...	...	-0.0643958	-0.0648543
v_1	...	...	...	0.0540447	0.0505836
w_1	...	...	...	-0.0187778	-0.0189058
z_1	...	...	...	-0.0698363	-0.0665402
t_3	...	...	...	...	-0.0142169

Table 3.3: The values of various modes of the string field at the stationary point of the potential for $R = \sqrt{3}$ calculated at various levels of approximation.

In general, the potential at a given level has many extrema. Two of them will be of particular interest for us:

1. We always find a translationally invariant minimum $\vec{T}_{vac}$ corresponding to the tachyon condensation. At this minimum, all fields with nonzero momentum have zero vev. We will use this solution when calculating the ratio $r^{(2)}$ defined in eq.(3.18).

2. If we start the numerical algorithm with initial values near $t_0 \approx 0.25$ and $t_1 \approx -0.4$ then our numerical algorithm converges to the one-lump solution $\vec{T}_{lump}$ that we are interested in.

The solution $\vec{T}_{vac}$ can be found in Chapter 2 or refs. [15, 19]. In Table 3.3 we give the solutions $\vec{T}_{lump}$ at various truncation levels. Having found $\vec{T}_{vac}$ and $\vec{T}_{lump}$ we can now calculate the ratio of the lump mass to the D0-brane mass using the two different

Level	$r^{(1)}$	$r^{(2)}$
$(1/3; 2/3)$	1.32002	0.77377
$(4/3; 8/3)$	1.25373	0.707471
$(2; 4)$	1.11278	1.02368
$(7/3; 14/3)$	1.07358	0.984467
$(3, 6)$	1.06421	0.993855

Table 3.4: The ratio of the calculated mass of the lump to the mass of the D0 brane in the two schemes described in equations (3.17) and (3.18).

methods (3.17) and (3.18). The results are given in Table 3.4. We see that the first method gives a monotonically decreasing lump mass whereas the second method is oscillating but gives a lump mass much closer to the expected mass.

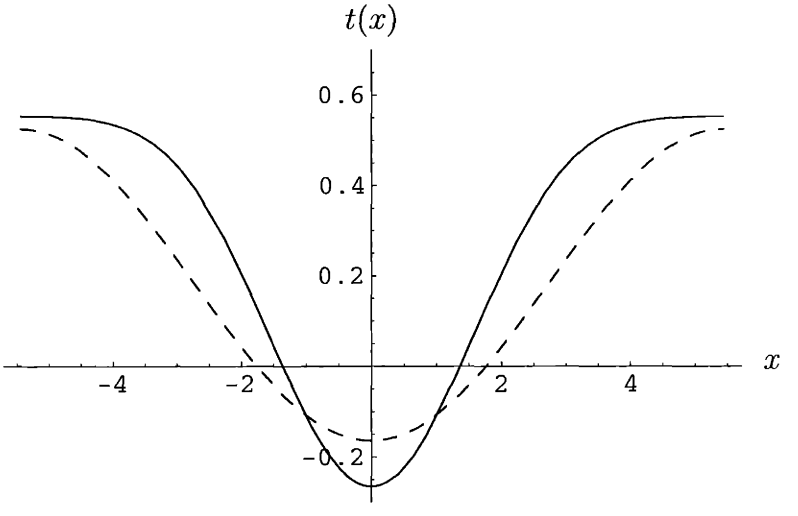

Figure 3-1: The dashed line shows a plot of $t(x)$ for $R = \sqrt{3}$ at level (1/3, 2/3) approximation. The solid line shows the plot of $t(x)$ for $R = \sqrt{3}$ at the level (3,6) approximation.

It is instructive to plot the profile of the tachyon field:

$$t(x) = \sum_n t_n \cos \frac{nx}{R}\,, \tag{3.44}$$

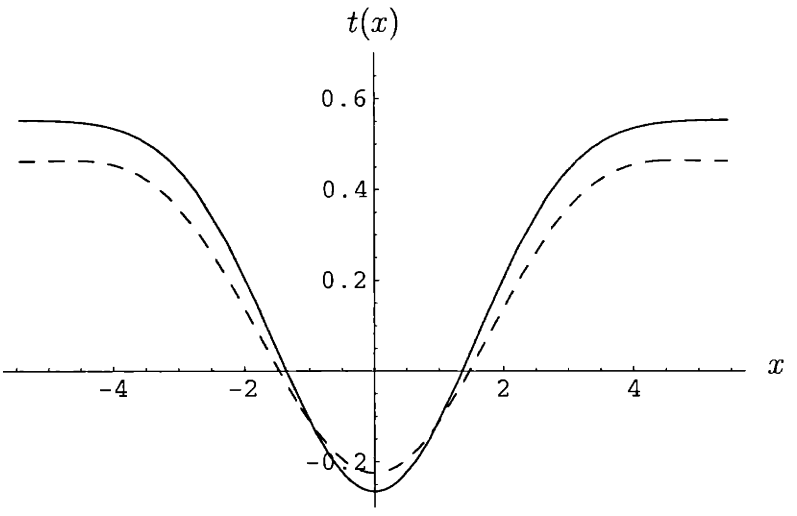

Figure 3-2: The dashed line shows a plot of $t(x)$ for $R = \sqrt{3}$ at level (4/3, 8/3) approximation. The solid line shows the plot of $t(x)$ for $R = \sqrt{3}$ at the level (3,6) approximation.

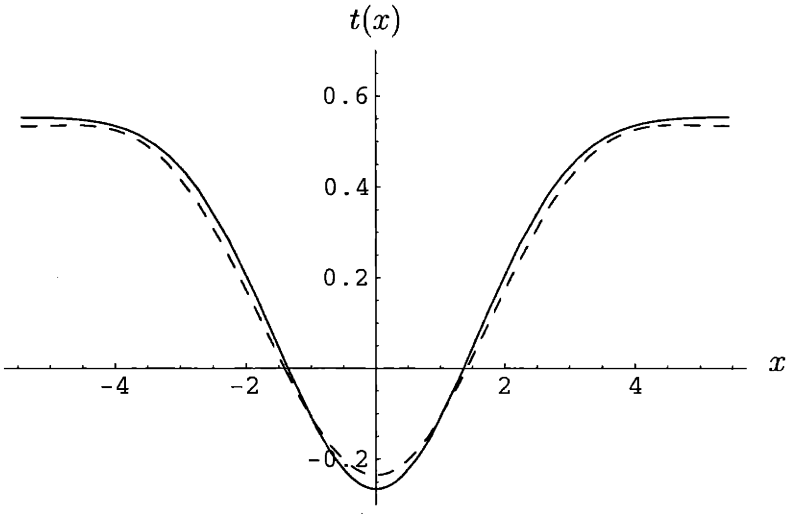

Figure 3-3: The dashed line shows a plot of $t(x)$ for $R = \sqrt{3}$ at level (2, 4) approximation. The solid line shows the plot of $t(x)$ for $R = \sqrt{3}$ at the level (3,6) approximation.

as a function of x and compare them at different approximations. In Figures 3-1 to 3-4 we have plotted the tachyon profiles at the level (1/3,2/3), (4/3,8/3), (2,4) and (7/3,14/3) approximation respectively, each of them being superimposed on the tachyon profile at the level (3,6) approximation.

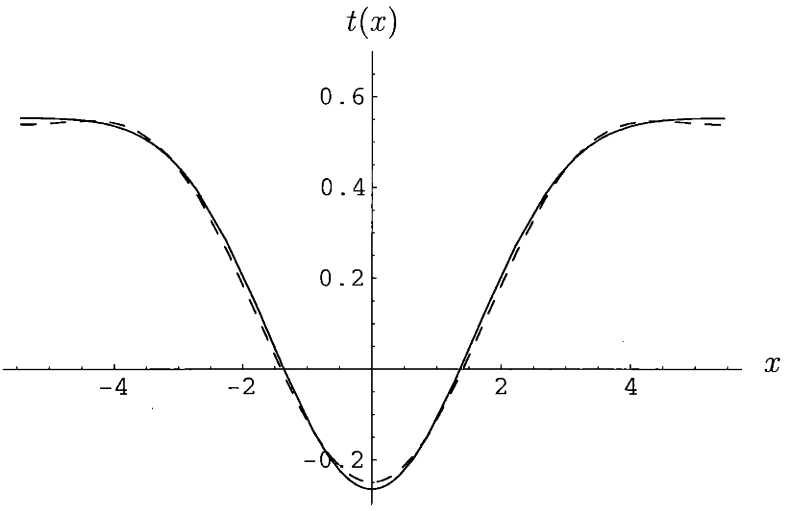

Figure 3-4: The dashed line shows a plot of $t(x)$ for $R = \sqrt{3}$ at level (7/3, 14/3) approximation. The solid line shows the plot of $t(x)$ for $R = \sqrt{3}$ at the level (3,6) approximation.

For future use, we shall now define two new functions F_0 and G_0 as follows:

$$\begin{aligned} F_0(t_0, t_1, t_2, u_0, v_0, w_0, u_1, v_1, w_1, z_1; R) &= \mathcal{V}_{(\frac{7}{3}, \frac{14}{3})}, \\ G_0(t_0, t_1, t_2, u_0, v_0, w_0, u_1, v_1, w_1, z_1; R) &= \mathcal{V}_{(3,6)} - V(3,6) - V(2, 14/3) - V(7/3, 4) \\ &\quad -V(7/3, 6) - V(3, 14/3) \end{aligned} \tag{3.45}$$

where $\mathcal{V}_{(\frac{7}{3}, \frac{14}{3})}$ and $\mathcal{V}_{(3,6)}$ have been defined in eqs.(3.36)-(3.43). The right hand side of this equation has to be interpreted as a function of the various modes $t_0, \ldots z_1$ and R, *without R being set to* $\sqrt{3}$. The function F_0 and G_0 defined here will be useful in constructing the potential $\mathcal{V}_{(M,N)}$ for other values of R, as will be discussed in the next section.

3.3 Tachyon lump at other radii

In this section we shall discuss the construction of the tachyonic lump solution on circles of radii other than $\sqrt{3}$, and compare the results with those obtained for $R = \sqrt{3}$. As the basic techniques have already been discussed in the previous two sections,

in this section we shall only quote the results.

3.3.1 $R > \sqrt{3}$

First we need to decide which values of R we shall use to study the lump. Although this choice is arbitrary, there is slight simplification of counting levels if we choose R such that the level of u_1, v_1, w_1 and z_1 coincide with that of one of the harmonics (say t_n) of the tachyon field. This requires

$$2 + \frac{1}{R^2} = \frac{n^2}{R^2}, \qquad \rightarrow \qquad R = \sqrt{\frac{n^2-1}{2}}. \tag{3.46}$$

We shall consider the values $n = 4, 5, 6$ corresponding to $R = \sqrt{\frac{15}{2}}, \sqrt{12}, \sqrt{\frac{35}{2}}$. In each case we shall be using the level $(2 + \frac{1}{R^2}, 4 + \frac{2}{R^2})$ approximation to the potential. For this we need to include up to the n-th harmonic of the tachyon field t and the first harmonics of the fields u, v, w and z.

For these additional R values all interactions present in $\mathcal{V}_{(\frac{7}{3},\frac{14}{3})}$ at $R = \sqrt{3}$ are still present. We need, however, further interactions as can be checked using the generating function (3.33). These additional interactions can be expressed in terms of the following functions:

$$\begin{aligned}
& F_1(t_0, \cdots, t_4, u_0, v_0, w_0, u_1, v_1, w_1, z_1; R) \\
= \; & -\frac{1}{4}\Big(1 - \frac{9}{R^2}\Big)t_3^2 - \frac{1}{4}\Big(1 - \frac{16}{R^2}\Big)t_4^2 \\
& + \frac{1}{2}K^{3-18/R^2} t_0 t_3^2 + \frac{1}{2}K^{3-32/R^2} t_0 t_4^2 + \frac{1}{2}K^{3-14/R^2} t_1 t_2 t_3 \\
& + \frac{1}{4}K^{3-24/R^2} t_2^2 t_4 + \frac{1}{2}K^{3-26/R^2} t_1 t_3 t_4 \\
& + \Big(\frac{11}{32}u_1 - \frac{125}{64}w_1 + \Big(\frac{25}{2R^4} - \frac{11}{16R^2}\Big)z_1 + \Big(\frac{11}{4R^2} - \frac{5}{64}\Big)v_1\Big) K^{1-14/R^2} t_2 t_3
\end{aligned} \tag{3.47}$$

$$F_2(t_0, \cdots, t_5, u_0, v_0, w_0, u_1, v_1, w_1, z_1; R)$$

$$
\begin{aligned}
= & -\frac{1}{4}\Big(1-\frac{25}{R^2}\Big)t_5^2+\frac{1}{2}K^{3-38/R^2}\,t_2\,t_3\,t_5+\frac{1}{2}K^{3-42/R^2}\,t_1\,t_4\,t_5+\frac{1}{2}K^{3-50/R^2}\,t_0\,t_5^2 \\
& +\Big(\frac{11}{32}u_0+\Big(-\frac{5}{64}+\frac{9}{2R^2}\Big)v_0-\frac{125}{64}w_0\Big)K^{1-18/R^2}t_3^2 \\
& +\Big(\frac{11}{32}u_1+\Big(-\frac{5}{64}+\frac{23}{4R^2}\Big)v_1-\frac{125}{64}w_1+\Big(\frac{49}{2R^4}-\frac{11}{16R^2}\Big)z_1\Big)K^{1-26/R^2}\,t_3\,t_4
\end{aligned}
\tag{3.48}
$$

$$
\begin{aligned}
& F_3(t_0,\cdots,t_6,u_0,v_0,w_0,u_1,v_1,w_1,z_1;R) \\
= & -\frac{1}{4}\Big(1-\frac{36}{R^2}\Big)t_6^2+\frac{1}{4}\,K^{3-54/R^2}\,t_3^2\,t_6+\frac{1}{2}\,K^{3-56/R^2}\,t_2\,t_4\,t_6+\frac{1}{2}K^{3-62/R^2}\,t_1\,t_5\,t_6 \\
& +\frac{1}{2}K^{3-72/R^2}\,t_0\,t_6^2+\Big(\frac{11}{32}\,u_0+\Big(-\frac{5}{64}+\frac{8}{R^2}\Big)\,v_0-\frac{125}{64}\,w_0\Big)\,K^{1-32/R^2}\,t_4^2\,.
\end{aligned}
\tag{3.49}
$$

We shall now write down our results for level $(2+\frac{1}{R^2},4+\frac{2}{R^2})$ approximation for the potential for $R^2=(n^2-1)/2$ in terms of the functions $F_0,\ldots F_3$ defined in eqs.(3.45), (3.47)-(3.49). These are as follows:

$$
\begin{aligned}
& \mathcal{V}_{(32/15,64/15)}(t_0,\cdots,t_4,u_0,v_0,w_0,u_1,v_1,w_1,z_1;R=\sqrt{15/2}) \\
= & \; F_0(t_0,t_1,t_2,u_0,v_0,w_0,u_1,v_1,w_1,z_1;R=\sqrt{15/2}) \\
& +F_1(t_0,\cdots,t_4,u_0,v_0,w_0,u_1,v_1,w_1,z_1;R=\sqrt{15/2})\,,
\end{aligned}
\tag{3.50}
$$

$$
\begin{aligned}
& \mathcal{V}_{(25/12,25/6)}(t_0,\cdots,t_5,u_0,v_0,w_0,u_1,v_1,w_1,z_1;R=\sqrt{12}) \\
= & \; F_0(t_0,t_1,t_2,u_0,v_0,w_0,u_1,v_1,w_1,z_1;R=\sqrt{12}) \\
& +F_1(t_0,\cdots,t_4,u_0,v_0,w_0,u_1,v_1,w_1,z_1;R=\sqrt{12}) \\
& +F_2(t_0,\cdots,t_5,u_0,v_0,w_0,u_1,v_1,w_1,z_1;R=\sqrt{12})\,,
\end{aligned}
\tag{3.51}
$$

$$
\begin{aligned}
& \mathcal{V}_{(72/35,144/35)}(t_0,\cdots,t_6,u_0,v_0,w_0,u_1,v_1,w_1,z_1;R=\sqrt{35/2}) \\
= & \; F_0(t_0,t_1,t_2,u_0,v_0,w_0,u_1,v_1,w_1,z_1;R=\sqrt{35/2})
\end{aligned}
$$

Field	$R=\sqrt{15/2}$	$R=\sqrt{12}$	$R=\sqrt{35/2}$	$R=\sqrt{11/10}$
t_0	0.363333	0.401189	0.424556	0.0804185
t_1	-0.308419	-0.255373	-0.218344	-0.31707
t_2	-0.19463	-0.190921	-0.176679	-0.00983574
t_3	-0.0849552	-0.122721	-0.132269	...
t_4	-0.0248729	-0.0575418	-0.0830114	...
t_5	...	-0.0210929	-0.0409281	...
t_6	...	...	-0.0178687	...
u_0	0.118792	0.131499	0.139048	0.0318155
v_0	0.0131977	0.020668	0.0263317	-0.0591248
w_0	0.0380389	0.0417417	0.0438076	0.0132021
u_1	-0.0712708	-0.0629211	-0.0567058	-0.0052739
v_1	-0.0958004	-0.0657449	-0.0476215	-0.0119114
w_1	-0.0181708	-0.0150031	-0.0131234	-0.000863176
z_1	0.0860302	0.058747	0.0418645	0.00570249

Table 3.5: The values of various modes of the string field at the stationary point of the potential for different radii.

$$
\begin{aligned}
&+F_1(t_0,\cdots,t_4,u_0,v_0,w_0,u_1,v_1,w_1,z_1;R=\sqrt{35/2})\\
&+F_2(t_0,\cdots,t_5,u_0,v_0,w_0,u_1,v_1,w_1,z_1;R=\sqrt{35/2})\\
&+F_3(t_0,\cdots,t_6,u_0,v_0,w_0,u_1,v_1,w_1,z_1;R=\sqrt{35/2})\,. \qquad (3.52)
\end{aligned}
$$

As in the previous section, we can find a tachyonic lump solution by starting with a non-zero seed value of t_1. The numerical solutions are given in Table 3.5. The result for the two ratios $r^{(1)}$ and $r^{(2)}$, defined in eqs.(3.17) and (3.18) are given in Table 3.6.

In Figures 3-5 to 3-7 we have plotted the tachyon field $t(x)$ defined in eq.(3.44) as a function of x for each of the three values of R. For reference we have also plotted on

R	$r^{(1)}$	$r^{(2)}$
$\sqrt{15/2}$	1.14625	1.00535
$\sqrt{12}$	1.19147	1.01324
$\sqrt{35/2}$	1.23876	1.02353
$\sqrt{11/10}$	1.02175	0.979149

Table 3.6: The ratio of the calculated mass of the lump to the mass of the D0 brane at various radii in the two schemes described in equations (3.17) and (3.18).

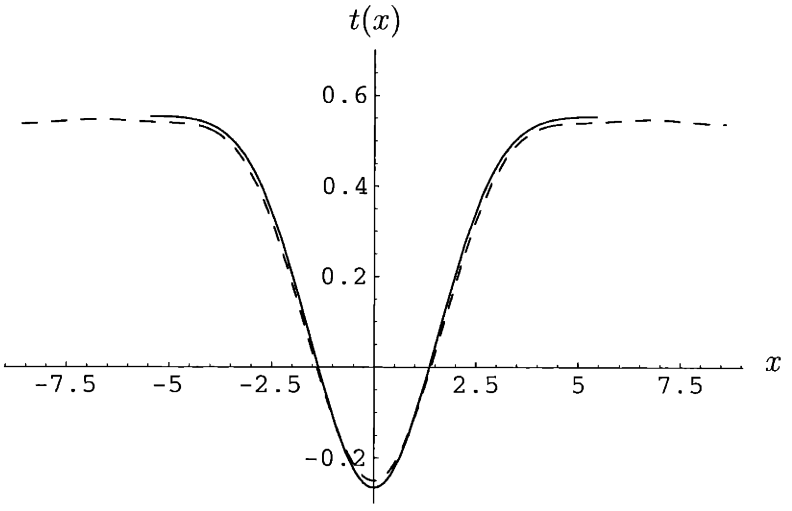

Figure 3-5: The dashed line shows a plot of $t(x)$ for $R = \sqrt{15/2}$ at level (32/15, 64/15) approximation. The solid line spanning a smaller range of x shows the plot of $t(x)$ for the level (3,6) approximation at $R = \sqrt{3}$.

the same graph the function $t(x)$ obtained in the level (3,6) approximation for $R = \sqrt{3}$. As is seen from these figures, the tachyon profiles for different radii are almost undistinguishable from each other even though they are obtained as superpositions of harmonics of very different wave-lengths.

3.3.2 $R < \sqrt{3}$

Finally we would like to study how the shape of the soliton changes when R is small. For this we take $R = \sqrt{1.1}$ and work at the level (40/11, 80/11) approximation of the

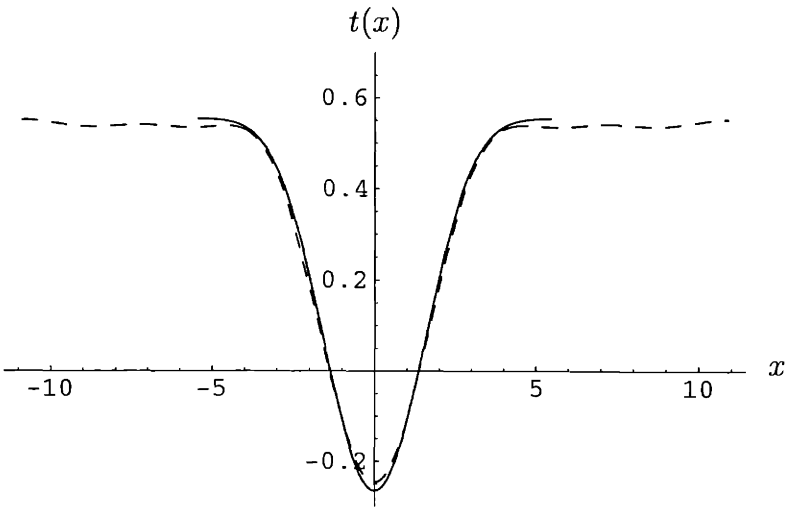

Figure 3-6: The dashed line shows a plot of $t(x)$ for $R = \sqrt{12}$ at level (25/12, 25/6) approximation. The solid line spanning a smaller range of x shows the plot of $t(x)$ for the level (3,6) approximation at $R = \sqrt{3}$.

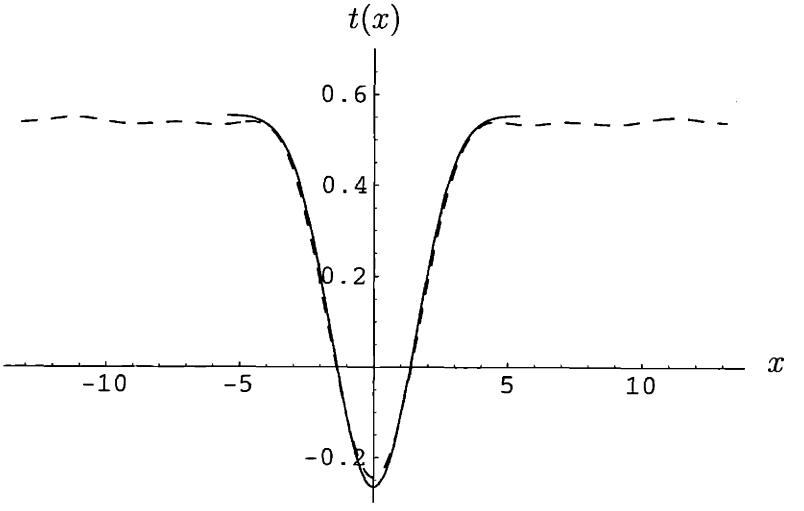

Figure 3-7: The dashed line shows a plot of $t(x)$ for $R = \sqrt{35/2}$ at level (72/35, 144/35) approximation. The solid line spanning a smaller range of x shows the plot of $t(x)$ for the level (3,6) approximation at $R = \sqrt{3}$.

potential. One can show that to this level of approximation the potential is given by,

$$\begin{aligned} & \mathcal{V}_{(40/11,80/11)}(t_0, t_1, t_2, u_0, v_0, w_0, u_1, v_1, w_1, z_1; R = \sqrt{1.1}) \\ = \; & G_0(t_0, t_1, t_2, u_0, v_0, w_0, u_1, v_1, w_1, z_1; R = \sqrt{1.1}) \,, \end{aligned} \tag{3.53}$$

where G_0 has been defined in eq.(3.45). The tachyonic lump solution for this potential is given in Table 3.5. The results for the two ratios $r^{(1)}$ and $r^{(2)}$ defined in eqs.(3.17) and (3.18) are given in Table 3.6.

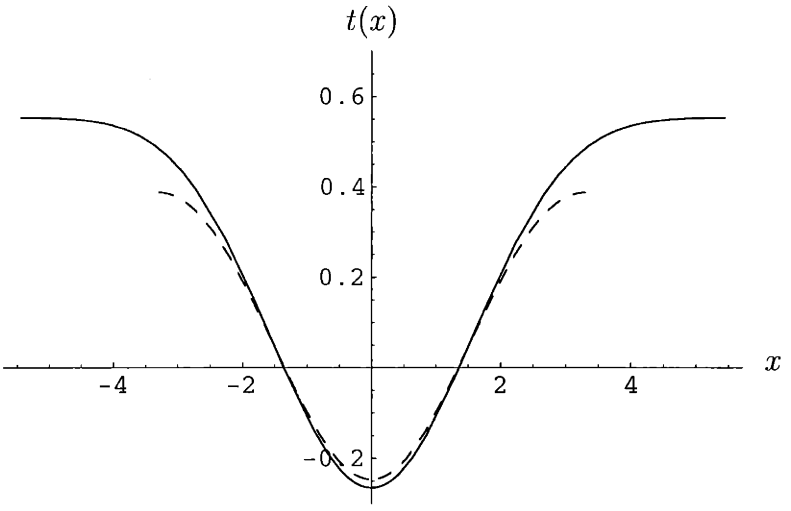

Figure 3-8: The dashed line shows a plot of $t(x)$ for $R = \sqrt{11/10}$ at level (40/11, 80/11) approximation. The solid line spanning a smaller range of x shows the plot of $t(x)$ for the level (3,6) approximation at $R = \sqrt{3}$.

We have displayed in Figure 3-8 the tachyon profile, superimposed on the tachyon profile for the level (3,6) approximation at $R = \sqrt{3}$. As can be seen from this figure, for $R = \sqrt{11/10}$ there is not enough room for the full lump solution to fit in, but the profile of the lump at smaller radius follows closely the profile at larger radius near the core.

3.3.3 Size of the lump

We can estimate the size of the lump at different radii in a somewhat systematic way by fitting the lump profile with a gaussian curve of the form:

$$G(x) = a + b \cdot e^{-x^2/(2\sigma^2)} . \tag{3.54}$$

We calculate the parameters a, b and σ using a nonlinear regression algorithm on a set of points chosen on the lump profile in the following way. For $R \geq \sqrt{3}$:

Radius	a	b	σ
$\sqrt{3}$	0.559814	-0.828599	1.52341
$\sqrt{15/2}$	0.546313	-0.804112	1.5595
$\sqrt{12}$	0.544226	-0.801652	1.54089
$\sqrt{35/2}$	0.54328	-0.799957	1.54477
$\sqrt{11/10}$	0.451678	-0.702596	1.41847

Table 3.7: The result for the best fit of the profile of the lump with the gaussian curve described in eq.(3.54).

- We take 100 points, regularly spaced in x, in the core of the lump from $x = -\sqrt{3}\pi$ to $x = \sqrt{3}\pi$.

- We take a smaller density of points, regularly spaced in x, on the rest of the circle (where the profile is essentially flat). Here we have taken 20, 30 and 40 points for $R = \sqrt{15/2}$, $R = \sqrt{12}$ and $R = \sqrt{35/2}$ respectively.

In the case of $R = \sqrt{11/10}$, we take 100 points from $x = -\sqrt{11/10}\pi$ to $x = \sqrt{11/10}\pi$

The results of the regression at the different radii are given in Table 3.7. We see that the size of the lump, which can be defined as a multiple of σ, is essentially independent of the radius (it increases by about 1.5 % when R increases from $\sqrt{3}$ to $\sqrt{35/2}$). Even when there is not enough room for the lump to fit in ($R = \sqrt{11/10}$), the lump is only slightly compressed (by about 7 %). A reasonable definition for the size would be $6\,\sigma$, with the solution extending by $3\,\sigma$ both along the positive and the negative x-axis. With this convention, the lump will have a size of approximately $9.3\sqrt{\alpha'}$. This is close to the answer obtained in ref.[29].

3.4 Conclusions and open questions

In this chapter we have developed and tested the level expansion method in string field theory beyond translationally invariant vacuum solutions. This enabled us to

give a systematic method for calculating quantities related to tachyon lumps and to give an accurate description of D-branes as tachyonic lumps in bosonic string field theory. Given the accuracy of our calculations (about 1% typically) we are confident that the profile of the lump that we have found is indeed very close to the exact one. As we have seen, as long as the radius is sufficiently big the lump has a definite radius independent profile. Indeed, when approximated by a gaussian, the lump representing a D-brane has $\sigma \simeq 1.55\sqrt{\alpha'}$. We also considered the profile of the tachyon lump for $R = \sqrt{1.1\alpha'}$, a radius sufficiently small that the large radius profile of the lump does not fit on the circle. We saw that the bottom part of the lump is essentially unchanged.

There are some questions related to the present work that we have not addressed. In particular we have not produced a lump solution in string field theory for $R = 1$, where the tachyon harmonic t_1 becomes exactly marginal and the D0 and D1 branes have the same mass. Presumably, for small $(R^2 - 1)$ one must go fairly high in the level expansion to produce an accurate description. We have also not discussed the case $R < 1$, where the D0 brane is unstable against decay into the D1 brane, or into the translationally invariant vacuum. We have also not tried to describe several D0 branes, all located at the same position.

We have not discussed issues related to the size of the lump representing a D-brane. While in the conformal field theory description a D-brane is an object with a well defined position, in string field theory it is a fat object, with thickness of the order of the string scale. Since string field theory is a gauge theory one may wonder if the size is an artifact of the chosen gauge. We do not at present know the answer to this question. The simplest way to get some insight into the nature of this extended solution would be to try to find out the energy density. This fails since the string field theory action is nonlocal, and hence there is no known expression for energy density in this theory. It would be interesting to examine some physical question that could help interpret the nature of this size [64]. According to the conjectures of refs.[7, 40, 41, 43], all physical quantities calculated in the background of the lump solution must agree with those calculated in the background of a lower dimensional

D-brane.

The methods used in this chapter should be able to deal with:

- Neveu-Schwarz string field theory, where tachyon kinks rather than lumps represent lower dimensional D-branes. One way to deal with the boundary conditions on a circle would be to place both a kink and an anti-kink at diametrically opposite points of the circle. Another, probably more efficient way would be to include a Wilson line along the circle in such a way that the tachyon boundary conditions are twisted [5].

- Higher codimension D-branes. In [29] it was observed that as the codimension is increased the naive use of the tachyon "bounce" gave increasingly worse approximations to the lump mass. We believe that our methods will enable calculations to any desired accuracy. The simplest situation would involve making two of the original brane dimensions into circles and including harmonics in both directions by simple extension of the methods of Section 3.1.2.

- Intersecting D-branes. The simplest setup would be to begin with a D2-brane on a torus and generate a pair of transverse D1 branes intersecting at one point.

We hope that our analysis will ultimately provide a more refined understanding of string field theory and its geometry. One application is already apparent; if we could get a formulation of string field theory around the translationally invariant vacuum where the original D-brane is no longer present, such formulation will have more unbroken symmetries than the current formulation.

It is interesting to note that the level expansion method used here incorporates into the calculational scheme an ultra-violet (UV) cutoff. Since $l = p^2 + \cdots$, working at fixed l implies a upper bound to the momentum (in the spatial directions). From this one is naturally led to propose a level expansion method for *quantum string field theory*. One approach could be to use the Euclidean version of the theory, and make periodic all directions including time[65], thus turning, at any fixed level M, the set of all relevant fields into a set of expansion coefficients c_n, with $l(|\phi_n\rangle) \leq M$. Since

we are setting the whole system in a box, we also have a natural infra-red cutoff. The whole quantum path integral $\int \prod [dc_n] \exp(-S(c_n)/\hbar)$ could then be evaluated.[9] Alternatively, one could make all dimensions except time periodic. In this case the result would be the quantum mechanics of the wave functions $c_n(t)$. It would be exciting if the level expansion gave a concrete calculational definition of quantum string field theory, a definition one could in practice feed to a computer in order to calculate observables to any desired degree of precision.

[9]Here S should be the truncation, to the given level of approximation, of the full quantum action satisfying the exact quantum Batalin-Vilkovisky master equation. It is not clear that the cubic open string field theory provides such solution[66, 67]. The open-closed string field theory introduced in ref. [68] does provide a well defined quantum action, but due to the non-polynomial nature of the action it is not clear how to carry out the level expansion in this theory.

Chapter 4

Codimension two lump solutions in string field theory and in tachyonic theories

In Chapter 3, a level truncation scheme has been developed which takes non-zero momentum into account. Applied to lump solutions in one dimension, it gave numerical results for the ratio of the tension of a D-p-brane and a D-$(p-1)$-brane with a precision of about 1%. In [69], de Mello Koch and Rodrigues applied this scheme to construct 2-dimensional lumps in open bosonic string field theory.

In this chapter, we want to present independent results on 2-dimensional lumps. We also describe these lumps in two theories involving only the tachyon: pure tachyonic SFT (string field theory in which we keep only the tachyon, including its higher derivatives), with action ([53]):

$$S = -2\pi^2 T_{25} \int d^{26}x \left(\frac{1}{2}\partial_\mu \phi \, \partial^\mu \phi - \frac{1}{2}\phi^2 + \frac{1}{3}K^3 \tilde{\phi}^3 \right) , \tag{4.1}$$

where T_{25} is the D-25-brane tension, $K = 3\sqrt{3}/4$ and $\tilde{\phi} = K^{\partial_\mu \partial^\mu}\phi$. And pure ϕ^3 theory (the usual scalar ϕ^3 theory of a tachyon, which doesn't include higher derivatives), with action

$$S = -2\pi^2 T_{25} \int d^{26}x \left(\frac{1}{2}\partial_\mu \phi \, \partial^\mu \phi - \frac{1}{2}\phi^2 + \frac{1}{3}K^3 \phi^3 \right) , \tag{4.2}$$

the only difference being that here we have ϕ^3 instead of $\tilde{\phi}^3$.

4.1 Calculating the potential

We will use the notation of Chapter 3, but we will compactify two dimensions, instead of one, on a torus. Let us name x and y the compact dimensions. We impose the identifications

$$\begin{aligned} x &\sim x + 2\pi R \,, \\ y &\sim y + 2\pi R \,. \end{aligned} \tag{4.3}$$

The x- and y-momenta will be quantized:

$$\begin{aligned} p_x &= m/R \,, \\ p_y &= n/R \,. \end{aligned} \tag{4.4}$$

For each zero-momentum state $|\Phi_i\rangle$ that appears in the non-compact theory, we will have states labeled by two indices $|\Phi_{i,mn}\rangle$ with levels

$$l(\Phi_{i,mn}) = l(\Phi_i) + (m^2 + n^2)/R^2 \,. \tag{4.5}$$

By definition, when we work at level (M, N), we keep fields of level $\leq M$, and terms in the potential of total level $\leq N$. In this chapter, we will work in string field theory at level (2, 4) and in pure tachyonic theories at arbitrary levels. Therefore all the fields we need are:

$$\begin{aligned} |T_{mn}\rangle &= \begin{cases} c_1 \cos\left(\frac{m\,x}{R}\right) \cos\left(\frac{n\,y}{R}\right) |0\rangle \;, & m = n \\ c_1 \left(\cos\left(\frac{m\,x}{R}\right) \cos\left(\frac{n\,y}{R}\right) + \cos\left(\frac{n\,x}{R}\right) \cos\left(\frac{m\,y}{R}\right)\right) |0\rangle \;, & m \neq n \end{cases} \\ |U_{00}\rangle &= c_{-1} |0\rangle \\ |V_{00}\rangle &= c_1 \left(L^X_{-2} + L^Y_{-2}\right) |0\rangle \\ |W_{00}\rangle &= c_1 L'_{-2} |0\rangle \,, \end{aligned} \tag{4.6}$$

where L^X_{-2} and L^Y_{-2} are Virasoro generators of the CFT of the compact dimensions x and y respectively, and L'_{-2} is a Virasoro generator of the CFT of the 24-dimensional co-space. The definition of $|T_{mn}\rangle$ ensures that the solutions we will find are symmetric under $x \leftrightarrow y$ as well as under $x \to -x$ and $y \to -y$. We will thus use the string field:

$$\left|\vec{T}\right\rangle = \sum_{m \leq n} t_{mn} \left|T_{mn}\right\rangle + u_{00} \left|U_{00}\right\rangle + v_{00} \left|V_{00}\right\rangle + w_{00} \left|W_{00}\right\rangle , \tag{4.7}$$

where the sum is restricted by the level truncation, the level of each field being

$$l(T_{mn}) = (m^2 + n^2)/R^2 \quad , \quad l(U_{00}) = l(V_{00}) = l(W_{00}) = 2 \ . \tag{4.8}$$

We will not repeat here how to calculate the potential $\mathcal{V}_{MN}(\vec{T})$ at level (M, N). We refer to Chapters 2 and 3 and the literature (see for example [20, 15, 30, 19, 71]). Note however that in theories involving only the tachyon, the coefficients of the terms in the potential can be calculated straightforwardly, the only difficulties being to keep track of momentum conservation at the vertex and to figure out the combinatorial factors. We have written computer codes calculating the potentials in the following theories:

- string field theory at arbitrary radius up to level (2, 4).
- pure tachyonic sft at arbitrary radius and arbitrary level.
- pure ϕ^3 theory at arbitrary radius and arbitrary level.

4.2 Codimension two lumps

4.2.1 String field theory truncated at level (2,4)

Before showing results, let us say a few words about how to find these lumps given the potential. In general, the tachyon potential has many extrema. In doing computations at high level, it might be difficult to setup the convergence on the right branch. The

method we've used here[1] is to go backwards: We know the approximate shape of the lump we are looking for, from it one can calculate its Fourier expansion. We can then plug these Fourier coefficients into our algorithm finding solutions of the equations of motion (by Newton's method). If we start the numerical algorithm with a seed close enough to the solution we want, it is fairly probable that it will converge to the sought solution.

Let us present our result in string field theory at level $(2, 4)$. In order to compare our result with [69], we have computed it at $R = \sqrt{3}$. Figure 4-1 shows a plot of the solution.

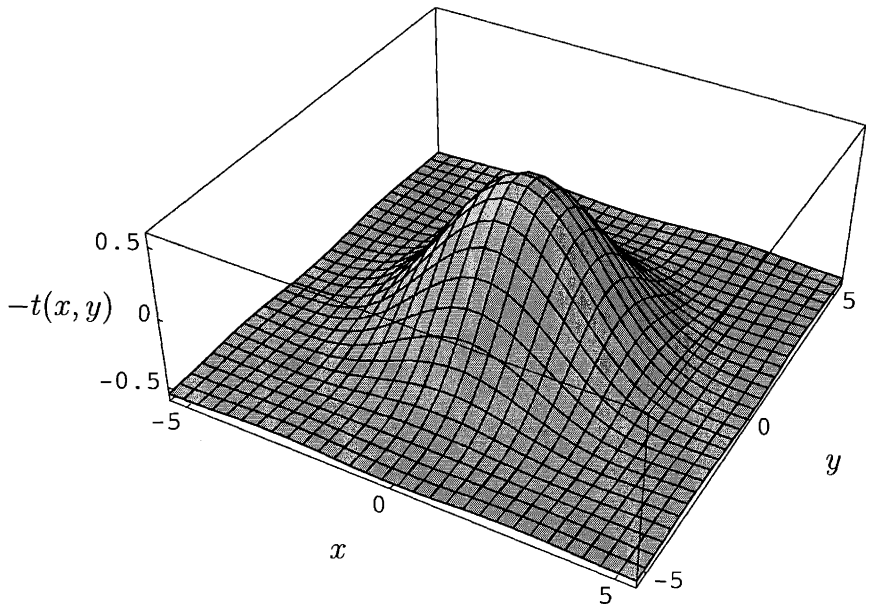

Figure 4-1: A lump in sft at level (2, 4) with $R = \sqrt{3}$. The plot represents $-t(x, y)$ as a function of x and y.

The ratio of the tension of a D-p-brane and a D-$(p-2)$-brane, when divided by its expected value $(2\pi)^2$, can be approximated by (see Chapter 3):

$$r^{(2)} \equiv R^2 \left(2\pi^2 \mathcal{V}_{(M,N)}(\vec{T}_{lump}) - 2\pi^2 \mathcal{V}_{(M,N)}(\vec{T}_{vac})\right), \tag{4.9}$$

where $\vec{T}_{lump}$ is the lump solution, $\vec{T}_{vac}$ is the solution corresponding to the true vacuum

[1] I thank B. Zwiebach for this suggestion.

at the given truncation level (M, N) and $\mathcal{V}_{(M,N)}$ is the potential at level (M, N). With our solution above, we find

$$r^{(2)}_{(2,4)} = 1.13025 \ , \tag{4.10}$$

13% away from the expected value of unity.[2]

To show that the size of the lump is, in the large radius limit, independent of the radius, let us compare with the solution at $R = 3$ (Figure 4-2). To compare the sizes

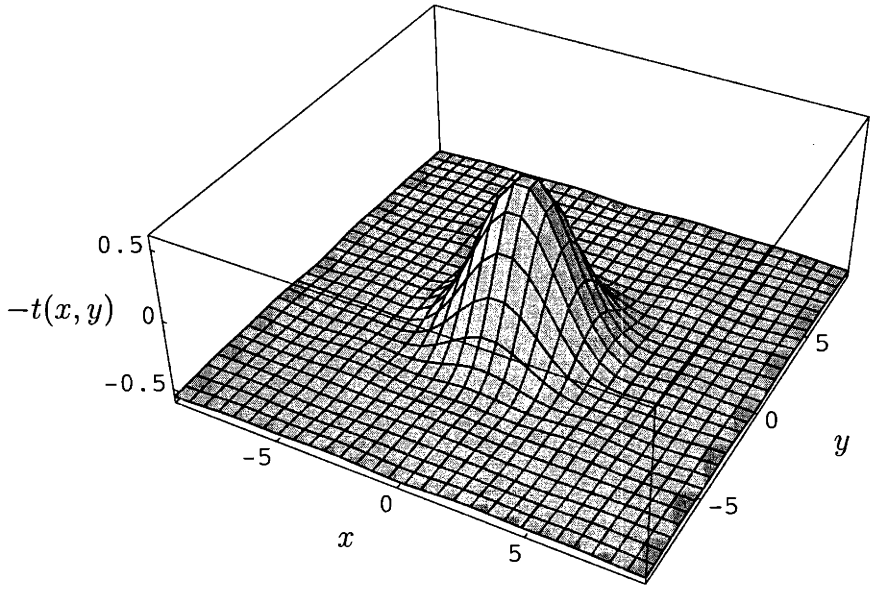

Figure 4-2: A lump in sft at level (2, 4) with $R = 3$. The plot represents $-t(x, y)$ as a function of x and y.

of this lumps, we plot together their profiles $-t(x, 0)$. Figure 4-3 clearly shows the radius-independence of the shape of the lump.

4.2.2 Pure tachyonic string field theory and pure ϕ^3 theory

We do find codimension two lump solutions in these theories. In Figure 4-4, we show the profiles $-t(x, 0)$ of the lumps in the three different theories. We have taken the three lumps to be at level (2, 4) with $R = 3$. The different asymptotic values of $t(x, 0)$ show the different vev's of the tachyon in the three theories.

[2]This number is in total agreement with the result in [69].

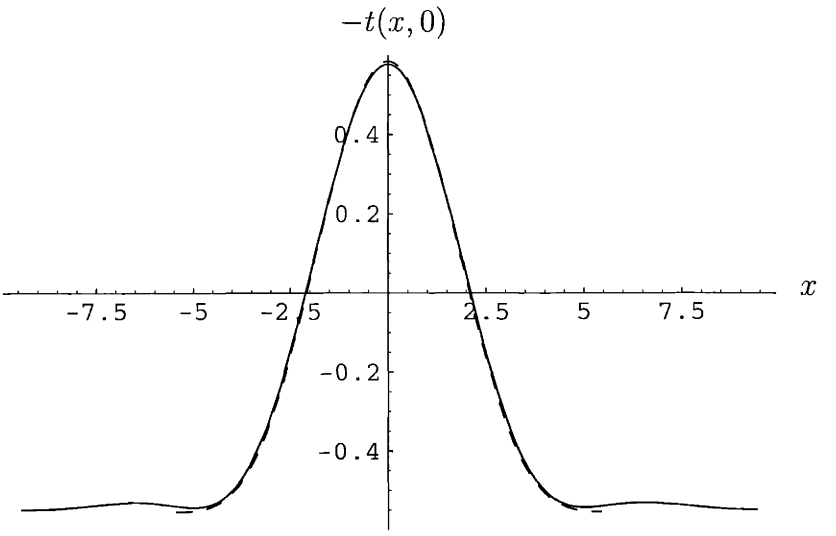

Figure 4-3: The dashed curve is the profile $-t(x,0)$ of the lump solution in sft at $R=\sqrt{3}$, the solid curve is the profile $-t(x,0)$ of the lump solution at $R=3$

The pure tachyonic theories are much more tractable for numerical computations. We have written codes giving the actions at arbitrary level. To illustrate the convergence of the level truncation scheme we show, in Figures 4-5 and 4-6, the lump profiles at different truncation levels.

It is interesting to see that the solution in pure ϕ^3 theory converges much slower than in pure tachyonic sft. This is due to the fact that in pure tachyonic sft, the coefficient of the term $t_{m_1n_1}t_{m_2n_2}t_{m_3n_3}$ in the potential is proportional to

$$K^{3-(m_1^2+n_1^2+m_2^2+n_2^2+m_3^2+n_3^2)/R^2}.$$

Since $K>1$, at high level these terms are much less important than in pure ϕ^3 theory where the same coefficients are proportional to K^3.

4.3 Conclusions

We do find codimension two lumps solutions in all three theories considered in this chapter. Note that there is an apparent conflict with Derrick's theorem which states that solitons in scalar field theory can exist only in codimension <2. But one of the

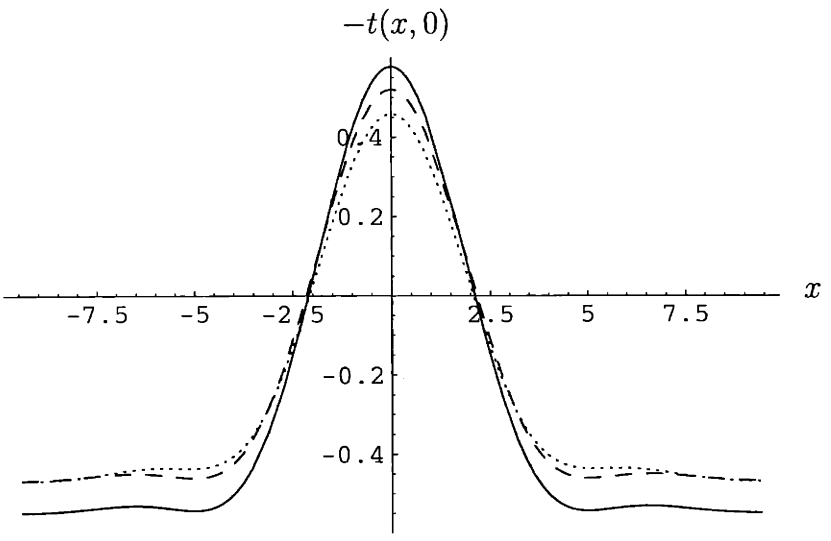

Figure 4-4: Lump profiles $-t(x,0)$ in string field theory (solid curve), pure tachyonic sft (dashed curve) and pure ϕ^3 theory (dotted curve) at level (2, 4) and $R = 3$.

assumptions used in the proof of the theorem is that the potential must be bounded below, which is not the case in the theories considered here.[3] This negativity allows the existence of solutions, as shown in [29].

As it is easy to use, pure tachyonic sft is an interesting toy model of full string field theory. We saw that it converges very fast when the truncation level is increased. Moreover we found a lump solution of approximately the same shape as in sft, this may show that we can study other kinds of sft solitons (like intersecting branes) by using the pure tachyonic approximation (work in progress [72]).

Finally, we saw the amusing fact that string field theory, due to the coefficients $K^{3-\text{level}}$ in front of every term, seems to be better fit for level truncation than the simple ϕ^3 theory which converges very slowly as the level is increased.

[3] I wish to thank B. Zwiebach for pointing this out.

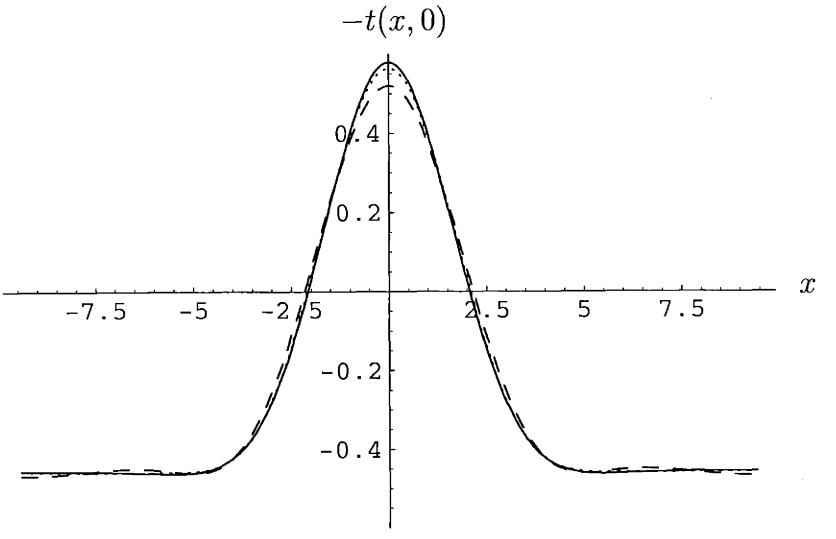

Figure 4-5: Lump profiles $-t(x,0)$ in pure tachyonic sft with $R = 3$, at level (2, 4) (dashed curve), (3, 9) (dotted curve) and (10, 30) (solid curve)

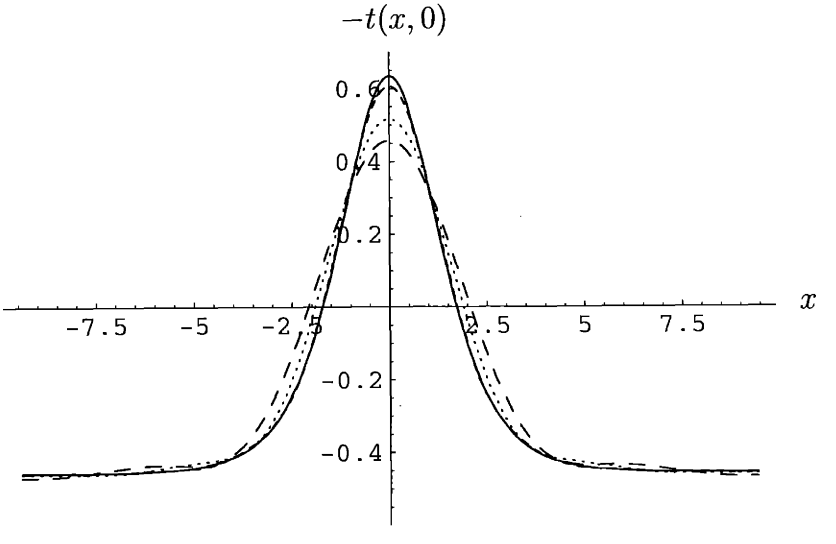

Figure 4-6: Lump profiles $-t(x,0)$ in pure ϕ^3 theory with $R = 3$, at level (2, 4) (big-dashed curve), (3, 9) (dotted curve), (7, 21) (small-dashed curve), and (20, 60) (solid curve)

Chapter 5

The identity string field and the tachyon vacuum

Thus far, Sen's first and third conjectures have been shown to be true to a very high level of accuracy; they have also been proved analytically in Boundary String Field Theory [10, 11, 12]. The second conjecture however, is still puzzling.

Let us clarify the meaning of this conjecture. From a physical point of view, after the tachyon condenses to the vacuum, the corresponding D-brane system disappears and there is no place for open strings to end on. Therefore at least all perturbative conventional open string excitations (of ghost number 1) should decouple from the theory. There has been a lot of work to check this statement, for example [83, 84, 85, 86, 87, 88, 89, 90, 92, 93, 94, 95]. In particular, using level truncation, [96] verifies that the scalar excitations at even levels (the Q-closed scalar fields, where Q is the BRST charge) are also Q-exact to very high accuracy.

However, as proposed in [97, 98] there is a little stronger version for the second conjecture. There, Rastelli, Sen and Zwiebach suggest that after a field redefinition, the new BRST operator may be taken[1] to be simply c_0, or more generally a linear combination of operators of the form $(c_n + (-)^n c_{-n})$. For such a new BRST operator, not only should the conventional excitations of ghost number 1 disappear, but more precisely the full cohomology of any ghost number of the new BRST operator around

[1]The first String Field Theory action with pure ghost kinetic operator was written down in [99].

the tachyon vacuum vanishes.[2] Hence these authors propose that Sen's second conjecture should hold in such a stronger level. In fact, Sen's second conjecture suggests also that around the tachyon vacuum, there should be only closed string dynamics. However, we will not touch upon the issue of closed strings here and leave the reader to the references [93, 100, 101, 105].

Considering the standing of the second conjecture, it is the aim of this chapter to address to what degree does it hold, i.e., whether the cohomology of the BRST operator in the true vacuum is trivial only for ghost number one fields or for fields of any ghost number. We will give evidence which shows that the second conjecture holds in the strong sense, and is hence consistent with the proposal in [97, 98].

Our discussion relies heavily upon the existence of a string field $\mathcal{I}$ of ghost number zero which is the identity of the $\star$-product. It satisfies

$$\mathcal{I} \star \psi = \psi \star \mathcal{I} = \psi$$

for any state[3] ψ. The state $\mathcal{I}$ was first constructed in the oscillator basis in [32]. Then a recent work [71] gave a recursive way of constructing the identity in the (background independent) total-Virasoro basis which shows its universal property in string field theory. As a by-product of our analysis, we have found a new and elegant analytic expression for $\mathcal{I}$ without recourse to the complicated recursions.

We recall that the BRST operator around the nonperturbative vacuum Ψ_0 is given by

$$Q_{\Psi_0}\phi = Q_B\phi + \Psi_0 \star \phi - (-1)^{\phi}\phi \star \Psi_0 \,. \tag{5.1}$$

Ignoring anomalies, the fact that Q_{Ψ_0} is a derivation of the $\star$-algebra implies that $\mathcal{I}$ is Q_{Ψ_0} closed. And the problem is to determine whether it is also Q_{Ψ_0} exact, i.e.,

[2] An evidence for the triviality of a subset of the discrete ghost number one cohomology was presented recently in [22] which complemented [96].

[3] There are some mysteries regarding of the identity. For example, in [71] the authors showed that this identity string field is subject to anomalies, with consequences that $\mathcal{I}$ may be the identity of the $\star$-algebra only on a subspace of the whole Hilbert space. In the following, we will first assume that $\mathcal{I}$ behaves well on the whole Hilbert space, and postpone some discussions thereupon to Section 5.3.

if there exists a ghost number -1 field A, such that $\mathcal{I} = Q_{\Psi_0} A$. If so, then for an arbitrary Q_{Ψ_0}-closed state ϕ we would have

$$\begin{aligned} Q_{\Psi_0}(A \star \phi) &= (Q_{\Psi_0} A) \star \phi - A \star (Q_{\Psi_0} \phi) \\ &= \mathcal{I} \star \phi \\ &= \phi, \end{aligned}$$

where in the second step, we used the fact that ϕ is Q_{Ψ_0}-closed, and in the last step, that $\mathcal{I}$ acts as the identity on ϕ. This means that any Q_{Ψ_0}-closed field ϕ is also Q_{Ψ_0}-exact, in other words, the entire cohomology of Q_{Ψ_0} is trivial. Our endeavor will be to use the level truncation scheme to find a string field A satisfying

$$Q_{\Psi_0} A = \mathcal{I}. \tag{5.2}$$

For a general solution ψ of the equations of motion, equation (5.2) can be written $Q_\psi A = Q_B A + \psi \star A + A \star \psi = \mathcal{I}$. For a general ψ, the string field A will not exist. For example in the perturbative vacuum, $\psi = 0$, Q_ψ is simply Q_B. It is easy to show here that there is no solution for A because the Q_B action preserves levels while $\mathcal{I}$ has a component at level one (namely $|0\rangle$), but the minimum level of a ghost number -1 state A is 3. Indeed, for a more general solution $\psi \neq 0$ (such as the tachyon vacuum), the star product will not preserve the level and so it may be possible to find A.

The chapter is structured as follows. We start, in Section 5.1, by presenting a new closed and simple form for the identity string field. In Section 5.2, we use two different methods to find the state A: one without gauge fixing and the other, in the Feynman-Siegel gauge. They give the results up to an accuracy of 2.4% and 3.2% respectively. In Section 5.3, we discuss the behaviour of $\mathcal{I}$ under level truncation and perform a few consistency checks on our approximations. Finally, in Section 5.4 we make some concluding remarks and address some further problems and directions.

5.1 The identity string field

To solve the condition (5.2), we first need an explicit expression of the identity $\mathcal{I}$. Such an expression has been presented in [32] and [71], differing by a mere normalization factor $-4i$. In this chapter, we will follow the conventions of [71] which has[4]

$$
\begin{aligned}
|\mathcal{I}\rangle &= e^{L_{-2}-\frac{1}{2}L_{-4}+\frac{1}{2}L_{-6}-\frac{7}{12}L_{-8}+\frac{2}{3}L_{-10}+\cdots}|0\rangle && (5.3)\\
&= |0\rangle + L_{-2}|0\rangle + \frac{1}{2}(L_{-2}^2 - L_{-4})|0\rangle \\
&\quad + \left(\frac{1}{6}L_{-2}^3 - \frac{1}{4}L_{-2}L_{-4} - \frac{1}{4}L_{-4}L_{-2} + \frac{1}{2}L_{-6}\right)|0\rangle \\
&\quad + \left(\frac{1}{24}L_{-2}^4 + \frac{1}{4}(L_{-2}L_{-6} + L_{-6}L_{-2}) + \frac{1}{8}L_{-4}^2 - \frac{7}{12}L_{-8}\right. \\
&\qquad \left. -\frac{1}{12}(L_{-2}^2L_{-4} + L_{-2}L_{-4}L_{-2} + L_{-4}L_{-2}^2)\right)|0\rangle && (5.4)\\
&\quad + \ldots && (5.5)
\end{aligned}
$$

where $L_n = L_n^m + L_n^g$, the sum of the ghost (L_n^g) and matter (L_n^m) parts, is the total Virasoro operator. For later usage we have expanded the exponential up to level 9. Furthermore, we split L_n into matter and ghost parts and expand the latter into b_n, c_n operators as
$L_m^g := \sum_{n=-\infty}^{\infty}(2m-n) : b_n c_{m-n} : -\delta_{m,0}$. In other words, we write the states in the so-called "Universal Basis" [71].

As a by-product, we have found an elegant expression for $\mathcal{I}$ which avoids the recursions[5] needed to generate the coefficients in the exponent. In fact, one can show that only L_{-m} for m being a power of 2 survive in the final expression, thus significantly reducing the complexity of the computation of level-truncation for $\mathcal{I}$:

$$
|\mathcal{I}\rangle = \left(\prod_{n=2}^{\overleftarrow{\infty}} \exp\left(-\frac{2}{2^n}L_{-2^n}\right)\right) e^{L_{-2}}|0\rangle \qquad (5.6)
$$

[4]With the normalization $\langle c_1, c_1, c_1\rangle = 3$ that we are using in this chapter, we should scale this expression by a factor of $K^3/3$, where $K = 3\sqrt{3}/4$. However, as the normalization of the identity will not change our analysis, we will use this right normalization only in Section 5.3, where we are dealing with expressions like $\mathcal{I} \star \Phi$.

[5]The expression given in [32] has no recursion either, however their oscillator expansion is not normal-ordered due to ghost insertions at the string mid-point.

$$= \quad \ldots \exp\left(-\frac{2}{2^3}L_{-2^3}\right) \exp\left(-\frac{2}{2^2}L_{-2^2}\right) \exp\left(L_{-2}\right)|0\rangle \ ,$$

where the left arrow means that the Virasoro's of higher index stack to the left. The rest of this section is devoted to the proof of this equation.

To prove (5.6), let us consider its BPZ conjugate form[6]

$$\langle \mathcal{I}| = \langle 0| U_h U_{f_2} U_{f_3} U_{f_4} \ldots \ , \tag{5.7}$$

where $U_{f_n} = e^{-\frac{2}{2^n}L_{2^n}}$ for $n \geq 2$ and $U_h = e^{L_2}$. In [71], the identity is given by $\langle \mathcal{I}| = \langle 0| U_{f_\mathcal{I}}$ where $U_{f_\mathcal{I}}$ is the operator corresponding to the function

$$f_\mathcal{I}(z) = \frac{z}{1-z^2} \, .$$

Using the composition law $U_{g_1} U_{g_2} = U_{g_1 \circ g_2}$, what we need to prove is therefore

$$U_h U_{f_2} U_{f_3} U_{f_4} \ldots = U_{h \circ f_2 \circ f_3 \circ \ldots} = U_{f_\mathcal{I}} \ ,$$

which is equivalent to proving

$$\lim_{k \to \infty} h \circ f_2 \circ \ldots \circ f_k(z) = f_\mathcal{I}(z) = \frac{z}{1-z^2} \, . \tag{5.8}$$

For the operator $U_f = e^{aL_n}$, the corresponding function f is given by [63]

$$f(z) = \exp\left(az^{n+1}\partial_z\right) z = \frac{z}{(1-anz^n)^{1/n}} \ ,$$

so we have

$$\begin{aligned} h(z) &= \frac{z}{(1-2z^2)^{1/2}} \\ f_n(z) &= \frac{z}{(1+2z^{2^n})^{1/2^n}} \, . \end{aligned}$$

[6]Notice that, besides the replacement $L_n \to (-1)^n L_{-n}$, the orders under BPZ-conjugation are also reversed. This is because we use L_n instead of the oscillators α_m, whose orders do not get reversed under BPZ.

A useful property of f_n is that $f_n(z) = (g(z^{2^n}))^{1/2^n}$, where

$$g(z) \equiv \frac{z}{1+2z} = \frac{1}{2+\frac{1}{z}}.$$

Before calculating the left hand side of (5.8) in the general case, let us first illustrate the method on an example:

$$\begin{aligned} f_2 \circ f_3 \circ f_4(z) &= f_2 \circ f_3[(g[z^{2^4}])^{1/2^4}] \\ &= f_2[(g[((g[z^{2^4}])^{1/2^4})^{2^3}])^{1/2^3}] \\ &= f_2[(g[g^{1/2}[z^{2^4}]])^{1/2^3}] \\ &= (g[((g[g^{1/2}[z^{2^4}]])^{1/2^3})^{2^2}])^{1/2^2} \\ &= (g[g^{1/2}[g^{1/2}[z^{2^4}]]])^{1/2^2} \\ &= (g^{1/2}[g^{1/2}[g^{1/2}[z^{2^4}]]])^{1/2}. \end{aligned}$$

Now it is easy to see that the general form is

$$h \circ f_2 \circ f_3 \circ \ldots \circ f_{k+1}(z) = h \circ (\underbrace{g^{\frac{1}{2}} \circ \ldots \circ g^{\frac{1}{2}}}_{k}(z^{2^{k+1}}))^{\frac{1}{2}}.$$

Thus (5.8) is equivalent to showing that

$$\lim_{k\to\infty} \underbrace{g^{\frac{1}{2}} \circ \ldots \circ g^{\frac{1}{2}}}_{k}(z^{2^{k+1}}) = (h^{-1}(f(z)))^2 = \frac{z^2}{1+z^4}.$$

The left hand side can be written as

$$(\underbrace{(2+(2+\ldots+(2}_{k}+\frac{1}{z^{2^{k+1}}})^{\frac{1}{2}}\ldots)^{\frac{1}{2}})^{\frac{1}{2}})^{-1} = z^2((2z^{2^2}+(2z^{2^3}+\ldots(2z^{2^{k+1}}+1)^{\frac{1}{2}}\ldots)^{\frac{1}{2}})^{\frac{1}{2}})^{-1}.$$

Thus (5.8) reduces to the verification of the equation

$$\lim_{k\to\infty}(2z^{2^2}+(2z^{2^3}+\ldots(2z^{2^{k+1}}+1)^{\frac{1}{2}}\ldots)^{\frac{1}{2}})^{\frac{1}{2}} = 1+z^{2^2}.$$

This can be done as follows. Consider first squaring both sides of the above equation and canceling $2z^{2^2}$ from the two sides, we get

$$\lim_{k\to\infty}(2z^{2^3}+\ldots(2z^{2^{k+1}}+1)^{\frac{1}{2}}\ldots)^{\frac{1}{2}})^{\frac{1}{2}}=1+z^{2^3}\,.$$

Repeating the above operation k times, the left hand side gives 1 while the right hand side gives $1+z^{2^{k+2}}$. Thus as long as $z<1$, we get that the left and right hand sides do converge to each other as $k\to\infty$. This establishes the identity (5.6).

5.2 Finding the state A

Let us now solve (5.2) by level truncation. To do so, let us proceed in two ways. We recall from the previous section that A is well-defined up to the gauge transformation $A\to A+Q_{\Psi_0}B$ where B is a state of ghost number -2. Because in the level truncation scheme, this gauge invariance is broken, we first try to find the best fit results without fixing the gauge of A. The fitting procedure is analogous to that used in [22] and we shall not delve too much into the details. We shall see below that at level 9, the result is accurate to 2.4%. However, when we check the behaviour of the numerical coefficients of A as we increase the accuracy from level 3 to 9, we found that they do not seem to converge. We shall explain this phenomenon as the consequence of the gauge freedom in the definition of A; we shall then redo the fitting in the Feynman-Siegel gauge. With this second method, we shall find that the coefficients do converge and the best fit at level 9 is to 3.2% accuracy. These results support strongly the existence of a state A in (5.2) and hence the statement that the cohomology around the tachyon vacuum is indeed trivial. In the following subsections let us present our methods and results in detail.

5.2.1 The fitting without gauge fixing A

It is worth noticing that in the expansion of $\mathcal{I}$ only odd levels have nonzero coefficients. This means that we can constrain the solution A of (5.2), if it exists, to have only

odd levels in its expansion. The reason for this is as follows. Equation (5.2) states that $Q_B A + \Psi_0 \star A + A \star \Psi_0 = \mathcal{I}$, moreover we recall that (cf. e.g. Appendix A.4 of [22]) the coefficient $k_{\ell,i}$ in the expansion of the star product $x \star y = \sum_{\ell,i} k_{\ell,i} \psi_{\ell,i}$ is $k_{\ell,i} = \langle \tilde{\psi}_{\ell,i}, x, y \rangle$ for the orthogonal basis $\tilde{\psi}$ to ψ. Now the triple correlator has the symmetry $\langle x, y, z \rangle = (-)^{1+g(x)g(y)+\ell(x)+\ell(y)+\ell(z)} \langle x, z, y \rangle$, where $g(x)$ and $\ell(x)$ are the ghost number and level of the field x respectively. Whence, one can see that the even levels of $\Psi_0 \star A + A \star \Psi_0$ will be zero because the tachyon vacuum Ψ_0 has only even levels and A is constrained to odd levels. Furthermore, $Q_B = \sum_n c_n L^m_{-n} + \frac{1}{2}(m-n) : c_m c_n b_{-m-n} : -c_0$ preserves level. Therefore, in order that both the left and right hand sides of (5.2) have only odd levels, A must also have only odd level fields.

Now the procedure is clear. We expand A into odd levels of ghost number -1 with coefficients as parameters and calculate $Q_{\Psi_0} A$. Indeed as with [22], all the states will be written as Euclidean vectors whose basis is prescribed by the fields at a given level; the components of the vectors are thus the expansion coefficients in each level. Then we compare $Q_{\Psi_0} A$ with $\mathcal{I}$ up to the same level and determine the coefficients of A by minimizing the quantity

$$\epsilon = \frac{|Q_{\Psi_0} A - \mathcal{I}|}{|\mathcal{I}|},$$

which we of course wish to be as close to zero as possible. We refer to this as the *"fitting of the coefficients"*. The norm $|.|$ is the Euclidean norm (for our basis, see Appendix A.5) . As observed in [96], different normalizations do not significantly change the values from the fitting procedure, so for simplicity we use the Euclidean norm to define the above measure of proximity ϵ. The minimum level of the ghost number -1 field A is 3, so we start our fitting from this level and continue to up to level 9 (higher levels will become computationally prohibitive).

First we list the number of components of odd levels for the fields A and $\mathcal{I}$ up to

given levels:

	level 3	level 5	level 7	level 9
Number of Components of A	1	4	14	43
Number of Components of $\mathcal{I}$	4	14	43	118

From this table, we see that at level 3, we have only one parameter to fit 4 components. At level 5, we have 4 parameters to fit 14 components. As the level is increased the number of components to be fitted increases faster that the number of free parameters. Therefore it is not a trivial fitting at all.

A up to level 3

At level 3 the identity is:

$$\begin{aligned}\mathcal{I}_3 &= |0\rangle + L_{-2}|0\rangle \\ &= |0\rangle - b_{-3}c_1|0\rangle - 2b_{-2}c_0|0\rangle + L^m_{-2}|0\rangle\end{aligned}$$

and we find the best fit of A (recall that at level 3 we have only 1 degree of freedom) to be

$$A_3 = 1.12237\, b_{-2}|0\rangle\,,$$

with an ϵ of 17.1%.

A up to level 5

Continuing to level 5, we have

$$\begin{aligned}\mathcal{I}_5 &= |0\rangle + L_{-2}|0\rangle + \tfrac{1}{2}(L^2_{-2} - L_{-4})|0\rangle \\ &= |0\rangle - b_{-3}c_1|0\rangle - 2b_{-2}c_0|0\rangle + L^m_{-2}|0\rangle + b_{-5}c_1|0\rangle - b_{-2}c_{-2}|0\rangle \\ &\quad + b_{-3}c_{-1}|0\rangle + 2b_{-3}b_{-2}c_0c_1|0\rangle + 2b_{-4}c_0|0\rangle - \tfrac{1}{2}L^m_{-4}|0\rangle \\ &\quad - b_{-3}c_1L^m_{-2}|0\rangle - 2b_{-2}c_0L^m_{-2}|0\rangle + \tfrac{1}{2}L^m_{-2}L^m_{-2}|0\rangle\,.\end{aligned}$$

To this level we have determined the best-fit A to be

$$A_5 = 1.01893\, b_{-2}\,|0\rangle + 0.50921\, b_{-3}b_{-2}c_1\,|0\rangle - 0.518516\, b_{-4}\,|0\rangle + 0.504193\, b_{-2}L^m_{-2}\,|0\rangle\,,$$

with an ϵ of 11.8%.

The detailed data of the field A to levels 7 and 9 are given in Appendix A.5.1. Here we just summarize the results of the best-fit measure ϵ:

	level 3	level 5	level 7	level 9
$\epsilon = \frac{\lvert Q_{\Psi_0}A-\mathcal{I}\rvert}{\lvert\mathcal{I}\rvert}$	0.171484	0.117676	0.0453748	0.0243515

This indicates that up to an accuracy of 2.4% at level 9, there exists an A that satisfies (5.2); moreover the accuracy clearly gets better with increasing levels. This is truly an encouraging result.

5.2.2 The stability of fitting

There is a problem however. Looking carefully at the coefficients of A given in Appendix A.5.1, especially the fitting coefficients between levels 7 and 9, we see that these two groups of data have a large difference. Naively it means that our solution for A does not converge as we increase level. How do we solve this puzzle?

We recall that A is well-defined only up to the gauge freedom

$$A \longrightarrow A + Q_{\Psi_0}B.$$

It means that the solutions of (5.2) should consist of a family of gauge equivalent A. However, because $Q^2_{\Psi_0} \neq 0$ under the level truncation approximation, the family (or the moduli space) is broken into isolated pieces. Similar phenomena were found in [96] where the momentum-dependent closed states were given by points instead of a continuous family. Using this fact, our explanation is that the fitting of levels 7 and 9 are related by $Q_{\Psi_0}B$ for some field B of ghost number -2. To show this, we solve

a new $\tilde{A}$ up to level 9 that minimizes

$$\frac{|(\tilde{A})_7 - A_7|}{|A_7|} + \frac{|Q_{\Psi_0}\tilde{A} - \mathcal{I}_9|}{|\mathcal{I}_9|}$$

where A_7 is the known fitting data at level seven, $\mathcal{I}_9$ is the identity up to level nine and $(\tilde{A})_7$ refers to the first 14 components (i.e., the components up to level seven) of the level 9 expansion of $\tilde{A}$. By minimizing this above quantity, we balance the stability of fitting from level 7 to 9. The data is given in the last column of Appendix A.5.1. Though having gained stability, the fitting for level 9 is a little worse, with ϵ increasing from 2.44% to 3.56%.

The next thing is to check whether $\tilde{A} - A_9$ is an exact state $Q_{\Psi_0}B$. We find that this is indeed true and we find a state B such that

$$\frac{|(\tilde{A} - A_9) - Q_{\Psi_0}B|}{|\tilde{A} - A_9|} = 0.28\%.$$

5.2.3 Fitting A in the Feynman-Siegel gauge

Alternatively, by gauge-fixing, we can also avoid the instability of the fit. If we require the state A to be in the Feynman-Siegel gauge, A will not have the gauge freedom anymore and the fitting result should converge as we do not have isolated points in the gauge moduli space to jump to. We have done so and do find much greater stability of the coefficients.

Notice that in the Feynman-Siegel gauge, A has the same field bases in levels 3 and 5, so the fitting at these two levels is the same as in Subsection 5.2.1. However, in this gauge it has one parameter less at level 7 and 5 less in level 9. Performing the fit with these parameters we have reached an accuracy of $\epsilon = 4.8\%$ at level 7 and $\epsilon = 3.2\%$ at level 9, which is still a good result. The details are presented in Appendix A.5.2.

5.3 Some subtleties of the identity

There are some mysterious and anomalous features of the identity $\mathcal{I}$. For example, $\mathcal{I}$ is not a normalizable state [102], moreover, c_0, contrary to expectation, does not annihilate $\mathcal{I}$ even though it is a derivation [71]. We shall show in the following that with a slight modification of the level truncation scheme, this unnormalizability does not effect the results and furthermore that in our approximation $Q_{\Psi_0}\mathcal{I}$ indeed vanishes as it must for consistency.

Let us first show how problems may arise in a naive attempt at level truncation. Consider the quantity $\mathcal{I}_\ell \star |\Omega\rangle - |\Omega\rangle$, where $\mathcal{I}_\ell$ denotes the identity truncated to level ℓ and $|\Omega\rangle := c_1 |0\rangle$. We of course expect this to approach 0 as we increase ℓ. Using the methods of the previous section, we shall define the measure of proximity

$$\eta \equiv \frac{|\mathcal{I}_\ell \star |\Omega\rangle - |\Omega\rangle\,|}{|\,|\Omega\rangle\,|} = |\mathcal{I}_\ell \star |\Omega\rangle - |\Omega\rangle\,|,$$

where $|.|$ is our usual norm. We list η to levels 3, 5, 7, and 9 in the following table:

level ℓ	3	5	7	9
$\eta = \|\mathcal{I}_\ell \star \|\Omega\rangle - \|\Omega\rangle\,\|$	2.06852	2.87917	3.56054	3.9452

Our η obviously does not converge to zero, hence star products involving $\mathcal{I}$ do not converge in the usual sense of level truncation. It is however not yet necessary to despair, as weak convergence will come to our rescue[7].

Indeed, instead of truncating the result to level ℓ, let us use a slightly different scheme. We truncate $\mathcal{I}_\ell \star |\Omega\rangle$ to a fixed level $m < \ell$ and observe how the coefficients of the fields up to level m converge as we increase ℓ. In the following table we list the values of the coefficients coeff(x) of the basis for $m = 2$ (i.e., fields x of level 0, 1 and 2) for the expression $\mathcal{I}_\ell \star |\Omega\rangle$.

[7] We thank B. Zwiebach for this suggestion.

$\mathcal{I}_\ell \star \|\Omega\rangle$	coeff($\|\Omega\rangle$)	coeff($b_{-1}c_0\|\Omega\rangle$)	coeff($b_{-1}c_{-1}\|\Omega\rangle$)	coeff($b_{-2}c_0\|\Omega\rangle$)	coeff($L^m_{-2}\|\Omega\rangle$)
$\ell = 3$	0.6875	0.505181	−0.905093	−0.930556	0.465278
$\ell = 5$	1.16898	−0.278874	0.38846	0.520748	−0.260374
$\ell = 7$	0.911094	0.16252	−0.197833	−0.296607	0.148304
$\ell = 9$	1.05767	−0.0971502	0.0902728	0.163579	−0.0817895

We see that the $|\Omega\rangle$ component converges to 1 while the others converge to 0, as was hoped. We note however that this (oscillating) convergence is rather slow and we thus expect slow weak convergence for other calculations involving the identity.

Having shown that as $\ell \to \infty$ we get a weak convergence $\mathcal{I}_\ell \star |\Omega\rangle \to |\Omega\rangle$, we now consider $Q_{\Psi_0}\mathcal{I}_\ell$ as $\ell \to \infty$, which should tend to zero. Since Q_B preserves level and $Q_B\mathcal{I} = 0$, we have that $Q_B\mathcal{I} = 0$ in the level expansion; thus $Q_{\Psi_0}\mathcal{I} = \Psi_0 \star \mathcal{I} - \mathcal{I} \star \Psi_0$, which should converge to zero.

As the expression $Q_{\Psi_0}\mathcal{I}$ is linear in every component of Ψ_0, that $\mathcal{I}$ is Q_{Ψ_0}-closed will be established if we can show that for each component ϕ in Ψ_0, $\phi\star\mathcal{I} - \mathcal{I}\star\phi \equiv [\phi\star, \mathcal{I}]$ converges to zero as the level of $\mathcal{I}$ is increased. We plot in Figure 5-1, the absolute

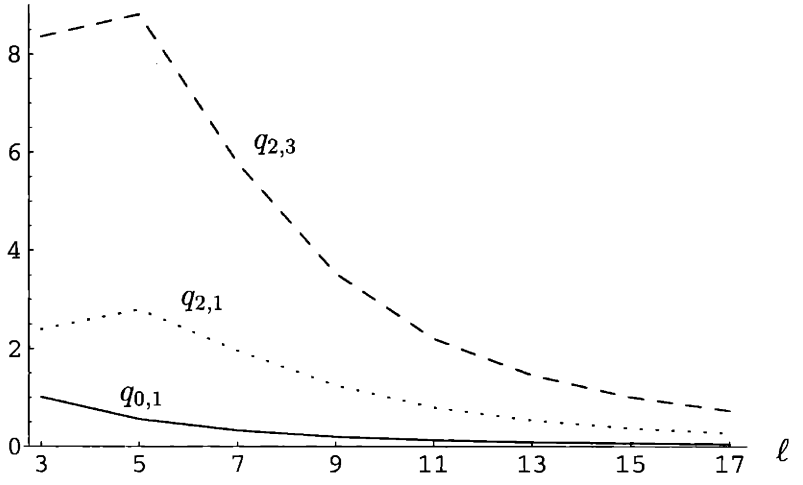

Figure 5-1: A plot of $q_{0,1}(\ell)$ (solid curve), $q_{2,1}(\ell)$ (dotted curve) and $q_{2,3}(\ell)$ (dashed curve) as functions of the level ℓ of the identity.

values of the coefficient of $c_0|0\rangle$ in the expressions $[(c_1|0\rangle)\star, \mathcal{I}_\ell]$, $[(c_{-1}|0\rangle)\star, \mathcal{I}_\ell]$ and $\left[(L^m_{-2}c_1)|0\rangle\star, \mathcal{I}_\ell\right]$, which we denote by $q_{0,1}(\ell)$, $q_{2,1}(\ell)$ and $q_{2,3}(\ell)$ respectively. It seems clear that the coefficients do converge to zero.

The weak convergence we have shown above can be interpreted in a more abstract setting. Let us examine the quantity $|\mathcal{I}_\ell \star \Phi - \Phi|$. It was shown in [103] that the $\star$-algebra of the open bosonic string field theory is a C^*-algebra. A well-known theorem dictates that any C^*-algebra M (with or without unit) has a so-called *approximate identity* which is a set of operators $\{\mathcal{I}_i\}$ in M indexed by i satisfying (i) $\|\mathcal{I}_i\| \leq 1$ for every i and (ii) $\|\mathcal{I}_i x - x\| \to 0$ and $\|x\mathcal{I}_i - x\| \to 0$ for all $x \in M$ with respect to the (Banach) norm $\|.\|$ of M (cf. e.g. [104]).

The level ℓ in our level truncation scheme is suggestive of an index for $\mathcal{I}$. Furthermore the weak convergence we have found in this section is analogous to property (ii) of the theorem (being of course a little cavalier about the distinction of the Banach norm of the C^*-algebra with the Euclidean norm used here). Barring this subtlety, it is highly suggestive that our $\mathcal{I}_\ell$ is an approximate identity of the $\star$-algebra indexed by level ℓ.

5.4 Conclusions and discussions

According to a strong version of Sen's Second Conjecture, there should be an absence of any open string states around the perturbatively stable tachyon vacuum Ψ_0. This disappearance of all states, not merely the physical ones of ghost number 1, means that the cohomology of the new BRST operator Q_{Ψ_0} should be completely trivial near the vacuum. It is the key observation of this chapter that this statement of triviality is implied by the existence of a ghost number -1 field A satisfying

$$Q_{\Psi_0} A = Q_B A + \Psi_0 \star A + A \star \Psi_0 = \mathcal{I}.$$

That is to say that if the identity of the $\star$-algebra $\mathcal{I}$ is a Q_{Ψ_0} exact state, then the cohomology of Q_{Ψ_0} would be trivial.

The level truncation scheme was subsequently applied to check our proposal. We have found that such a state A exists up to an accuracy of 3.2% at level 9. Although these numerical results give a strong support to the proposal for the existence of A

and hence the triviality of Q_{Ψ_0}-cohomology near the vacuum, an analytic expression for A would be most welcome. However, to obtain such an analytic form of A, it seems that we would require the analytic expression for the vacuum Ψ_0, bringing us back to an old problem. It is perhaps possible that by choosing different gauges other than the Feynman-Siegel gauge we may find such a solution.

Our solution A satisfies $\{A, Q\} = I$. It would be nice to see whether we can choose A cleverly to make $A \star A = 0$ (our Feynman-Siegel gauge fitting may not satisfy this equation). We are interested with this case because for the proposal of $Q_B = c_n + (-)^n c_{-n}$ made in [97, 98], one could find that $A = \frac{1}{2}(b_{-n} + (-)^n b_n)$ which does satisfy $A^2 = 0$. It would be interesting to mimic this nilpotency within the $\star$-algebra. Furthermore, it would be fascinating to see if we can make a field redefinition to reduce A to a simple operator such as b_0, and at the same time reduce Q_{Ψ_0} to a new BRST operator as suggested in [98], for example, c_0.

Last but not least, an interesting question is about the identity $\mathcal{I}$. In this chapter we have given an elegant analytic expression for $\mathcal{I}$ which avoids the usage of complicated recursion relations. Furthermore, we have suggested that though the $\star$-algebra of OSFT may be a non-unital C^*-algebra, $\mathcal{I}$ still may serve as a so-called approximate identity. However, as we discussed before, anomalies related to the identity in the String Field Theory make the calculation in level truncation converge very slowly. It will be useful to understand more about $\mathcal{I}$.

Chapter 6

Dynamics with infinitely many time derivatives and rolling tachyons

Some of the most intriguing and fascinating aspects of string theory center around the role of locality. More precisely, string theory appears to be a consistent theory that is not local in the sense of local quantum field theory. Indeed, the covariant string field theory action governing the dynamics of the infinite set of spacetime fields contains spacetime derivatives of all orders. Not only we have spatial derivatives of all orders, as in non-commutative field theory, but we also have time derivatives of all orders, and mixed derivatives of all orders.

The possible difficulties with theories having a high number of time derivatives are familiar. They include possible violations of unitarity and causality, the appearance of spurious solutions, complications setting up an initial value problem, and difficulties quantizing the theory and/or finding a stable Hamiltonian [110]. There is, however, evidence that in the case of string theory the higher derivative structure does not threat the consistency of the theory. The perturbative S-matrix of string theory is unitary. Even though covariant string field theory cannot be quantized using a Hamiltonian, path integral quantization is possible and elegantly done with the use of the Batalin-Vilkovisky formalism [111, 66, 100, 112]. While infinitely many spatial

derivatives are possible in non-commutative *field* theory, infinitely many mixed spatial and time derivatives appear to require string theory for consistency [113, 114]. Finally, the higher derivative structure of string theory is certainly very special – when passing to the light-cone gauge the theory becomes local in light-cone time. Indeed, light-cone string field theory has only first order time derivatives [115].

Motivated by the recent work of Sen on tachyon matter [16, 17, 18] we examine the rolling of the tachyon down its potential. Tachyon matter is a classical open string theory solution where at large times the tachyon $T(t)$ approaches the tachyon vacuum $T = \infty$ with constant velocity $\dot{T}(t)$. This solution represents a pressureless gas and its possible cosmological relevance has been studied in [116]. The evidence for such solutions comes mostly from the conformal field theory approach. Recently, related solutions have been obtained from considerations of boundary string field theory [117, 118]. These actions, truncated to include all powers of first derivatives of fields exhibit similar, though not identical behavior. The purpose of the present chapter is to examine tachyon dynamics in the setup of open string field theory [13], where the equations of motion contain infinitely many time derivatives. Most of our work, however, will concentrate in the case of p-adic string theory [119]. This string theory is essentially a theory of a scalar field with infinitely many spacetime derivatives. Indeed many of the properties of the tachyon field of open string theory are also exhibited by the p-adic string model [86, 91, 92]. One has a tachyon, and a potential with a locally stable minimum where the scalar field has no conventional excitations. Lump-like solutions exist representing p-adic D-branes of various dimensionalities. We will find here interesting phenomena regarding tachyon solutions in p-adic string theory, and we will also see that some solutions in string field theory are quite analogous to p-adic string solutions. None of the solutions we find, should be said, appears to represent tachyon matter.

In order to explain our results we briefly review the p-adic string model. The model is defined by an action S for a scalar field. Formulated with an arbitrary spacetime dimensionality, the model has a parameter p, which is initially taken to be a prime number. The action, however, makes sense for other values of p, and even in

the limit $p \to 1$, where it reduces to the tachyon action of [88] as noted in [10]. In this chapter we will take p to be an integer that is greater than or equal to two. The p-adic action is given by

$$S = \int d^d x \mathcal{L} = \frac{1}{g_p^2} \int d^d x \left[-\frac{1}{2} \phi \, p^{-\frac{1}{2}\Box} \phi + \frac{1}{p+1} \phi^{p+1} \right], \quad \frac{1}{g_p^2} \equiv \frac{1}{g^2} \frac{p^2}{p-1}. \tag{6.1}$$

The infinite number of spacetime derivatives are manifest in the differential operator $p^{-\frac{1}{2}\Box}$. Here, we have

$$\Box = -\frac{\partial^2}{\partial t^2} + \nabla \cdot \nabla \,, \tag{6.2}$$

and one defines

$$p^{-\frac{1}{2}\Box} = \exp\Big(-\frac{1}{2} \ln p \, \Box\Big) = \sum_{n=0}^{\infty} \Big(-\frac{1}{2} \ln p\Big)^n \frac{1}{n!} \, \Box^n \,. \tag{6.3}$$

The equation of motion following from the action is rather simple looking:

$$p^{-\frac{1}{2}\Box} \phi = \phi^p \,. \tag{6.4}$$

For the case of time dependent but spatially homogeneous solutions – the only kind we will study in this chapter – the equation is

$$p^{\frac{1}{2}\partial_t^2} \, \phi = \phi^p \,. \tag{6.5}$$

Finally, we note that the scalar potential is given by

$$V(\phi) = \frac{1}{g_p^2} \left(\frac{1}{2} \phi^2 - \frac{1}{p+1} \phi^{p+1} \right). \tag{6.6}$$

The cases odd p and even p are qualitatively different (see Figure 6-1), although both have potentials unbounded from below. For odd p the potentials are even in ϕ, while for even p they fail to be even. In both cases there is a local maximum at $\phi = 1$, where the tachyon has $M^2 = -2$, and a local minimum at $\phi = 0$ where the field seems naively to have no dynamics as its mass-squared goes to infinity.

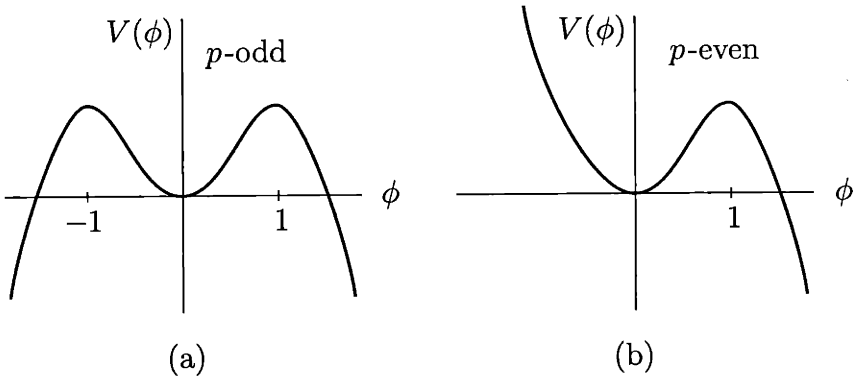

Figure 6-1: The p-adic string potentials. For odd p the potential is even and has two unstable maxima. For even p there is only one unstable maximum.

In order to study effectively these theories and their solutions we need expressions for the components of the energy-momentum tensor. For the case of a higher derivative theory we extend the conventional Noether procedure and find an expression for T^{μ}_{α} as an infinite series involving all numbers of derivatives. These expressions are formally local and can also be used for open string field theory. The energy of a solution does involve infinite number of derivatives and it is conserved. Its evaluation can sometimes be done in closed form. It is also determined unambiguously from the above Noether method. The Noether calculation of T^{i}_{i}, where from we must read the pressure, has improvement ambiguities and we use the metric variation of the covariantized p-adic action to calculate its value.

We also discuss the nature of the initial value problem for equations such as (6.5) containing infinitely many time derivatives. While an equation of motion containing up to N derivatives requires N independent initial conditions, we show that in the case of infinite number of time derivatives the infinite number of "initial conditions" are not independent but are actually subject to (possibly) infinitely many constraints. It may even happen that the space of consistent initial conditions is parametrized by a finite number of parameters. If this were the case we would have a surprising example of a theory with infinitely many time derivatives whose solution space is not altogether different to that following from equations with two time derivatives.

The first time dependent solution in p-adic string theory was found by Brekke

et.al. [119]. The equation of motion (6.5) was studied by expressing the differential operator in the left hand side as a convolution of ϕ with a gaussian, as will be reviewed in Section 6.1.1. The equation of motion then becomes a non-linear integral equation. For the case of odd p the authors found numerically a kink solution of the integral equation. The solution interpolates in time between the vacua $\phi = \pm 1$. No solution was obtained for even p.

In this chapter we study in detail time dependent solutions of p-adic string theory. We use a combination of analytic and numerical methods. In particular we show how to use the convolution approach to constrain solutions and to rule out certain behaviors. Some of the numerical methods are based on considerations of [16, 17] and the recent work [120]. While we have no exact closed forms for any solution, we have analytic expressions valid in certain limits. As the solutions are sometimes quite surprising we try to check them in two ways. We verify they hold numerically both as solutions of the nonlinear integral equation, and after evaluating several derivatives of the solution, we confirm that they directly satisfy (6.5) with the derivatives expanded as in (6.3). This not only increases our confidence on the solutions, but it is of some theoretical significance in that the exponentiated differential operator and the convolution form do not agree when acting on certain kinds of smooth functions.

After confirming the kink solution of [119] to high accuracy and checking it does satisfy both versions of the equation of motion, we turn to finding families of solutions for odd p potentials. We find nontrivial field oscillations around the tachyon vacuum $\phi = 0$. These are rather surprising. It is well known that the linearized equations of motion of the tachyon around the vacuum admit no solutions. This is the p-adic version of the familiar statement that there are no conventional open string excitations at the tachyon vacuum [7, 3, 4, 5]. The solutions we find exist because they solve the complete nonlinear equations. The oscillations are completely anharmonic and the basic frequency goes to infinity as the amplitude of the oscillation goes to zero. The solutions are of the form $\phi \simeq A(\cos(\omega t))^{1/p}$, with $\omega^2 \sim -\ln(A)$ and provide an explicit example of a non-standard open string excitation capable of carrying energy at the tachyon vacuum. These solutions are obtained by a level analysis of the dif-

ferential equation and were checked also by the integral form. There are two possible interpretations for these oscillations. In the first one, they would represent oscillating solutions with a nontrivial energy-momentum tensor which would be expected to radiate quite efficiently into closed string modes, thus converting the tachyon energy into closed strings. In the second interpretation these oscillations, suitably quantized would be the closed string excitations themselves. We will discuss both possibilities, but believe the former is more likely to be correct.

In the studies of tachyon matter the tachyon vacuum is at infinity and the tachyon never reaches this point. Moreover, there is no meaning to configurations beyond the tachyon vacuum. On the other hand, in string field theory or in p-adic theory, the tachyon vacuum is at a finite point in the field configuration space and there are field values beyond the tachyon vacuum. In the solutions we obtained the field typically speeds by the tachyon vacuum without difficulty. The case of even p, in particular $p = 2$, where the potential is cubic resembles open string field theory. For even p we have found no constant amplitude oscillations around the tachyon vacuum (but we lack a proof that they cannot exist). For $p = 2$ a rolling solution down the unstable maximum at $\phi = 1$ is seen to zoom by the tachyon vacuum $\phi = 0$ and after an excursion to negative values having potential energies higher than that of the original unstable vacuum, ever growing oscillations occur. In this solution the pressure does not go to zero for large times. The analog for even p of the family of odd p bounded oscillations is a family of solutions that has ever growing oscillations (ever growing oscillations also seem possible for odd p).

Last but not least we study the rolling problem in the full open string field theory using the analytic continuation of the marginal deformation solution of [84] as advocated in [16]. We find that the tachyon rolls down towards the vacuum, goes beyond it by a large factor, and that a pattern of growing oscillations appears to set it. This surprising result, in many ways, motivated our full analysis of the p-adic string model. Indeed, the results summarized above concerning the p-adic model indicate that rolling in OSFT appear to be remarkably similar to rolling on the $p = 2$ potential. This lends credence to the idea that the OSFT solution can be trusted and

is not an artifact of some approximation scheme. On the other hand it also suggests that this solution is not tachyon matter.

Some concluding remarks and observations, as well as a detailed list of open questions can be found in the conclusion section.

6.1 Convolution and initial value problem

In this section we begin by considering the convolution form of the p-adic string equation of motion. In this form, the equation is a nonlinear integral equation with a gaussian kernel. The convolution form and the differential form of the equation of motion appear to be equivalent only in the space of real analytic functions.

We then show that the convolution form of the equation of motion is a useful tool that allows qualitative analysis of solutions. We use it to show that there cannot exist solutions of p-adic string theory where the field approaches monotonically the tachyon vacuum for large times. We also use it to find constraints on possible oscillatory solutions and to rule out certain types of lump solutions.

Finally, we discuss the crucial issue of the initial value problem in a theory with infinite number of derivatives.

6.1.1 Convolution form of the p-adic equation of motion

In this subsection we discuss the convolution form of the p-adic string dynamics obtained by [119]. Let us first derive this form. To this end we recall the differential form of the equation of motion (6.5):

$$p^{\frac{1}{2}\partial_t^2}\phi = \phi^p \,. \tag{6.7}$$

As a first step we assume a well defined Fourier transform $\hat{\phi}(k)$ of the p-adic field $\phi(t)$:

$$\hat{\phi}(k) = \frac{1}{\sqrt{2\pi}} \int_{-\infty}^{\infty} e^{ikt}\, \phi(t) dt \,,$$

giving $\phi(t)$ by inverse Fourier transformation:

$$\phi(t) = \frac{1}{\sqrt{2\pi}} \int_{-\infty}^{\infty} e^{-ikt}\, \hat{\phi}(k) dk\,.$$

Then, the left hand side of the equation of motion (6.7) can be written as:

$$\begin{aligned} p^{\frac{1}{2}\partial_t^2}\phi(t) &= \frac{1}{\sqrt{2\pi}} \int_{-\infty}^{\infty} p^{-\frac{1}{2}k^2} e^{-ikt} \hat{\phi}(k) dk \\ &= \frac{1}{\sqrt{2\pi}} \int_{-\infty}^{\infty} dk \left(\frac{1}{\sqrt{2\pi \ln p}} \int_{-\infty}^{\infty} e^{-\frac{t'^2}{2\ln p}} e^{-ik(t-t')} dt' \right) \hat{\phi}(k) \\ &= \frac{1}{\sqrt{2\pi \ln p}} \int_{-\infty}^{\infty} e^{-\frac{1}{2\ln p}(t-t')^2} \phi(t') dt'\,. \end{aligned} \tag{6.8}$$

Defining the gaussian convolution $\mathcal{C}[\phi]$

$$\mathcal{C}[\phi](t) \equiv \frac{1}{\sqrt{2\pi \ln p}} \int_{-\infty}^{\infty} e^{-\frac{1}{2\ln p}(t-t')^2} \phi(t') dt'\,, \tag{6.9}$$

the equation of motion can then be rewritten as

$$\phi(t)^p = \mathcal{C}[\phi](t)\,. \tag{6.10}$$

This is a nonlinear integral equation. Note that the convolution operator is correctly normalized to represent the differential operator: acting on a constant it gives the constant back

$$\mathcal{C}[a] = a\,. \tag{6.11}$$

Constant solutions $\phi(t) = \phi_0$ of the p-adic field equation (6.10) therefore arise when :

$$\phi_0^p = \phi_0 \qquad p > 1. \tag{6.12}$$

This gives $\phi_0 = 0$ and $\phi_0 = 1$ valid for all $p \geq 2$. For odd p we also have $\phi_0 = -1$. These solutions all correspond to the tachyon sitting on a critical point of the p-adic string potentials.

Before we go on and solve either (6.7) or (6.10), we should note that there are

smooth functions $\psi(t)$ (*i.e.* continuous functions with continuous derivatives of all orders) for which the convolution does not represent the action of the differential operator:

$$p^{-\frac{1}{2}\partial_t^2}\psi(t) \neq \mathcal{C}[\psi](t)\,.$$

A simple example is provided by the following smooth function with compact support:

$$\psi(t) = \begin{cases} 0, & |t| > b \\ 1, & |t| < a\,. \end{cases} \tag{6.13}$$

where a and b are positive numbers such that $b > a$. When $a \leq |t| \leq b$, ψ interpolates

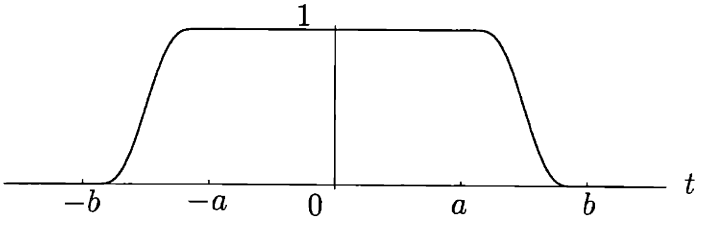

Figure 6-2: A smooth function that is identically one for $|t| < a$, and identically zero when $|t| > b$. For such a function the differential form of the equation of motion does not coincide with the convolution form.

smoothly between 0 and 1. Since all the derivatives of ψ are zero at $t = 0$, we have $p^{-\frac{1}{2}\Box}\psi(0) = \psi(0) = 1$; but on the other hand $\mathcal{C}[\psi](0) < 1$ since $\mathcal{C}[1] = 1$ and ψ is strictly smaller than one when $|t| > a$. Therefore equation (6.8) does not hold for this smooth function. We expect, however, that (6.8) holds for *real analytic* functions whenever the convolution exists. We have checked many of the solutions obtained in this chapter and verified that they solve both forms (6.7) and (6.10) of the equations of motion. This seems to mean that solutions of the p-adic string theory lie on the space of real analytic functions.

6.1.2 Convolution constraints on solutions

General features of a solution to the equation of motion can be gleaned from the properties of the gaussian convolution. We will illustrate this by proving three results

that give us insight into the questions we are trying to address.

The first result rules out the possibility that the tachyon may roll monotonically down from $\phi = 1$ reaching the tachyon vacuum $\phi = 0$.

Claim 1: There is no solution $\phi(t)$ such that $\phi(t = -\infty) = 1$ and $\phi(t = +\infty) = 0$ with $\phi(t)$ decreasing monotonically in time.

Proof: Consider a monotonically decreasing function $\phi(t)$ satisfying the above conditions, as illustrated in Figure 6-3. Since the function approaches zero, there is a time t_0 such that $\phi(t_0) = a$, with $a > 0$ and sufficiently small such that

$$a^p < \frac{a}{2}. \tag{6.14}$$

On the other hand the equation of motion requires

$$a^p = \mathcal{C}[\phi](t_0). \tag{6.15}$$

Consider now the auxiliary function $\psi(t)$ such that $\psi(t) = a$ for $t < t_0$, and $\psi(t) = 0$ for $t > t_0$. It is clear from the monotonicity property that $\phi(t) > \psi(t)$ for all t. Moreover, ψ has a very simple gaussian convolution. Using (6.15) we have

$$a^p = \mathcal{C}[\phi](t_0) > \mathcal{C}[\psi](t_0) = \frac{a}{2}. \tag{6.16}$$

This violates the inequality in (6.14) and proves the claim that no solution exists satisfying the stated conditions.

The second result concerns the possibility of solutions bounded in time. These could be bounded oscillations or otherwise. The ranges of variation are constrained by the following claim:

Claim 2: Consider a solution $\phi(t)$ and constants $a < b$ such that $a \leq \phi(t) \leq b$ for all times t. Moreover, assume that the values a, and b are actually attained for some specific times. Then $0 < b < 1$ and $a < 0$. For odd p we must also have $a > -1$.

Proof: Let t_0 denote a time when $\phi(t_0) = b$ and t_1 denote a time when $\phi(t_1) = a$ (see

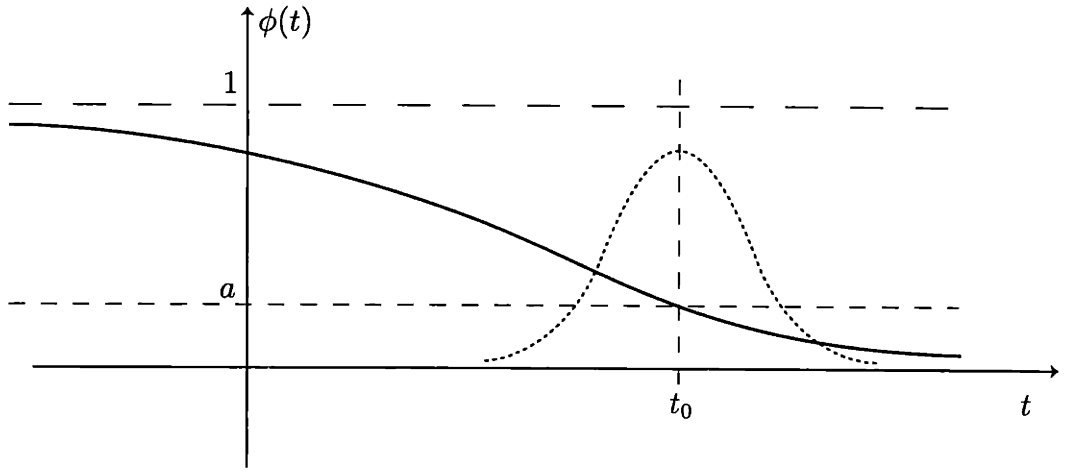

Figure 6-3: A monotonically decreasing field configuration going from the top of the potential all the way to the tachyon vacuum. Such field configuration cannot satisfy the equation of motion.

Figure 6-4). From the equation of motion we must have

$$b^p = \mathcal{C}[\phi](t_0)\,, \qquad a^p = \mathcal{C}[\phi](t_1)\,. \tag{6.17}$$

Since $\phi(t_1) \leq \phi(t) \leq \phi(t_0)$ we have

$$b^p = \mathcal{C}[\phi](t_0) < \mathcal{C}[\phi(t_0)] = b\,, \qquad a^p = \mathcal{C}[\phi](t_1) > \mathcal{C}[\phi(t_1)] = a\,, \tag{6.18}$$

giving us the inequalities

$$b^p < b\,, \qquad a^p > a\,, \qquad b > a\,, \tag{6.19}$$

where the last inequality is that from the definition of parameters. We rewrite them as

$$b(b^{p-1} - 1) < 0\,, \qquad a(a^{p-1} - 1) > 0\,, \qquad b > a\,. \tag{6.20}$$

Note that $p - 1$ is a positive integer. Consider the a inequality. If both factors are positive we must have $a > 1$. If both factors are negative there are two cases: (i) even p requires $a < 0$, and (ii) odd p requires $-1 < a < 0$. Consider now the b inequality.

If $b > 0$ then $0 < b < 1$. If $b < 0$ there is no solution for even p, and for odd p we see that actually $b < -1$. The inequality $b > a$ allows now selection of the final ranges. Since $b < 1$ in all cases, the possibility $a > 1$ cannot be realized. Thus $a < 0$ always. If p is even then $a < 0$ and $0 < b < 1$. If p is odd then $-1 < a < 0$. This is not consistent with $b < -1$, and therefore we get again $0 < b < 1$. This is the statement in the claim.

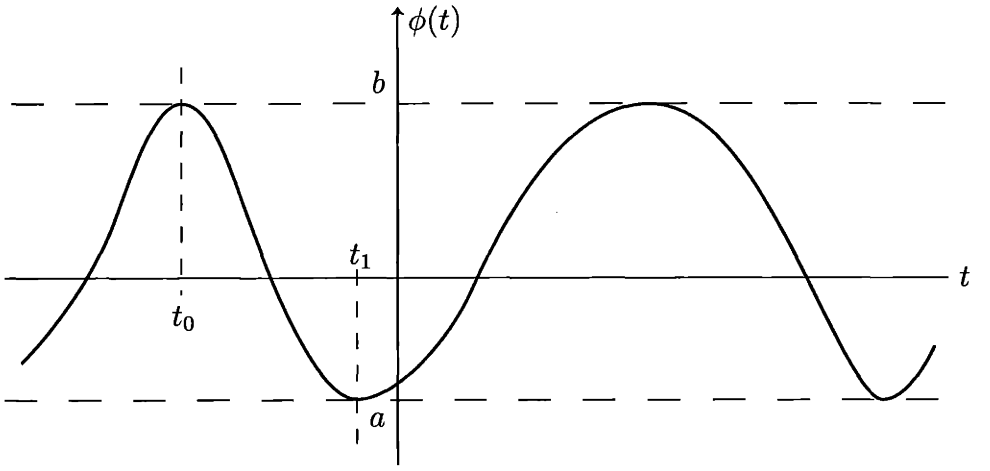

Figure 6-4: A bounded field configuration attaining a maximum value of b and a minimum value of a. The field equation gives constraints on the possible values of a and b.

Our third result will concern the absence of certain lump solutions for the case of even p. In order to establish this result we first note that for any bounded function $\phi(t)$ the derivative of its convolution equals the convolution of its derivative:

$$\frac{dC[\phi]}{dt}(t) = C\left[\frac{d\phi}{dt}\right](t)\,. \tag{6.21}$$

This result follows by noting that $\frac{d}{dt}$ equals to $\left(-\frac{d}{dt'}\right)$ acting on the gaussian appearing in the convolution (6.9). This derivative can be integrated by parts without picking any boundary contributions and one can let it act on the function ϕ thus obtaining the result.

Let us now define a *monotonic lump* associated to a bounded solution as in claim 2. This is a solution having $\phi(-\infty) = \phi(\infty) = b$ and $\phi(t_0) = a$ for some unique t_0. In

addition ϕ decreases monotonically for $t < t_0$ and increases monotonically for $t > t_0$. An example of such ϕ is shown in Figure 6-5.

Claim 3: There are no monotonic lump solutions for even p.

Proof: Because of claim 2, we have $\phi(t_0) = a < 0$. Since ϕ has a minimum at t_0, the convolution $\mathcal{C}[\phi](t) = \phi^p$ must have a maximum at t_0. This requires

$$\frac{d^2\mathcal{C}[\phi]}{dt^2}(t_0) < 0\,. \tag{6.22}$$

We differentiate (6.21) once more to obtain

$$\frac{d^2\mathcal{C}[\phi]}{dt^2}(t_0) = \frac{1}{\sqrt{2\pi \ln p}} \frac{1}{\ln p} \int_{-\infty}^{\infty} e^{-\frac{1}{2\ln p}(t'-t_0)^2} \left[(t'-t_0)\frac{d\phi(t')}{dt'}\right] dt'\,. \tag{6.23}$$

From the monotonicity condition we see that the factor in brackets is positive both for $t' < t_0$ and for $t' > t_0$. Therefore the above integral is positive, in contradiction with (6.22). This establishes claim 3.

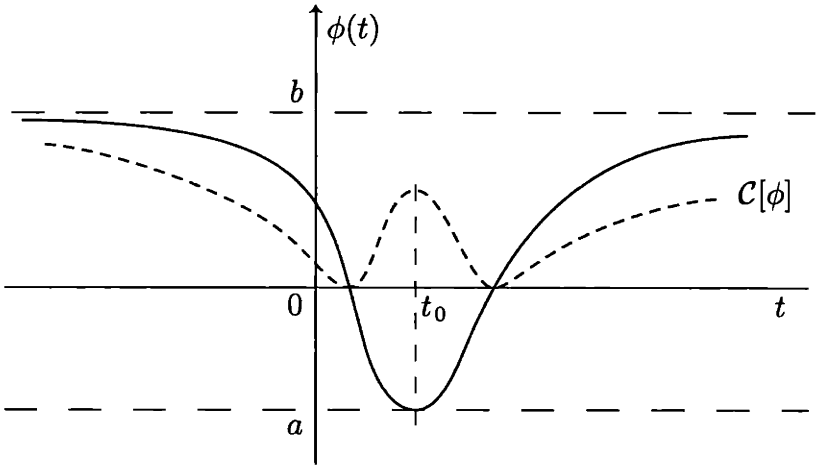

Figure 6-5: A monotonic lump with endpoint values b and unique minimum value of a. This kind of lump solution cannot exist for even p. The dashed line represents the gaussian convolution of the field configuration.

6.1.3 The fate of the initial value problem

In this subsection we will make some basic observations about the initial value problem for the equation

$$p^{\frac{1}{2}\partial_t^2}\phi = \phi^p \,. \tag{6.24}$$

In doing so, we view this as a differential equation for time evolution. This equation has an infinite number of derivatives and it is therefore unclear how to define the initial value problem.

We will argue that an equation as the one above is qualitatively very different from a differential equation having a large but finite number of time derivatives. In solving the initial value problem for a differential equation having time derivatives up to order N, one must specify N initial conditions – the values of the field and those of its first $(N-1)$ derivatives at an initial time, for example. Typically, those values are unconstrained, and solutions regular for some finite time exist for any choice of initial conditions.

In an equation such as that in (6.24) one would be led to believe that one can specify an infinite number of independent initial conditions. More precisely, an infinite number minus one – that is, if we specify all derivatives of ϕ at zero time, we could use the equation to read the value of ϕ at zero time. But a puzzle arises – if the function and all of its derivatives are specified at zero time, the natural assumption of analyticity would imply that the function is known and can be reconstructed from its Taylor expansion. It seems the differential equation is not needed anymore!

We will see below that equation (6.24) actually imposes an intricate set of conditions for the initial conditions! We believe the analyticity assumption, and thus think that the evolution is determined fully by the values of the function and all of its time derivatives at the initial time – nevertheless finding consistent initial conditions is now *the problem.* In the system with infinite number of time derivatives *the problem is not that of evolving an initial value configuration, but rather that of constructing a consistent initial value configuration.*

In an equation with up to N derivatives, and with N initial conditions, taking

further derivatives of the equation typically does not yield constraints for the chosen initial values. The resulting equations simply determine the higher order derivatives at the initial time. On the other hand for equation (6.24) taking arbitrary numbers of time derivatives yields new constraints that must be satisfied by the infinite set of initial conditions. This is what makes the problem different.

To show that there are indeed many constraints implied in (6.24) consider the following example. Let the first derivative of ϕ be non-vanishing at zero time, but all higher derivatives vanish:

$$\phi'(0) = a \neq 0, \quad \phi''(0) = \phi'''(0) = \ldots = 0\,. \tag{6.25}$$

Consider now equation (6.24) for $p = 2$. Consistent with the above initial conditions we find

$$p^{\frac{1}{2}\partial_t^2}\phi(0) = \phi(0) = \phi^2(0)\,. \tag{6.26}$$

Consider now choosing $\phi(0) = 1$ to satisfy this constraint. Since we now have the field and all of its derivatives specified at zero time, the (analytic) field is thus determined to be $\phi = 1 + at$, and this does not solve equation (6.24)! What went wrong? We did not have a consistent set of initial conditions. Indeed, taking two derivatives of equation (6.24) we have

$$p^{\frac{1}{2}\partial_t^2}\partial_t^2\phi(0) = 2\phi'(0)\phi'(0) + 2\phi(0)\phi''(0)\,, \tag{6.27}$$

which at zero time gives a new constraint on the initial conditions

$$0 = 2a^2\,. \tag{6.28}$$

This constraint indicates that we should not have expected a solution for nonzero a. It also shows that derivatives of the equation of motion yields new constraints on the initial values.

It does not seem altogether unreasonable to expect that equation (6.24) together

with all of its derivatives impose an infinite number of consistency conditions on the initial values. Could it be that that consistent initial values are parametrized by a finite number of parameters? More exploration is necessary to answer this question.

6.2 Energy-momentum in higher derivative theories

Both p-adic string theory and string field theory have actions where fields appear with infinitely many derivatives, both spatial and temporal. It is also the case that the action of p-adic string theory has no explicit dependence on the spacetime coordinates. The same occurs for open string field theory in many important backgrounds. It therefore follows that we expect to be able to define a conserved energy-momentum tensor through a generalized Noether procedure. Since the Noether procedure does not yield automatically a symmetric energy momentum tensor, we do not necessarily obtain the energy-momentum tensor that acts as a source of the gravitational field. This causes no complication for the case of the energy, which is unambiguous. But there are total derivative ambiguities in identifying the pressure from the Noether construction of $(-T_i^i)$. Therefore pressure is calculated by doing a metric variation in the relativistic covariantization of the p-adic action. We focus on the values of energy and pressure in the case of time dependent but space independent backgrounds, and then specialize further to the p-adic string model.

6.2.1 Generalized Noether construction

The situation in case is described by an action S of the type

$$S = \int d^D x dt \, \mathcal{L}\left(\phi,\ \partial_{\nu_1}\phi\,,\ \partial_{\nu_1}\partial_{\nu_2}\phi\,,\ \partial_{\nu_1}\partial_{\nu_2}\partial_{\nu_3}\phi\,,\ \cdots\right), \tag{6.29}$$

where the dots denote the dependence on fields acted upon by an ever increasing number of derivatives. The symbol ϕ in the above action may represent a collection of fields, but for notational simplicity we will not include an extra index. We emphasize

that this collection of fields can include, in addition to scalars, fields of arbitrary tensor type. This is indeed required for the results to be useful in string field theory. All the results below are trivially extended when ϕ is a collection of fields.

For a Lagrangian without explicit coordinate dependence the transformation

$$\delta\phi = \epsilon^\alpha \partial_\alpha \phi, \tag{6.30}$$

where ϵ^α is a spacetime constant, gives rise to a conserved current. Under this transformation the Lagrangian varies into a total derivative

$$\delta\mathcal{L} = \epsilon^\alpha \partial_\alpha \mathcal{L} = \partial_\alpha(\epsilon^\alpha \mathcal{L})\,. \tag{6.31}$$

If the Lagrangian $\mathcal{L}$ only contained first order derivatives the stress tensor would be given as

$$T^\mu_\alpha = -\delta^\mu_\alpha\,\mathcal{L} + \frac{\partial\mathcal{L}}{\partial\phi_\mu}\,\phi_\alpha\,. \tag{6.32}$$

Here we are using the notation

$$\phi_\alpha \equiv \partial_\alpha\phi\,, \tag{6.33}$$

or more generally, for any object A, we define

$$A_{\alpha_1\alpha_2\cdots\alpha_k} \equiv \partial_{\alpha_1}\partial_{\alpha_2}\cdots\partial_{\alpha_k}A\,. \tag{6.34}$$

The familiar result in (6.32) holds for any field ϕ of any tensor type.[1] This is because under *constant* space translations any tensor field transforms as indicated in (6.30). What we wish to have now is the generalization of (6.32) for the case when the action contains all possible numbers of derivatives. Our result will be an expression for the stress tensor involving all numbers of derivatives, and reducing to the above if $\mathcal{L}$ only depends on first derivatives.

We begin the derivation of the general formula by writing the equation of motion

[1] For fields other than scalars the resulting energy-momentum tensor $T_{\mu\alpha}$ may not be symmetric.

following from the action in (6.29). One finds

$$0 = \frac{\partial \mathcal{L}}{\partial \phi} - \Big(\frac{\partial \mathcal{L}}{\partial \phi_{\mu_1}}\Big)_{\mu_1} + \Big(\frac{\partial \mathcal{L}}{\partial \phi_{\mu_1\mu_2}}\Big)_{\mu_1\mu_2} - \cdots + (-1)^k \Big(\frac{\partial \mathcal{L}}{\partial \phi_{\mu_1\cdots\mu_k}}\Big)_{\mu_1\cdots\mu_k} + \cdots \,. \tag{6.35}$$

In here the derivatives are defined as

$$\frac{\partial \phi_{\mu_1\cdots\mu_k}}{\partial \phi_{\nu_1\cdots\nu_k}} = \delta^{\nu_1}_{\mu_1}\cdots\delta^{\nu_k}_{\mu_k}\,, \tag{6.36}$$

with no additional symmetrizations. Thus while $\phi_{\mu_1\cdots\mu_k}$ is by definition symmetric in all indices, $\frac{\partial}{\partial \phi_{\nu_1\cdots\nu_k}}$ is not. It is also useful to note that

$$\partial_\alpha \mathcal{L} = \frac{\partial \mathcal{L}}{\partial \phi}\,\phi_\alpha + \frac{\partial \mathcal{L}}{\partial \phi_{\nu_1}}\,\phi_{\alpha\nu_1} + \frac{\partial \mathcal{L}}{\partial \phi_{\nu_1\nu_2}}\,\phi_{\alpha\nu_1\nu_2} + \cdots + \frac{\partial \mathcal{L}}{\partial \phi_{\nu_1\cdots\nu_k}}\,\phi_{\alpha\nu_1\cdots\nu_k} + \cdots \,. \tag{6.37}$$

This equation encodes the lack of explicit coordinate dependence in the Lagrangian.

At this stage it is simplest to state the result for the energy-momentum tensor and then confirm it is conserved. We find

$$\begin{aligned}
T^\mu_\alpha = \quad & -\delta^\mu_\alpha \mathcal{L} \\
& + \frac{\partial \mathcal{L}}{\partial \phi_\mu}\,\phi_\alpha \\
& - \Big\{ \Big(\frac{\partial \mathcal{L}}{\partial \phi_{\nu_1\mu}}\Big)_{\nu_1} \phi_\alpha - \Big(\frac{\partial \mathcal{L}}{\partial \phi_{\mu\nu_1}}\Big)\,\phi_{\alpha\nu_1} \Big\} \\
& + \Big\{ \Big(\frac{\partial \mathcal{L}}{\partial \phi_{\nu_1\nu_2\mu}}\Big)_{\nu_1\nu_2} \phi_\alpha - \Big(\frac{\partial \mathcal{L}}{\partial \phi_{\nu_1\mu\nu_2}}\Big)_{\nu_1} \phi_{\alpha\nu_2} + \Big(\frac{\partial \mathcal{L}}{\partial \phi_{\mu\nu_1\nu_2}}\Big)\,\phi_{\alpha\nu_1\nu_2} \Big\} \\
& \quad \vdots \\
& + (-1)^k \Big\{ \Big(\frac{\partial \mathcal{L}}{\partial \phi_{\nu_1\nu_2\cdots\nu_k\mu}}\Big)_{\nu_1\nu_2\cdots\nu_k} \phi_\alpha - \Big(\frac{\partial \mathcal{L}}{\partial \phi_{\nu_1\nu_2\cdots\mu\nu_k}}\Big)_{\nu_1\nu_2\cdots\nu_{k-1}} \phi_{\alpha\nu_k} \\
& \qquad \cdots + (-1)^k \Big(\frac{\partial \mathcal{L}}{\partial \phi_{\mu\nu_1\nu_2\cdots\nu_k}}\Big)\,\phi_{\alpha\nu_1\nu_2\cdots\nu_k} \Big\} \\
& \quad \vdots
\end{aligned} \tag{6.38}$$

We must now verify that

$$\partial_\mu T^\mu_\alpha = 0\,, \tag{6.39}$$

when we use the equation of motion (6.35) and equation (6.37). The verification is straightforward once we note that each group of terms in between braces has a simple derivative. When taking a ∂_μ on any such group the only contributions are from: ∂_μ acting on the $\mathcal{L}$ derivative in the first term, and, from ∂_μ acting on the field derivative in the last term. All other derivatives cancel each other due to the alternating signs in the set of terms. As a result we find

$$\begin{aligned}
\partial_\mu T^\mu_\alpha = \quad & -\partial_\alpha \mathcal{L} \\
& + \Big(\frac{\partial \mathcal{L}}{\partial \phi_\mu}\Big)_\mu \phi_\alpha + \Big(\frac{\partial \mathcal{L}}{\partial \phi_\mu}\Big) \phi_{\alpha\mu} \\
& + \Big\{ -\Big(\frac{\partial \mathcal{L}}{\partial \phi_{\nu_1\mu}}\Big)_{\nu_1\mu} \phi_\alpha + \Big(\frac{\partial \mathcal{L}}{\partial \phi_{\mu\nu_1}}\Big) \phi_{\alpha\mu\nu_1} \Big\} \\
& + \Big\{ \Big(\frac{\partial \mathcal{L}}{\partial \phi_{\nu_1\nu_2\mu}}\Big)_{\nu_1\nu_2\mu} \phi_\alpha + \Big(\frac{\partial \mathcal{L}}{\partial \phi_{\mu\nu_1\nu_2}}\Big) \phi_{\alpha\mu\nu_1\nu_2} \Big\} \\
& \quad \vdots \\
& + \Big\{ (-1)^k \Big(\frac{\partial \mathcal{L}}{\partial \phi_{\nu_1\nu_2\cdots\nu_k\mu}}\Big)_{\nu_1\nu_2\cdots\nu_k\mu} \phi_\alpha + \Big(\frac{\partial \mathcal{L}}{\partial \phi_{\mu\nu_1\nu_2\cdots\nu_k}}\Big) \phi_{\alpha\mu\nu_1\nu_2\cdots\nu_k} \Big\} \\
& \vdots
\end{aligned} \tag{6.40}$$

Using the equation of motion (6.35) one finds that the terms multiplying ϕ_α add up to $\frac{\partial \mathcal{L}}{\partial \phi}$. Using (6.37) one then sees that indeed $\partial_\mu T^\mu_\alpha = 0$.

As written, the expression for the energy-momentum tensor can be used directly to obtain its form in p-adic string theory. As mentioned before, this result can be readily extended to a collection of fields ϕ^i. In this case one simply sums over the various fields by replacing in (6.38) the terms

$$\frac{\partial \mathcal{L}}{\partial \phi_{\ldots}}\, \phi_{\ldots} \to \frac{\partial \mathcal{L}}{\partial \phi^i_{\ldots}}\, \phi^i_{\ldots} \tag{6.41}$$

With this replacement we can use (6.38) to find the energy-momentum tensor asso-

ciated to a solution in open string field theory.

6.2.2 Energy in time dependent solutions

The focus in this chapter is on solutions that have time dependence but no spatial dependence. For these class of solutions the expression (6.38) for the energy momentum tensor simplifies considerably and all the tensor components can only have time dependence. From the conservation law, and with i, j, denoting spatial indices,

$$0 = \partial_\mu T_0^\mu = \partial_0 T_0^0 + \partial_i T_0^i = \partial_0 T_0^0 \,. \tag{6.42}$$

Since the energy $T_0^0(t)$ is conserved we do not have ambiguities in its construction – an additive constant ambiguity is fixed by the condition that when the field does not vary in time, the energy must coincide with the potential energy.

For solutions with no spatial dependence we also have that

$$\phi_{\mu_1 \cdots i \cdots \mu_k} = 0 \,, \tag{6.43}$$

since all space derivatives must vanish. Therefore, the terms involving field derivatives in (6.38) vanish when calculating T_i^0 and T_j^i. We find

$$T_i^0 = 0 \,, \qquad T_j^i = -\delta_j^i \mathcal{L} \,. \tag{6.44}$$

Note that the conservation law $\partial_\mu T_i^\mu = 0$ gives $\partial_0 T_i^0 + \partial_j T_i^j = 0$ or equivalently $\partial_j T_i^j = 0$. This conservation does not rule out time dependent improvement terms in T_i^j. Therefore the identification of the pressure as $p(t) = -T_{11} = -T_{22} = \cdots = +\mathcal{L}(t)$ is ambiguous. This is also clear from the fact that it is set to equal the Lagrangian, a quantity for which total time derivatives are ambiguous. We will give a computation of the pressure using the methods of general relativity in the following subsection.

Let us now calculate the energy density T_0^0. Denoting, for any quantity $A(t)$

$$A_n \equiv \frac{\partial^n}{\partial t^n} A \,, \tag{6.45}$$

we find from (6.38) that the k^{th} term in braces becomes

$$(-1)^k\Big\{\Big(\frac{\partial\mathcal{L}}{\partial\phi_{k+1}}\Big)_k\phi_1-\Big(\frac{\partial\mathcal{L}}{\partial\phi_{k+1}}\Big)_{k-1}\phi_2+\cdots+(-1)^k\Big(\frac{\partial\mathcal{L}}{\partial\phi_{k+1}}\Big)_0\phi_{k+1}\Big\}, \tag{6.46}$$

and can be rewritten as

$$\sum_{m=0}^{k}(-1)^m\Big(\frac{\partial\mathcal{L}}{\partial\phi_{k+1}}\Big)_m\phi_{k+1-m}\,. \tag{6.47}$$

We then recognize that the complete expression for the energy is simply

$$E=T_0^0=-\mathcal{L}+\sum_{k=0}^{\infty}\sum_{m=0}^{k}(-1)^m\Big(\frac{\partial\mathcal{L}}{\partial\phi_{k+1}}\Big)_m\phi_{k+1-m}\,. \tag{6.48}$$

Shifting the sum over k by one unit we write

$$E(t)=-\mathcal{L}\;+\;\sum_{k=1}^{\infty}\sum_{m=0}^{k-1}(-1)^m\Big(\frac{\partial\mathcal{L}}{\partial\phi_k}\Big)_m\phi_{k-m}\,. \tag{6.49}$$

This is the result we needed. It provides an expansion for the energy in terms of time derivatives of the field. If the Lagrangian depends only on finite number of derivatives then the expansion terminates for some finite value of k. If the Lagrangian has infinite number of time derivatives then the expression for the energy is an infinite series. That series may or may not be possible to sum in closed form. Nevertheless the expression for the energy is formally local – it gives the value of $E(t)$ in terms of derivatives all of which are evaluated at t.

We will now evaluate the above expression for the energy in the case of the p-adic string theory (6.1). For any solution $p^{-\frac{1}{2}\Box}\phi=\phi^p$ of the equation of motion the Lagrangian density evaluated at the solution becomes

$$\mathcal{L}=\frac{1}{g_p^2}\,\frac{1}{2}\,\frac{1-p}{1+p}\,\phi^{p+1}\,. \tag{6.50}$$

In addition, the derivative $\frac{\partial \mathcal{L}}{\partial \phi_k}$ only exists for even k, and reads:

$$\frac{\partial \mathcal{L}}{\partial \phi_{2\ell}} = -\frac{1}{2g_p^2}\phi\left(\frac{1}{2}\ln p\right)^{\ell}\frac{1}{\ell!}\,. \tag{6.51}$$

With this result, the expression for the energy in (6.49) becomes

$$E(t) = -\mathcal{L} \;+\; \frac{1}{g_p^2}\sum_{\ell=1}^{\infty}\sum_{m=0}^{2\ell-1} -\frac{1}{2}\left(\frac{1}{2}\ln p\right)^{\ell}\frac{1}{\ell!}(-1)^m\phi_m\;\phi_{2\ell-m}\,, \tag{6.52}$$

or, after minor rearrangements,

$$E(t) = -\mathcal{L} \;-\; \frac{1}{2g_p^2}\sum_{\ell=1}^{\infty}\left(\frac{1}{2}\ln p\right)^{\ell}\frac{1}{\ell!}\sum_{m=0}^{2\ell-1}(-1)^m\phi_m\,\phi_{2\ell-m}\,. \tag{6.53}$$

This formula will be used to confirm the correctness of certain solutions of p-adic string theory by testing energy conservation. We will also use it in Section 6.4 to compute the energy of oscillatory solutions.

6.2.3 Calculation of the pressure

In this section we use the unambiguous definition of the energy-momentum tensor from general relativity. We make the p-adic model action invariant under coordinate transformations by including a spacetime metric $g_{\alpha\beta}$ and calculate the energy-momentum tensor as

$$T_{\alpha\beta} = \frac{2}{\sqrt{-g}}\frac{\delta S}{\delta g^{\alpha\beta}}\,. \tag{6.54}$$

The action of the p-adic model, with derivatives expanded and covariantized reads

$$\begin{aligned} S \;&=\; \frac{1}{g_p^2}\int d^dx\sqrt{-g}\left(-\frac{1}{2}\phi^2+\frac{1}{p+1}\phi^{p+1}\right)\\ &\quad -\frac{1}{2g_p^2}\sum_{\ell=1}^{\infty}\left(-\frac{1}{2}\ln p\right)^{\ell}\frac{1}{\ell!}\int d^dx\sqrt{-g}\phi\,\Box^{\ell}\,\phi\,. \end{aligned} \tag{6.55}$$

Here the box operators are the covariant ones, and since all of them act on scalars they can be all written as

$$\Box\,\phi = \frac{1}{\sqrt{-g}}\partial_\mu(\sqrt{-g}g^{\mu\nu}\partial_\nu\,\phi)\,. \tag{6.56}$$

The terms that are delicate to vary involve repeated action of box operators:

$$\begin{aligned}\int dx\sqrt{-g}\phi\,\Box^\ell\,\phi \;\;=\;\; & \int dx\;\phi\;\partial_{\mu_1}\sqrt{-g}g^{\mu_1\nu_1}\partial_{\nu_1}\;\frac{1}{\sqrt{-g}}\partial_{\mu_2}\sqrt{-g}g^{\mu_2\nu_2}\partial_{\nu_2}\;\cdots \\ & \cdots\frac{1}{\sqrt{-g}}\partial_{\mu_\ell}\sqrt{-g}g^{\mu_\ell\nu_\ell}\partial_{\nu_\ell}\,\phi\,,\end{aligned} \tag{6.57}$$

where all derivatives act to the right. Since we are interested in pressure we will only consider the computation of the components of the energy-momentum tensor $T_{\alpha\beta}$ having spatial indices. Since the solutions we focus on are only time dependent, this means that we need not vary the metric components $g^{\mu_i\nu_i}$ appearing above for these would yield contributions to the pressure that have explicit spatial derivatives. It therefore suffices to vary the factors of $\sqrt{-g}$, which is done with the help of

$$\delta\sqrt{-g} = -\frac{1}{2}\sqrt{-g}\;g_{\alpha\beta}\,\delta g^{\alpha\beta}\,,\quad \delta\frac{1}{\sqrt{-g}} = \frac{1}{2}\frac{1}{\sqrt{-g}}\;g_{\alpha\beta}\,\delta g^{\alpha\beta}\,. \tag{6.58}$$

When we vary a particular $\sqrt{-g}$ in (6.57) we must integrate by parts all the derivatives to the left of the variation. There are $(2\ell-1)$ such variations in (6.57), each one giving a different splitting of the derivatives between the two fields. All in all we find (with i not summed) that the pressure is given by

$$p(t) = -T^i_i = \frac{1}{g_p^2}\Big(-\frac{1}{2}\phi^2 + \frac{1}{p+1}\phi^{p+1}\Big) + \frac{1}{2g_p^2}\sum_{\ell=1}^{\infty}\Big(\frac{1}{2}\ln p\Big)^\ell\frac{1}{\ell!}\sum_{m=1}^{2\ell-1}\phi_m\phi_{2\ell-m}\,. \tag{6.59}$$

This pressure formula will be used to analyze rolling solutions.

6.3 Rolling down the unstable p-adic vacuum

In this section we construct solutions representing rolling of the tachyon from the unstable vacuum. That is, we want solutions where in the infinite past the tachyon approaches the unstable vacuum. We will obtain a solution for the case of odd p (even potentials) and another very different solution for the case of even p.

It was already pointed out in [119] that (6.10) has a kink and an anti-kink solution when p is odd. These are the solutions we are interested in for they start on one maximum at $t \to -\infty$. As it turns out they end up on the other maximum at $t \to +\infty$. We will construct such solutions to high accuracy, and verify that they not only solve the convolution form of the field equation, but also the differential form.

The case of even p is much more surprising. Here one could have expected a lump solution, but as we saw in Section 6.1.2 these are not expected to exist. Essentially the difficulties arise because even though the field can go into negative values the convolution, that must equal an even power of the field, cannot. What we find (for $p = 2$) is rolling down, an overshooting and then ever-growing oscillations. This is the result of a calculation using an ansatz for the solution in the form of a sum of exponentials. The result is so surprising that we check it in two ways. One by verifying that the solution thus constructed satisfies the convolution form of the field equation, and second, by evaluating the energy and checking that it is conserved for the indicated motion. We also calculate the pressure and find that it does not go to zero. We will see in Section 6.6 that this behavior seems to occur also in OSFT.

6.3.1 Kink solution for odd p

Even though the analytical form of the kinks are not known, it is relatively easy to construct them numerically. For example, one can use the iterative procedure where a given field configuration $\phi(t)$ is used to calculate the function $\mathcal{C}[\phi]$. The field equation then implies that $(\mathcal{C}[\phi])^{1/p}$ gives a new (and possibly improved) approximation to $\phi(t)$.

Thus we hope for a situation where the iteration

$$\phi(t) \longrightarrow \left(\frac{1}{\sqrt{2\pi \ln p}} \int e^{-\frac{1}{2\ln p}(t-t')^2} \phi(t') dt' \right)^{1/p} , \tag{6.60}$$

converges to some definite answer. Note that for odd p there is no complication taking the root – positive numbers are taken to have positive roots, and negative numbers are taken to have negative roots.

Starting with the step function

$$\phi(t) = \begin{cases} +1, & t < 0 , \\ 0, & t = 0 , \\ -1, & t > 0 , \end{cases} \tag{6.61}$$

$\phi(t)$ will converge to the kink solution when we iterate (6.60). Figure 6-6 shows the kink solutions for $p = 3$, $p = 5$ and $p = 11$. As can be seen from (6.10) (and as already noted in [119]), near $\phi = 0$ the field behaves like $\phi(t) \sim t^{1/p}$. Also when $p \to \infty$, the kink tends to a step function. Note that this means the field zooms by the tachyon vacuum crossing it with infinite velocity and spending the least possible amount of time in its vicinity.

Our numerical kink solutions have been constructed from (6.10). As mentioned before, it is important to check that they also satisfy equation (6.7). From equation (6.3) we have that

$$p^{-\frac{1}{2}\Box} = \exp\left(\frac{1}{2} \ln p \, \partial_t^2\right) = \sum_{m=0}^{\infty} \left(\frac{\ln p}{2}\right)^m \frac{1}{m!} \, \partial_t^{2m} . \tag{6.62}$$

We are thus led to define an approximate version $D^{(2n)}$ of this differential operator where we include time derivatives of order less than or equal to $2n$:

$$D^{(2n)}\phi(t_0) \equiv \sum_{m=0}^{n} \left(\frac{\ln p}{2}\right)^m \frac{1}{m!} \, (\partial_t)^{2m} \, \phi(t_0) . \tag{6.63}$$

In Table 6.1 we perform a check of the solutions obtained for $p = 3$. We choose two

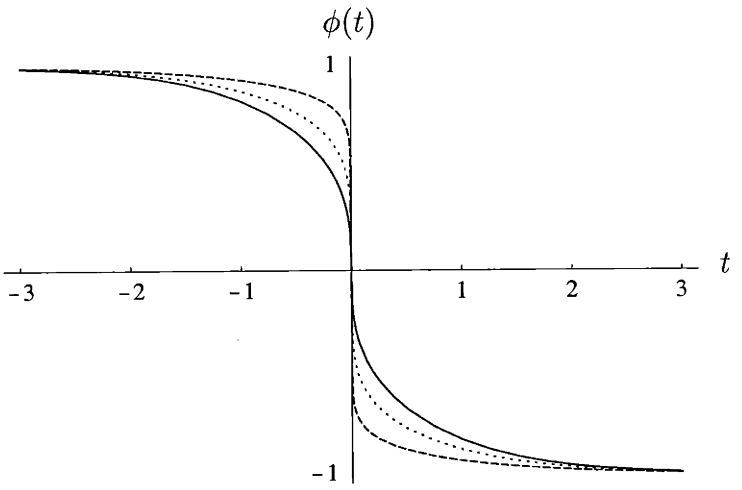

Figure 6-6: Kink solutions for $p = 3$ (solid line), $p = 5$ (dotted line), and $p = 11$ (dashed line). The horizontal axis is time, and the value of the field $\phi(t)$ interpolates between the unstable vacuum $\phi = 1$ in the far past and the unstable vacuum $\phi = -1$ in the far future.

t_0	$\phi(t_0)$	$D^{(2)}\phi(t_0)$	$D^{(4)}\phi(t_0)$	$D^{(6)}\phi(t_0)$	$D^{(8)}\phi(t_0)$	$\phi^3(t_0)$
−4.67086	0.999	0.997905	0.997309	0.997067	0.996974	0.997002
−3.04298	0.99	0.978765	0.972588	0.971867		0.970299

Table 6.1: Checking eqn. (6.7) on the numerical kink solution ($p = 3$) computed from (6.10).

values of the field $\phi = 0.999,\ 0.99$ to do our check. For these values we compare ϕ^3 to $D^{(2n)}\phi$, where the derivatives are evaluated using the numerical solution for the $p = 3$ kink. If $\phi(t_0)$ satisfies (6.7), then $D^{(2n)}\phi(t_0)$ should converge to $\phi^3(t_0)$ when $n \to \infty$. In the first case, only eight derivatives can be evaluated accurately; in the second case, we can trust only six derivatives. In both cases, this suffices to see a relatively good agreement between $D^{(2n)}\phi(t_0)$ and $\phi^3(t_0)$. We thus conclude that the kink obtained by the convolution form of the equation of motion satisfies also the differential form.

If we try to repeat the same check for smaller values of the field, we see that high derivatives have large absolute values, and it would then be necessary to sum a large number of them to observe convergence. Finer numerical methods would be needed to evaluate enough derivatives. It will become clear in Section 6.4 that the kink is

the zero-frequency limit of solutions describing anharmonic oscillations; and this will give us further evidence that the differential form of the equation is indeed satisfied for the kink.

6.3.2 Rolling tachyons for p-adic strings with even p

The case of even p is rather different from the case of odd p. When p is even the potential has only one maximum ($\phi = 1$) and we cannot have a kink solution. We could expect that the kink gets replaced by a lump-like solution, but as we showed in Section 6.1.2, a typical lump solution does not exist. We will see that if the tachyon rolls down the unstable maximum towards the tachyon vacuum it overshoots it and then ever growing oscillations begin. We will first argue qualitatively why such behavior occurs. Then we will calculate the field evolution using a suitable expansion. Finally we will test the solution in two ways.

Qualitative discussion of rolling solution

We now imagine the tachyon starts to roll down from $\phi = 1$ in the infinite past towards the tachyon vacuum $\phi = 0$. Because of claim 1 of Section 6.1.2 we know that the field cannot go asymptotically to the tachyon vacuum for large time. Thus we expect the field to go past $\phi = 0$ into negative values, as illustrated in Figure 6-7 where at some time t_0 we have $\phi(t_0) = 0$. As soon as the field turns negative it becomes delicate satisfying the equation of motion, since the convolution must remain positive. This would be very hard to achieve if the field remains negative for a long time. We can therefore expect the field to reach a minimum at some time t_1 and then go back to zero value at some time t_2.

In Figure 6-7 a dashed line shows the convolution, which must equal ϕ^p. The convolution at t_0 must be zero, and this is possible since the field is substantially negative to the right of t_0. But right after t_0 the convolution must increase. How can that happen when the gaussian peak is moving towards values where ϕ is turning more negative ? This can happen if after t_2 the field $\phi(t)$ is becoming positive very

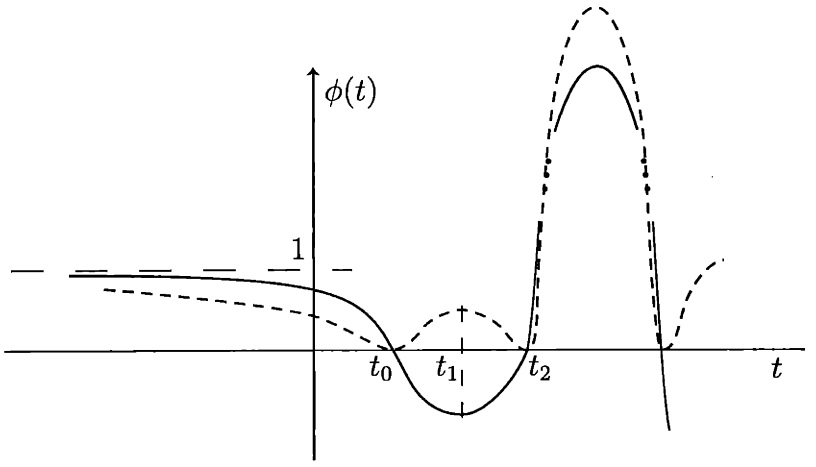

Figure 6-7: A rolling solution for even p and a consistency analysis based on the value of the convolution $C[\phi]$ shown in dashed lines.

quickly. It must become so large and positive that even the fast-decreasing gaussian tail manages to pick up a significant contribution.

Now consider the convolution at t_1. It can be positive because of the large positive values of the field beyond t_2. But this convolution must start decreasing to the right of t_1. It must do so even though the gaussian peak is moving towards values of the field that are large and positive. This can only happen if shortly after t_2 the field turns negative again and does so extremely fast. All in all we find a pattern of ever growing oscillations. We will now confirm this somewhat qualitative analysis with a computation.

Rolling with ever-growing oscillations

We now look for a solution where the tachyon rolls down from its maximum. We shall make the following ansatz

$$\phi(t) = 1 - \sum_{n=1}^{\infty} a_n \, e^{\alpha n t}, \tag{6.64}$$

where $\alpha > 0$ is a constant to be determined. Note that we are using "harmonics" of the basic exponential $e^{\alpha t}$. This is sensible due to the structure of the equation we are trying to solve. With α positive, moreover, we guarantee that as $t \to -\infty$ the field

is at the maximum. This kind of expansion has also been discussed in [120].

It is possible to anticipate the value of α. It should correspond to $\sqrt{-M^2}$, where M^2 is the value of the mass-squared at the maximum. This can also be derived from the field equation, where we will confirm that a_1 plays the role of a "marginal" parameter. Since $M^2 = -2$ at the maximum (for any p) we must have $\alpha = \sqrt{2}$.

The ansatz (6.64) for the solution is plugged into the left hand side of (6.7) and for $p = 2$ we find

$$p^{\frac{1}{2}}\partial_t^2\phi(t) = 1 - \sum_{n=1}^{\infty} a_n \, 2^{\frac{1}{2}\alpha^2 n^2} \, e^{\alpha n t} \,. \tag{6.65}$$

In addition, the right hand side of (6.7), letting $a_0 \equiv -1$ takes the form:

$$(\phi(t))^2 = \sum_{n=0}^{\infty}\Big(\sum_{m=0}^{n} a_m a_{n-m}\Big) \, e^{\alpha n t} \,. \tag{6.66}$$

Therefore the equation gives the set of relations

$$-a_n \, 2^{\frac{1}{2}\alpha^2 n^2} = \sum_{m=0}^{n} a_m a_{n-m} \,, \qquad n \geq 1 \,. \tag{6.67}$$

For the case $n = 1$ we find the condition:

$$-a_1 2^{\frac{1}{2}\alpha^2} = -2a_1 \,, \tag{6.68}$$

which implies that $\alpha = \sqrt{2}$, and a_1 is arbitrary. The relations in (6.67) then give

$$a_n \, (2^{n^2} - 2) = -\sum_{m=1}^{n-1} a_m a_{n-m} \,. \qquad n \geq 2 \,. \tag{6.69}$$

It is clear from this equation that we can determine the *exact* values of the coefficients a_n iteratively. For example, we readily find

$$a_2 = -\frac{a_1^2}{14} \,. \tag{6.70}$$

It may seem at first sight that we have the freedom to choose a_1, but a shift in time

can be used to rescale it to one (or to minus one if a_1 is negative, in which case the tachyon rolls towards the unbounded side of the potential). This is possible because $a_n \sim a_1^n$, as can be seen from (6.69) and (6.70), and the structure of the ansatz (6.64).

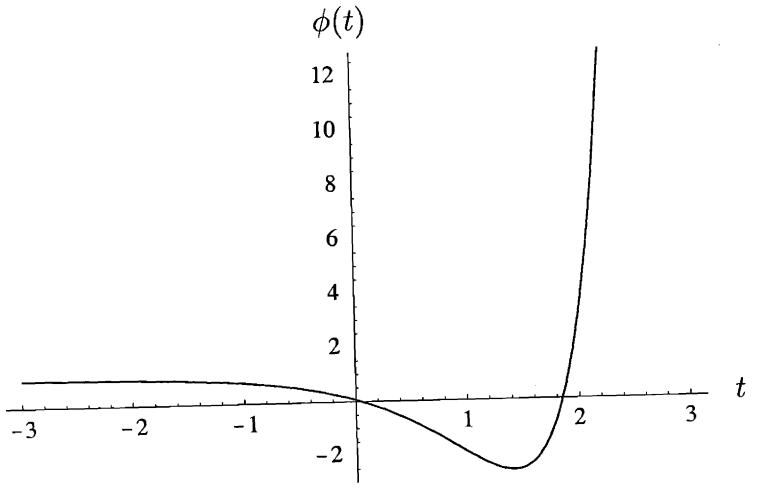

Figure 6-8: The first oscillation of $\phi(t)$ as function of time. The field oscillates with ever-growing amplitude.

The above iterative procedure can be carried to any desired order to find a solution that is accurate for longer and longer times. Here we show the result for $\phi(t)$ to level five

$$\begin{aligned}\phi(t) &= 1 - e^{\sqrt{2}t} + \frac{1}{14}e^{2\sqrt{2}t} - \frac{1}{3570}e^{3\sqrt{2}t} \\ &\quad + \frac{283}{3275389320}e^{4\sqrt{2}t} - \frac{7313}{6105767870038200}e^{5\sqrt{2}t} + \cdots . \end{aligned} \tag{6.71}$$

The signs of a_n alternate, that will make the field oscillate. In Figure 6-8, we plot the first oscillation. We see that the tachyon starts with the value one, rolls slowly towards the minimum, then overshoots the point $\phi = -\frac{1}{2}$ – the point where the tachyon would turn around in a theory with the same potential and with a canonical kinetic term. Here the field goes down to a value of about $\phi = -2.6$. In doing so the field has climbed a height which is about 55 times that of the original height of the unstable minimum! This can be consistent with energy conservation because in the p-adic string model the kinetic energy can be negative. The field turns around

	$t_0 = 0$	$t_0 = 1$	$t_0 = 2$	$t_0 = 3$	$t_0 = 4$	$t_0 = 5$
$\phi(t_0)$	0.0711485	−1.92423	3.17788	184.953	−424.634	−196021
$\phi^2(t_0)$	0.00506212	3.70267	10.0989	34207.7	180314	$3.8424 \cdot 10^{10}$
$\mathcal{C}[\phi](t_0)$	0.00506212	3.70267	10.0989	34207.7	180314	$3.8424 \cdot 10^{10}$

Table 6.2: Comparison between $\phi^2(t_0)$ and $\mathcal{C}[\phi](t_0)$, where ϕ is the solution to level 30. The agreement is remarkable.

at $\phi = -2.6$, overshooting the maximum and continuing to grow until it reaches a value of about $\phi = 593$, a very large value indeed. At this point the potential is very negative and therefore the kinetic energy must be very large and positive. The field then manages to climb up the potential to go to lower values, and continues to oscillate with ever-growing amplitude.

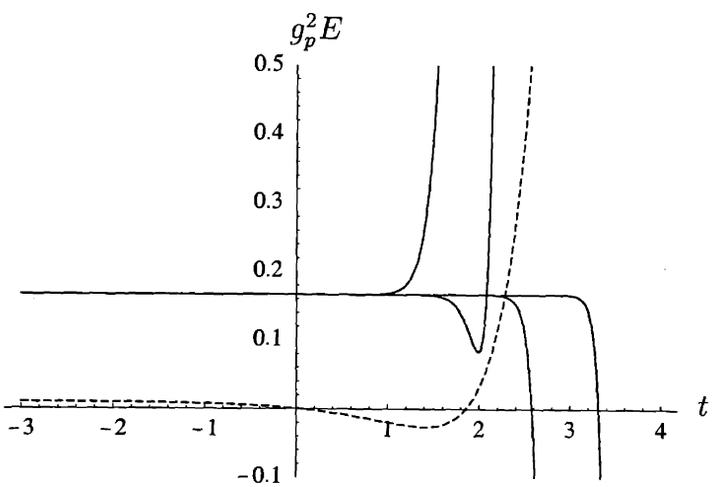

Figure 6-9: Testing the constancy of the energy $E(t)$ for the rolling solution with ever growing oscillations. This figure shows $g_p^2 E(t)$, calculated from (6.53), using a level 30 solution (6.64). The successively flatter (solid) curves are calculated from (6.53), keeping respectively 40, 60, 100, and 150 time derivatives. The dashed curve is $0.01\phi(t)$ and is just shown as a reference.

Testing and exploring the solution

We want to do two kinds of check on this solution. First, since it was constructed from the derivative form of the equation of motion, we want to make sure that it satisfies the convolution form of the equation of motion. This will also confirm the

correctness of the intuition that suggested that convolution requires ever growing oscillations. Then we want to measure the energy of the solution. In particular, we want to confirm the rather unusual property that ever growing oscillations can be compatible with the constancy of the total energy.

In Table 6.2, we compare $\phi^2(t_0)$ to the convolution $\mathcal{C}[\phi](t_0)$ calculated numerically. We have taken $\phi(t)$ to level 30. We see that the agreement holds to at least six digits accuracy. This is impressive given that the field values include very large numbers and therefore are sampling at least two cycles of oscillation.

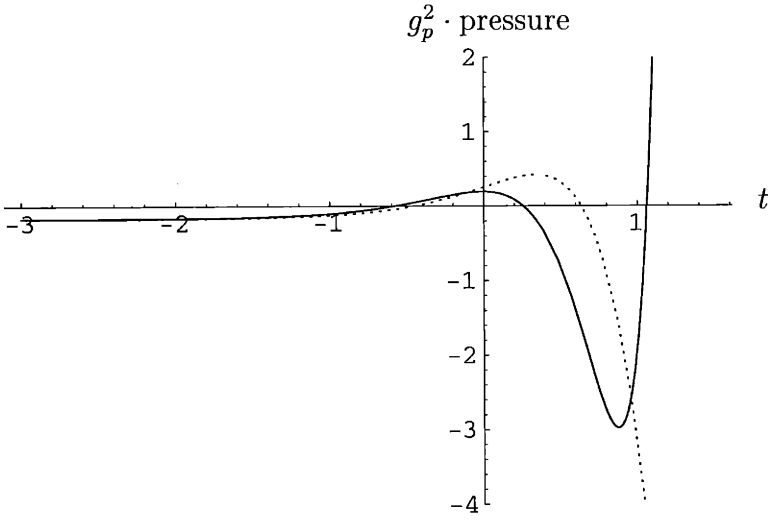

Figure 6-10: Calculating the pressure of the maximal rolling solution for the $p = 2$ potential. Shown in dashed lines is the pressure (multiplied by g_p^2) as calculated including only first derivatives in (6.59). In continuous line is the pressure including all derivatives that are relevant in the interval shown.

In the second test we use the energy formula (6.53) to see if the solution satisfies the requirement that the energy is constant. Since the energy formula includes infinite number of derivatives we expect better accuracy as we include more and more terms. This is indeed what we observe in Figure 6-9. We note that including more derivatives in the energy formula makes it constant for longer times (when the higher derivatives of $\phi(t)$ become more important). It is also clear on this graph, that the energy of the rolling solution is $\frac{1}{6\,g_p^2}$, the height of the maximum of the potential.

In Figure 6-10 we show the pressure (multiplied by g_p^2) as a function of time.

This was calculated using (6.59) and (6.71) evaluating the solution to level 14, and using up to 80 derivatives in the pressure formula. Note that for large negative times the value is negative and equal to $(-1/6)$. Shown in dashed lines, for comparison is the pressure including only the first derivative contribution. We see no sign that the pressure is going to zero for large times, therefore no evidence that this solution represents tachyon matter.

It is of interest to compare this solution with similar rolling solutions in ordinary field theory. As noted in [120] the perturbative expansion of a rolling solution in a ϕ^3 theory using the exponentials associated to the unstable maximum breaks down at a finite time. This does not happen with the p-adic string solution. The expansion coefficients a_n fall off extremely fast due to the factor of 2^{n^2} in (6.69).

6.4 Anharmonic oscillations around the vacuum

The p-adic string model, as reviewed at the beginning of this chapter, satisfies one important property expected from the tachyon. At the minimum, the mass of the field goes to infinity and there are no conventional degrees of freedom. Indeed, for $\phi(t)$ small, the linearized equation of motion is $p^{-\frac{1}{2}\Box}\phi = 0$, which requires $\Box = +\infty$, that is, $m^2 = \infty$. We therefore have no conventional harmonic oscillations at the bottom of the potential.

It will be seen, however, that while there are no oscillations that solve the linearized equations of motion, there are oscillatory solutions of the nonlinear equations of motion. This is the case when p is odd, and the potential is even. Such oscillations do not appear to exist when p is even.

The oscillations represent a family of solutions – in the limit as the frequency goes to zero they go into the kink solution discussed earlier. In the anharmonic oscillations to be constructed below the amplitude of oscillation is a function of the frequency. As the frequency goes to infinity, the amplitude will go to zero. These oscillations can be found numerically, either by solving the convolution equation by iteration (6.60) starting from a periodic $\phi_0(t)$, or by a "level" truncation analysis of the differential

form of the equation of motion, applied on a Fourier expansion of ϕ. We will explain this last method in detail, because it will be useful in order to understand the analytic form of $\phi(t)$ in the large frequency limit. It will also allow us to calculate both the amplitude/frequency relation, and the energy of the oscillations in the large ω limit.

6.4.1 Series construction and amplitude/frequency relation

Let us write a Fourier series for $\phi(t)$ which we imagine oscillates with some amplitude A and period T around the tachyon vacuum $\phi = 0$ of an odd p potential. First, we choose the origin of time axis such that $\phi(0) = A$ and $\partial_t\phi(0) = 0$. Also, since the equation of motion is invariant under $\phi \to -\phi$, we can demand that $-\phi(t) = \phi(t+\frac{T}{2})$, where $T = \frac{2\pi}{\omega}$, with ω the fundamental frequency. This implies that ϕ can be written in terms of odd modes only

$$\phi(t) = \sum_{n=0}^{\infty} a_{2n+1} \cos\left((2n+1)\omega t\right). \tag{6.72}$$

Since ω is defined to be the fundamental frequency we assume $a_1 \neq 0$. It is easily seen that

$$p^{\frac{1}{2}\partial_t^2}\phi(t) = \sum_{n=0}^{\infty} a_{2n+1}\, p^{-\frac{1}{2}\omega^2(2n+1)^2} \cos\left((2n+1)\omega t\right). \tag{6.73}$$

The right hand side $\phi^p(t)$ of the equation of motion can also be expressed as a sum of cosines with odd modes only because p is odd.

Now we want to truncate $\phi(t)$ to level $(2N+1)$: $\phi(t) = \sum_{n=0}^{N} a_{2n+1} \cos\left((2n+1)\omega t\right)$, and for concreteness we will take $p = 3$. To level one, $\phi(t) = a_1 \cos(\omega t)$. Plugging this into the equation of motion gives

$$p^{-\frac{1}{2}\omega^2} a_1 \cos(\omega t) = \left(a_1 \cos(\omega t)\right)^3 = \frac{3}{4}\, a_1^3 \cos(\omega t) + \frac{1}{4}\, a_1^3 \cos(3\omega t), \tag{6.74}$$

and, since we work to level one, we keep only the $\cos(\omega t)$ term:

$$p^{-\frac{1}{2}\omega^2} a_1 = \frac{3}{4}\, a_1^3. \tag{6.75}$$

This equation has the nontrivial solutions

$$a_1 = \pm \frac{2}{\sqrt{3}} 3^{-\frac{1}{4}w^2} . \tag{6.76}$$

With $\omega = 1$, this is $a_1 = \pm 0.877383$. Note that at this level a_1 is the amplitude of oscillation, and it depends nontrivially on the frequency. To level three, $\phi(t) = a_1 \cos(\omega t) + a_3 \cos(3\omega t)$, and we have two equations

$$p^{-\frac{\omega^2}{2}} a_1 = \frac{3}{4} a_1^3 + \frac{3}{4} a_1^2 a_3 - \frac{3}{2} a_1 a_3^2 , \tag{6.77}$$

$$p^{-\frac{9\omega^2}{2}} a_3 = \frac{1}{4} a_1^3 + \frac{3}{2} a_1^2 a_3 - \frac{3}{4} a_3^3 . \tag{6.78}$$

With $\omega = 1$, we have, apart from trivial solutions and obvious sign flips,

$$a_1 = 0.930367 , \qquad a_3 = -0.153804 . \tag{6.79}$$

With these values the amplitude $A \simeq 0.777$. This is not too far from the value $A \simeq 0.818$ obtained by a rather accurate iterative convolution calculation. In Figure 6-11, we show the solutions to level 1, 3 and 9, compared to the very accurate solution obtained from convolution. At level nine the two different numerical methods give almost the same solution. This means that the oscillations satisfy both the convolution and the differential form of the equations of motion. Since the $\omega \to 0$ limit of the anharmonic oscillation is the kink, we also expect that the kink is a solution of both equations of motion, as verified to some degree in Section 6.3.1.

We emphasize that in this example we started by choosing a frequency ω and the numerical solution was then found to be unique (up to obvious time shifts). In particular, the amplitude is given uniquely in terms of ω. In addition, there are solutions for any value of the frequency. This situation is drastically different from the case of classical harmonic oscillations in conventional field theory, where the frequency is given by the mass of the field, but the amplitude is free to take any value.

Although we do not have a closed form solution describing the oscillations, we can

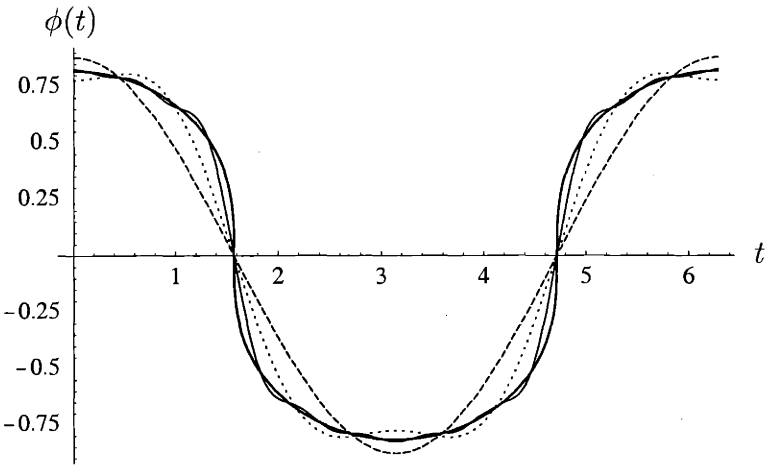

Figure 6-11: Solutions for the anharmonic oscillation with $p = 3$ and $\omega = 1$, to levels 1 (dashed line), 3 (dotted line), 9 (thin solid line), and the more accurate solution from the iteration procedure (thick line). The horizontal axis is time. The amplitude is $A = 0.817615$

derive such closed form in the $\omega \to \infty$ limit. Indeed, in this limit, the right hand side of (6.73) is dominated by the first term in the sum:

$$p^{-\frac{1}{2}\Box}\phi(t) = a_1\, p^{-\frac{1}{2}\omega^2} \cos(\omega t) + \mathcal{O}\left(p^{-\frac{9}{2}\omega^2}\right) . \tag{6.80}$$

From the equation of motion, we thus have

$$\phi^p(t) = a_1\, p^{-\frac{1}{2}\omega^2} \cos(\omega t) + \mathcal{O}\left(p^{-\frac{9}{2}\omega^2}\right) . \tag{6.81}$$

In the $\omega \to \infty$, the $\mathcal{O}(..)$ terms can be neglected and the above equation implies that

$$\phi(t) \overset{\omega\to\infty}{\longrightarrow} A\left[\cos(\omega t)\right]^{1/p} , \tag{6.82}$$

where the amplitude A is related to a_1 and to ω as:

$$A^p = a_1 p^{-\frac{\omega^2}{2}} . \tag{6.83}$$

Recall that since p is odd, there is no problem in taking the root in (6.82) – for negative

arguments the root is defined to be negative. The evaluation of a_1 is possible from the approximate form of $\phi(t)$. Indeed a_1 is the first harmonic in the expansion of $[\cos(\omega t)]^{1/p}$. Using (6.72) we have

$$A\,[\cos(\omega t)]^{1/p} = a_1 \cos(\omega t) + a_3 \cos(3\omega t) + \cdots\,, \tag{6.84}$$

and therefore we can calculate

$$\begin{aligned} a_1 = \frac{\omega}{\pi}\int_0^{\frac{2\pi}{\omega}} \cos(\omega t)\phi(t)dt \quad &\overset{\omega\to\infty}{\longrightarrow} \quad \frac{A}{\pi}\int_0^{2\pi} (\cos x)^{1+\frac{1}{p}}\,dx \\ &= \quad A\,\frac{2\,\Gamma\left(1+\frac{1}{2p}\right)}{\sqrt{\pi}\,\Gamma\left(\frac{3}{2}+\frac{1}{2p}\right)}\,. \end{aligned} \tag{6.85}$$

Now combining (6.83) and (6.85), we find the asymptotic expression for the amplitude:

$$A^{p-1} \overset{\omega\to\infty}{\longrightarrow} \frac{2\,\Gamma\left(1+\frac{1}{2p}\right)}{\sqrt{\pi}\,\Gamma\left(\frac{3}{2}+\frac{1}{2p}\right)}\,p^{-\frac{\omega^2}{2}}\,. \tag{6.86}$$

To illustrate the asymptotic forms we show in Figure 6-12 one period of oscillations for various values of ω and the asymptotic profile (6.82).

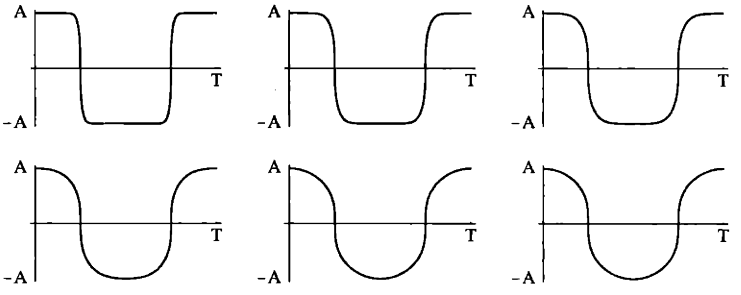

Figure 6-12: One period T of anharmonic oscillations for $p = 3$. On the first row from left to right: $\omega = 0.1$, $\omega = 0.2$, and $\omega = 0.3$. On the second row from left to right: $\omega = 0.5$, $\omega = 2$, and the last graph shows the asymptotic profile $(\cos\omega t)^{1/3}$. The scale has been adjusted to show all periods as equal.

At last, in Table 6.3, we compare the amplitudes of some $p = 3$ numerical solutions (whose absolute accuracy is about 10^{-6}) to the asymptotic amplitudes (6.86). We

	$\omega = 0.6$	$\omega = 0.8$	$\omega = 1$	$\omega = 1.5$	$\omega = 2$
Numerical amplitude	0.962253	0.899904	0.817615	0.580459	0.358948
Amplitude from (6.86)	0.975466	0.903262	0.818225	0.58046	0.358948

Table 6.3: Comparison of the amplitudes of the $p = 3$ anharmonic oscillations, calculated from the numerical solutions and from the asymptotic formula (6.86).

see that both the profile and the amplitude approach rapidly their asymptotic limits. The asymptotic amplitude is already precise to six digits when $\omega \geq 2$.

6.4.2 Energy of anharmonic oscillations

It is possible to simplify the formula (6.53) for the energy in the case of anharmonic oscillations. We will eventually find the following asymptotic expression for the energy

$$E \overset{\omega\to\infty}{\longrightarrow} \frac{h_p}{g_p^2}\,\omega^2\,A^{p+1}\,, \tag{6.87}$$

where h_p is a p-dependent constant that will be determined in the following calculation.

Let us plug the expansion (6.72) into (6.53). Since the energy is conserved, we can evaluate it at $t = 0$; at this particular time, all the odd derivatives of ϕ vanish; and the m-th derivative, for m even, is

$$\phi_m(0) = \sum_{n=0}^{\infty} a_{2n+1}(-1)^{\frac{m}{2}}(2n+1)^m\omega^m\,. \tag{6.88}$$

Thus (6.53) becomes

$$\begin{aligned} E \;=\; & -\mathcal{L}(t=0) - \frac{1}{2g_p^2}\sum_{\ell=1}^{\infty}\left(\frac{1}{2}\ln p\right)^{\ell}\frac{1}{\ell!}\sum_{\substack{m=0\\ m\text{ even}}}^{2\ell-2}(-1)^m \times \\ & \times\sum_{n=0}^{\infty} a_{2n+1}(-1)^{\frac{m}{2}}(2n+1)^m\omega^m\sum_{k=0}^{\infty} a_{2k+1}(-1)^{\ell-\frac{m}{2}}(2k+1)^{2\ell-m}\omega^{2\ell-m}\,. \end{aligned}$$

After obvious simplifications, and rearranging the order of summation, we get

$$E = -\mathcal{L}(t=0) - \frac{1}{2g_p^2}\sum_{n,k=0}^{\infty} a_{2n+1}a_{2k+1}\sum_{\ell=1}^{\infty}\Big(-\frac{\omega^2(2k+1)^2}{2}\ln p\Big)^{\ell}\frac{1}{\ell!}\sum_{\substack{m=0\\ m\text{ even}}}^{2\ell-2}\left(\frac{2n+1}{2k+1}\right)^m .$$

The last sum is a finite geometric series, it can thus be summed explicitly

$$\sum_{\substack{m=0\\ m\text{ even}}}^{2\ell-2}\left(\frac{2n+1}{2k+1}\right)^m = \begin{cases} \ell & , \quad n=k \\ \frac{1-\left(\frac{2n+1}{2k+1}\right)^{2\ell}}{1-\left(\frac{2n+1}{2k+1}\right)^2} & , \quad n\neq k \end{cases} .$$

The energy then becomes

$$\begin{aligned} E \;=\; & -\mathcal{L}(t=0) - \frac{1}{2g_p^2}\sum_{n=0}^{\infty} a_{2n+1}^2\Big(-\frac{\omega^2(2n+1)^2}{2}\ln p\Big)\sum_{\ell=0}^{\infty}\Big(-\frac{\omega^2(2n+1)^2}{2}\ln p\Big)^{\ell}\frac{1}{\ell!} - \\ & -\frac{1}{2g_p^2}\sum_{\substack{n,k=0\\ n\neq k}}^{\infty} a_{2n+1}a_{2k+1}\frac{1}{1-\left(\frac{2n+1}{2k+1}\right)^2}\sum_{\ell=1}^{\infty}\Big(-\frac{\omega^2}{2}\ln p\Big)^{\ell}\frac{1}{\ell!}\left((2k+1)^{2\ell}-(2n+1)^{2\ell}\right) . \end{aligned}$$

We can now do explicitly the ℓ sums and they give simply exponentials. And since ϕ is a solution of the equation of motion, we have

$$\mathcal{L}(t=0) = \frac{1}{2g_p^2}\frac{1-p}{1+p}A^{p+1} ,$$

where $A = \phi(0)$ is the amplitude of the oscillation. The expression for the energy thus simplifies to

$$\begin{aligned} E \;=\; & \frac{1}{2g_p^2}\frac{p-1}{p+1}A^{p+1} + \omega^2\frac{\ln p}{4g_p^2}\sum_{n=0}^{\infty} a_{2n+1}^2(2n+1)^2 p^{-\frac{\omega^2(2n+1)^2}{2}} + \\ & +\frac{1}{2g_p^2}\sum_{\substack{n,k=0\\ n\neq k}}^{\infty} a_{2n+1}a_{2k+1}\frac{1}{1-\left(\frac{2n+1}{2k+1}\right)^2}\left(p^{-\frac{\omega^2(2n+1)^2}{2}} - p^{-\frac{\omega^2(2k+1)^2}{2}}\right) . \end{aligned} \tag{6.89}$$

We now want to find the asymptotic behavior of (6.89) when $\omega \to \infty$. This is easily done by noting, from (6.86), that $p^{-\frac{\omega^2}{2}} \sim A^{p-1}$, and from (6.84), that $a_{2n+1}^2 \sim A^2$. With this we see that the leading term in the first sum of (6.89) is the first term, and it is of order $\omega^2 A^{p+1}$. On the other hand the leading term in the second sum is of

order A^{p+1}. This is also the order of the first term in the equation. Therefore, in the limit that we are considering, the leading term in the energy is

$$\frac{1}{g_p^2}\,\omega^2\,\frac{\ln p}{4}a_1^2 p^{-\frac{\omega^2}{2}} = \frac{1}{g_p^2}\,\frac{\ln p}{2\sqrt{\pi}}\frac{\Gamma\left(1+\frac{1}{2p}\right)}{\Gamma\left(\frac{3}{2}+\frac{1}{2p}\right)}\,\omega^2\,A^{p+1}\,,$$

where we have used (6.85) and (6.86). In total the final expression is

$$E = \frac{1}{g_p^2}\left(\frac{\ln p}{2\sqrt{\pi}}\frac{\Gamma\left(1+\frac{1}{2p}\right)}{\Gamma\left(\frac{3}{2}+\frac{1}{2p}\right)}\,\omega^2\,A^{p+1} + \mathcal{O}(A^{p+1}) + \text{higher powers of } A\right)\,, \qquad (6.90)$$

where the first correction is of order A^{p+1}, without an ω^2 in front of it. The next terms are higher powers of A, and their relative contributions are thus exponentially vanishing when $\omega \to \infty$. It is straightforward to confirm that the above result would arise by computing the energy using simply $\phi = a_1 \cos(\omega t)$. Thus in this large frequency approximation the first harmonic carries the leading contribution to the energy.

In harmonic oscillations, the energy goes like $A^2\omega^2$, where A is the amplitude and ω is the frequency. The frequency dependence of the energy for the anharmonic oscillations is the same, but the amplitude dependence is different – the amplitude appears with the same power as it appears in the potential. Of course, in the present case the amplitude and frequency are not independent variables.

In summary, we have found physical, energy-carrying excitations around the tachyon vacuum. If we try to interpret them in the context of string theory, they could correspond to non-conventional open string excitations that may radiate into closed strings. In the Sen conjecture, where the tachyon vacuum is supposed to be the closed string vacuum, physical excitations around the closed string vacuum would naturally be interpreted as closed strings. Could the above anharmonic oscillations represent closed strings? Perhaps, but there are a few complications. First, these solutions do not have analogs for even p potentials where any oscillation must eventually grow without limit. In some ways the even p case seems more closely related to bosonic string theory. In addition, we have calculated what would be the analog

of *classical* open string solutions. The closed string states would correspond to the quantization of the above oscillations. Since the closed string spectrum should be coupling constant independent, the quantization must somehow cancel out the factor $1/g_o^2$ present in the energy of the classical solutions. For other discussion of closed strings and the tachyon vacuum see [105, 70, 121].

6.5 Family of Solutions for Even p

We have already found a family of solutions for the case of odd p – the anharmonic oscillations around the tachyon vacuum. In this section we will present a continuous family of solutions for even p that are, in some sense the closest analog to the anharmonic oscillations of the odd p theory. The oscillations, however, will be unbounded. This can happen even in the limit when the energy can be vanishingly small.

In studying the maximal rolling solution for even p in Section 6.3.2, we saw that the "frequency" α in the expansion (6.64) was forced to take the value $\sqrt{2}$. We will now describe a family of solutions labelled by a parameter α such that $0 < \alpha < \sqrt{2}$. For simplicity we will consider only the case $p = 2$. Our ansatz is therefore

$$\phi(t) = \sum_{n=0}^{\infty} a_n \cosh(n\alpha t)\,. \tag{6.91}$$

A solution of this form has time-reversal symmetry $\phi(-t) = \phi(t)$. And at $t = 0$, the tachyon field has value $\phi(0) = \sum_{n=0}^{\infty} a_n$. Let us set up the level truncation scheme for this ansatz. For convenience is it useful to rewrite the expansion as

$$\phi(t) = \frac{1}{2} \sum_{n=-\infty}^{\infty} \bar{a}_n\, e^{n\alpha t}\,, \tag{6.92}$$

with

$$\bar{a}_{-n} = \bar{a}_n = a_n\,, \quad \text{for} \quad n \neq 0\,, \qquad \bar{a}_0 = 2a_0\,. \tag{6.93}$$

Again, the left hand side of the equation of motion is simple

$$p^{\frac{1}{2}}\partial_t^2\phi(t) = \frac{1}{2}\sum_{n=-\infty}^{\infty}\bar{a}_n\, p^{\frac{1}{2}n^2\alpha^2}e^{n\alpha t}\,. \tag{6.94}$$

The right hand side of the equation of motion gives:

$$\phi^2(t) = \frac{1}{4}\sum_{n=-\infty}^{\infty}\Big(\sum_{m=-\infty}^{\infty}\bar{a}_m\,\bar{a}_{n-m}\Big)\,e^{n\alpha t}\,. \tag{6.95}$$

The last two equations imply that the equation of motion is equivalent to the set of equations:

$$\bar{a}_n\, p^{\frac{1}{2}n^2\alpha^2} = \frac{1}{2}\sum_{m=-\infty}^{\infty}\bar{a}_m\,\bar{a}_{n-m}\,. \tag{6.96}$$

The structure of these equations ensures that it suffices to consider $n \geq 0$. Moreover it is clear that given that the sum in the right hand side is infinite one cannot solve these equations exactly. A level expansion, of course, is possible. To work at level N means to keep all equations above with $0 \leq n \leq N$ and to keep all $\bar{a}_q$ with $|q| \leq N$. Finally, let us note that given a solution with expansion coefficients a_n we get another solution by letting

$$a_n \to (-1)^n a_n\,. \tag{6.97}$$

To level zero the equation of motion is $a_0 = a_0^2$, and has for solution a tachyon sitting either at the maximum or at the minimum of the potential. To level one, we have two equations for a_0 and a_1

$$a_0 = a_0^2 + \frac{a_1^2}{2}\,, \tag{6.98}$$

$$2^{\frac{1}{2}\alpha^2}a_1 = 2a_0a_1\,. \tag{6.99}$$

Apart from trivial solutions, one finds

$$\begin{aligned} a_0 &= 2^{\frac{\alpha^2}{2}-1}\,, \\ a_1 &= \pm 2^{\frac{\alpha^2}{4}-\frac{1}{2}}\sqrt{2-2^{\frac{\alpha^2}{2}}}\,. \end{aligned} \tag{6.100}$$

α	1.41	1.4	1.3	1.2	1	0.8
$g_p^2 E$	0.16082	0.147657	0.0592576	0.0205954	0.00114305	$6.59996 \cdot 10^{-6}$

Table 6.4: Energy of the solution for some values of the parameter α. When α is close to $\sqrt{2}$, we have $g_p^2 E \approx \frac{1}{6}$. And as α decreases, the energy goes to zero very fast.

Some interesting features can already be seen to this level. First of all, note that we have two branches, indexed by the sign of a_1, and as could be anticipated by (6.97). If a_1 is positive, a higher level analysis indicates that so will be all higher coefficients a_n, and the solution diverges to positive field values without oscillating. When a_1 is negative, the signs of the a_n will alternate, making the solution oscillate with ever-increasing amplitude.

It is also clear from (6.100) that α has to be smaller than $\sqrt{2}$ in order for a_1 to be real. In this regard, the maximal rolling solution of Section 6.3.2, having $\alpha = \sqrt{2}$ can be thought as a limit case. It cannot be obtained, however, by taking the $\alpha \to \sqrt{2}$ limit of (6.91), that would only give a trivial solution.

The values of the field at $t = 0$ and at this present level one approximation are (taking a_1 to be negative)

$$\lim_{\alpha \to \sqrt{2}} \phi(0) = 1\,, \qquad \lim_{\alpha \to 0} \phi(0) = \frac{1}{2} - \frac{1}{\sqrt{2}} \approx -0.207\,. \tag{6.101}$$

Higher level analysis shows that for any α between 0 and $\sqrt{2}$, the solution oscillates without a bound. When $\alpha \to \sqrt{2}$, we have $\phi(0) \to 1$, and the energy tends to $\frac{1}{6 g_p^2}$, the height of the potential at its maximum. When $\alpha \to 0$ however, $\phi(0) \to 0$ and the field becomes flatter near $t = 0$, in other words one has to wait for longer times before we see it taking large values. This is illustrated in Figure 6-13. Moreover the energy goes to zero very fast as α becomes small. Even though in these solutions the field can spend a long time oscillating around the tachyon vacuum their energy is necessarily very small, and thus they cannot represent tachyon matter. In Table 6.4, we show a few values calculated from the formula (6.53) applied on numerical solutions at level 30.

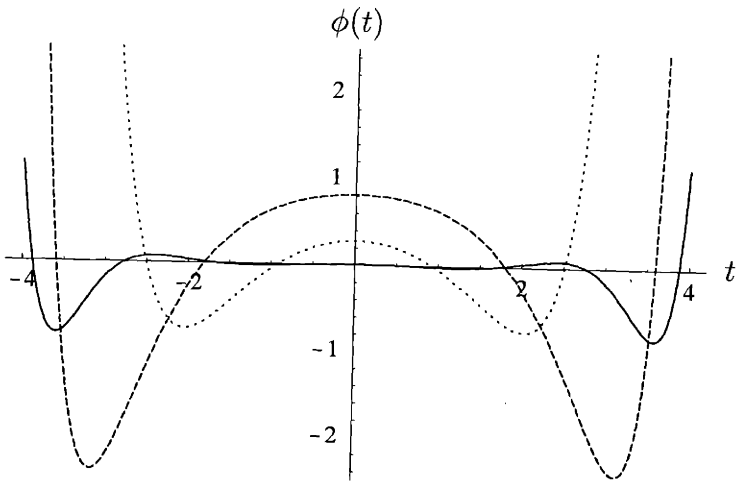

Figure 6-13: Tachyon profiles as functions of t for $\alpha = 1.4$ (dashed line), $\alpha = 1.2$ (dotted line), and $\alpha = 0.8$ (solid line). The curves become flatter near the origin when α is decreased.

6.6 Rolling the tachyon in open string field theory

In this section we study the rolling of the tachyon in OSFT. There are at least two ways we could do this analysis. In the first one, we would use level expansion to focus on a few low levels, write the equations of motion (containing infinitely many time derivatives) and solve them as in the p-adic string case. A second method was proposed in ref. [16] (Section 2), and it uses the analytic continuation of the marginal string field theory solution of ref.[84]. This is the method we will follow here to examine the rolling tachyon.

We will consider the solution representing a marginal deformation of a D1 brane stretched along a circle of unit radius. This marginal deformation can be used to interpolate from the D1 into a D0 brane, and it involves tachyon and higher field harmonics of the type $\cos(nX)$, where X is a coordinate along the circle. The analytic continuation requires replacing $\cos(nX) \to \cosh(nt)$. We use the solutions of [84], Section 3, and let the radius go to one. In addition, we work including fields up to level four and interactions up to level eight, using the action given in Appendix B of [84]. In this way we can include up to the second harmonic of the tachyon. The marginal direction is represented by the first tachyon harmonic T_1 appearing in the

tachyon field expansion

$$T(t) = T_0 + T_1 \cosh(t) + T_2 \cosh(2t) + \cdots . \tag{6.102}$$

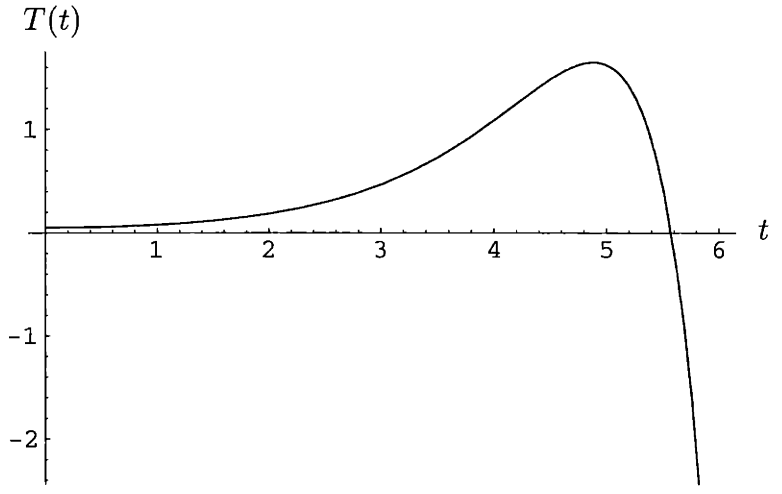

Figure 6-14: The tachyon profile as a function of time as it rolls down in OSFT. The initial conditions are $T(0) = 0.05144$ and $T'(0) = 0$. The tachyon rolls past the tachyon vacuum $T \simeq 0.55$ and the first turning point is at about $T \simeq 1.65$.

The string field equations are solved by setting a value for T_1 and solving for the other components of the string field. We take $T_1 = 0.05$ and the equations of motion give

$$T(t) = 0.00162997 + 0.05 \cosh(t) - 0.000189714 \cosh(2t) . \tag{6.103}$$

It is in fact this result that motivated much of the analysis in the present chapter, and a few comments are thus in order. First note that use of the cosh expansion implies that the field satisfies $\dot{T}(0) = 0$. The other initial condition could be viewed as giving the value of the tachyon at $t = 0$. But certainly that is not the way the equation is solved. Fixing T_1 one solves for all other harmonics $T_0, T_2, \cdots$, and all of them together fix the initial value of the tachyon. For $T_1 = 0.05$ we find from the above equation that $T(0) = 0.05144$ and $T'(0) = 0$. The first harmonic $\cosh(t)$ reflects the blowing up of the tachyon in the approximation where the potential is quadratic. Note that the second harmonic comes about with negative sign, thus at some time the

tachyon stops growing and turns around. We had expected naively that this turning point would be around the tachyon vacuum, thus signaling in this approximation that the tachyon does not cross over. But the result does not support this expectation. In here the tachyon overshoots the tachyon vacuum by a large factor. The maximum is reached for $t \simeq 4.88$ and gives $T = 1.649$, which is about three times the value $T \simeq 0.55$ representing the tachyon vacuum. The tachyon as a function of time, is shown in Figure 6-14. We have verified that the turning point $T \simeq 1.65$ is quite stable under small changes of the marginal parameter T_1, supporting the conclusion that the tachyon generically overshoots the tachyon vacuum before turning around.

The analogy with the $p = 2$ maximal rolling solution is actually quite striking. Recall the discussion below eqn. (6.71), where we observed that the p-adic tachyon climbs a height equal to about 55 times the height of the unstable vacuum. We can estimate easily the corresponding quantity in the above OSFT computation. Taking the tachyon potential to be the level zero one $V = -\frac{1}{2}T^2 + \frac{27\sqrt{3}}{64}T^3$, an overshooting to $T = 1.65$ implies that the OSFT tachyon climbs up about 56 times the height of the unstable vacuum! While such close agreement is most likely a coincidence, the fact that these quantities are close confirms that the p-adic model seems to capture quite well OSFT features in a simpler context.

What happens next? To answer this we would need the value of T_3 the third tachyon harmonic. This, however, would require a level (9,18) computation which is a major new task. There are indications, however, that the next coefficient in (6.103) would be positive, and that ever growing oscillations occur, just as in the case of p-adic strings with even p.

For the value $T_1 = 0.05$ used above, the next three fields u, v and w, all of them at level 2, are:

$$\begin{aligned} u(t) &= 0.000663831 + 9.216 \times 10^{-7} \cosh(t)\,, \\ v(t) &= -0.00162516 + 0.00003999 \cosh(t)\,, \\ w(t) &= 0.000301312 - 6.325 \times 10^{-6} \cosh(t)\,. \end{aligned} \tag{6.104}$$

With such small values for the first harmonic, these fields do not appear to change significantly the physics of the tachyon. This was also the case in the original marginal deformation problem, where level expansion was seen to operate quite well. In this level (4,8) solution there are additional fields at level three and at level four. We will not write here their values.

We will not attempt here a computation of the pressure in this OSFT solution, but such computation would be of interest. With the behavior of the solution strikingly similar to that of the p-adic string solution for $p = 2$, we see no reason to expect that the pressure goes to zero asymptotically, but there could be surprises. A computation would settle this important issue.

6.7 Concluding remarks and open questions

In this chapter we have studied tachyon dynamics in string field theory and in p-adic string theory facing up to the novelties due to the infinite number of time derivatives in the field equations.

Several classes of rolling solutions of p-adic string theory have been studied. We have not been exhaustive in showing all of them nor in trying to show that we have a complete set of solutions. For example, there are non-oscillatory diverging solutions for $p = 2$ related by the sign change in (6.97) to the oscillatory solutions. In addition there are similar solutions for $p = 3$ (and possibly all odd p). These solutions also show ever growing oscillations, and can be modified by the sign change in (6.97) and by an overall change of sign. There are also additional solutions (both for even and odd p) arising from the analytic continuation of the familiar lump solutions of p-adic string theory. At present, for any value of the energy we know of a finite number of solutions.

In general terms our analysis has revealed a few surprises:

- The solution space of the equations of motions appears to consist of real analytic (smooth) functions. Solutions appear to be in one-to-one correspondence with *consistent* initial values for the field and all of its derivatives. The dynamical

equation imposes a possibly infinite number of conditions on the initial values and thus restricts considerably the solution space. This remarkable feature of the equation of motion was not anticipated by the consideration of systems with finite number of time derivatives.

- There are energy-carrying solutions of the field equations around the tachyon vacuum. These bounded but anharmonic oscillations shown to exist in the case of p-adic strings with even potentials, represent solutions of the non-linear equations not anticipated by the linearized (cohomology-like) problem that admits no solutions.

- There exist oscillatory solutions with ever-growing amplitudes and constant energy. In fact, such solutions exist even for energies that approach zero. These solutions exhibit behaviors not seen in Lagrangians quadratic in first time derivatives where the kinetic energy is positive definite. In the systems considered here the kinetic energy can be negative and thus one can see the tachyon move to higher and higher heights on the tachyon potential while conserving the total energy.

At the technical level we have calculated the energy-momentum tensor in higher derivative theories, finding useful expressions for the energy and the pressure in the case of time dependent solutions. We have also learned how to extract qualitative behavior of the solutions using the convolution form of the field equation. Finally, we have shown how to obtain solutions by numerical methods, and by analytic methods in certain limits.

Interesting open questions remain. We list below a few of them:

- From the physical viewpoint, the most puzzling result has been that none of the rolling solutions obtained here appear to represent tachyon matter. That is, we have not found solutions where with varying values of the energy the pressure goes to zero for long times. The rolling solutions described in this chapter would seem to yield oscillating energy-momentum tensors that could

effectively convert the D-brane energy into closed string excitations. This had been the conventional wisdom (see, for example [122]) before studies of tachyon matter. Given the exciting possibility that a stable form of tachyon matter could have astrophysical consequences it seems of utmost importance to confirm its (theoretical!) existence using string field theory. Since the tachyon vacuum is at a finite and apparently regular value in the field space of string field theory, tachyon matter must be, if present, an exotic solution.

- For the case of even p-adic potentials, the anharmonic excitations around the tachyon vacuum do represent non-conventional type of excitations. The most straightforward interpretation is that they are degrees of freedom that would radiate their energy into closed strings. Could they actually represent closed strings? While preliminary indications do not support this interpretation, further investigation of the physics and interpretation of these solutions are of interest.

- We have seen that there is no conventional initial value problem in the sense that finding *consistent initial conditions* appears to be the same problem as finding the solution. The space of consistent initial conditions appears to be strongly constrained in the nonlinear equations of motion of p-adic string theory. How many parameters does the space of consistent initial conditions have?

- Our work has given an explicit construction for the energy density of spatially homogeneous solutions in OSFT. The calculation of the pressure was more subtle and was only done for the p-adic string. The OSFT pressure should be computed to test if, as opposed to the case of the p-adic model, the ever growing oscillations could have an asymptotically vanishing pressure. A more geometrical construction would use open/closed string field theory [68], where the energy-momentum tensor would arise from a variation of the closed string field. It may be of interest to give such stringy construction.

- One feature of string field theory is that the infinitely many time derivatives of

the covariant formulation turn into first order time derivatives in the light cone formulation. Studies of gauge fixing in string field theory have not revealed how this transformation actually happens. It would therefore be of interest to understand if there is a light-cone gauge p-adic string theory. If the answer is affirmative the passage from covariant to light-cone formulation could be tractable and provide much insight.

- The convolution form of the field equation seems to hide completely the causality properties of the time evolution. It would be of interest to formulate and explore a test of causality in p-adic string theory.

It is clear that in p-adic string theory and in OSFT we have a rich set of problems and issues that should allow us to improve our understanding of time evolution in string theory. Such understanding seems essential for the development of string theory cosmology.

Appendix A

Tables

A.1 Table of scalar states at levels ≤ 6

The following table describes the scalar states at levels $0, 2, 4$ and 6. The SZ column relates these fields to the background-independent fields used in [15]. m and g are the indices of the matter and ghost states into which each scalar decomposes through (2.9). $g\langle\psi^i\rangle_L$ denote expectation values of the scalar fields in level truncations (4, 12), (6, 18) and (10, 20).

ψ^i	SZ	state	m	g	$g\langle\psi^i\rangle_4$	$g\langle\psi^i\rangle_6$	$g\langle\psi^i\rangle_{10}$
ψ^1	ϕ	$\|\Omega\rangle$	1	1	1.09680	1.09586	1.09259
ψ^2	$v/\sqrt{52}$	$(\alpha_{-1}\cdot\alpha_{-1})\ \|\Omega\rangle$	2	1	0.05692	0.05714	0.05723
ψ^3	$-u$	$b_{-1}c_{-1}\ \|\Omega\rangle$	1	2	-0.41135	-0.42363	-0.43372
ψ^4	$A+B$	$(\alpha_{-1}\cdot\alpha_{-3})\ \|\Omega\rangle$	4	1	-0.01142	-0.01146	-0.01148
ψ^5	$A/2$	$(\alpha_{-2}\cdot\alpha_{-2})\ \|\Omega\rangle$	5	1	-0.00512	-0.00511	-0.00509
ψ^6	$B/4$	$(\alpha_{-1}\cdot\alpha_{-1})(\alpha_{-1}\cdot\alpha_{-1})\ \|\Omega\rangle$	6	1	-0.00029	-0.00031	-0.00032
ψ^7	$-F$	$(\alpha_{-1}\cdot\alpha_{-1})\,b_{-1}c_{-1}\ \|\Omega\rangle$	2	2	0.00686	0.00740	0.00786
ψ^8	$-C$	$b_{-1}c_{-3}\ \|\Omega\rangle$	1	5	0.11242	0.11478	0.11654
ψ^9	E	$b_{-2}c_{-2}\ \|\Omega\rangle$	1	6	0.06621	0.06813	0.06990
ψ^{10}	D	$b_{-3}c_{-1}\ \|\Omega\rangle$	1	7	0.03747	0.03826	0.03885
ψ^{11}		$(\alpha_{-1}\cdot\alpha_{-5})\ \|\Omega\rangle$	10	1		0.00349	0.00350
ψ^{12}		$(\alpha_{-2}\cdot\alpha_{-4})\ \|\Omega\rangle$	11	1		0.00293	0.00291
ψ^{13}		$(\alpha_{-3}\cdot\alpha_{-3})\ \|\Omega\rangle$	12	1		0.00144	0.00143
ψ^{14}		$(\alpha_{-1}\cdot\alpha_{-3})(\alpha_{-1}\cdot\alpha_{-1})\ \|\Omega\rangle$	13	1		0.00028	0.00028
ψ^{15}		$(\alpha_{-2}\cdot\alpha_{-2})(\alpha_{-1}\cdot\alpha_{-1})\ \|\Omega\rangle$	14	1		0.00015	0.00015
ψ^{16}		$(\alpha_{-1}\cdot\alpha_{-2})(\alpha_{-1}\cdot\alpha_{-2})\ \|\Omega\rangle$	15	1		0.00001	0.00001
ψ^{17}		$(\alpha_{-1}\cdot\alpha_{-1})(\alpha_{-1}\cdot\alpha_{-1})(\alpha_{-1}\cdot\alpha_{-1})\ \|\Omega\rangle$	16	1		-0.00000	-0.00000
ψ^{18}		$(\alpha_{-1}\cdot\alpha_{-3})\,b_{-1}c_{-1}\ \|\Omega\rangle$	4	2		-0.00263	-0.00280
ψ^{19}		$(\alpha_{-2}\cdot\alpha_{-2})\,b_{-1}c_{-1}\ \|\Omega\rangle$	5	2		-0.00116	-0.00121
ψ^{20}		$(\alpha_{-1}\cdot\alpha_{-1})(\alpha_{-1}\cdot\alpha_{-1})\,b_{-1}c_{-1}\ \|\Omega\rangle$	6	2		-0.00008	-0.00009
ψ^{21}		$(\alpha_{-1}\cdot\alpha_{-2})\,b_{-1}c_{-2}\ \|\Omega\rangle$	3	3		-0.00013	-0.00015
ψ^{22}		$(\alpha_{-1}\cdot\alpha_{-2})\,b_{-2}c_{-1}\ \|\Omega\rangle$	3	4		-0.00006	-0.00007
ψ^{23}		$(\alpha_{-1}\cdot\alpha_{-1})\,b_{-1}c_{-3}\ \|\Omega\rangle$	2	5		-0.00336	-0.00351
ψ^{24}		$(\alpha_{-1}\cdot\alpha_{-1})\,b_{-2}c_{-2}\ \|\Omega\rangle$	2	6		-0.00283	-0.00295
ψ^{25}		$(\alpha_{-1}\cdot\alpha_{-1})\,b_{-3}c_{-1}\ \|\Omega\rangle$	2	7		-0.00112	-0.00117
ψ^{26}		$b_{-1}c_{-5}\ \|\Omega\rangle$	1	12		-0.06003	-0.06094
ψ^{27}		$b_{-2}c_{-4}\ \|\Omega\rangle$	1	13		-0.03750	-0.03816
ψ^{28}		$b_{-3}c_{-3}\ \|\Omega\rangle$	1	14		-0.02283	-0.02291
ψ^{29}		$b_{-4}c_{-2}\ \|\Omega\rangle$	1	15		-0.01875	-0.01908
ψ^{30}		$b_{-5}c_{-1}\ \|\Omega\rangle$	1	16		-0.01201	-0.01219
ψ^{31}		$b_{-2}b_{-1}c_{-2}c_{-1}\ \|\Omega\rangle$	1	17		0.01547	0.01612

A.2 Table of matter and ghost states at levels ≤ 6

The following tables list the matter and ghost states which contribute to scalar fields at levels ≤ 6. The quadratic terms involving each state are listed in the last column.

Matter states

$\|\eta_m\rangle$	state	quadratic terms
$\|\eta_1\rangle$	$\|\Omega\rangle$	$d^{\text{mat}}_{1\,1} = -\frac{1}{2}$
$\|\eta_2\rangle$	$(\alpha_{-1}\cdot\alpha_{-1})\,\|\Omega\rangle$	$d^{\text{mat}}_{2\,2} = 2\cdot 13$
$\|\eta_3\rangle$	$(\alpha_{-1}\cdot\alpha_{-2})\,\|\Omega\rangle$	$d^{\text{mat}}_{3\,3} = 2^2\cdot 13$
$\|\eta_4\rangle$	$(\alpha_{-1}\cdot\alpha_{-3})\,\|\Omega\rangle$	$d^{\text{mat}}_{4\,4} = 3^2\cdot 13$
$\|\eta_5\rangle$	$(\alpha_{-2}\cdot\alpha_{-2})\,\|\Omega\rangle$	$d^{\text{mat}}_{5\,5} = 2^3\cdot 3\cdot 13$
$\|\eta_6\rangle$	$(\alpha_{-1}\cdot\alpha_{-1})(\alpha_{-1}\cdot\alpha_{-1})\,\|\Omega\rangle$	$d^{\text{mat}}_{6\,6} = 2^5\cdot 3\cdot 7\cdot 13$
$\|\eta_{10}\rangle$	$(\alpha_{-1}\cdot\alpha_{-5})\,\|\Omega\rangle$	$d^{\text{mat}}_{10\,10} = 5^2\cdot 13$
$\|\eta_{11}\rangle$	$(\alpha_{-2}\cdot\alpha_{-4})\,\|\Omega\rangle$	$d^{\text{mat}}_{11\,11} = 2^3\cdot 5\cdot 13$
$\|\eta_{12}\rangle$	$(\alpha_{-3}\cdot\alpha_{-3})\,\|\Omega\rangle$	$d^{\text{mat}}_{12\,12} = 2\cdot 3^2\cdot 5\cdot 13$
$\|\eta_{13}\rangle$	$(\alpha_{-1}\cdot\alpha_{-3})(\alpha_{-1}\cdot\alpha_{-1})\,\|\Omega\rangle$	$d^{\text{mat}}_{13\,13} = 2^3\cdot 3\cdot 5\cdot 7\cdot 13$
$\|\eta_{14}\rangle$	$(\alpha_{-2}\cdot\alpha_{-2})(\alpha_{-1}\cdot\alpha_{-1})\,\|\Omega\rangle$	$d^{\text{mat}}_{14\,14} = 2^5\cdot 5\cdot 13^2$, $d^{\text{mat}}_{14\,15} = 2^4\cdot 5\cdot 13$
$\|\eta_{15}\rangle$	$(\alpha_{-1}\cdot\alpha_{-2})(\alpha_{-1}\cdot\alpha_{-2})\,\|\Omega\rangle$	$d^{\text{mat}}_{15\,14} = 2^4\cdot 5\cdot 13$, $d^{\text{mat}}_{15\,15} = 2^3\cdot 3^3\cdot 5\cdot 13$
$\|\eta_{16}\rangle$	$(\alpha_{-1}\cdot\alpha_{-1})(\alpha_{-1}\cdot\alpha_{-1})(\alpha_{-1}\cdot\alpha_{-1})\,\|\Omega\rangle$	$d^{\text{mat}}_{16\,16} = 2^7\cdot 3^2\cdot 5^2\cdot 7\cdot 13$

Ghost states

$\lvert\chi_g\rangle$	state	quadratic terms
$\lvert\chi_1\rangle$	$\lvert\Omega\rangle$	$d^{\rm gh}_{1\,1} = -\frac{1}{2}$
$\lvert\chi_2\rangle$	$b_{-1}c_{-1}\lvert\Omega\rangle$	$d^{\rm gh}_{2\,2} = -\frac{1}{2}$
$\lvert\chi_3\rangle$	$b_{-1}c_{-2}\lvert\Omega\rangle$	$d^{\rm gh}_{3\,4} = -1$
$\lvert\chi_4\rangle$	$b_{-2}c_{-1}\lvert\Omega\rangle$	$d^{\rm gh}_{4\,3} = -1$
$\lvert\chi_5\rangle$	$b_{-1}c_{-3}\lvert\Omega\rangle$	$d^{\rm gh}_{5\,7} = -\frac{3}{2}$
$\lvert\chi_6\rangle$	$b_{-2}c_{-2}\lvert\Omega\rangle$	$d^{\rm gh}_{6\,6} = -\frac{3}{2}$
$\lvert\chi_7\rangle$	$b_{-3}c_{-1}\lvert\Omega\rangle$	$d^{\rm gh}_{7\,5} = -\frac{3}{2}$
$\lvert\chi_{12}\rangle$	$b_{-1}c_{-5}\lvert\Omega\rangle$	$d^{\rm gh}_{12\,16} = -\frac{5}{2}$
$\lvert\chi_{13}\rangle$	$b_{-2}c_{-4}\lvert\Omega\rangle$	$d^{\rm gh}_{13\,15} = -\frac{5}{2}$
$\lvert\chi_{14}\rangle$	$b_{-3}c_{-3}\lvert\Omega\rangle$	$d^{\rm gh}_{14\,14} = -\frac{5}{2}$
$\lvert\chi_{15}\rangle$	$b_{-4}c_{-2}\lvert\Omega\rangle$	$d^{\rm gh}_{15\,13} = -\frac{5}{2}$
$\lvert\chi_{16}\rangle$	$b_{-5}c_{-1}\lvert\Omega\rangle$	$d^{\rm gh}_{16\,12} = -\frac{5}{2}$
$\lvert\chi_{17}\rangle$	$b_{-2}b_{-1}c_{-2}c_{-1}\lvert\Omega\rangle$	$d^{\rm gh}_{17\,17} = \frac{5}{2}$

A.3 Cubic interactions at levels (6, 16)

In the following pages we give tables of all cubic interactions between the pure matter and ghost scalar fields listed in Appendix A.2 which contribute to cubic interactions of total dimension ≤ 16 between the scalar fields listed in Appendix A.1. All cubic interactions of level less or equal to (6, 16) between the scalar fields listed in Appendix A.1 can be reproduced using these tables and (2.10).

Cubic matter field coefficients t^{mat}_{ijk}

		i					
j	k	1	2	3	4	5	6
1	1	1	$-\frac{2\cdot5\cdot13}{3^3}$	0	$\frac{2^6\cdot13}{3^5}$	$\frac{2^2\cdot13^2}{3^5}$	$\frac{2^3\cdot5^2\cdot7\cdot13}{3^6}$
1	2	$-\frac{2\cdot5\cdot13}{3^3}$	$\frac{2^2\cdot7\cdot13\cdot83}{3^6}$	$\frac{2^{12}\cdot13\sqrt{3}}{3^8}$	$-\frac{2^7\cdot13\cdot73}{3^8}$	$-\frac{2^3\cdot13\cdot487}{3^9}$	$-\frac{2^4\cdot5\cdot7\cdot13\cdot31}{3^6}$
1	3	0	$-\frac{2^{12}\cdot13\sqrt{3}}{3^8}$	$-\frac{2^{15}\cdot13}{3^9}$	$-\frac{2^{12}\cdot7\cdot13\sqrt{3}}{3^{10}}$	$-\frac{2^{16}\cdot13\sqrt{3}}{3^{10}}$	$\frac{2^{15}\cdot5\cdot7\cdot13\sqrt{3}}{3^{11}}$
1	4	$\frac{2^6\cdot13}{3^5}$	$-\frac{2^7\cdot13\cdot73}{3^8}$	$\frac{2^{12}\cdot7\cdot13\sqrt{3}}{3^{10}}$	$\frac{2^{10}\cdot13\cdot479}{3^{11}}$	$\frac{2^8\cdot13\cdot163}{3^9}$	$\frac{2^9\cdot5\cdot7\cdot13}{3^7}$
1	5	$\frac{2^2\cdot13^2}{3^5}$	$-\frac{2^3\cdot13\cdot487}{3^9}$	$\frac{2^{16}\cdot13\sqrt{3}}{3^{10}}$	$\frac{2^8\cdot13\cdot163}{3^9}$	$\frac{2^4\cdot13\cdot17\cdot1093}{3^{10}}$	$-\frac{2^5\cdot5\cdot7^2\cdot13\cdot223}{3^{12}}$
1	6	$\frac{2^3\cdot5^2\cdot7\cdot13}{3^6}$	$-\frac{2^4\cdot5\cdot7\cdot13\cdot31}{3^6}$	$-\frac{2^{15}\cdot5\cdot7\cdot13\sqrt{3}}{3^{11}}$	$\frac{2^9\cdot5\cdot7\cdot13}{3^7}$	$-\frac{2^5\cdot5\cdot7^2\cdot13\cdot223}{3^{12}}$	$\frac{2^6\cdot7\cdot13\cdot100537}{3^{11}}$
1	10	$-\frac{2^6\cdot5\cdot13^2}{3^9}$	$\frac{2^7\cdot5\cdot13^2\cdot73}{3^{12}}$	$-\frac{2^{12}\cdot5\cdot13\cdot43\sqrt{3}}{3^{14}}$	$-\frac{2^{10}\cdot5\cdot13\cdot251}{3^{13}}$	$-\frac{2^8\cdot5\cdot13\cdot31\cdot139}{3^{14}}$	$-\frac{2^9\cdot5^2\cdot7\cdot13^2}{3^{11}}$
1	11	$-\frac{2^{12}\cdot13}{3^9}$	$\frac{2^{13}\cdot13\cdot41}{3^{12}}$	$-\frac{2^{18}\cdot5\cdot13\sqrt{3}}{3^{14}}$	$-\frac{2^{16}\cdot13}{3^{14}}$	$-\frac{2^{14}\cdot13\cdot233}{3^{14}}$	$-\frac{2^{15}\cdot5\cdot7\cdot13\cdot17}{3^{15}}$
1	12	$-\frac{2\cdot13\cdot19\cdot47}{3^8}$	$\frac{2^2\cdot13\cdot103\cdot571}{3^{11}}$	$-\frac{2^{12}\cdot5\cdot13\sqrt{3}}{3^{11}}$	$-\frac{2^7\cdot11\cdot13\cdot1523}{3^{13}}$	$\frac{2^3\cdot7\cdot13\cdot44269}{3^{13}}$	$-\frac{2^4\cdot5\cdot7\cdot13\cdot59581}{3^{14}}$
1	13	$-\frac{2^8\cdot5\cdot7\cdot13}{3^8}$	$\frac{2^9\cdot7\cdot13\cdot23}{3^8}$	$-\frac{2^{14}\cdot7\cdot13\sqrt{3}}{3^{12}}$	$-\frac{2^{12}\cdot7\cdot13\cdot47\cdot53}{3^{14}}$	$-\frac{2^{10}\cdot7\cdot13\cdot17\cdot311}{3^{14}}$	$-\frac{2^{11}\cdot7\cdot13\cdot19\cdot599}{3^{13}}$
1	14	$-\frac{2^3\cdot5\cdot13^3}{3^8}$	$\frac{2^4\cdot11\cdot13^2\cdot1129}{3^{12}}$	$-\frac{2^{14}\cdot13^2\sqrt{3}}{3^{10}}$	$-\frac{2^9\cdot13^2\cdot2549}{3^{13}}$	$-\frac{2^5\cdot7\cdot13^2\cdot36013}{3^{14}}$	$\frac{2^6\cdot7\cdot13\cdot257981}{3^{15}}$
1	15	$-\frac{2^2\cdot5\cdot13^2}{3^8}$	$\frac{2^3\cdot11\cdot13\cdot1129}{3^{12}}$	$-\frac{2^{13}\cdot13\sqrt{3}}{3^{10}}$	$-\frac{2^8\cdot13\cdot2549}{3^{13}}$	$-\frac{2^4\cdot7\cdot13\cdot36013}{3^{14}}$	$\frac{2^5\cdot7\cdot13\cdot678779}{3^{14}}$
1	16	$-\frac{2^4\cdot5^4\cdot7\cdot13}{3^8}$	$\frac{2^5\cdot5^3\cdot7\cdot13\cdot1093}{3^{11}}$	$\frac{2^{15}\cdot5^3\cdot7\cdot13\sqrt{3}}{3^{12}}$	$-\frac{2^{10}\cdot5^3\cdot7\cdot13\cdot89}{3^{13}}$	$\frac{2^6\cdot5^3\cdot7\cdot13\cdot401}{3^{12}}$	$-\frac{2^7\cdot5^2\cdot7\cdot13\cdot522283}{3^{14}}$
2	2	$\frac{2^2\cdot7\cdot13\cdot83}{3^6}$	$-\frac{2^3\cdot7\cdot13\cdot41\cdot73}{3^8}$	0	$\frac{2^8\cdot7\cdot13\cdot397}{3^{10}}$	$-\frac{2^4\cdot13\cdot79\cdot157}{3^{11}}$	$\frac{2^5\cdot7\cdot13\cdot61\cdot3119}{3^{11}}$
2	3	$\frac{2^{12}\cdot13\sqrt{3}}{3^8}$	0	$\frac{2^{16}\cdot13\cdot19}{3^{11}}$	$\frac{2^{13}\cdot13\cdot743\sqrt{3}}{3^{13}}$	$\frac{2^{14}\cdot13\cdot23\cdot101\sqrt{3}}{3^{14}}$	$-\frac{2^{15}\cdot7\cdot13\cdot31\sqrt{3}}{3^{11}}$
2	4	$-\frac{2^7\cdot13\cdot73}{3^8}$	$\frac{2^8\cdot7\cdot13\cdot397}{3^{10}}$	$-\frac{2^{13}\cdot13\cdot743\sqrt{3}}{3^{13}}$	$-\frac{2^{11}\cdot5\cdot13\cdot5683}{3^{14}}$	$-\frac{2^9\cdot13\cdot113\cdot257}{3^{13}}$	$-\frac{2^{10}\cdot7\cdot13\cdot21247}{3^{13}}$
2	5	$-\frac{2^3\cdot13\cdot487}{3^9}$	$-\frac{2^4\cdot13\cdot79\cdot157}{3^{11}}$	$-\frac{2^{14}\cdot13\cdot23\cdot101\sqrt{3}}{3^{14}}$	$-\frac{2^9\cdot13\cdot113\cdot257}{3^{13}}$	$-\frac{2^5\cdot13\cdot53\cdot15137}{3^{13}}$	$\frac{2^6\cdot7^2\cdot13^2\cdot17351}{3^{15}}$
2	6	$-\frac{2^4\cdot5\cdot7\cdot13\cdot31}{3^6}$	$\frac{2^5\cdot7\cdot13\cdot61\cdot3119}{3^{11}}$	$\frac{2^{15}\cdot7\cdot13\cdot31\sqrt{3}}{3^{11}}$	$-\frac{2^{10}\cdot7\cdot13\cdot21247}{3^{13}}$	$\frac{2^6\cdot7^2\cdot13^2\cdot17351}{3^{15}}$	$-\frac{2^7\cdot7\cdot13\cdot13224697}{3^{14}}$
2	10	$\frac{2^7\cdot5\cdot13^2\cdot73}{3^{12}}$	$-\frac{2^8\cdot5\cdot7\cdot13^2\cdot397}{3^{14}}$	$\frac{2^{13}\cdot5\cdot13\cdot7307\sqrt{3}}{3^{17}}$	$\frac{2^{11}\cdot5\cdot13\cdot58321}{3^{17}}$	$\frac{2^9\cdot5^2\cdot7\cdot13\cdot6047}{3^{17}}$	$\frac{2^{10}\cdot5\cdot7\cdot13^2\cdot21247}{3^{17}}$
2	11	$\frac{2^{13}\cdot13\cdot41}{3^{12}}$	$-\frac{2^{14}\cdot5\cdot13\cdot733}{3^{15}}$	$\frac{2^{19}\cdot13\cdot773\sqrt{3}}{3^{17}}$	$-\frac{2^{17}\cdot7\cdot13\cdot233}{3^{17}}$	$-\frac{2^{15}\cdot11\cdot13\cdot109}{3^{17}}$	$\frac{2^{16}\cdot7\cdot13^2\cdot283}{3^{17}}$
2	12	$\frac{2^2\cdot13\cdot103\cdot571}{3^{11}}$	$-\frac{2^3\cdot7\cdot13\cdot31\cdot53\cdot593}{3^{14}}$	$\frac{2^{14}\cdot13\cdot6883\sqrt{3}}{3^{16}}$	$\frac{2^8\cdot13\cdot1109113}{3^{16}}$	$-\frac{2^4\cdot13\cdot80863921}{3^{17}}$	$\frac{2^5\cdot7\cdot13\cdot811\cdot6779}{3^{15}}$
2	13	$\frac{2^9\cdot7\cdot13\cdot23}{3^8}$	$-\frac{2^{10}\cdot7\cdot13\cdot23623}{3^{13}}$	$\frac{2^{15}\cdot7^2\cdot13\cdot151\sqrt{3}}{3^{15}}$	$\frac{2^{13}\cdot5\cdot7\cdot13\cdot17909}{3^{16}}$	$\frac{2^{11}\cdot7^2\cdot13\cdot28387}{3^{16}}$	$\frac{2^{12}\cdot7\cdot13\cdot1536989}{3^{16}}$
2	14	$\frac{2^4\cdot11\cdot13^2\cdot1129}{3^{12}}$	$\frac{2^5\cdot7^2\cdot13\cdot19^2\cdot43}{3^{14}}$	$\frac{2^{18}\cdot13\cdot27043\sqrt{3}}{3^{17}}$	$\frac{2^{10}\cdot13\cdot929\cdot3673}{3^{16}}$	$\frac{2^6\cdot13\cdot619\cdot1542007}{3^{18}}$	$-\frac{2^7\cdot7\cdot13\cdot199109}{3^{12}}$
2	15	$\frac{2^3\cdot11\cdot13\cdot1129}{3^{12}}$	$-\frac{2^4\cdot7\cdot13\cdot599\cdot6691}{3^{15}}$	$-\frac{2^{17}\cdot13\cdot71\cdot359\sqrt{3}}{3^{17}}$	$-\frac{2^9\cdot13\cdot67\cdot137\cdot587}{3^{17}}$	$-\frac{2^5\cdot13\cdot131\cdot1447\cdot3187}{3^{18}}$	$\frac{2^6\cdot7\cdot11\cdot13^2\cdot79\cdot4133}{3^{17}}$
2	16	$\frac{2^5\cdot5^3\cdot7\cdot13\cdot1093}{3^{11}}$	$-\frac{2^6\cdot5^2\cdot7\cdot13\cdot958361}{3^{14}}$	$-\frac{2^{17}\cdot5^2\cdot7\cdot13\cdot1093\sqrt{3}}{3^{16}}$	$\frac{2^{11}\cdot5^2\cdot7\cdot13\cdot241\cdot373}{3^{16}}$	$-\frac{2^7\cdot5^2\cdot7\cdot13\cdot1483\cdot2711}{3^{17}}$	$\frac{2^8\cdot5\cdot7\cdot13\cdot131\cdot419\cdot2389}{3^{16}}$
3	3	$-\frac{2^{15}\cdot13}{3^9}$	$\frac{2^{16}\cdot13\cdot19}{3^{11}}$	0	$-\frac{2^{19}\cdot13\cdot17}{3^{13}}$	$-\frac{2^{17}\cdot5\cdot7\cdot13}{3^{13}}$	$-\frac{2^{18}\cdot7\cdot13\cdot167}{3^{14}}$
3	4	$-\frac{2^{12}\cdot7\cdot13\sqrt{3}}{3^{10}}$	$\frac{2^{13}\cdot13\cdot743\sqrt{3}}{3^{13}}$	$-\frac{2^{19}\cdot13\cdot17}{3^{13}}$	0	$\frac{2^{14}\cdot13\cdot1889\sqrt{3}}{3^{15}}$	$-\frac{2^{15}\cdot7\cdot13\cdot1889\sqrt{3}}{3^{15}}$
3	5	$-\frac{2^{16}\cdot13\sqrt{3}}{3^{10}}$	$\frac{2^{14}\cdot13\cdot23\cdot101\sqrt{3}}{3^{14}}$	$-\frac{2^{17}\cdot5\cdot7\cdot13}{3^{13}}$	$-\frac{2^{14}\cdot13\cdot1889\sqrt{3}}{3^{15}}$	0	$-\frac{2^{17}\cdot7\cdot13\cdot1889\sqrt{3}}{3^{16}}$
3	6	$\frac{2^{15}\cdot5\cdot7\cdot13\sqrt{3}}{3^{11}}$	$-\frac{2^{15}\cdot7\cdot13\cdot31\sqrt{3}}{3^{11}}$	$-\frac{2^{18}\cdot7\cdot13\cdot167}{3^{14}}$	$\frac{2^{15}\cdot7\cdot13\cdot1889\sqrt{3}}{3^{15}}$	$\frac{2^{17}\cdot7\cdot13\cdot1889\sqrt{3}}{3^{16}}$	0

Table of t_{ijk}^{mat} (continued)

		i					
j	k	1	2	3	4	5	6
3	10	$\frac{2^{12}5\cdot13\cdot43\sqrt{3}}{3^{14}}$	$-\frac{2^{13}5\cdot13\cdot7307\sqrt{3}}{3^{17}}$	$\frac{2^{19}5\cdot13^2 17}{3^{17}}$	$-\frac{2^{21}5^3 13\sqrt{3}}{3^{18}}$	$-\frac{2^{14}5\cdot13\cdot149\cdot233\sqrt{3}}{3^{19}}$	$\frac{2^{15}5\cdot7^2 13\cdot31\cdot101\sqrt{3}}{3^{19}}$
3	11	$\frac{2^{18}5\cdot13\sqrt{3}}{3^{14}}$	$-\frac{2^{19}13\cdot773\sqrt{3}}{3^{17}}$	$\frac{2^{25}13\cdot17}{3^{17}}$	$\frac{2^{24}13\sqrt{3}}{3^{16}}$	$-\frac{2^{20}5\cdot13\cdot599\sqrt{3}}{3^{19}}$	$\frac{2^{21}7\cdot13\cdot1523\sqrt{3}}{3^{19}}$
3	12	$\frac{2^{12}5\cdot13\sqrt{3}}{3^{11}}$	$-\frac{2^{14}13\cdot6883\sqrt{3}}{3^{16}}$	$\frac{2^{16}13\cdot8513}{3^{17}}$	$-\frac{2^{13}13\cdot144847\sqrt{3}}{3^{18}}$	$-\frac{2^{14}13\cdot50707\sqrt{3}}{3^{18}}$	$\frac{2^{15}7\cdot13\cdot43\cdot2897\sqrt{3}}{3^{19}}$
3	13	$\frac{2^{14}7\cdot13\sqrt{3}}{3^{12}}$	$-\frac{2^{15}7^2 13\cdot151\sqrt{3}}{3^{15}}$	$-\frac{2^{21}7\cdot13}{3^{17}}$	$-\frac{2^{24}5\cdot7\cdot13\cdot41\sqrt{3}}{3^{19}}$	$-\frac{2^{16}7\cdot13\cdot47\cdot2081\sqrt{3}}{3^{19}}$	$\frac{2^{17}5\cdot7\cdot11\cdot13\cdot23\cdot83\sqrt{3}}{3^{18}}$
3	14	$\frac{2^{14}13^2\sqrt{3}}{3^{10}}$	$-\frac{2^{18}13\cdot27043\sqrt{3}}{3^{17}}$	$-\frac{2^{18}13\cdot73\cdot757}{3^{18}}$	$-\frac{2^{15}5\cdot13\cdot19\cdot419\sqrt{3}}{3^{19}}$	$-\frac{2^{16}13\cdot915379\sqrt{3}}{3^{19}}$	$\frac{2^{17}7\cdot13\cdot211\cdot9221\sqrt{3}}{3^{20}}$
3	15	$\frac{2^{13}13\sqrt{3}}{3^{10}}$	$\frac{2^{17}13\cdot71\cdot359\sqrt{3}}{3^{17}}$	$\frac{2^{17}13\cdot72101}{3^{17}}$	$\frac{2^{14}5\cdot13\cdot139\cdot739\sqrt{3}}{3^{18}}$	$\frac{2^{15}13^2311\cdot419\sqrt{3}}{3^{19}}$	$-\frac{2^{16}7\cdot11\cdot13\cdot47\cdot1163\sqrt{3}}{3^{19}}$
3	16	$-\frac{2^{15}5^3 7\cdot13\sqrt{3}}{3^{12}}$	$\frac{2^{17}5^2 7\cdot13\cdot1093\sqrt{3}}{3^{16}}$	$\frac{2^{19}5^2 7^2 13\cdot139}{3^{17}}$	$-\frac{2^{16}5^2 7\cdot13\cdot47\cdot173\sqrt{3}}{3^{18}}$	$-\frac{2^{17}5^2 7\cdot13\cdot773\sqrt{3}}{3^{17}}$	$-\frac{2^{18}5\cdot7\cdot13\cdot522283\sqrt{3}}{3^{19}}$
4	4	$\frac{2^{10}13\cdot479}{3^{11}}$	$-\frac{2^{11}5\cdot13\cdot5683}{3^{14}}$	0	$\frac{2^{17}13\cdot2357}{3^{15}}$	$\frac{2^{12}13\cdot463781}{3^{17}}$	$\frac{2^{13}7^2 13\cdot41\cdot151}{3^{16}}$
4	5	$\frac{2^8 13\cdot163}{3^9}$	$-\frac{2^9 13\cdot113\cdot257}{3^{13}}$	$\frac{2^{14}13\cdot1889\sqrt{3}}{3^{15}}$	$\frac{2^{12}13\cdot463781}{3^{17}}$	$\frac{2^{10}13\cdot653\cdot661}{3^{15}}$	$\frac{2^{11}7\cdot13\cdot361687}{3^{17}}$
4	6	$\frac{2^9 5\cdot7\cdot13}{3^7}$	$-\frac{2^{10}7\cdot13\cdot21247}{3^{13}}$	$-\frac{2^{15}7\cdot13\cdot1889\sqrt{3}}{3^{15}}$	$\frac{2^{13}7^2 13\cdot41\cdot151}{3^{16}}$	$\frac{2^{11}7\cdot13\cdot361687}{3^{17}}$	$\frac{2^{12}7\cdot13\cdot1516037}{3^{16}}$
5	5	$\frac{2^4 13\cdot17\cdot1093}{3^{10}}$	$-\frac{2^5 13\cdot53\cdot15137}{3^{13}}$	0	$\frac{2^{10}13\cdot653\cdot661}{3^{15}}$	$\frac{2^6 11\cdot13\cdot19\cdot7151}{3^{14}}$	$\frac{2^7 7\cdot13\cdot331\cdot79283}{3^{18}}$
5	6	$-\frac{2^5 5\cdot7^2 13\cdot223}{3^{12}}$	$\frac{2^6 7^2 13^2 17351}{3^{15}}$	$-\frac{2^{17}7\cdot13\cdot1889\sqrt{3}}{3^{16}}$	$\frac{2^{11}7\cdot13\cdot361687}{3^{17}}$	$\frac{2^7 7\cdot13\cdot331\cdot79283}{3^{18}}$	$-\frac{2^8 5\cdot7\cdot13\cdot11099833}{3^{17}}$
6	6	$\frac{2^6 7\cdot13\cdot100537}{3^{11}}$	$-\frac{2^7 7\cdot13\cdot13224697}{3^{14}}$	0	$\frac{2^{12}7\cdot13\cdot1516037}{3^{16}}$	$-\frac{2^8 5\cdot7\cdot13\cdot11099833}{3^{17}}$	$\frac{2^9 7\cdot11\cdot13\cdot997\cdot10181}{3^{15}}$
4	10	$-\frac{2^{10}5\cdot13\cdot251}{3^{13}}$	$\frac{2^{11}5\cdot13\cdot58321}{3^{17}}$	$\frac{2^{21}5^3 13\sqrt{3}}{3^{18}}$	$-\frac{2^{17}5\cdot13\cdot42323}{3^{20}}$	$-\frac{2^{12}5^2 11\cdot13\cdot7727}{3^{19}}$	$-\frac{2^{13}5\cdot7\cdot13\cdot4261}{3^{16}}$
4	11	$-\frac{2^{16}13}{3^{14}}$	$-\frac{2^{17}7\cdot13\cdot233}{3^{17}}$	$-\frac{2^{24}13\sqrt{3}}{3^{16}}$	$-\frac{2^{26}11\cdot13\cdot19}{3^{20}}$	$-\frac{2^{18}13\cdot14249}{3^{19}}$	$\frac{2^{19}7\cdot13\cdot673}{3^{17}}$
4	12	$-\frac{2^7 11\cdot13\cdot1523}{3^{13}}$	$\frac{2^8 13\cdot1109113}{3^{16}}$	$\frac{2^{13}13\cdot144847\sqrt{3}}{3^{18}}$	$-\frac{2^{11}13\cdot137\cdot27823}{3^{19}}$	$-\frac{2^9 13^2 278269}{3^{18}}$	$-\frac{2^{10}7\cdot13\cdot1886231}{3^{18}}$
4	13	$-\frac{2^{12}7\cdot13\cdot47\cdot53}{3^{14}}$	$\frac{2^{13}5\cdot7\cdot13\cdot17909}{3^{16}}$	$\frac{2^{24}5\cdot7\cdot13\cdot41\sqrt{3}}{3^{19}}$	$-\frac{2^{19}7\cdot13\cdot89\cdot137}{3^{18}}$	$-\frac{2^{14}7\cdot13\cdot19\cdot28961}{3^{19}}$	$-\frac{2^{15}5\cdot7\cdot13\cdot23\cdot36217}{3^{19}}$
4	14	$-\frac{2^9 13^2 2549}{3^{13}}$	$\frac{2^{10}13\cdot929\cdot3673}{3^{16}}$	$\frac{2^{15}5\cdot13\cdot19\cdot419\sqrt{3}}{3^{19}}$	$-\frac{2^{13}11\cdot13\cdot47\cdot61441}{3^{20}}$	$-\frac{2^{11}13\cdot1002523}{3^{15}}$	$-\frac{2^{12}7\cdot11\cdot13\cdot149\cdot13171}{3^{19}}$
4	15	$-\frac{2^8 13\cdot2549}{3^{13}}$	$-\frac{2^9 13\cdot67\cdot137\cdot587}{3^{17}}$	$-\frac{2^{14}5\cdot13\cdot139\cdot739\sqrt{3}}{3^{18}}$	$-\frac{2^{12}13\cdot18654169}{3^{20}}$	$-\frac{2^{10}11\cdot13\cdot1621\cdot3121}{3^{19}}$	$\frac{2^{11}7\cdot13\cdot293\cdot313}{3^{14}}$
4	16	$-\frac{2^{10}5^3 7\cdot13\cdot89}{3^{13}}$	$\frac{2^{11}5^2 7\cdot13\cdot241\cdot373}{3^{16}}$	$\frac{2^{16}5^2 7\cdot13\cdot47\cdot173\sqrt{3}}{3^{18}}$	$-\frac{2^{14}5^2 7^2 13^3 101}{3^{19}}$	$-\frac{2^{12}5^2 7\cdot11\cdot13\cdot7727}{3^{18}}$	$-\frac{2^{13}5\cdot7^2 13\cdot787\cdot2477}{3^{18}}$
5	10	$-\frac{2^8 5\cdot13\cdot31\cdot139}{3^{14}}$	$\frac{2^9 5^2 7\cdot13\cdot6047}{3^{17}}$	$\frac{2^{14}5\cdot13\cdot149\cdot233\sqrt{3}}{3^{19}}$	$-\frac{2^{12}5^2 11\cdot13\cdot7727}{3^{19}}$	$-\frac{2^{10}5\cdot13\cdot4394717}{3^{19}}$	$-\frac{2^{11}5\cdot7^2 13\cdot37\cdot61\cdot109}{3^{21}}$
5	11	$-\frac{2^{14}13\cdot233}{3^{14}}$	$-\frac{2^{15}11\cdot13\cdot109}{3^{17}}$	$\frac{2^{20}5\cdot13\cdot599\sqrt{3}}{3^{19}}$	$-\frac{2^{18}13\cdot14249}{3^{19}}$	$-\frac{2^{16}13\cdot82267}{3^{18}}$	$\frac{2^{17}7\cdot13\cdot23\cdot2389}{3^{20}}$
5	12	$\frac{2^3 7\cdot13\cdot44269}{3^{13}}$	$-\frac{2^4 13\cdot80863921}{3^{17}}$	$\frac{2^{14}13\cdot50707\sqrt{3}}{3^{18}}$	$-\frac{2^9 13^2 278269}{3^{18}}$	$\frac{2^5 13\cdot58008371}{3^{18}}$	$\frac{2^6 7\cdot13\cdot1597\cdot319129}{3^{20}}$
5	13	$-\frac{2^{10}7\cdot13\cdot17\cdot311}{3^{14}}$	$\frac{2^{11}7^2 13\cdot28387}{3^{16}}$	$\frac{2^{16}7\cdot13\cdot47\cdot2081\sqrt{3}}{3^{19}}$	$-\frac{2^{14}7\cdot13\cdot19\cdot28961}{3^{19}}$	$-\frac{2^{12}7\cdot13\cdot257\cdot15359}{3^{19}}$	$-\frac{2^{13}7\cdot13\cdot19\cdot5501}{3^{15}}$
5	14	$-\frac{2^5 7\cdot13^2 36013}{3^{14}}$	$\frac{2^6 13\cdot619\cdot1542007}{3^{18}}$	$\frac{2^{16}13\cdot915379\sqrt{3}}{3^{19}}$	$-\frac{2^{11}13\cdot1002523}{3^{15}}$	$\frac{2^7 13\cdot523\cdot87049}{3^{18}}$	$-\frac{2^8 7\cdot13\cdot8867\cdot199049}{3^{20}}$
5	15	$-\frac{2^4 7\cdot13\cdot36013}{3^{14}}$	$-\frac{2^5 13\cdot131\cdot1447\cdot3187}{3^{18}}$	$-\frac{2^{15}13^2311\cdot419\sqrt{3}}{3^{19}}$	$-\frac{2^{10}11\cdot13\cdot1621\cdot3121}{3^{19}}$	$-\frac{2^6 13\cdot19\cdot491\cdot192547}{3^{19}}$	$\frac{2^7 7\cdot13\cdot8422919627}{3^{21}}$
5	16	$\frac{2^6 5^3 7\cdot13\cdot401}{3^{12}}$	$-\frac{2^7 5^2 7\cdot13\cdot1483\cdot2711}{3^{17}}$	$\frac{2^{17}5^2 7\cdot13\cdot773\sqrt{3}}{3^{17}}$	$-\frac{2^{12}5^2 7\cdot11\cdot13\cdot7727}{3^{18}}$	$-\frac{2^8 5^2 7^2 11^2 13\cdot9749}{3^{19}}$	$\frac{2^9 5\cdot7\cdot13\cdot19\cdot113681761}{3^{20}}$
6	10	$-\frac{2^9 5^2 7\cdot13^2}{3^{11}}$	$\frac{2^{10}5\cdot7\cdot13^2 21247}{3^{17}}$	$-\frac{2^{15}5\cdot7^2 13\cdot31\cdot101\sqrt{3}}{3^{19}}$	$-\frac{2^{13}5\cdot7\cdot13\cdot4261}{3^{16}}$	$-\frac{2^{11}5\cdot7^2 13\cdot37\cdot61\cdot109}{3^{21}}$	$-\frac{2^{12}5\cdot7\cdot13^2 1516037}{3^{20}}$
6	11	$-\frac{2^{15}5\cdot7\cdot13\cdot17}{3^{15}}$	$\frac{2^{16}7\cdot13^2 283}{3^{17}}$	$-\frac{2^{21}7\cdot13\cdot1523\sqrt{3}}{3^{19}}$	$\frac{2^{19}7\cdot13\cdot673}{3^{17}}$	$\frac{2^{17}7\cdot13\cdot23\cdot2389}{3^{20}}$	$-\frac{2^{18}7^2 13\cdot8467}{3^{20}}$
6	12	$-\frac{2^4 5\cdot7\cdot13\cdot59581}{3^{14}}$	$\frac{2^5 7\cdot13\cdot811\cdot6779}{3^{15}}$	$-\frac{2^{15}7\cdot13\cdot43\cdot2897\sqrt{3}}{3^{19}}$	$-\frac{2^{10}7\cdot13\cdot1886231}{3^{18}}$	$\frac{2^6 7\cdot13\cdot1597\cdot319129}{3^{20}}$	$-\frac{2^7 7^3 13\cdot47\cdot193\cdot2671}{3^{19}}$
6	13	$-\frac{2^{11}7\cdot13\cdot19\cdot599}{3^{13}}$	$\frac{2^{12}7\cdot13\cdot1536989}{3^{16}}$	$-\frac{2^{17}5\cdot7\cdot11\cdot13\cdot23\cdot83\sqrt{3}}{3^{18}}$	$-\frac{2^{15}5\cdot7\cdot13\cdot23\cdot36217}{3^{19}}$	$-\frac{2^{13}7\cdot13\cdot19\cdot5501}{3^{15}}$	$-\frac{2^{14}7\cdot13\cdot12167927}{3^{17}}$
6	14	$\frac{2^6 7\cdot13\cdot257981}{3^{15}}$	$-\frac{2^7 7\cdot13\cdot199109}{3^{12}}$	$-\frac{2^{17}7\cdot13\cdot211\cdot9221\sqrt{3}}{3^{20}}$	$-\frac{2^{12}7\cdot11\cdot13\cdot149\cdot13171}{3^{19}}$	$-\frac{2^8 7\cdot13\cdot8867\cdot199049}{3^{20}}$	$\frac{2^9 5^2 7^2 13\cdot473411}{3^{16}}$
6	15	$\frac{2^5 7\cdot13\cdot678779}{3^{14}}$	$\frac{2^6 7\cdot11\cdot13^2 79\cdot4133}{3^{17}}$	$\frac{2^{16}7\cdot11\cdot13\cdot47\cdot1163\sqrt{3}}{3^{19}}$	$\frac{2^{11}7\cdot13\cdot293\cdot313}{3^{14}}$	$\frac{2^7 7\cdot13\cdot8422919627}{3^{21}}$	$-\frac{2^8 5^2 7\cdot13\cdot29\cdot2539\cdot4441}{3^{20}}$
6	16	$-\frac{2^7 5^2 7\cdot13\cdot522283}{3^{14}}$	$\frac{2^8 5\cdot7\cdot13\cdot131\cdot419\cdot2389}{3^{16}}$	$\frac{2^{18}5\cdot7\cdot13\cdot522283\sqrt{3}}{3^{19}}$	$-\frac{2^{13}5\cdot7^2 13\cdot787\cdot2477}{3^{18}}$	$\frac{2^9 5\cdot7\cdot13\cdot19\cdot113681761}{3^{20}}$	$-\frac{2^{10}5\cdot7\cdot13\cdot19\cdot185072623}{3^{18}}$

Table of t_{ijk}^{mat} (continued)

		i				
j	k	1	2	4	5	6
10	10	$\frac{2^{10}\cdot 5\cdot 13\cdot 109\cdot 839}{3^{17}}$	$-\frac{2^{11}\cdot 5\cdot 13\cdot 251\cdot 59107}{3^{21}}$	$\frac{2^{17}\cdot 5^2\cdot 7\cdot 13\cdot 17033}{3^{22}}$	$\frac{2^{12}\cdot 5\cdot 13\cdot 16686323}{3^{22}}$	$\frac{2^{13}\cdot 5^2\cdot 7\cdot 13\cdot 31\cdot 42743}{3^{22}}$
10	11	$\frac{2^{16}\cdot 5\cdot 13\cdot 29}{3^{14}}$	$-\frac{2^{17}\cdot 5\cdot 13\cdot 168013}{3^{21}}$	$\frac{2^{27}\cdot 5\cdot 13\cdot 599}{3^{23}}$	$\frac{2^{18}\cdot 5\cdot 13\cdot 768437}{3^{23}}$	$\frac{2^{19}\cdot 5\cdot 7\cdot 13\cdot 31\cdot 28927}{3^{24}}$
10	12	$\frac{2^{7}\cdot 5\cdot 7^2\cdot 13\cdot 47\cdot 67}{3^{17}}$	$-\frac{2^{8}\cdot 5\cdot 13\cdot 11307557}{3^{20}}$	$\frac{2^{11}\cdot 5^2\cdot 13\cdot 773063}{3^{21}}$	$-\frac{2^{9}\cdot 5\cdot 13\cdot 709\cdot 37567}{3^{22}}$	$\frac{2^{10}\cdot 5\cdot 7\cdot 13\cdot 47\cdot 149143}{3^{21}}$
10	13	$\frac{2^{12}\cdot 5\cdot 7\cdot 13\cdot 37\cdot 113}{3^{17}}$	$-\frac{2^{13}\cdot 5\cdot 7\cdot 13\cdot 19^2\cdot 463}{3^{19}}$	$\frac{2^{19}\cdot 5\cdot 7\cdot 13^2\cdot 79^2}{3^{22}}$	$\frac{2^{14}\cdot 5\cdot 7\cdot 13\cdot 5795159}{3^{23}}$	$\frac{2^{15}\cdot 5\cdot 7\cdot 13\cdot 97\cdot 32327}{3^{21}}$
10	14	$\frac{2^{9}\cdot 5\cdot 7\cdot 13^2\cdot 3271}{3^{17}}$	$-\frac{2^{10}\cdot 5^2\cdot 13\cdot 97\cdot 101\cdot 557}{3^{20}}$	$\frac{2^{13}\cdot 5\cdot 13\cdot 43^2\cdot 52291}{3^{23}}$	$\frac{2^{11}\cdot 5\cdot 13\cdot 843766543}{3^{23}}$	$\frac{2^{12}\cdot 5\cdot 7\cdot 13\cdot 37\cdot 601\cdot 6133}{3^{23}}$
10	15	$\frac{2^{8}\cdot 5\cdot 7\cdot 13\cdot 3271}{3^{17}}$	$\frac{2^{9}\cdot 5^2\cdot 11\cdot 13\cdot 575251}{3^{21}}$	$\frac{2^{12}\cdot 5\cdot 13\cdot 43\cdot 67\cdot 1567}{3^{21}}$	$\frac{2^{10}\cdot 5\cdot 13\cdot 5171\cdot 23747}{3^{22}}$	$-\frac{2^{11}\cdot 5\cdot 7\cdot 13\cdot 17\cdot 3763033}{3^{22}}$
10	16	$\frac{2^{10}\cdot 5^4\cdot 7\cdot 13^2\cdot 89}{3^{17}}$	$-\frac{2^{11}\cdot 5^3\cdot 7\cdot 13^2\cdot 241\cdot 373}{3^{20}}$	$\frac{2^{14}\cdot 5^3\cdot 7\cdot 13\cdot 29\cdot 1553}{3^{20}}$	$-\frac{2^{12}\cdot 5^3\cdot 7\cdot 13\cdot 43\cdot 1213}{3^{22}}$	$\frac{2^{13}\cdot 5^2\cdot 7^2\cdot 13^2\cdot 787\cdot 2477}{3^{22}}$
11	11	$\frac{2^{22}\cdot 13\cdot 151}{3^{17}}$	$-\frac{2^{23}\cdot 7^2\cdot 13\cdot 167}{3^{20}}$	$\frac{2^{31}\cdot 7\cdot 13\cdot 31}{3^{22}}$	$\frac{2^{24}\cdot 11\cdot 13\cdot 2887}{3^{23}}$	$\frac{2^{25}\cdot 7\cdot 13\cdot 53\cdot 647}{3^{23}}$
11	12	$\frac{2^{13}\cdot 13\cdot 173\cdot 373}{3^{17}}$	$-\frac{2^{14}\cdot 5\cdot 13\cdot 777317}{3^{20}}$	$\frac{2^{17}\cdot 13\cdot 37\cdot 227\cdot 311}{3^{22}}$	$\frac{2^{15}\cdot 13\cdot 12201337}{3^{22}}$	$\frac{2^{16}\cdot 7\cdot 13\cdot 2081\cdot 8581}{3^{23}}$
11	13	$-\frac{2^{18}\cdot 7^2\cdot 13^2}{3^{17}}$	$\frac{2^{19}\cdot 7\cdot 13^2\cdot 461}{3^{19}}$	$\frac{2^{29}\cdot 7\cdot 13\cdot 83}{3^{23}}$	$\frac{2^{20}\cdot 5\cdot 7\cdot 13\cdot 1993}{3^{22}}$	$-\frac{2^{21}\cdot 7\cdot 13\cdot 529531}{3^{22}}$
11	14	$\frac{2^{15}\cdot 13^2\cdot 853}{3^{17}}$	$-\frac{2^{16}\cdot 13\cdot 103\cdot 13469}{3^{21}}$	$\frac{2^{19}\cdot 5\cdot 13\cdot 188767}{3^{23}}$	$\frac{2^{17}\cdot 13\cdot 8037049}{3^{22}}$	$-\frac{2^{18}\cdot 7\cdot 13\cdot 31\cdot 73\cdot 5527}{3^{24}}$
11	15	$\frac{2^{14}\cdot 13\cdot 853}{3^{17}}$	$\frac{2^{15}\cdot 13\cdot 181\cdot 7927}{3^{20}}$	$\frac{2^{18}\cdot 5\cdot 13\cdot 262153}{3^{22}}$	$\frac{2^{16}\cdot 13\cdot 37143319}{3^{23}}$	$-\frac{2^{17}\cdot 7\cdot 13\cdot 191\cdot 131449}{3^{23}}$
11	16	$-\frac{2^{16}\cdot 5^3\cdot 7^2\cdot 13}{3^{17}}$	$\frac{2^{17}\cdot 5^2\cdot 7\cdot 13\cdot 8539}{3^{20}}$	$-\frac{2^{20}\cdot 5^2\cdot 7\cdot 13\cdot 29723}{3^{22}}$	$-\frac{2^{18}\cdot 5^2\cdot 7\cdot 13\cdot 83\cdot 857}{3^{22}}$	$-\frac{2^{19}\cdot 5\cdot 7\cdot 11\cdot 13\cdot 625367}{3^{23}}$
12	12	$\frac{2^{2}\cdot 13\cdot 1733\cdot 67057}{3^{16}}$	$-\frac{2^{3}\cdot 13\cdot 22571\cdot 334751}{3^{19}}$	$\frac{2^{8}\cdot 13\cdot 37\cdot 13732591}{3^{20}}$	$-\frac{2^{4}\cdot 13\cdot 540822211}{3^{21}}$	$\frac{2^{5}\cdot 7\cdot 13\cdot 37789649033}{3^{22}}$
12	13	$\frac{2^{9}\cdot 7\cdot 13\cdot 84533}{3^{16}}$	$-\frac{2^{10}\cdot 7^2\cdot 13\cdot 469801}{3^{18}}$	$\frac{2^{13}\cdot 7^2\cdot 13^2\cdot 257\cdot 857}{3^{22}}$	$\frac{2^{11}\cdot 7\cdot 13\cdot 79\cdot 304153}{3^{22}}$	$\frac{2^{12}\cdot 7\cdot 13\cdot 167962661}{3^{21}}$
12	14	$-\frac{2^{4}\cdot 13^2\cdot 233\cdot 6607}{3^{16}}$	$\frac{2^{5}\cdot 13\cdot 21221\cdot 396061}{3^{20}}$	$\frac{2^{10}\cdot 11\cdot 13\cdot 2083\cdot 8609}{3^{21}}$	$-\frac{2^{6}\cdot 13\cdot 1628880601}{3^{22}}$	$-\frac{2^{7}\cdot 7\cdot 13\cdot 593\cdot 126649637}{3^{23}}$
12	15	$-\frac{2^{3}\cdot 13\cdot 233\cdot 6607}{3^{16}}$	$\frac{2^{4}\cdot 13\cdot 15641\cdot 122557}{3^{20}}$	$\frac{2^{9}\cdot 13^2\cdot 463\cdot 17911}{3^{21}}$	$\frac{2^{5}\cdot 13\cdot 31\cdot 137\cdot 229\cdot 10321}{3^{22}}$	$-\frac{2^{6}\cdot 7\cdot 11\cdot 13\cdot 1175551529}{3^{22}}$
12	16	$\frac{2^{5}\cdot 5^3\cdot 7\cdot 13\cdot 29\cdot 2081}{3^{16}}$	$-\frac{2^{6}\cdot 5^2\cdot 7^2\cdot 13\cdot 19\cdot 53\cdot 9257}{3^{19}}$	$\frac{2^{11}\cdot 5^2\cdot 7\cdot 13\cdot 23\cdot 251483}{3^{21}}$	$-\frac{2^{7}\cdot 5^2\cdot 7\cdot 13\cdot 23\cdot 995369}{3^{19}}$	$\frac{2^{8}\cdot 5\cdot 7\cdot 13\cdot 83\cdot 3407\cdot 109579}{3^{22}}$
13	13	$\frac{2^{14}\cdot 7\cdot 13^2\cdot 3943}{3^{16}}$	$-\frac{2^{15}\cdot 7^2\cdot 13\cdot 61\cdot 12433}{3^{19}}$	$\frac{2^{21}\cdot 5\cdot 7\cdot 13\cdot 49669}{3^{20}}$	$\frac{2^{16}\cdot 7\cdot 13\cdot 1187\cdot 67577}{3^{23}}$	$\frac{2^{17}\cdot 7\cdot 13\cdot 89\cdot 3588601}{3^{22}}$
13	14	$\frac{2^{11}\cdot 7\cdot 13\cdot 723103}{3^{17}}$	$-\frac{2^{12}\cdot 7^2\cdot 13\cdot 61\cdot 51607}{3^{19}}$	$\frac{2^{15}\cdot 7\cdot 13\cdot 19\cdot 4108801}{3^{22}}$	$\frac{2^{13}\cdot 7\cdot 13\cdot 83\cdot 127^2\cdot 397}{3^{22}}$	$\frac{2^{14}\cdot 7\cdot 13\cdot 19\cdot 71\cdot 443\cdot 659}{3^{21}}$
13	15	$\frac{2^{10}\cdot 7\cdot 13\cdot 23^2\cdot 313}{3^{16}}$	$-\frac{2^{11}\cdot 7\cdot 11\cdot 13\cdot 397\cdot 1759}{3^{19}}$	$\frac{2^{14}\cdot 7\cdot 13\cdot 31^2\cdot 25183}{3^{22}}$	$\frac{2^{12}\cdot 7\cdot 13\cdot 683\cdot 836203}{3^{23}}$	$-\frac{2^{13}\cdot 7\cdot 11\cdot 13\cdot 1471\cdot 8779}{3^{21}}$
13	16	$\frac{2^{12}\cdot 5^2\cdot 7\cdot 13\cdot 23\cdot 2113}{3^{16}}$	$-\frac{2^{13}\cdot 5\cdot 7\cdot 13\cdot 79\cdot 157\cdot 1091}{3^{18}}$	$\frac{2^{16}\cdot 5\cdot 7\cdot 13\cdot 349\cdot 215801}{3^{22}}$	$\frac{2^{14}\cdot 5\cdot 7\cdot 13\cdot 1823\cdot 63391}{3^{22}}$	$\frac{2^{15}\cdot 5^2\cdot 7\cdot 13\cdot 73609741}{3^{20}}$
14	14	$\frac{2^{6}\cdot 13\cdot 397\cdot 487\cdot 6247}{3^{18}}$	$-\frac{2^{7}\cdot 5^3\cdot 13\cdot 823116673}{3^{21}}$	$\frac{2^{12}\cdot 13\cdot 167\cdot 191\cdot 856721}{3^{23}}$	$-\frac{2^{8}\cdot 5\cdot 13\cdot 19\cdot 401\cdot 547\cdot 4007}{3^{23}}$	$\frac{2^{9}\cdot 7\cdot 11\cdot 13\cdot 31\cdot 2441317421}{3^{24}}$
14	15	$\frac{2^{5}\cdot 13\cdot 770448241}{3^{18}}$	$-\frac{2^{6}\cdot 5^2\cdot 13^2\cdot 90630013}{3^{21}}$	$\frac{2^{11}\cdot 13\cdot 19\cdot 293\cdot 2519347}{3^{23}}$	$\frac{2^{7}\cdot 5\cdot 13\cdot 80743100293}{3^{23}}$	$-\frac{2^{8}\cdot 7\cdot 13\cdot 379\cdot 6581\cdot 201997}{3^{24}}$
14	16	$-\frac{2^{7}\cdot 5^2\cdot 7\cdot 13\cdot 269\cdot 2939}{3^{16}}$	$\frac{2^{8}\cdot 5\cdot 7\cdot 13\cdot 9743\cdot 261631}{3^{20}}$	$\frac{2^{13}\cdot 5\cdot 7^2\cdot 11\cdot 13\cdot 19\cdot 77479}{3^{21}}$	$\frac{2^{9}\cdot 5\cdot 7\cdot 13\cdot 3361619981}{3^{21}}$	$-\frac{2^{10}\cdot 5\cdot 7\cdot 13^2\cdot 21979487743}{3^{23}}$
15	15	$\frac{2^{4}\cdot 13\cdot 622014119}{3^{17}}$	$-\frac{2^{5}\cdot 5^2\cdot 13\cdot 13037\cdot 90523}{3^{20}}$	$\frac{2^{10}\cdot 13^3\cdot 3433\cdot 13883}{3^{22}}$	$\frac{2^{6}\cdot 5\cdot 13\cdot 2549\cdot 3228103}{3^{22}}$	$\frac{2^{7}\cdot 7\cdot 13\cdot 89\cdot 161993441}{3^{20}}$
15	16	$-\frac{2^{6}\cdot 5^2\cdot 7\cdot 13\cdot 151\cdot 13757}{3^{16}}$	$\frac{2^{7}\cdot 5\cdot 7\cdot 13\cdot 17\cdot 353\cdot 265541}{3^{20}}$	$-\frac{2^{12}\cdot 5\cdot 7\cdot 13\cdot 193\cdot 1099547}{3^{21}}$	$-\frac{2^{8}\cdot 5\cdot 7^2\cdot 13\cdot 359\cdot 8876653}{3^{22}}$	$\frac{2^{9}\cdot 5\cdot 7\cdot 11\cdot 13\cdot 29333\cdot 163613}{3^{22}}$
16	16	$\frac{2^{8}\cdot 5\cdot 7\cdot 13\cdot 23\cdot 67\cdot 101\cdot 317}{3^{15}}$	$-\frac{2^{9}\cdot 5\cdot 7\cdot 13\cdot 89\cdot 4973\cdot 16369}{3^{18}}$	$\frac{2^{14}\cdot 5^2\cdot 7\cdot 13\cdot 153516109}{3^{20}}$	$-\frac{2^{10}\cdot 5\cdot 7\cdot 13^2\cdot 307\cdot 2791\cdot 4457}{3^{21}}$	$\frac{2^{11}\cdot 5^2\cdot 7\cdot 13\cdot 121821760531}{3^{21}}$

Cubic ghost field coefficients $t^{\rm gh}_{ijk}$

		i						
j	k	1	2	3	4	5	6	7
1	1	1	$-\frac{11}{3^3}$	0	0	$\frac{2^4\cdot 5}{3^6}$	$\frac{19}{3^5}$	$\frac{2^4\cdot 5}{3^5}$
1	2	$-\frac{11}{3^3}$	$\frac{19}{3^5}$	$-\frac{2^6\cdot 5\sqrt{3}}{3^8}$	$-\frac{2^7\cdot 5\sqrt{3}}{3^8}$	$-\frac{2^4\cdot 5^2}{3^8}$	$-\frac{43\cdot 89}{3^9}$	$-\frac{2^4\cdot 5^2}{3^7}$
1	3	0	$\frac{2^6\cdot 5\sqrt{3}}{3^8}$	$\frac{2^6\cdot 5^2}{3^9}$	$\frac{2^7\cdot 7}{3^8}$	$\frac{2^6\cdot 5^2\sqrt{3}}{3^{11}}$	$\frac{2^7\cdot 5\cdot 7\sqrt{3}}{3^{10}}$	$\frac{2^6\cdot 19\sqrt{3}}{3^9}$
1	4	0	$\frac{2^7\cdot 5\sqrt{3}}{3^8}$	$\frac{2^7\cdot 7}{3^8}$	$\frac{2^8\cdot 5^2}{3^9}$	$\frac{2^7\cdot 19\sqrt{3}}{3^{10}}$	$\frac{2^8\cdot 5\cdot 7\sqrt{3}}{3^{10}}$	$\frac{2^7\cdot 5^2\sqrt{3}}{3^{10}}$
1	5	$\frac{2^4\cdot 5}{3^6}$	$-\frac{2^4\cdot 5^2}{3^8}$	$-\frac{2^6\cdot 5^2\sqrt{3}}{3^{11}}$	$-\frac{2^7\cdot 19\sqrt{3}}{3^{10}}$	$\frac{2^6\cdot 5^2}{3^{11}}$	$-\frac{2^4\cdot 5\cdot 7\cdot 19}{3^{11}}$	$-\frac{2^6\cdot 17\cdot 47}{3^{12}}$
1	6	$\frac{19}{3^5}$	$-\frac{43\cdot 89}{3^9}$	$-\frac{2^7\cdot 5\cdot 7\sqrt{3}}{3^{10}}$	$-\frac{2^8\cdot 5\cdot 7\sqrt{3}}{3^{10}}$	$-\frac{2^4\cdot 5\cdot 7\cdot 19}{3^{11}}$	$-\frac{31\cdot 131}{3^9}$	$-\frac{2^4\cdot 5\cdot 7\cdot 19}{3^{10}}$
1	7	$\frac{2^4\cdot 5}{3^5}$	$-\frac{2^4\cdot 5^2}{3^7}$	$-\frac{2^6\cdot 19\sqrt{3}}{3^9}$	$-\frac{2^7\cdot 5^2\sqrt{3}}{3^{10}}$	$-\frac{2^6\cdot 17\cdot 47}{3^{12}}$	$-\frac{2^4\cdot 5\cdot 7\cdot 19}{3^{10}}$	$\frac{2^6\cdot 5^2}{3^9}$
1	12	$-\frac{2^4\cdot 71}{3^9}$	$\frac{2^4\cdot 5\cdot 71}{3^{11}}$	$\frac{2^6\cdot 5\cdot 71\sqrt{3}}{3^{14}}$	$\frac{2^7\cdot 43\sqrt{3}}{3^{12}}$	$-\frac{2^6\cdot 5\cdot 71}{3^{14}}$	$\frac{2^4\cdot 37\cdot 103}{3^{14}}$	$-\frac{2^6\cdot 2089}{3^{14}}$
1	13	$-\frac{2^5\cdot 5^2}{3^9}$	$\frac{2^5\cdot 5\cdot 211}{3^{12}}$	$\frac{2^7\cdot 7\cdot 13\sqrt{3}}{3^{12}}$	$-\frac{2^8\cdot 5^3\sqrt{3}}{3^{14}}$	$\frac{2^7\cdot 1723}{3^{15}}$	$-\frac{2^5\cdot 5^4}{3^{13}}$	$-\frac{2^7\cdot 5^2\cdot 269}{3^{14}}$
1	14	$-\frac{2099}{3^9}$	$\frac{18289}{3^{12}}$	$-\frac{2^6\cdot 5\cdot 19\sqrt{3}}{3^{12}}$	$-\frac{2^7\cdot 5\cdot 19\sqrt{3}}{3^{12}}$	$-\frac{2^4\cdot 5^2\cdot 433}{3^{14}}$	$-\frac{17^2\cdot 19\cdot 83}{3^{14}}$	$-\frac{2^4\cdot 5^2\cdot 433}{3^{13}}$
1	15	$-\frac{2^6\cdot 5^2}{3^9}$	$\frac{2^6\cdot 5\cdot 211}{3^{12}}$	$-\frac{2^8\cdot 5^3\sqrt{3}}{3^{14}}$	$\frac{2^9\cdot 7\cdot 13\sqrt{3}}{3^{12}}$	$-\frac{2^8\cdot 5^2\cdot 269}{3^{15}}$	$-\frac{2^6\cdot 5^4}{3^{13}}$	$\frac{2^8\cdot 1723}{3^{14}}$
1	16	$-\frac{2^4\cdot 5\cdot 71}{3^9}$	$\frac{2^4\cdot 5^2\cdot 71}{3^{11}}$	$\frac{2^6\cdot 5\cdot 43\sqrt{3}}{3^{12}}$	$\frac{2^7\cdot 5^2\cdot 71\sqrt{3}}{3^{14}}$	$-\frac{2^6\cdot 5\cdot 2089}{3^{15}}$	$\frac{2^4\cdot 5\cdot 37\cdot 103}{3^{14}}$	$-\frac{2^6\cdot 5^2\cdot 71}{3^{13}}$
1	17	$-\frac{11\cdot 19}{3^8}$	$\frac{38449}{3^{12}}$	$\frac{2^6\cdot 5^2\sqrt{3}}{3^{10}}$	$\frac{2^7\cdot 5^2\sqrt{3}}{3^{10}}$	$\frac{2^4\cdot 5\cdot 19\cdot 73}{3^{14}}$	$\frac{103\cdot 3313}{3^{14}}$	$\frac{2^4\cdot 5\cdot 19\cdot 73}{3^{13}}$
2	2	$\frac{19}{3^5}$	$-\frac{1}{3^4}$	0	0	$\frac{2^4\cdot 5}{3^8}$	$\frac{19\cdot 6571}{3^{12}}$	$\frac{2^4\cdot 5}{3^7}$
2	3	$-\frac{2^6\cdot 5\sqrt{3}}{3^8}$	0	$-\frac{2^6\cdot 5^2}{3^9}$	$\frac{2^7\cdot 137}{3^{12}}$	$-\frac{2^6\cdot 5^2\sqrt{3}}{3^{11}}$	$-\frac{2^6\cdot 5^2\cdot 7\cdot 13\sqrt{3}}{3^{14}}$	$-\frac{2^6\cdot 257\sqrt{3}}{3^{12}}$
2	4	$-\frac{2^7\cdot 5\sqrt{3}}{3^8}$	0	$\frac{2^7\cdot 137}{3^{12}}$	$-\frac{2^8\cdot 5^2}{3^9}$	$-\frac{2^7\cdot 257\sqrt{3}}{3^{13}}$	$-\frac{2^7\cdot 5^2\cdot 7\cdot 13\sqrt{3}}{3^{14}}$	$-\frac{2^7\cdot 5^2\sqrt{3}}{3^{10}}$
2	5	$-\frac{2^4\cdot 5^2}{3^8}$	$\frac{2^4\cdot 5}{3^8}$	$\frac{2^6\cdot 5^2\sqrt{3}}{3^{11}}$	$\frac{2^7\cdot 257\sqrt{3}}{3^{13}}$	$-\frac{2^6\cdot 5^2}{3^{11}}$	$\frac{2^4\cdot 5\cdot 7\cdot 887}{3^{15}}$	$-\frac{2^6\cdot 7\cdot 11\cdot 13}{3^{14}}$
2	6	$-\frac{43\cdot 89}{3^9}$	$\frac{19\cdot 6571}{3^{12}}$	$\frac{2^6\cdot 5^2\cdot 7\cdot 13\sqrt{3}}{3^{14}}$	$\frac{2^7\cdot 5^2\cdot 7\cdot 13\sqrt{3}}{3^{14}}$	$\frac{2^4\cdot 5\cdot 7\cdot 887}{3^{15}}$	$-\frac{131\cdot 3331}{3^{14}}$	$\frac{2^4\cdot 5\cdot 7\cdot 887}{3^{14}}$
2	7	$-\frac{2^4\cdot 5^2}{3^7}$	$\frac{2^4\cdot 5}{3^7}$	$\frac{2^6\cdot 257\sqrt{3}}{3^{12}}$	$\frac{2^7\cdot 5^2\sqrt{3}}{3^{10}}$	$-\frac{2^6\cdot 7\cdot 11\cdot 13}{3^{14}}$	$\frac{2^4\cdot 5\cdot 7\cdot 887}{3^{14}}$	$-\frac{2^6\cdot 5^2}{3^9}$
2	12	$\frac{2^4\cdot 5\cdot 71}{3^{11}}$	$-\frac{2^4\cdot 71}{3^{11}}$	$-\frac{2^6\cdot 5\cdot 71\sqrt{3}}{3^{14}}$	$-\frac{2^7\cdot 7\cdot 461\sqrt{3}}{3^{16}}$	$\frac{2^6\cdot 5\cdot 71}{3^{14}}$	$-\frac{2^4\cdot 5\cdot 31\cdot 773}{3^{18}}$	$\frac{2^6\cdot 103^2}{3^{16}}$
2	13	$\frac{2^5\cdot 5\cdot 211}{3^{12}}$	$-\frac{2^5\cdot 5\cdot 19\cdot 109}{3^{14}}$	$-\frac{2^7\cdot 43\cdot 227\sqrt{3}}{3^{17}}$	$\frac{2^8\cdot 5^2\cdot 109\sqrt{3}}{3^{16}}$	$-\frac{2^7\cdot 41\cdot 73}{3^{16}}$	$\frac{2^5\cdot 5\cdot 7^2\cdot 1667}{3^{18}}$	$\frac{2^7\cdot 5^2\cdot 13\cdot 137}{3^{16}}$
2	14	$\frac{18289}{3^{12}}$	$-\frac{107\cdot 283}{3^{14}}$	$-\frac{2^7\cdot 5\cdot 17\cdot 29\sqrt{3}}{3^{17}}$	$-\frac{2^8\cdot 5\cdot 17\cdot 29\sqrt{3}}{3^{17}}$	$\frac{2^4\cdot 5\cdot 12491}{3^{17}}$	$\frac{47\cdot 53\cdot 61\cdot 199}{3^{18}}$	$\frac{2^4\cdot 5\cdot 12491}{3^{16}}$
2	15	$\frac{2^6\cdot 5\cdot 211}{3^{12}}$	$-\frac{2^6\cdot 5\cdot 19\cdot 109}{3^{14}}$	$\frac{2^8\cdot 5^2\cdot 109\sqrt{3}}{3^{16}}$	$-\frac{2^9\cdot 43\cdot 227\sqrt{3}}{3^{17}}$	$\frac{2^8\cdot 5^2\cdot 13\cdot 137}{3^{17}}$	$\frac{2^6\cdot 5\cdot 7^2\cdot 1667}{3^{18}}$	$-\frac{2^8\cdot 41\cdot 73}{3^{15}}$
2	16	$\frac{2^4\cdot 5^2\cdot 71}{3^{11}}$	$-\frac{2^4\cdot 5\cdot 71}{3^{11}}$	$-\frac{2^6\cdot 5\cdot 7\cdot 461\sqrt{3}}{3^{16}}$	$-\frac{2^7\cdot 5^2\cdot 71\sqrt{3}}{3^{14}}$	$\frac{2^6\cdot 5\cdot 103^2}{3^{17}}$	$-\frac{2^4\cdot 5^2\cdot 31\cdot 773}{3^{18}}$	$\frac{2^6\cdot 5^2\cdot 71}{3^{13}}$
2	17	$\frac{38449}{3^{12}}$	$-\frac{6571}{3^{11}}$	$\frac{2^7\cdot 5\cdot 137\sqrt{3}}{3^{14}}$	$\frac{2^8\cdot 5\cdot 137\sqrt{3}}{3^{14}}$	$\frac{2^4\cdot 5\cdot 13\cdot 31}{3^{15}}$	$\frac{463\cdot 116167}{3^{18}}$	$\frac{2^4\cdot 5\cdot 13\cdot 31}{3^{14}}$
3	3	$\frac{2^6\cdot 5^2}{3^9}$	$-\frac{2^6\cdot 5^2}{3^9}$	0	0	0	$\frac{2^6\cdot 5^2}{3^9}$	$-\frac{2^{15}\cdot 5}{3^{14}}$
3	4	$\frac{2^7\cdot 7}{3^8}$	$\frac{2^7\cdot 137}{3^{12}}$	0	0	$\frac{2^{13}\cdot 5^2}{3^{14}}$	$-\frac{2^7\cdot 7^2\cdot 97}{3^{14}}$	$\frac{2^{13}\cdot 5^2}{3^{13}}$
4	4	$\frac{2^8\cdot 5^2}{3^9}$	$-\frac{2^8\cdot 5^2}{3^9}$	0	0	$-\frac{2^{17}\cdot 5}{3^{15}}$	$\frac{2^8\cdot 5^2}{3^9}$	0
3	5	$\frac{2^6\cdot 5^2\sqrt{3}}{3^{11}}$	$-\frac{2^6\cdot 5^2\sqrt{3}}{3^{11}}$	0	$\frac{2^{13}\cdot 5^2}{3^{14}}$	0	$-\frac{2^6\cdot 5^2\cdot 397\sqrt{3}}{3^{16}}$	$\frac{2^{14}\cdot 5\cdot 23\sqrt{3}}{3^{17}}$
3	6	$\frac{2^7\cdot 5\cdot 7\sqrt{3}}{3^{10}}$	$-\frac{2^6\cdot 5^2\cdot 7\cdot 13\sqrt{3}}{3^{14}}$	$\frac{2^6\cdot 5^2}{3^9}$	$-\frac{2^7\cdot 7^2\cdot 97}{3^{14}}$	$\frac{2^6\cdot 5^2\cdot 397\sqrt{3}}{3^{16}}$	0	$\frac{2^6\cdot 7^2\cdot 13\sqrt{3}}{3^{13}}$
3	7	$\frac{2^6\cdot 19\sqrt{3}}{3^9}$	$-\frac{2^6\cdot 257\sqrt{3}}{3^{12}}$	$-\frac{2^{15}\cdot 5}{3^{14}}$	$\frac{2^{13}\cdot 5^2}{3^{13}}$	$-\frac{2^{14}\cdot 5\cdot 23\sqrt{3}}{3^{17}}$	$-\frac{2^6\cdot 7^2\cdot 13\sqrt{3}}{3^{13}}$	0
4	5	$\frac{2^7\cdot 19\sqrt{3}}{3^{10}}$	$-\frac{2^7\cdot 257\sqrt{3}}{3^{13}}$	$\frac{2^{13}\cdot 5^2}{3^{14}}$	$-\frac{2^{17}\cdot 5}{3^{15}}$	0	$-\frac{2^7\cdot 7^2\cdot 13\sqrt{3}}{3^{14}}$	$-\frac{2^{15}\cdot 5\cdot 23\sqrt{3}}{3^{17}}$
4	6	$\frac{2^8\cdot 5\cdot 7\sqrt{3}}{3^{10}}$	$-\frac{2^7\cdot 5^2\cdot 7\cdot 13\sqrt{3}}{3^{14}}$	$-\frac{2^7\cdot 7^2\cdot 97}{3^{14}}$	$\frac{2^8\cdot 5^2}{3^9}$	$\frac{2^7\cdot 7^2\cdot 13\sqrt{3}}{3^{14}}$	0	$\frac{2^7\cdot 5^2\cdot 397\sqrt{3}}{3^{15}}$
4	7	$\frac{2^7\cdot 5^2\sqrt{3}}{3^{10}}$	$-\frac{2^7\cdot 5^2\sqrt{3}}{3^{10}}$	$\frac{2^{13}\cdot 5^2}{3^{13}}$	0	$\frac{2^{15}\cdot 5\cdot 23\sqrt{3}}{3^{17}}$	$-\frac{2^7\cdot 5^2\cdot 397\sqrt{3}}{3^{15}}$	0

Table of t_{ijk}^{gh} (continued)

		i						
j	k	1	2	3	4	5	6	7
3	12	$-\frac{2^6\cdot5\cdot71\sqrt{3}}{3^{14}}$	$\frac{2^6\cdot5\cdot71\sqrt{3}}{3^{14}}$	0	$-\frac{2^{13}\cdot89}{3^{16}}$	0	$\frac{2^6\cdot5\cdot5641\sqrt{3}}{3^{18}}$	$\frac{2^{14}\cdot373\sqrt{3}}{3^{19}}$
3	13	$-\frac{2^7\cdot7\cdot13\sqrt{3}}{3^{12}}$	$\frac{2^7\cdot43\cdot227\sqrt{3}}{3^{17}}$	$-\frac{2^{15}\cdot5\cdot59}{3^{18}}$	$\frac{2^{14}\cdot5\cdot7}{3^{16}}$	$-\frac{2^{13}\cdot5\cdot349\sqrt{3}}{3^{20}}$	$\frac{2^7\cdot7\cdot17\cdot331\sqrt{3}}{3^{18}}$	$-\frac{2^{13}\cdot5^2\cdot71\sqrt{3}}{3^{18}}$
3	14	$\frac{2^6\cdot5\cdot19\sqrt{3}}{3^{12}}$	$\frac{2^7\cdot5\cdot17\cdot29\sqrt{3}}{3^{17}}$	$-\frac{2^6\cdot5^3\cdot967}{3^{18}}$	$\frac{2^7\cdot11\cdot1409}{3^{17}}$	$-\frac{2^6\cdot5^2\cdot863\sqrt{3}}{3^{19}}$	$-\frac{2^6\cdot5\cdot197\sqrt{3}}{3^{19}}$	$\frac{2^6\cdot19\cdot11491\sqrt{3}}{3^{18}}$
3	15	$\frac{2^8\cdot5^3\sqrt{3}}{3^{14}}$	$-\frac{2^8\cdot5^2\cdot109\sqrt{3}}{3^{16}}$	0	$\frac{2^{15}\cdot5\cdot7}{3^{16}}$	$\frac{2^{14}\cdot5^3\cdot11\sqrt{3}}{3^{19}}$	$\frac{2^8\cdot5^3\sqrt{3}}{3^{14}}$	$-\frac{2^{14}\cdot5\cdot211\sqrt{3}}{3^{19}}$
3	16	$-\frac{2^6\cdot5\cdot43\sqrt{3}}{3^{12}}$	$\frac{2^6\cdot5\cdot7\cdot461\sqrt{3}}{3^{16}}$	$\frac{2^{15}\cdot5^2}{3^{18}}$	$-\frac{2^{13}\cdot5\cdot89}{3^{16}}$	$-\frac{2^{14}\cdot5^3\cdot7\sqrt{3}}{3^{20}}$	$\frac{2^6\cdot5\cdot7\cdot11489\sqrt{3}}{3^{19}}$	$\frac{2^{15}\cdot5\cdot11\sqrt{3}}{3^{17}}$
3	17	$-\frac{2^6\cdot5^2\sqrt{3}}{3^{10}}$	$-\frac{2^7\cdot5\cdot137\sqrt{3}}{3^{14}}$	$-\frac{2^6\cdot5^2}{3^9}$	$-\frac{2^7\cdot7\cdot97\cdot137}{3^{18}}$	$-\frac{2^6\cdot5^2\cdot397\sqrt{3}}{3^{16}}$	$-\frac{2^6\cdot5\cdot7\cdot97\sqrt{3}}{3^{14}}$	$-\frac{2^6\cdot663797\sqrt{3}}{3^{19}}$
4	12	$-\frac{2^7\cdot43\sqrt{3}}{3^{12}}$	$\frac{2^7\cdot7\cdot461\sqrt{3}}{3^{16}}$	$-\frac{2^{13}\cdot89}{3^{16}}$	$\frac{2^{17}\cdot5}{3^{18}}$	$\frac{2^{16}\cdot11\sqrt{3}}{3^{18}}$	$\frac{2^7\cdot7\cdot11489\sqrt{3}}{3^{19}}$	$-\frac{2^{15}\cdot5^2\cdot7\sqrt{3}}{3^{19}}$
4	13	$\frac{2^8\cdot5^3\sqrt{3}}{3^{14}}$	$-\frac{2^8\cdot5^2\cdot109\sqrt{3}}{3^{16}}$	$\frac{2^{14}\cdot5\cdot7}{3^{16}}$	0	$-\frac{2^{14}\cdot5\cdot211\sqrt{3}}{3^{20}}$	$\frac{2^8\cdot5^3\sqrt{3}}{3^{14}}$	$\frac{2^{14}\cdot5^3\cdot11\sqrt{3}}{3^{18}}$
4	14	$\frac{2^7\cdot5\cdot19\sqrt{3}}{3^{12}}$	$\frac{2^8\cdot5\cdot17\cdot29\sqrt{3}}{3^{17}}$	$\frac{2^7\cdot11\cdot1409}{3^{17}}$	$-\frac{2^8\cdot5^3\cdot967}{3^{18}}$	$\frac{2^7\cdot19\cdot11491\sqrt{3}}{3^{19}}$	$-\frac{2^7\cdot5\cdot197\sqrt{3}}{3^{19}}$	$-\frac{2^7\cdot5^2\cdot863\sqrt{3}}{3^{18}}$
4	15	$-\frac{2^9\cdot7\cdot13\sqrt{3}}{3^{12}}$	$\frac{2^9\cdot43\cdot227\sqrt{3}}{3^{17}}$	$\frac{2^{15}\cdot5\cdot7}{3^{16}}$	$-\frac{2^{18}\cdot5\cdot59}{3^{18}}$	$-\frac{2^{15}\cdot5^2\cdot71\sqrt{3}}{3^{19}}$	$\frac{2^9\cdot7\cdot17\cdot331\sqrt{3}}{3^{18}}$	$-\frac{2^{15}\cdot5\cdot349\sqrt{3}}{3^{19}}$
4	16	$-\frac{2^7\cdot5^2\cdot71\sqrt{3}}{3^{14}}$	$\frac{2^7\cdot5^2\cdot71\sqrt{3}}{3^{14}}$	$-\frac{2^{13}\cdot5\cdot89}{3^{16}}$	0	$\frac{2^{15}\cdot5\cdot373\sqrt{3}}{3^{20}}$	$\frac{2^7\cdot5^2\cdot5641\sqrt{3}}{3^{18}}$	0
4	17	$-\frac{2^7\cdot5^2\sqrt{3}}{3^{10}}$	$-\frac{2^8\cdot5\cdot137\sqrt{3}}{3^{14}}$	$-\frac{2^7\cdot7\cdot97\cdot137}{3^{18}}$	$-\frac{2^8\cdot5^2}{3^9}$	$-\frac{2^7\cdot663797\sqrt{3}}{3^{20}}$	$-\frac{2^7\cdot5\cdot7\cdot97\sqrt{3}}{3^{14}}$	$-\frac{2^7\cdot5^2\cdot397\sqrt{3}}{3^{15}}$
5	5	$\frac{2^6\cdot5^2}{3^{11}}$	$-\frac{2^6\cdot5^2}{3^{11}}$	0	0	0	$-\frac{2^6\cdot5^2\cdot19\cdot29}{3^{17}}$	$-\frac{2^{20}\cdot5}{3^{17}}$
5	6	$-\frac{2^4\cdot5\cdot7\cdot19}{3^{11}}$	$\frac{2^4\cdot5\cdot7\cdot887}{3^{15}}$	$-\frac{2^6\cdot5^2\cdot397\sqrt{3}}{3^{16}}$	$-\frac{2^7\cdot7^2\cdot13\sqrt{3}}{3^{14}}$	$-\frac{2^6\cdot5^2\cdot19\cdot29}{3^{17}}$	$-\frac{2^4\cdot5\cdot131\cdot397}{3^{16}}$	$\frac{2^6\cdot7^2\cdot5641}{3^{18}}$
5	7	$-\frac{2^6\cdot17\cdot47}{3^{12}}$	$-\frac{2^6\cdot7\cdot11\cdot13}{3^{14}}$	$\frac{2^{14}\cdot5\cdot23\sqrt{3}}{3^{17}}$	$-\frac{2^{15}\cdot5\cdot23\sqrt{3}}{3^{17}}$	$-\frac{2^{20}\cdot5}{3^{17}}$	$\frac{2^6\cdot7^2\cdot5641}{3^{18}}$	$-\frac{2^{20}\cdot5}{3^{16}}$
6	6	$-\frac{31\cdot131}{3^9}$	$-\frac{131\cdot3331}{3^{14}}$	0	0	$-\frac{2^4\cdot5\cdot131\cdot397}{3^{16}}$	$\frac{31^2}{3^8}$	$-\frac{2^4\cdot5\cdot131\cdot397}{3^{15}}$
6	7	$-\frac{2^4\cdot5\cdot7\cdot19}{3^{10}}$	$\frac{2^4\cdot5\cdot7\cdot887}{3^{14}}$	$\frac{2^6\cdot7^2\cdot13\sqrt{3}}{3^{13}}$	$\frac{2^7\cdot5^2\cdot397\sqrt{3}}{3^{15}}$	$\frac{2^6\cdot7^2\cdot5641}{3^{18}}$	$-\frac{2^4\cdot5\cdot131\cdot397}{3^{15}}$	$-\frac{2^6\cdot5^2\cdot19\cdot29}{3^{15}}$
7	7	$\frac{2^6\cdot5^2}{3^9}$	$-\frac{2^6\cdot5^2}{3^9}$	0	0	$-\frac{2^{20}\cdot5}{3^{16}}$	$-\frac{2^6\cdot5^2\cdot19\cdot29}{3^{15}}$	0
5	12	$-\frac{2^6\cdot5\cdot71}{3^{14}}$	$\frac{2^6\cdot5\cdot71}{3^{14}}$	0	$-\frac{2^{16}\cdot11\sqrt{3}}{3^{18}}$	0	$\frac{2^6\cdot5\cdot89\cdot313}{3^{20}}$	$\frac{2^{22}\cdot7}{3^{20}}$
5	13	$\frac{2^7\cdot1723}{3^{15}}$	$-\frac{2^7\cdot41\cdot73}{3^{16}}$	$\frac{2^{13}\cdot5\cdot349\sqrt{3}}{3^{20}}$	$\frac{2^{14}\cdot5\cdot211\sqrt{3}}{3^{20}}$	$\frac{2^{14}\cdot5\cdot7\cdot11}{3^{20}}$	$\frac{2^7\cdot487\cdot599}{3^{20}}$	$-\frac{2^{14}\cdot5\cdot1019}{3^{21}}$
5	14	$-\frac{2^4\cdot5^2\cdot433}{3^{14}}$	$\frac{2^4\cdot5\cdot12491}{3^{17}}$	$\frac{2^6\cdot5^2\cdot863\sqrt{3}}{3^{19}}$	$-\frac{2^7\cdot19\cdot11491\sqrt{3}}{3^{19}}$	$-\frac{2^6\cdot5^2}{3^{11}}$	$\frac{2^4\cdot5\cdot19\cdot227\cdot307}{3^{20}}$	$-\frac{2^6\cdot3760769}{3^{20}}$
5	15	$-\frac{2^8\cdot5^2\cdot269}{3^{15}}$	$\frac{2^8\cdot5^2\cdot13\cdot137}{3^{17}}$	$-\frac{2^{14}\cdot5^3\cdot11\sqrt{3}}{3^{19}}$	$\frac{2^{15}\cdot5^2\cdot71\sqrt{3}}{3^{19}}$	$-\frac{2^{15}\cdot5^3\cdot11}{3^{20}}$	$-\frac{2^8\cdot5^2\cdot7\cdot4657}{3^{20}}$	$-\frac{2^{15}\cdot5\cdot1019}{3^{21}}$
5	16	$-\frac{2^6\cdot5\cdot2089}{3^{15}}$	$\frac{2^6\cdot5\cdot103^2}{3^{17}}$	$\frac{2^{14}\cdot5^3\cdot7\sqrt{3}}{3^{20}}$	$-\frac{2^{15}\cdot5\cdot373\sqrt{3}}{3^{20}}$	$-\frac{2^{20}\cdot5^2}{3^{20}}$	$\frac{2^6\cdot5\cdot7\cdot73\cdot491}{3^{20}}$	$\frac{2^{22}\cdot5\cdot7}{3^{20}}$
5	17	$\frac{2^4\cdot5\cdot19\cdot73}{3^{14}}$	$\frac{2^4\cdot5\cdot13\cdot31}{3^{15}}$	$\frac{2^6\cdot5^2\cdot397\sqrt{3}}{3^{16}}$	$\frac{2^7\cdot663797\sqrt{3}}{3^{20}}$	$\frac{2^6\cdot5^2\cdot19\cdot29}{3^{17}}$	$\frac{2^4\cdot5^2\cdot397\cdot1499}{3^{20}}$	$-\frac{2^6\cdot1130627}{3^{21}}$
6	12	$\frac{2^4\cdot37\cdot103}{3^{14}}$	$-\frac{2^4\cdot5\cdot31\cdot773}{3^{18}}$	$-\frac{2^6\cdot5\cdot5641\sqrt{3}}{3^{18}}$	$-\frac{2^7\cdot7\cdot11489\sqrt{3}}{3^{19}}$	$\frac{2^6\cdot5\cdot89\cdot313}{3^{20}}$	$\frac{2^4\cdot131\cdot5641}{3^{18}}$	$\frac{2^6\cdot7\cdot73\cdot491}{3^{19}}$
6	13	$-\frac{2^5\cdot5^4}{3^{13}}$	$\frac{2^5\cdot5\cdot7^2\cdot1667}{3^{18}}$	$-\frac{2^7\cdot7\cdot17\cdot331\sqrt{3}}{3^{18}}$	$-\frac{2^8\cdot5^3\sqrt{3}}{3^{14}}$	$\frac{2^7\cdot487\cdot599}{3^{20}}$	$\frac{2^5\cdot5^2\cdot31}{3^{13}}$	$-\frac{2^7\cdot5^2\cdot7\cdot4657}{3^{19}}$
6	14	$-\frac{17^2\cdot19\cdot83}{3^{14}}$	$\frac{47\cdot53\cdot61\cdot199}{3^{18}}$	$\frac{2^6\cdot5\cdot197\sqrt{3}}{3^{19}}$	$\frac{2^7\cdot5\cdot197\sqrt{3}}{3^{19}}$	$\frac{2^4\cdot5\cdot19\cdot227\cdot307}{3^{20}}$	$-\frac{11\cdot131\cdot19289}{3^{18}}$	$\frac{2^4\cdot5\cdot19\cdot227\cdot307}{3^{19}}$
6	15	$-\frac{2^6\cdot5^4}{3^{13}}$	$\frac{2^6\cdot5\cdot7^2\cdot1667}{3^{18}}$	$-\frac{2^8\cdot5^3\sqrt{3}}{3^{14}}$	$-\frac{2^9\cdot7\cdot17\cdot331\sqrt{3}}{3^{18}}$	$-\frac{2^8\cdot5^2\cdot7\cdot4657}{3^{20}}$	$\frac{2^6\cdot5^2\cdot31}{3^{13}}$	$\frac{2^8\cdot487\cdot599}{3^{19}}$
6	16	$\frac{2^4\cdot5\cdot37\cdot103}{3^{14}}$	$-\frac{2^4\cdot5^2\cdot31\cdot773}{3^{18}}$	$-\frac{2^6\cdot5\cdot7\cdot11489\sqrt{3}}{3^{19}}$	$-\frac{2^7\cdot5^2\cdot5641\sqrt{3}}{3^{18}}$	$\frac{2^6\cdot5\cdot7\cdot73\cdot491}{3^{20}}$	$\frac{2^4\cdot5\cdot131\cdot5641}{3^{18}}$	$\frac{2^6\cdot5^2\cdot89\cdot313}{3^{19}}$
6	17	$\frac{103\cdot3313}{3^{14}}$	$\frac{463\cdot116167}{3^{18}}$	$\frac{2^6\cdot5\cdot7\cdot97\sqrt{3}}{3^{14}}$	$\frac{2^7\cdot5\cdot7\cdot97\sqrt{3}}{3^{14}}$	$\frac{2^4\cdot5^2\cdot397\cdot1499}{3^{20}}$	$\frac{31\cdot3331}{3^{13}}$	$\frac{2^4\cdot5^2\cdot397\cdot1499}{3^{19}}$
7	12	$-\frac{2^6\cdot2089}{3^{14}}$	$\frac{2^6\cdot103^2}{3^{16}}$	$-\frac{2^{14}\cdot373\sqrt{3}}{3^{19}}$	$\frac{2^{15}\cdot5^2\cdot7\sqrt{3}}{3^{19}}$	$\frac{2^{22}\cdot7}{3^{20}}$	$\frac{2^6\cdot7\cdot73\cdot491}{3^{19}}$	$-\frac{2^{20}\cdot5}{3^{18}}$
7	13	$-\frac{2^7\cdot5^2\cdot269}{3^{14}}$	$\frac{2^7\cdot5^2\cdot13\cdot137}{3^{16}}$	$\frac{2^{13}\cdot5^2\cdot71\sqrt{3}}{3^{18}}$	$-\frac{2^{14}\cdot5^3\cdot11\sqrt{3}}{3^{18}}$	$-\frac{2^{14}\cdot5\cdot1019}{3^{21}}$	$-\frac{2^7\cdot5^2\cdot7\cdot4657}{3^{19}}$	$-\frac{2^{14}\cdot5^3\cdot11}{3^{18}}$
7	14	$-\frac{2^4\cdot5^2\cdot433}{3^{13}}$	$\frac{2^4\cdot5\cdot12491}{3^{16}}$	$-\frac{2^6\cdot19\cdot11491\sqrt{3}}{3^{18}}$	$\frac{2^7\cdot5^2\cdot863\sqrt{3}}{3^{18}}$	$-\frac{2^6\cdot3760769}{3^{20}}$	$\frac{2^4\cdot5\cdot19\cdot227\cdot307}{3^{19}}$	$-\frac{2^6\cdot5^2}{3^9}$
7	15	$\frac{2^8\cdot1723}{3^{14}}$	$-\frac{2^8\cdot41\cdot73}{3^{15}}$	$\frac{2^{14}\cdot5\cdot211\sqrt{3}}{3^{19}}$	$\frac{2^{15}\cdot5\cdot349\sqrt{3}}{3^{19}}$	$-\frac{2^{15}\cdot5\cdot1019}{3^{21}}$	$\frac{2^8\cdot487\cdot599}{3^{19}}$	$\frac{2^{15}\cdot5\cdot7\cdot11}{3^{18}}$
7	16	$-\frac{2^6\cdot5^2\cdot71}{3^{13}}$	$\frac{2^6\cdot5^2\cdot71}{3^{13}}$	$-\frac{2^{15}\cdot5\cdot11\sqrt{3}}{3^{17}}$	0	$\frac{2^{22}\cdot5\cdot7}{3^{20}}$	$\frac{2^6\cdot5^2\cdot89\cdot313}{3^{19}}$	0
7	17	$\frac{2^4\cdot5\cdot19\cdot73}{3^{13}}$	$\frac{2^4\cdot5\cdot13\cdot31}{3^{14}}$	$\frac{2^6\cdot663797\sqrt{3}}{3^{19}}$	$\frac{2^7\cdot5^2\cdot397\sqrt{3}}{3^{15}}$	$-\frac{2^6\cdot1130627}{3^{21}}$	$\frac{2^4\cdot5^2\cdot397\cdot1499}{3^{19}}$	$\frac{2^6\cdot5^2\cdot19\cdot29}{3^{15}}$

Table of t^{gh}_{ijk} (continued)

		i				
j	k	1	2	5	6	7
12	12	$\frac{2^6\cdot 71^2}{3^{17}}$	$-\frac{2^6\cdot 71^2}{3^{17}}$	0	$-\frac{2^6\cdot 71\cdot 5531}{3^{22}}$	$\frac{2^{20}\cdot 71}{3^{22}}$
12	13	$-\frac{2^7\cdot 7993}{3^{18}}$	$\frac{2^7\cdot 7723}{3^{19}}$	$-\frac{2^{14}\cdot 11^2\cdot 31}{3^{23}}$	$-\frac{2^7\cdot 189187}{3^{21}}$	$\frac{2^{14}\cdot 5^2\cdot 563}{3^{23}}$
12	14	$\frac{2^4\cdot 11\cdot 19\cdot 521}{3^{18}}$	$-\frac{2^4\cdot 5\cdot 106921}{3^{20}}$	$\frac{2^6\cdot 5\cdot 67\cdot 10343}{3^{23}}$	$\frac{2^4\cdot 25908643}{3^{23}}$	$\frac{2^6\cdot 7^2\cdot 13\cdot 17\cdot 109}{3^{22}}$
12	15	$-\frac{2^8\cdot 5\cdot 277}{3^{14}}$	$\frac{2^8\cdot 5\cdot 409831}{3^{21}}$	$-\frac{2^{15}\cdot 5^2\cdot 11\cdot 23}{3^{24}}$	$-\frac{2^8\cdot 5\cdot 41\cdot 74887}{3^{23}}$	$-\frac{2^{15}\cdot 1213}{3^{21}}$
12	16	$-\frac{2^6\cdot 67\cdot 11083}{3^{18}}$	$\frac{2^6\cdot 7^2\cdot 53^2}{3^{20}}$	$-\frac{2^{22}\cdot 5\cdot 7\cdot 13}{3^{23}}$	$\frac{2^6\cdot 13\cdot 229\cdot 29453}{3^{23}}$	$-\frac{2^{22}\cdot 5\cdot 7\cdot 13}{3^{22}}$
12	17	$-\frac{2^4\cdot 5^2\cdot 487}{3^{16}}$	$-\frac{2^4\cdot 79301}{3^{18}}$	$-\frac{2^6\cdot 5\cdot 89\cdot 313}{3^{20}}$	$-\frac{2^4\cdot 5\cdot 1499\cdot 5641}{3^{22}}$	$-\frac{2^6\cdot 7^2\cdot 317621}{3^{23}}$
13	13	$\frac{2^8\cdot 5^4}{3^{17}}$	$-\frac{2^8\cdot 5^3\cdot 263}{3^{20}}$	$-\frac{2^{15}\cdot 5^2\cdot 7\cdot 11}{3^{23}}$	$\frac{2^8\cdot 5^4}{3^{17}}$	$\frac{2^{15}\cdot 5^4\cdot 11}{3^{22}}$
13	14	$-\frac{2^5\cdot 5\cdot 71\cdot 2251}{3^{18}}$	$\frac{2^5\cdot 5\cdot 181\cdot 10159}{3^{21}}$	$-\frac{2^7\cdot 29\cdot 338839}{3^{23}}$	$-\frac{2^5\cdot 5\cdot 6828197}{3^{22}}$	$\frac{2^7\cdot 5^2\cdot 277903}{3^{21}}$
13	15	$-\frac{2^9\cdot 11\cdot 14887}{3^{18}}$	$-\frac{2^9\cdot 193601}{3^{21}}$	$-\frac{2^{16}\cdot 5\cdot 33427}{3^{24}}$	$\frac{2^9\cdot 181\cdot 29207}{3^{22}}$	$-\frac{2^{16}\cdot 5\cdot 33427}{3^{23}}$
13	16	$-\frac{2^7\cdot 5^2\cdot 277}{3^{14}}$	$\frac{2^7\cdot 5^2\cdot 409831}{3^{21}}$	$-\frac{2^{14}\cdot 5\cdot 1213}{3^{22}}$	$-\frac{2^7\cdot 5^2\cdot 41\cdot 74887}{3^{23}}$	$-\frac{2^{14}\cdot 5^3\cdot 11\cdot 23}{3^{23}}$
13	17	$\frac{2^5\cdot 5\cdot 17\cdot 139}{3^{16}}$	$-\frac{2^5\cdot 5^4\cdot 47\cdot 109}{3^{20}}$	$-\frac{2^7\cdot 61\cdot 367781}{3^{24}}$	$-\frac{2^5\cdot 5\cdot 7\cdot 13^2\cdot 43}{3^{18}}$	$\frac{2^7\cdot 5^2\cdot 96911}{3^{21}}$
14	14	$-\frac{23\cdot 97\cdot 10891}{3^{17}}$	$\frac{7^2\cdot 13\cdot 23\cdot 97\cdot 173}{3^{20}}$	$-\frac{2^4\cdot 5\cdot 23\cdot 97}{3^{14}}$	$\frac{19\cdot 47\cdot 263\cdot 10891}{3^{22}}$	$-\frac{2^4\cdot 5\cdot 23\cdot 97}{3^{13}}$
14	15	$-\frac{2^6\cdot 5\cdot 71\cdot 2251}{3^{18}}$	$\frac{2^6\cdot 5\cdot 181\cdot 10159}{3^{21}}$	$\frac{2^8\cdot 5^2\cdot 277903}{3^{22}}$	$-\frac{2^6\cdot 5\cdot 6828197}{3^{22}}$	$-\frac{2^8\cdot 29\cdot 338839}{3^{22}}$
14	16	$\frac{2^4\cdot 5\cdot 11\cdot 19\cdot 521}{3^{18}}$	$-\frac{2^4\cdot 5^2\cdot 106921}{3^{20}}$	$\frac{2^6\cdot 5\cdot 7^2\cdot 13\cdot 17\cdot 109}{3^{23}}$	$\frac{2^4\cdot 5\cdot 25908643}{3^{23}}$	$\frac{2^6\cdot 5^2\cdot 67\cdot 10343}{3^{22}}$
14	17	$\frac{19\cdot 29\cdot 8933}{3^{17}}$	$-\frac{41\cdot 3928843}{3^{21}}$	$-\frac{2^4\cdot 5\cdot 11\cdot 19\cdot 49877}{3^{23}}$	$\frac{613\cdot 9025327}{3^{23}}$	$-\frac{2^4\cdot 5\cdot 11\cdot 19\cdot 49877}{3^{22}}$
15	15	$\frac{2^{10}\cdot 5^4}{3^{17}}$	$-\frac{2^{10}\cdot 5^3\cdot 263}{3^{20}}$	$\frac{2^{17}\cdot 5^4\cdot 11}{3^{23}}$	$\frac{2^{10}\cdot 5^4}{3^{17}}$	$-\frac{2^{17}\cdot 5^2\cdot 7\cdot 11}{3^{22}}$
15	16	$-\frac{2^8\cdot 5\cdot 7993}{3^{18}}$	$\frac{2^8\cdot 5\cdot 7723}{3^{19}}$	$\frac{2^{15}\cdot 5^3\cdot 563}{3^{24}}$	$-\frac{2^8\cdot 5\cdot 189187}{3^{21}}$	$-\frac{2^{15}\cdot 5\cdot 11^2\cdot 31}{3^{22}}$
15	17	$\frac{2^6\cdot 5\cdot 17\cdot 139}{3^{16}}$	$-\frac{2^6\cdot 5^4\cdot 47\cdot 109}{3^{20}}$	$\frac{2^8\cdot 5^2\cdot 96911}{3^{22}}$	$-\frac{2^6\cdot 5\cdot 7\cdot 13^2\cdot 43}{3^{18}}$	$-\frac{2^8\cdot 61\cdot 367781}{3^{23}}$
16	16	$\frac{2^6\cdot 5^2\cdot 71^2}{3^{17}}$	$-\frac{2^6\cdot 5^2\cdot 71^2}{3^{17}}$	$\frac{2^{20}\cdot 5^2\cdot 71}{3^{23}}$	$-\frac{2^6\cdot 5^2\cdot 71\cdot 5531}{3^{22}}$	0
16	17	$-\frac{2^4\cdot 5^3\cdot 487}{3^{16}}$	$-\frac{2^4\cdot 5\cdot 79301}{3^{18}}$	$-\frac{2^6\cdot 5\cdot 7^2\cdot 317621}{3^{24}}$	$-\frac{2^4\cdot 5^2\cdot 1499\cdot 5641}{3^{22}}$	$-\frac{2^6\cdot 5^2\cdot 89\cdot 313}{3^{19}}$
17	17	$-\frac{11\cdot 29\cdot 151\cdot 191}{3^{18}}$	$-\frac{23\cdot 29\cdot 127\cdot 151}{3^{17}}$	$-\frac{2^4\cdot 5\cdot 29\cdot 151\cdot 397}{3^{20}}$	$-\frac{11\cdot 23\cdot 127\cdot 191}{3^{17}}$	$-\frac{2^4\cdot 5\cdot 29\cdot 151\cdot 397}{3^{19}}$

A.4 The perturbatively stable vacuum in the universal basis at level $(M, 3M)$

We tabulate the coefficient of the expansion of the stable vacuum solution Ψ_0 at various levels and interaction [19].

$gh = 1$ field basis	level $(2,6)$	level $(4,12)$	level $(6,18)$	level $(8,24)$
$\|\Omega\rangle$	0.397655	0.400720	0.400379	0.399736
$b_{-1}c_{-1}\|\Omega\rangle$	−0.138974	−0.150287	−0.154775	−0.157121
$L_{-2}^m\|\Omega\rangle$	0.0408931	0.0415945	0.0417553	0.0418068
$b_{-1}c_{-3}\|\Omega\rangle$		0.0410734	0.0419369	0.0423586
$b_{-2}c_{-2}\|\Omega\rangle$		0.0241917	0.0248902	0.0253018
$b_{-3}c_{-1}\|\Omega\rangle$		0.0136911	0.0139790	0.0141195
$L_{-4}^m\|\Omega\rangle$		−0.00374192	−0.00373316	−0.00372790
$b_{-1}c_{-1}L_{-2}^m\|\Omega\rangle$		0.00501319	0.00541066	0.00562071
$L_{-2}^mL_{-2}^m\|\Omega\rangle$		−0.000430640	−0.000454546	−0.000465402
$b_{-1}c_{-5}\|\Omega\rangle$			−0.0219311	−0.0221614
$b_{-2}c_{-4}\|\Omega\rangle$			−0.0137020	−0.0138528
$b_{-3}c_{-3}\|\Omega\rangle$			−0.00834273	−0.00835965
$b_{-4}c_{-2}\|\Omega\rangle$			−0.00685102	−0.00692638
$b_{-5}c_{-1}\|\Omega\rangle$			−0.00438622	−0.00443228
$b_{-2}b_{-1}c_{-2}c_{-1}\|\Omega\rangle$			−0.00565149	−0.00580655
$L_{-6}^m\|\Omega\rangle$			0.00106584	0.00106174
$b_{-1}c_{-1}L_{-4}^m\|\Omega\rangle$			−0.000849860	−0.000873223
$b_{-1}c_{-2}L_{-3}^m\|\Omega\rangle$			−0.0000467691	−0.0000522841
$b_{-2}c_{-1}L_{-3}^m\|\Omega\rangle$			−0.0000233846	−0.0000261421
$L_{-3}^mL_{-3}^m\|\Omega\rangle$			4.47944×10^{-6}	5.08049×10^{-6}
$b_{-1}c_{-3}L_{-2}^m\|\Omega\rangle$			−0.00245779	−0.00252866
$b_{-2}c_{-2}L_{-2}^m\|\Omega\rangle$			−0.00206802	−0.00212542
$b_{-3}c_{-1}L_{-2}^m\|\Omega\rangle$			−0.000819263	−0.000842886
$L_{-4}^mL_{-2}^m\|\Omega\rangle$			0.000223304	0.000225002
$b_{-1}c_{-1}L_{-2}^mL_{-2}^m\|\Omega\rangle$			−0.000111315	−0.000128173
$L_{-2}^mL_{-2}^mL_{-2}^m\|\Omega\rangle$			-7.24101×10^{-6}	-6.24006×10^{-6}

continued...

$gh=1$ field basis	level $(2,6)$	level $(4,12)$	level $(6,18)$	level $(8,24)$
$b_{-1}c_{-7}\|\Omega\rangle$				0.0143120
$b_{-2}c_{-6}\|\Omega\rangle$				0.00915820
$b_{-3}c_{-5}\|\Omega\rangle$				0.00567427
$b_{-4}c_{-4}\|\Omega\rangle$				0.00483896
$b_{-5}c_{-3}\|\Omega\rangle$				0.00340456
$b_{-6}c_{-2}\|\Omega\rangle$				0.00305273
$b_{-2}b_{-1}c_{-3}c_{-2}\|\Omega\rangle$				-0.00354226
$b_{-7}c_{-1}\|\Omega\rangle$				0.00204457
$b_{-2}b_{-1}c_{-4}c_{-1}\|\Omega\rangle$				0.00375276
$b_{-3}b_{-1}c_{-3}c_{-1}\|\Omega\rangle$				0.000430243
$b_{-3}b_{-2}c_{-2}c_{-1}\|\Omega\rangle$				-0.00118075
$b_{-4}b_{-1}c_{-2}c_{-1}\|\Omega\rangle$				0.00187638
$L_{-8}^{m}\|\Omega\rangle$				-0.000418010
$b_{-1}c_{-1}L_{-6}^{m}\|\Omega\rangle$				0.000293298
$b_{-1}c_{-2}L_{-5}^{m}\|\Omega\rangle$				6.28149×10^{-6}
$b_{-2}c_{-1}L_{-5}^{m}\|\Omega\rangle$				3.14074×10^{-6}
$b_{-1}c_{-3}L_{-4}^{m}\|\Omega\rangle$				0.000500528
$b_{-2}c_{-2}L_{-4}^{m}\|\Omega\rangle$				0.000303792
$b_{-3}c_{-1}L_{-4}^{m}\|\Omega\rangle$				0.000166843
$L_{-4}^{m}L_{-4}^{m}\|\Omega\rangle$				-0.0000219997
$b_{-1}c_{-4}L_{-3}^{m}\|\Omega\rangle$				0.0000349615
$b_{-2}c_{-3}L_{-3}^{m}\|\Omega\rangle$				-3.27536×10^{-6}
$b_{-3}c_{-2}L_{-3}^{m}\|\Omega\rangle$				-2.18357×10^{-6}
$b_{-4}c_{-1}L_{-3}^{m}\|\Omega\rangle$				8.74037×10^{-6}
$L_{-5}^{m}L_{-3}^{m}\|\Omega\rangle$				-1.31968×10^{-6}
$b_{-1}c_{-1}L_{-3}^{m}L_{-3}^{m}\|\Omega\rangle$				1.25944×10^{-6}
$b_{-1}c_{-5}L_{-2}^{m}\|\Omega\rangle$				0.00153453
$b_{-2}c_{-4}L_{-2}^{m}\|\Omega\rangle$				0.00135567
$b_{-3}c_{-3}L_{-2}^{m}\|\Omega\rangle$				0.000616606
$b_{-4}c_{-2}L_{-2}^{m}\|\Omega\rangle$				0.000677835
$b_{-5}c_{-1}L_{-2}^{m}\|\Omega\rangle$				0.000306907
$b_{-2}b_{-1}c_{-2}c_{-1}L_{-2}^{m}\|\Omega\rangle$				0.000578281
$L_{-6}^{m}L_{-2}^{m}\|\Omega\rangle$				-0.0000762460
$b_{-1}c_{-1}L_{-4}^{m}L_{-2}^{m}\|\Omega\rangle$				0.0000637562
$b_{-1}c_{-2}L_{-3}^{m}L_{-2}^{m}\|\Omega\rangle$				5.96264×10^{-6}
$b_{-2}c_{-1}L_{-3}^{m}L_{-2}^{m}\|\Omega\rangle$				2.98132×10^{-6}
$L_{-3}^{m}L_{-3}^{m}L_{-2}^{m}\|\Omega\rangle$				-5.42280×10^{-7}
$b_{-1}c_{-3}L_{-2}^{m}L_{-2}^{m}\|\Omega\rangle$				0.0000472816
$b_{-2}c_{-2}L_{-2}^{m}L_{-2}^{m}\|\Omega\rangle$				0.000100119
$b_{-3}c_{-1}L_{-2}^{m}L_{-2}^{m}\|\Omega\rangle$				0.0000157605
$L_{-4}^{m}L_{-2}^{m}L_{-2}^{m}\|\Omega\rangle$				-4.37157×10^{-6}
$b_{-1}c_{-1}L_{-2}^{m}L_{-2}^{m}L_{-2}^{m}\|\Omega\rangle$				-3.759767×10^{-7}
$L_{-2}^{m}L_{-2}^{m}L_{-2}^{m}L_{-2}^{m}\|\Omega\rangle$				7.25908×10^{-7}

A.5 Fitting of the parameters of A

A.5.1 A up to Level 9 without gauge fixing

As A is of ghost number -1 and has only odd levels, we here tabulate such field basis at levels 3, 5, 7 and 9. The best-fit numbers are the coefficients of A obtained by best-fit via minimizing $\epsilon = \frac{|Q_{\Psi_0} A - \mathcal{I}|}{|\mathcal{I}|}$. The stable fit at level 9 is constructed so as to control the convergence behaviour of the coefficients.

Field Basis	level 3 fit	level 5 fit	level 7 fit	level 9 fit	stable level 9 fit
$b_{-2}\|0\rangle$	1.12237	1.01893	0.948316	1.25995	0.931864
$b_{-3}b_{-2}c_1\|0\rangle$		0.50921	0.37306	0.660674	0.401547
$b_{-4}\|0\rangle$		−0.518516	−0.753272	−0.25828	−0.753004
$b_{-2}L_{-2}^m\|0\rangle$		0.504193	0.50695	0.400769	0.496562
$b_{-4}b_{-3}c_1\|0\rangle$			0.698601	−0.10683	0.691255
$b_{-5}b_{-2}c_1\|0\rangle$			0.893251	−1.8453	0.888407
$b_{-6}\|0\rangle$			−0.531323	1.40819	−0.541737
$-b_{-3}b_{-2}c_{-1}\|0\rangle$			−1.87167	3.14822	−1.86475
$-b_{-4}b_{-2}c_0\|0\rangle$			−2.54254	3.2966	−2.54625
$b_{-2}L_{-4}^m\|0\rangle$			0.264611	−0.750856	0.255304
$b_{-3}L_{-3}^m\|0\rangle$			0.00193005	−0.0539165	−0.0191971
$b_{-3}b_{-2}c_1L_{-2}^m\|0\rangle$			0.358002	0.301463	0.338645
$b_{-4}L_{-2}^m\|0\rangle$			−0.724095	0.163428	−0.744985
$b_{-2}L_{-2}^mL_{-2}^m\|0\rangle$			0.166002	0.180328	0.169096
$b_{-5}b_{-4}c_1\|0\rangle$				0.0796036	0.273844
$b_{-6}b_{-3}c_1\|0\rangle$				−1.09893	−0.107261
$b_{-7}b_{-2}c_1\|0\rangle$				0.847731	0.195816
$b_{-8}\|0\rangle$				−0.313743	−0.277211
$b_{-3}c_{-3}b_{-2}\|0\rangle$				−19.0376	−4.11409
$-b_{-4}b_{-2}c_{-2}\|0\rangle$				−0.147445	−0.626872
$-b_{-4}b_{-3}c_{-1}\|0\rangle$				1.80597	−0.0745503
$-b_{-5}b_{-2}c_{-1}\|0\rangle$				−0.172462	−0.356920
$b_{-4}b_{-3}b_{-2}c_0c_1\|0\rangle$				1.05994	−0.102556
$-b_{-5}b_{-3}c_0\|0\rangle$				1.48397	−0.319450
$-b_{-6}b_{-2}c_0\|0\rangle$				−0.784562	0.0949989
$b_{-2}L_{-6}^m\|0\rangle$				0.103719	−0.00879977
$b_{-3}L_{-5}^m\|0\rangle$				−0.530976	−0.0537990
$b_{-3}b_{-2}c_1L_{-4}^m\|0\rangle$				0.428303	0.0633010
$b_{-4}L_{-4}^m\|0\rangle$				0.114766	0.111182
$b_{-4}b_{-2}c_1L_{-3}^m\|0\rangle$				0.687831	0.200100
$b_{-5}L_{-3}^m\|0\rangle$				−0.165379	−0.134011
$-b_{-3}b_{-2}c_0L_{-3}^m\|0\rangle$				−2.72288	−0.722198
$b_{-2}L_{-3}^mL_{-3}^m\|0\rangle$				0.3427	0.0910701
$b_{-4}b_{-3}c_1L_{-2}^m\|0\rangle$				−0.01845	0.304266
$b_{-5}b_{-2}c_1L_{-2}^m\|0\rangle$				−0.628564	−0.137309
$b_{-6}L_{-2}^m\|0\rangle$				0.39923	0.195490
$-b_{-3}b_{-2}c_{-1}L_{-2}^m\|0\rangle$				−0.537685	−0.289167
$-b_{-4}b_{-2}c_0L_{-2}^m\|0\rangle$				0.951973	−0.288878
$b_{-2}L_{-4}^mL_{-2}^m\|0\rangle$				−0.237783	−0.0856879
$b_{-3}L_{-3}^mL_{-2}^m\|0\rangle$				−0.332135	−0.0868470
$b_{-3}b_{-2}c_1L_{-2}^mL_{-2}^m\|0\rangle$				0.128844	0.126029
$b_{-4}L_{-2}^mL_{-2}^m\|0\rangle$				−0.00185911	−0.160345
$b_{-2}L_{-2}^mL_{-2}^mL_{-2}^m\|0\rangle$				0.0403381	0.0402361
$\epsilon = \|Q_{\Psi_0}A - \mathcal{I}\|/\|\mathcal{I}\|$	0.171484	0.117676	0.0453748	0.0243515	0.0356226

A.5.2 Fitting A in the Feynman-Siegel gauge

As A enjoys the gauge freedom $A \to A + Q_{\Psi_0} B$, we can fix it to be in the Feynman-Siegel gauge. This is another way to control the convergence behaviour of the coefficients.

fields	level 3 fit	level 5 fit	level 7 fit	level 9 fit
$b_{-2}\|0\rangle$	1.12237	1.01893	1.12465	1.05322
$b_{-3}b_{-2}c_1\|0\rangle$		0.50921	0.467	0.500266
$b_{-4}\|0\rangle$		−0.518516	−0.503772	−0.53228
$b_{-2}L_{-2}^m\|0\rangle$		0.504193	0.476325	0.504269
$b_{-4}b_{-3}c_1\|0\rangle$			0.333428	0.326986
$b_{-5}b_{-2}c_1\|0\rangle$			−0.330557	−0.328381
$b_{-6}\|0\rangle$			0.346811	0.331188
$-b_{-3}b_{-2}c_{-1}\|0\rangle$			0.325862	0.327997
$-b_{-4}b_{-2}c_0\|0\rangle$			0	0
$b_{-2}L_{-4}^m\|0\rangle$			−0.166799	−0.164306
$b_{-3}L_{-3}^m\|0\rangle$			0.00133026	0.000334022
$b_{-3}b_{-2}c_1L_{-2}^m\|0\rangle$			0.341592	0.328637
$b_{-4}L_{-2}^m\|0\rangle$			−0.332864	−0.327326
$b_{-2}L_{-2}^mL_{-2}^m\|0\rangle$			0.1686	0.165931
$b_{-5}b_{-4}c_1\|0\rangle$				0.245489
$b_{-6}b_{-3}c_1\|0\rangle$				−0.253014
$b_{-7}b_{-2}c_1\|0\rangle$				0.250149
$b_{-8}\|0\rangle$				−0.257672
$b_{-3}c_{-3}b_{-2}\|0\rangle$				0.249999
$-b_{-4}b_{-2}c_{-2}\|0\rangle$				−0.256812
$-b_{-4}b_{-3}c_{-1}\|0\rangle$				0.246526
$-b_{-5}b_{-2}c_{-1}\|0\rangle$				−0.25213
$b_{-4}b_{-3}b_{-2}c_0c_1\|0\rangle$				0
$-b_{-5}b_{-3}c_0\|0\rangle$				0
$-b_{-6}b_{-2}c_0\|0\rangle$				0
$b_{-2}L_{-6}^m\|0\rangle$				0.00104113
$b_{-3}L_{-5}^m\|0\rangle$				0.0000151443
$b_{-3}b_{-2}c_1L_{-4}^m\|0\rangle$				−0.126025
$b_{-4}L_{-4}^m\|0\rangle$				0.12448
$b_{-4}b_{-2}c_1L_{-3}^m\|0\rangle$				−0.0004548
$b_{-5}L_{-3}^m\|0\rangle$				−0.000819122
$-b_{-3}b_{-2}c_0L_{-3}^m\|0\rangle$				0
$b_{-2}L_{-3}^mL_{-3}^m\|0\rangle$				0.0000905036
$b_{-4}b_{-3}c_1L_{-2}^m\|0\rangle$				0.250728
$b_{-5}b_{-2}c_1L_{-2}^m\|0\rangle$				−0.251499
$b_{-6}L_{-2}^m\|0\rangle$				0.250865
$-b_{-3}b_{-2}c_{-1}L_{-2}^m\|0\rangle$				0.249179
$-b_{-4}b_{-2}c_0L_{-2}^m\|0\rangle$				0
$b_{-2}L_{-4}^mL_{-2}^m\|0\rangle$				−0.123363
$b_{-3}L_{-3}^mL_{-2}^m\|0\rangle$				0.000457948
$b_{-3}b_{-2}c_1L_{-2}^mL_{-2}^m\|0\rangle$				0.126358
$b_{-4}L_{-2}^mL_{-2}^m\|0\rangle$				−0.125248
$b_{-2}L_{-2}^mL_{-2}^mL_{-2}^m\|0\rangle$				0.0406385
$\epsilon = \|Q_{\Psi_0}A - \mathcal{I}\|/\|\mathcal{I}\|$	0.171484	0.117676	0.0480658	0.0320384

Bibliography

[1] K. Bardakci, "Spontaneous Symmetry Breakdown In The Standard Dual String Model," Nucl. Phys. B **133**, 297 (1978).

[2] K. Bardakci, "Dual Models And Spontaneous Symmetry Breaking," Nucl. Phys. B **68**, 331 (1974). K. Bardakci and M. B. Halpern, "Explicit Spontaneous Breakdown In A Dual Model," Phys. Rev. D **10**, 4230 (1974). K. Bardakci and M. B. Halpern, "Explicit Spontaneous Breakdown In A Dual Model. 2. N Point Functions," Nucl. Phys. B **96**, 285 (1975).

[3] A. Sen, "Stable non-BPS bound states of BPS D-branes," JHEP **9808**, 010 (1998) [arXiv:hep-th/9805019].

[4] A. Sen, "Tachyon condensation on the brane antibrane system," JHEP **9808**, 012 (1998) [arXiv:hep-th/9805170].

[5] A. Sen, "SO(32) spinors of type I and other solitons on brane-antibrane pair," JHEP **9809**, 023 (1998) [arXiv:hep-th/9808141].

[6] A. Sen, "BPS D-branes on non-supersymmetric cycles," JHEP **9812**, 021 (1998) [arXiv:hep-th/9812031].

[7] A. Sen, "Descent relations among bosonic D-branes," Int. J. Mod. Phys. A **14**, 4061 (1999) [arXiv:hep-th/9902105].

[8] A. Sen, "Non-BPS states and branes in string theory," arXiv:hep-th/9904207.

[9] A. Sen, "Universality of the tachyon potential," JHEP **9912**, 027 (1999) [arXiv:hep-th/9911116].

[10] A. A. Gerasimov and S. L. Shatashvili, "On exact tachyon potential in open string field theory," JHEP **0010**, 034 (2000) [arXiv:hep-th/0009103].

[11] D. Kutasov, M. Marino and G. W. Moore, "Some exact results on tachyon condensation in string field theory," JHEP **0010**, 045 (2000) [arXiv:hep-th/0009148].

[12] D. Ghoshal and A. Sen, "Normalisation of the background independent open string field theory action," JHEP **0011**, 021 (2000) [arXiv:hep-th/0009191].

[13] E. Witten, "Noncommutative Geometry And String Field Theory," Nucl. Phys. B **268**, 253 (1986).

[14] V. A. Kostelecky and S. Samuel, "On A Nonperturbative Vacuum For The Open Bosonic String," Nucl. Phys. B **336**, 263 (1990).

[15] A. Sen and B. Zwiebach, "Tachyon condensation in string field theory," JHEP **0003**, 002 (2000) [arXiv:hep-th/9912249].

[16] A. Sen, "Rolling tachyon," JHEP **0204**, 048 (2002) [arXiv:hep-th/0203211].

[17] A. Sen, "Tachyon matter," JHEP **0207**, 065 (2002) [arXiv:hep-th/0203265].

[18] A. Sen, "Field theory of tachyon matter," Mod. Phys. Lett. A **17**, 1797 (2002) [arXiv:hep-th/0204143].

[19] N. Moeller and W. Taylor, "Level truncation and the tachyon in open bosonic string field theory," Nucl. Phys. B **583**, 105 (2000) [arXiv:hep-th/0002237].

[20] N. Moeller, A. Sen and B. Zwiebach, "D-branes as tachyon lumps in string field theory," JHEP **0008**, 039 (2000) [arXiv:hep-th/0005036].

[21] N. Moeller, "Codimension two lump solutions in string field theory and tachyonic theories," arXiv:hep-th/0008101.

[22] B. Feng, Y. H. He and N. Moeller, "Testing the uniqueness of the open bosonic string field theory vacuum," arXiv:hep-th/0103103.

[23] I. Ellwood, B. Feng, Y. H. He and N. Moeller, "The identity string field and the tachyon vacuum," JHEP **0107**, 016 (2001) [arXiv:hep-th/0105024].

[24] N. Moeller and B. Zwiebach, "Dynamics with infinitely many time derivatives and rolling tachyons," JHEP **0210**, 034 (2002) [arXiv:hep-th/0207107].

[25] J. Polchinski, "Dirichlet-Branes and Ramond-Ramond Charges," Phys. Rev. Lett. **75**, 4724 (1995) [arXiv:hep-th/9510017].

[26] V. A. Kostelecky and R. Potting, "Expectation Values, Lorentz Invariance, and CPT in the Open Bosonic String," Phys. Lett. B **381**, 89 (1996) [arXiv:hep-th/9605088].

[27] N. Berkovits, "The tachyon potential in open Neveu-Schwarz string field theory," JHEP **0004**, 022 (2000) [arXiv:hep-th/0001084].

[28] N. Berkovits, A. Sen and B. Zwiebach, "Tachyon condensation in superstring field theory," Nucl. Phys. B **587**, 147 (2000) [arXiv:hep-th/0002211].

[29] J. A. Harvey and P. Kraus, "D-branes as unstable lumps in bosonic open string field theory," JHEP **0004**, 012 (2000) [arXiv:hep-th/0002117].

[30] W. Taylor, "D-brane effective field theory from string field theory," Nucl. Phys. B **585**, 171 (2000) [arXiv:hep-th/0001201].

[31] M. R. Gaberdiel and B. Zwiebach, "Tensor constructions of open string theories I: Foundations," Nucl. Phys. B **505**, 569 (1997) [arXiv:hep-th/9705038]. M. R. Gaberdiel and B. Zwiebach, "Tensor constructions of open string theories. II: Vector bundles, D-branes and orientifold groups," Phys. Lett. B **410**, 151 (1997) [arXiv:hep-th/9707051].

[32] D. J. Gross and A. Jevicki, "Operator Formulation Of Interacting String Field Theory," Nucl. Phys. B **283**, 1 (1987). D. J. Gross and A. Jevicki, "Operator Formulation Of Interacting String Field Theory. 2," Nucl. Phys. B **287**, 225 (1987).

[33] E. Cremmer, A. Schwimmer and C. B. Thorn, "The Vertex Function In Witten's Formulation Of String Field Theory," Phys. Lett. B **179**, 57 (1986).

[34] S. Samuel, "The Ghost Vertex In E. Witten's String Field Theory," Phys. Lett. B **181**, 255 (1986).

[35] V. A. Kostelecky and S. Samuel, "The Static Tachyon Potential In The Open Bosonic String Theory," Phys. Lett. B **207**, 169 (1988).

[36] M. Srednicki, "IIB or not IIB," JHEP **9808**, 005 (1998) [arXiv:hep-th/9807138].

[37] E. Witten, "D-branes and K-theory," JHEP **9812**, 019 (1998) [arXiv:hep-th/9810188].

[38] P. Yi, "Membranes from five-branes and fundamental strings from Dp branes," Nucl. Phys. B **550**, 214 (1999) [arXiv:hep-th/9901159].

[39] J. A. Harvey, P. Horava and P. Kraus, "D-sphalerons and the topology of string configuration space," JHEP **0003**, 021 (2000) [arXiv:hep-th/0001143].

[40] C. G. Callan, I. R. Klebanov, A. W. Ludwig and J. M. Maldacena, "Exact solution of a boundary conformal field theory," Nucl. Phys. B **422**, 417 (1994) [arXiv:hep-th/9402113].

[41] J. Polchinski and L. Thorlacius, "Free Fermion Representation Of A Boundary Conformal Field Theory," Phys. Rev. D **50**, 622 (1994) [arXiv:hep-th/9404008].

[42] P. Fendley, H. Saleur and N. P. Warner, "Exact solution of a massless scalar field with a relevant boundary interaction," Nucl. Phys. B **430**, 577 (1994) [arXiv:hep-th/9406125].

[43] A. Recknagel and V. Schomerus, "Boundary deformation theory and moduli spaces of D-branes," Nucl. Phys. B **545**, 233 (1999) [arXiv:hep-th/9811237].

[44] E. Witten, "Interacting Field Theory Of Open Superstrings," Nucl. Phys. B **276**, 291 (1986).

[45] D. J. Gross and A. Jevicki, "Operator Formulation Of Interacting String Field Theory. 3. Nsr Superstring," Nucl. Phys. B **293**, 29 (1987).

[46] C. Wendt, "Scattering Amplitudes And Contact Interactions In Witten's Superstring Field Theory," Nucl. Phys. B **314**, 209 (1989).

[47] J. Greensite and F. R. Klinkhamer, "Superstring Amplitudes And Contact Interactions," Nucl. Phys. B **304**, 108 (1988).

[48] I. Y. Arefeva, P. B. Medvedev and A. P. Zubarev, "Background Formalism For Superstring Field Theory," Phys. Lett. B **240**, 356 (1990).

[49] C. R. Preitschopf, C. B. Thorn and S. A. Yost, "Superstring Field Theory," Nucl. Phys. B **337**, 363 (1990).

[50] N. Berkovits, "SuperPoincare invariant superstring field theory," Nucl. Phys. B **450**, 90 (1995) [Erratum-ibid. B **459**, 439 (1996)] [arXiv:hep-th/9503099].

[51] O. Bergman and M. R. Gaberdiel, "Stable non-BPS D-particles," Phys. Lett. B **441**, 133 (1998) [arXiv:hep-th/9806155].

[52] P. Horava, "Type IIA D-branes, K-theory, and matrix theory," Adv. Theor. Math. Phys. **2**, 1373 (1999) [arXiv:hep-th/9812135].

[53] R. de Mello Koch, A. Jevicki, M. Mihailescu and R. Tatar, "Lumps and p-branes in open string field theory," Phys. Lett. B **482**, 249 (2000) [arXiv:hep-th/0003031].

[54] P. J. De Smet and J. Raeymaekers, "Level four approximation to the tachyon potential in superstring field theory," JHEP **0005**, 051 (2000) [arXiv:hep-th/0003220].

[55] A. Iqbal and A. Naqvi, "Tachyon condensation on a non-BPS D-brane," arXiv:hep-th/0004015.

[56] N. Drukker, D. J. Gross and N. Itzhaki, "Sphalerons, merons and unstable branes in AdS," Phys. Rev. D **62**, 086007 (2000) [arXiv:hep-th/0004131].

[57] N. Berkovits, "A new approach to superstring field theory," Fortsch. Phys. **48**, 31 (2000) [arXiv:hep-th/9912121].

[58] N. Berkovits and C. T. Echevarria, "Four-point amplitude from open superstring field theory," Phys. Lett. B **478**, 343 (2000) [arXiv:hep-th/9912120].

[59] O. Bergman, private communication.

[60] A. Iqbal and A. Naqvi, private communication.

[61] J. A. Harvey, D. Kutasov and E. J. Martinec, "On the relevance of tachyons," arXiv:hep-th/0003101.

[62] P. Ginsparg, "Applied Conformal Field Theory," HUTP-88-A054 *Lectures given at Les Houches Summer School in Theoretical Physics, Les Houches, France, Jun 28 - Aug 5, 1988*, arXiv:hep-th/9108028.

[63] A. LeClair, M. E. Peskin and C. R. Preitschopf, "String Field Theory On The Conformal Plane. 1. Kinematical Principles," Nucl. Phys. B **317**, 411 (1989). A. LeClair, M. E. Peskin and C. R. Preitschopf, "String Field Theory On The Conformal Plane. 2. Generalized Gluing," Nucl. Phys. B **317**, 464 (1989).

[64] M. R. Douglas, D. Kabat, P. Pouliot and S. H. Shenker, "D-branes and short distances in string theory," Nucl. Phys. B **485**, 85 (1997) [arXiv:hep-th/9608024].

[65] G. W. Moore, "Finite In All Directions," arXiv:hep-th/9305139.

[66] C. B. Thorn, "String Field Theory," Phys. Rept. **175**, 1 (1989).

[67] A. R. Bogojevic, "Brst Invariance Of The Measure In String Field Theory," Phys. Lett. B **198**, 479 (1987). M. Maeno, "Canonical Quantization Of Witten's String Field Theory Using Midpoint Light Cone Time," Phys. Rev. D **43**, 4006 (1991).

[68] B. Zwiebach, "Oriented open-closed string theory revisited," Annals Phys. **267**, 193 (1998) [arXiv:hep-th/9705241].

[69] R. de Mello Koch and J. P. Rodrigues, "Lumps in level truncated open string field theory," Phys. Lett. B **495**, 237 (2000) [arXiv:hep-th/0008053].

[70] J. A. Harvey, P. Kraus, F. Larsen and E. J. Martinec, "D-branes and strings as non-commutative solitons," JHEP **0007**, 042 (2000) [arXiv:hep-th/0005031].

[71] L. Rastelli and B. Zwiebach, "Tachyon potentials, star products and universality," JHEP **0109**, 038 (2001) [arXiv:hep-th/0006240].

[72] N. Moeller, A. Sen and B. Zwiebach, unpublished.

[73] E. Witten, "On background independent open string field theory," Phys. Rev. D **46**, 5467 (1992) [arXiv:hep-th/9208027].

[74] E. Witten, "Some computations in background independent off-shell string theory," Phys. Rev. D **47**, 3405 (1993) [arXiv:hep-th/9210065].

[75] S. L. Shatashvili, "Comment on the background independent open string theory," Phys. Lett. B **311**, 83 (1993) [arXiv:hep-th/9303143].

[76] S. L. Shatashvili, "On the problems with background independence in string theory," arXiv:hep-th/9311177.

[77] A. A. Tseytlin, "Sigma model approach to string theory effective actions with tachyons," J. Math. Phys. **42**, 2854 (2001) [arXiv:hep-th/0011033].

[78] H. Hata and S. Shinohara, "BRST invariance of the non-perturbative vacuum in bosonic open string field theory," JHEP **0009**, 035 (2000) [arXiv:hep-th/0009105].

[79] P. Mukhopadhyay and A. Sen, "Test of Siegel gauge for the lump solution," JHEP **0102**, 017 (2001) [arXiv:hep-th/0101014].

[80] P. J. De Smet and J. Raeymaekers, "The tachyon potential in Witten's superstring field theory," JHEP **0008**, 020 (2000) [arXiv:hep-th/0004112].

[81] J. R. David, "Tachyon condensation in the D0/D4 system," JHEP **0010**, 004 (2000) [arXiv:hep-th/0007235].

[82] A. Iqbal and A. Naqvi, "On marginal deformations in superstring field theory," JHEP **0101**, 040 (2001) [arXiv:hep-th/0008127].

[83] W. Taylor, "Mass generation from tachyon condensation for vector fields on D-branes," JHEP **0008**, 038 (2000) [arXiv:hep-th/0008033].

[84] A. Sen and B. Zwiebach, "Large marginal deformations in string field theory," JHEP **0010**, 009 (2000) [arXiv:hep-th/0007153].

[85] H. Hata and S. Teraguchi, "Test of the absence of kinetic terms around the tachyon vacuum in cubic string field theory," JHEP **0105**, 045 (2001) [arXiv:hep-th/0101162].

[86] D. Ghoshal and A. Sen, "Tachyon condensation and brane descent relations in p-adic string theory," Nucl. Phys. B **584**, 300 (2000) [arXiv:hep-th/0003278].

[87] B. Zwiebach, "A solvable toy model for tachyon condensation in string field theory," JHEP **0009**, 028 (2000) [arXiv:hep-th/0008227].

[88] J. A. Minahan and B. Zwiebach, "Field theory models for tachyon and gauge field string dynamics," JHEP **0009**, 029 (2000) [arXiv:hep-th/0008231].

[89] J. A. Minahan and B. Zwiebach, "Effective tachyon dynamics in superstring theory," JHEP **0103**, 038 (2001) [arXiv:hep-th/0009246].

[90] J. A. Minahan and B. Zwiebach, "Gauge fields and fermions in tachyon effective field theories," JHEP **0102**, 034 (2001) [arXiv:hep-th/0011226].

[91] J. A. Minahan, "Quantum corrections in p-adic string theory," arXiv:hep-th/0105312.

[92] J. A. Minahan, "Mode interactions of the tachyon condensate in p-adic string theory," JHEP **0103**, 028 (2001) [arXiv:hep-th/0102071].

[93] G. Chalmers, "Open string decoupling and tachyon condensation," JHEP **0106**, 012 (2001) [arXiv:hep-th/0103056].

[94] A. A. Gerasimov and S. L. Shatashvili, "Stringy Higgs mechanism and the fate of open strings," JHEP **0101**, 019 (2001) [arXiv:hep-th/0011009].

[95] S. L. Shatashvili, "On field theory of open strings, tachyon condensation and closed strings," arXiv:hep-th/0105076.

[96] Ian Ellwood and Washington Taylor, I. Ellwood and W. Taylor, "Open string field theory without open strings," Phys. Lett. B **512**, 181 (2001) [arXiv:hep-th/0103085].

[97] L. Rastelli, A. Sen and B. Zwiebach, "String field theory around the tachyon vacuum," Adv. Theor. Math. Phys. **5**, 353 (2002) [arXiv:hep-th/0012251].

[98] L. Rastelli, A. Sen and B. Zwiebach, "Classical solutions in string field theory around the tachyon vacuum," Adv. Theor. Math. Phys. **5**, 393 (2002) [arXiv:hep-th/0102112].

[99] G. T. Horowitz, J. Morrow-Jones, S. P. Martin and R. P. Woodard, "New Exact Solutions For The Purely Cubic Bosonic String Field Theory," Phys. Rev. Lett. **60**, 261 (1988).

[100] B. Zwiebach, "Closed string field theory: Quantum action and the B-V master equation," Nucl. Phys. B **390**, 33 (1993) [arXiv:hep-th/9206084].

[101] M. Saadi and B. Zwiebach, "Closed String Field Theory From Polyhedra," Annals Phys. **192**, 213 (1989). M. Kaku, "Geometric Derivation Of String Field Theory From First Principles: Closed Strings And Modular Invariance," Phys. Rev. D **38**, 3052 (1988). T. Kugo and K. Suehiro, "Nonpolynomial Closed String Field Theory: Action And Its Gauge Invariance," Nucl. Phys. B **337**, 434 (1990).

[102] G. T. Horowitz and A. Strominger, "Translations As Inner Derivations And Associativity Anomalies In Open String Field Theory," Phys. Lett. B **185**, 45 (1987).

[103] H. W. Wiesbrock, "The C* Algebra Of Bosonic Strings," Commun. Math. Phys. **136**, 369 (1991). H. W. Wiesbrock, "A Note On The Construction Of The C* Algebra Of Bosonic Strings," J. Math. Phys. **33**, 1837 (1992).

[104] K.-H. Zhu, "An Introduction to Operator Algebras," Studies in Advanced Mathematics, CRC Press 1993.

[105] M. Kleban, A. E. Lawrence and S. H. Shenker, "Closed strings from nothing," Phys. Rev. D **64**, 066002 (2001) [arXiv:hep-th/0012081].

[106] I. Ellwood and W. Taylor, "Gauge invariance and tachyon condensation in open string field theory," arXiv:hep-th/0105156.

[107] W. Taylor, "A perturbative analysis of tachyon condensation," arXiv:hep-th/0208149.

[108] D. Gaiotto and L. Rastelli, "Experimental string field theory," arXiv:hep-th/0211012.

[109] W. Taylor, "Perturbative diagrams in string field theory," arXiv:hep-th/0207132.

[110] D. A. Eliezer and R. P. Woodard, "The Problem Of Nonlocality In String Theory," Nucl. Phys. B **325**, 389 (1989). R. P. Woodard, "A canonical formalism for Lagrangians with nonlocality of finite extent," Phys. Rev. A **62**, 052105 (2000) [arXiv:hep-th/0006207]. D. L. Bennett, H. B. Nielsen and R. P. Woodard, "The initial value problem for maximally non-local actions," Phys. Rev. D **57**, 1167 (1998) [arXiv:hep-th/9707088]. D. A. Eliezer and R. P. Woodard, "Instability Of Higher Difference Initial Value Theories," Phys. Rev. D **40**, 465 (1989). T. C. Cheng, P. M. Ho and M. C. Yeh, "Perturbative approach to higher derivative and nonlocal theories," Nucl. Phys. B **625**, 151 (2002) [arXiv:hep-th/0111160]. K. Bering, "A note on non-locality and Ostrogradski's construction," arXiv:hep-th/0007192. T. Nakamura and S. Hamamoto, "Higher Derivatives and Canonical Formalisms,"

Prog. Theor. Phys. **95**, 469 (1996) [arXiv:hep-th/9511219]. H. J. Schmidt, "Stability And Hamiltonian Formulation Of Higher Derivative Theories," Phys. Rev. D **49**, 6354 (1994) [Erratum-ibid. D **54**, 7906 (1996)] [arXiv:gr-qc/9404038]. F. Muller-Hoissen, "Higher Derivative Versus Second Order Field Equations," Annalen Phys. **48**, 543 (1991). J. Z. Simon, "Higher Derivative Lagrangians, Nonlocality, Problems And Solutions," Phys. Rev. D **41**, 3720 (1990). M. Ostogradski, Mem. Ac. St. Petersbourg **VI 4** 385 (1850).

[111] I. A. Batalin and G. A. Vilkovisky, "Quantization Of Gauge Theories With Linearly Dependent Generators," Phys. Rev. D **28**, 2567 (1983) [Erratum-ibid. D **30**, 508 (1984)]. A. Schwarz, "Geometry of Batalin-Vilkovisky quantization," Commun. Math. Phys. **155**, 249 (1993) [arXiv:hep-th/9205088].

[112] W. Siegel, "Introduction To String Field Theory," Adv. Ser. Math. Phys. **8**, 1 (1988).

[113] J. L. Barbon and E. Rabinovici, "Stringy fuzziness as the custodian of time-space noncommutativity," Phys. Lett. B **486**, 202 (2000) [arXiv:hep-th/0005073].

[114] L. Alvarez-Gaume, J. L. Barbon and R. Zwicky, "Remarks on time-space noncommutative field theories," JHEP **0105**, 057 (2001) [arXiv:hep-th/0103069].

[115] M. Kaku and K. Kikkawa, "The Field Theory Of Relativistic Strings, Pt. 1: Trees," Phys. Rev. D **10**, 1110 (1974). "The Field Theory Of Relativistic Strings. Pt. 2: Loops And Pomerons," Phys. Rev. D **10**, 1823 (1974).

[116] G. W. Gibbons, Phys. Lett. B **537**, 1 (2002) [arXiv:hep-th/0204008]. M. Fairbairn and M. H. Tytgat, Phys. Lett. B **546**, 1 (2002) [arXiv:hep-th/0204070]. C. M. Chen, D. V. Gal'tsov and M. Gutperle, Phys. Rev. D **66**, 024043 (2002) [arXiv:hep-th/0204071]. S. Mukohyama, Phys. Rev. D **66**, 024009 (2002) [arXiv:hep-th/0204084]. A. Feinstein, Phys. Rev. D **66**, 063511 (2002) [arXiv:hep-th/0204140]. T. Padmanabhan, Phys. Rev. D **66**, 021301 (2002) [arXiv:hep-th/0204150]. A. V. Frolov, L. Kofman and A. A. Starobinsky, Phys. Lett. B **545**, 8

(2002) [arXiv:hep-th/0204187]. K. Hashimoto, JHEP **0207**, 035 (2002) [arXiv:hep-th/0204203]. D. Choudhury, D. Ghoshal, D. P. Jatkar and S. Panda, Phys. Lett. B **544**, 231 (2002) [arXiv:hep-th/0204204]. X. z. Li, J. g. Hao and D. j. Liu, Chin. Phys. Lett. **19**, 1584 (2002) [arXiv:hep-th/0204252]. G. Shiu and I. Wasserman, Phys. Lett. B **541**, 6 (2002) [arXiv:hep-th/0205003]. T. Padmanabhan and T. R. Choudhury, Phys. Rev. D **66**, 081301 (2002) [arXiv:hep-th/0205055]. L. Kofman and A. Linde, JHEP **0207**, 004 (2002) [arXiv:hep-th/0205121]. H. B. Benaoum, arXiv:hep-th/0205140. M. Sami, Mod. Phys. Lett. A **18**, 691 (2003) [arXiv:hep-th/0205146]. M. Sami, P. Chingangbam and T. Qureshi, Phys. Rev. D **66**, 043530 (2002) [arXiv:hep-th/0205179].

[117] S. Sugimoto and S. Terashima, "Tachyon matter in boundary string field theory," JHEP **0207**, 025 (2002) [arXiv:hep-th/0205085].

[118] J. A. Minahan, "Rolling the tachyon in super BSFT," JHEP **0207**, 030 (2002) [arXiv:hep-th/0205098].

[119] L. Brekke, P. G. Freund, M. Olson and E. Witten, "Nonarchimedean String Dynamics," Nucl. Phys. B **302**, 365 (1988).

[120] A. Sen, "Time evolution in open string theory," JHEP **0210**, 003 (2002) [arXiv:hep-th/0207105].

[121] D. Gaiotto, L. Rastelli, A. Sen and B. Zwiebach, "Ghost structure and closed strings in vacuum string field theory," hep-th/0111129. A. Hashimoto and N. Itzhaki, "Observables of string field theory," JHEP **0201**, 028 (2002) [arXiv:hep-th/0111092]. G. Moore and W. Taylor, "The singular geometry of the sliver," JHEP **0201**, 004 (2002) [arXiv:hep-th/0111069]. A. Sen, "Fundamental strings in open string theory at the tachyonic vacuum," J. Math. Phys. **42**, 2844 (2001) [arXiv:hep-th/0010240]. G. W. Gibbons, K. Hori and P. Yi, "String fluid from unstable D-branes," Nucl. Phys. B **596**, 136 (2001) [arXiv:hep-th/0009061]. O. Bergman, K. Hori and P. Yi, "Confinement on the brane," Nucl. Phys. B **580**, 289 (2000) [arXiv:hep-th/0002223].

[122] M. Gutperle and A. Strominger, "Spacelike branes," JHEP **0204**, 018 (2002) [arXiv:hep-th/0202210].